Entry targeted lentiviral vectors for the specific modification of distinct subsets of immune cells

Vom Fachbereich Biologie der Technischen Universität Darmstadt

zur Erlangung des akademischen Grades

eines Doctor rerum naturalium

genehmigte Dissertation von

Diplom-Biologin Katharina Uhlig

aus Karl-Marx-Stadt

1. Referentin: Prof. Dr. Beatrix Süß

2. Referent: Prof. Dr. Bodo Laube

3. Referent: Prof. Dr. Christian Buchholz

Tag der Einreichung: 14.07.2015

Tag der mündlichen Prüfung: 25.09.2015

Darmstadt 2015

D 17

Für meine Eltern und für Gregor

- In Liebe und Dankbarkeit -

Wege entstehen dadurch, dass wir sie gehen.

- Franz Kafka

Table of contents

1. Introduction

1.1. Lentiviral vectors

Lentiviruses (*Lentiviridae*) are a genus of the retrovirus family (*Retroviridae*), a family which comprises a multiplicity of enveloped viruses characterized by the eponymous reverse transcription of their RNA genome into DNA. This DNA intermediate is then integrated into the host genome as provirus and subsequently transcribed and translated by the host cell machinery. Among the *Retroviridae*, lentiviruses possess the remarkable ability to infect not only dividing but also non-dividing cells (Weinberg et al., 1991; Lewis et al., 1992). They are not depending on the mitotic dissolution of the nuclear membrane as the viral pre-integration complex can rather be imported into the nucleus passing through the nuclear pore complex (Bukrinsky, 2004). Lentiviral vectors (LV) are derived from lentiviruses such as the Human Immunodeficiency Virus-1 (HIV-1) or -2 (HIV-2), Simian Immunodeficiency Virus (SIV) or Equine Infectious Anemia Virus (EIAV). In contrast to the viruses they originate from, vectors are not replication competent, since the genetic information indispensable for the assembly of progeny is not packaged within the particles. Hence, each LV is only able to transfer its genetic information into one single target cell, a process called transduction, which is distinguished from infection by replication-competent viruses.

1.1.1. Structure

Lentiviruses are enveloped viruses of approximately 100 nm in diameter. Their pseudodiploid, positive sense, single stranded RNA genome of 7 - 12 kbp (per single RNA strand) comprises three major genes named *gag*, *pol*, and *env* (5'-*gag*-*pol*-*env*-3', see Figure 1C). *Gag* codes for matrix (MA, p17), capsid (CA, p24), nucleocapsid (NC, p7), and p6 protein. Since MA, CA, and NC organize the structure of mature particles, with membrane-associated matrix proteins surrounding the core shell-forming capsid proteins, which in turn inclose viral RNA-bound nucleocapsid proteins (Figure 1B), these proteins are termed structural proteins. In contrast, p6 has no structural role, but is required for budding and release of particles. The *pol* gene includes the information for the viral enzymes protease (PR), reverse transcriptase (RT, reverse transcription of viral RNA into cDNA), and integrase (IN, integration of proviral sequences into host chromosomes). Both Gag and Gag/Pol are synthesized as polyproteins with cleavage sites of the viral protease separating all functional domains. Thereby, Pol is translated upon a programmed -1 ribosomal frameshift changing the open reading frame from *gag* to *pol* (Jacks et al., 1988), which occurs in about 5% - 10%, of translational events. The single polyprotein components are subsequently released by the action of the viral protease starting with an autocatalytic cleavage of the enzyme itself from the precursor (Louis et al., 2000). Processing of Gag and Gag/Pol takes place concomitant with or after budding. It is indispensable for particle maturation

which is accompanied by the reorganization of the spherically arranged Gag layer into a cone-shaped core and infectivity (Figure 1A) (Peng et al., 1989). However, proteolysis is not necessary for particle formation or budding of immature viral particles, which only requires Gag polyprotein assembly at the plasma membrane. Each immature virion contains approximately 5,000 Gag molecules (Briggs et al., 2004) which are membrane-anchored via the myristylated, N-terminally located matrix protein (Hearps and Jans, 2007). Interaction of matrix with the *env* encoded envelope proteins, embedded within the plasma membrane, ensures selective incorporation of the envelope proteins in the particle (Yu et al., 1992). The envelope proteins mediate the specific interaction with the cellular receptor(s) and are responsible for the subsequent pH-independent membrane fusion. Thus, they determine the host cell spectrum of the virus. In addition to the three named major genes, lentiviruses possess different accessory genes, which influence stages of the viral life cycle and pathogenesis. In HIV-1, the auxillary genes are *tat*, *rev*, *nef*, *vif*, *vpu*, and *vpr* (Li et al., 2005) (Figure 1C).
The entire lentiviral genome, including major and accessory genes, is flanked by two identical long terminal repeats (LTRs), containing the viral promoter, enhancer elements, a transcription termination sequence, a polyaldenylation signal and at their ends the attachment sites for viral integration into the host chromosome. Initiation of viral RNA genome dimerization and its encapsidation in infective particles, the so-called virions, depend on the cis-acting RNA packaging sequence Ψ, which is located between 5' LTR and the start codon of the *gag* reading frame (Lever et al., 1989; Clever and Parslow, 1997).

In contrast to lentiviruses, thereof derived lentiviral vectors are replication-incompetent and thus only able to transfer their genetic information, commonly therapeutic or marker genes, into a single transduced target cell. LVs are generated by transfecting so-called packaging cells with the genetic information indispensable for vector particle production (Figure 1C). The required genes are usually provided by three to four different plasmids (split genome approach), encoding Gag/Pol (packaging plasmid), Env (Env protein expression plasmid) and the transgene of interest (transfer vector). The packaging plasmid may additionally encode Tat and Rev, which are essential for viral transcription and nuclear export of unspliced transcripts, respectively, and are therefore indispensable for vector production (Zufferey et al., 1997). Alternatively, these proteins are provided by another expression plasmid. All other accessory genes besides *tat* and *rev* are deleted. *Gag/pol* and *env* expression is under control of strong heterologous promoters such as CMV (derived from the **c**yto**m**egalo**v**irus) or SFFV promoter (derived from the **s**pleen **f**ocus-**f**orming **v**irus) whereas the transfer vector still harbors lentiviral LTRs. Thereby, safety of current lentiviral vectors is improved by deleting parts of the 3' LTR abolishing promoter activity of the resulting self-inactivating (SIN)-LTR without affecting vector titers or transgene expression (Miyoshi et al., 1998; Zufferey et al., 1998). As only the transfer vector still harbors the packaging signal Ψ, just the transgene RNA is encapsidated into the vector particle

and transferred into transduced target cells. Ψ is deleted from packaging plasmid and Env protein expression construct(s), hampering the formation of viral progeny.

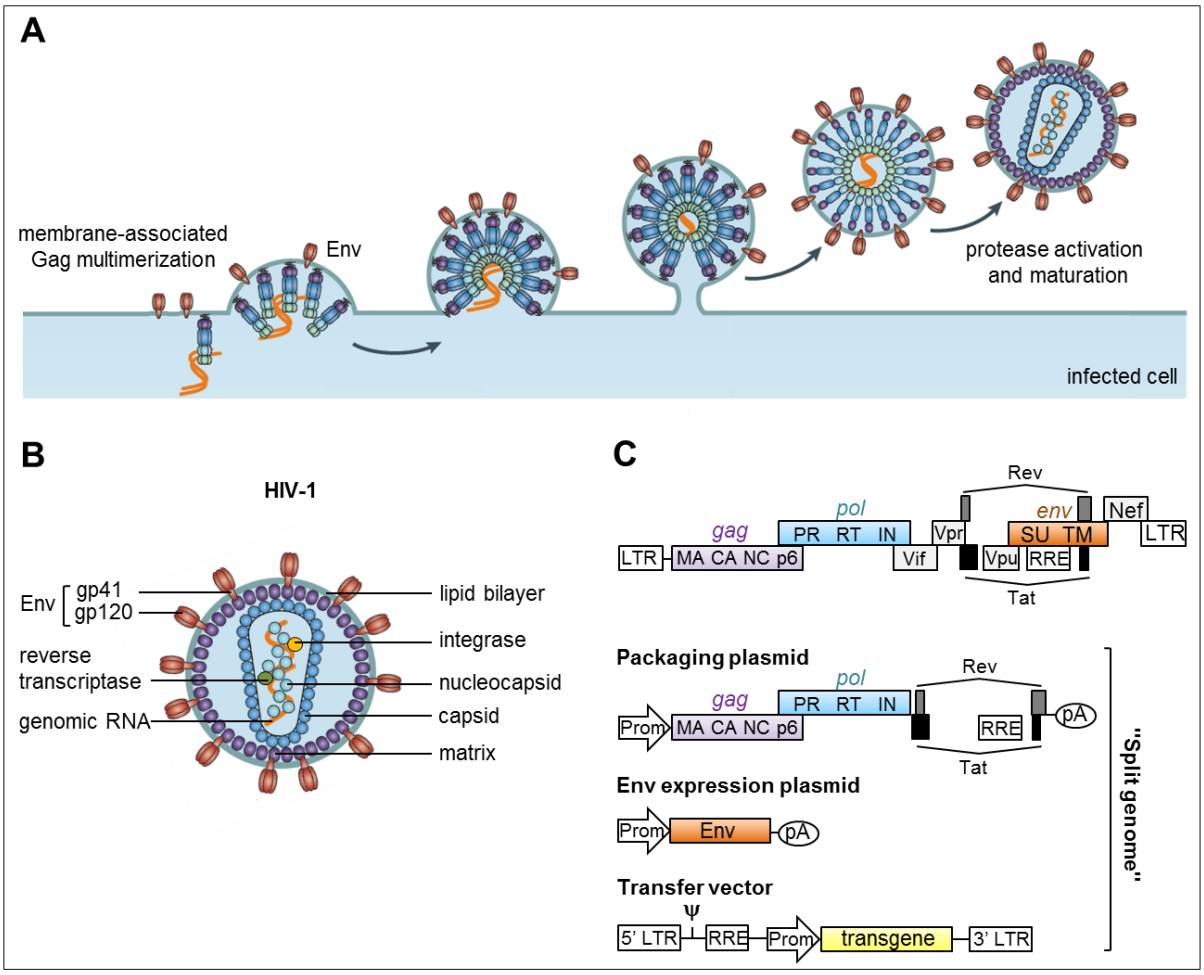

Figure 1: HIV-1 particle structure and release. (A) HIV-1 particle assembly and release. HIV-1 Gag/Pol is produced in the cytoplasm of HIV-1 infected cells, where it already starts to oligomerize and associates with genomic RNA. N-myristylation of matrix (purple) anchors Gag-RNA complexes at the plasma membrane, where Gag/Pol further multimerizes and the budding process is initialized. The interaction of matrix and envelope glycoproteins (Env) ensures incorporation of envelope proteins in the virion. Activation of the viral protease and subsequent cleavage of Gag and Gag/Pol polyproteins leads to particle maturation and gives rise to the infectious virion. **(B)** Structure of a HIV-1 virion. The viral genome, comprised of two single stranded RNAs, is bound to nucleocapsid proteins and associated with the viral enzymes integrase and reverse transcriptase. A core, composed of capsid proteins, surrounds these RNA-protein complexes. It is itself enclosed in matrix proteins, which are membrane-anchored and connected with the envelope proteins. HIV-1 envelope proteins consist of gp120, the surface unit, and transmembrane unit gp41. **(C)** Genome structure of HIV-1 and thereof derived second generation lentiviral vectors. Top: The HIV-1 genome is flanked by long terminal repeats (LTRs) and is composed of three main genes (*gag*, *pol*, and *env*) and six accessory genes (*vif*, *vpr*, *tat*, *rev*, *vpu* and *nef*). *Gag* encodes for matrix (MA), capsid (CA), nucleocapsid (NC), and p6. *Pol* comprises the information for the viral enzymes protease (PR), reverse transcriptase (RT) and integrase (IN). The envelope glycoproteins of HIV-1 are encoded by *env*. Env is cleaved into a surface unit (SU) and transmembrane domain (TM) by the host cell protease furin. Tat and Rev are involved in regulation of viral transcription and bind to the 5' LTR (Tat) or the Rev responsible element (RRE). Bottom: Second generation lentiviral vectors are produced by transfection of packaging cells with three different plasmids (split genome approach). The packaging plasmid encodes for Gag, Pol, Tat and Rev. Env is expressed by the Env expression plasmid. In both, packaging plasmid and Env expression plasmid, LTRs are replaced by a strong heterologous promoter (Prom) and a polyadenylation signal (pA). Only the transfer vector, harboring the transgene, contains Ψ and is thus packaged into vector particles. *Vif*, *vpr*, *vpu*, and *nef* are deleted. Panels A and B modified after Martin-Serrano and Neil, 2011, panel C modified after Sakuma et al., 2012.

However, the described split genome approach does not only lead to increased safety of the vectors due to the avoidance of recombination events, which may cause production of fully replicative lentiviruses. It also facilitates the manipulation of viral vectors, e.g. the exchange of the vector's own envelope proteins against heterologous ones (pseudotyping, see 1.2.1). Moreover, as only Gag is required for spontaneous self-assembly of particles (Lingappa et al., 2014), particles with different characteristics can be produced by leaving out single components of the vector. Omitting the Env encoding plasmid(s) for instance, leads to the production of "bald" particles where no envelope glycoproteins are incorporated into the membrane. Particles without a transgene are called "virus-like particles" as they closely resemble infectious viruses. They may or may not be equipped with envelope proteins.

1.1.2. Lentiviral vectors as vehicles for gene and protein transfer

Lentiviral vectors are frequently used in gene therapy or basic research for the genetic manipulation of cells. Their broad application is justified by several beneficial features, some of which are unique to LVs: (1) Stable integration of the transgene into the host chromosome guarantees a sustained gene expression (Blömer et al., 1997; Kafri et al., 1997), which is of special interest in the clinical setting aiming for long-term correction of genetic defects. LVs were shown to preferentially integrate into transcriptionally active genes (Mitchell et al., 2004), but no particular enrichment in proto-oncogenes, cancer-associated common integration sites, or growth-controlling genes was observed (Cattoglio et al., 2007), accounting for the low genotoxicity and low oncogenic potential of LVs (Montini et al., 2006). (2) Moreover, as they are able to transduce not only dividing but also non-dividing cells (Naldini et al., 1996), LVs are applicable for gene transfer into a variety of cell types, which are not accessible with other vectors. Nevertheless, a few cell types, particularly resting lymphocytes (Maurice et al., 2002; Frecha et al., 2009) or monocytes (Neil et al., 2001), proved to be rather resistant to genetic modification by conventionally used HIV-1 derived vectors like VSV-G pseudotyped LVs (VSV-LV). Commonly, productive transduction of T cells required minimal stimulation to induce entry of cells into the G_1b phase of cell cycle (Cavalieri et al., 2003) as already shown for the parental HIV-1 virus (Korin and Zack, 1998). (3) Another advantage of LVs is their high packaging capacity. An analysis systematically determining the packaging capacity of HIV-1 derived LVs revealed that there seems to be no absolute packaging limit although titers semilogarithmically decrease with the transfer vector length (Kumar et al., 2001). Generally, packaging of 8 – 10 kb heterologous DNA is considered feasible (Kumar et al., 2001; Sinn et al., 2005). Due to their high packaging capacities, LVs can transfer more than only one gene. Successful transfer of tricistronic expression cassettes has been described (Mitta et al., 2002; Ibrahimi et al., 2009). Thereby, insertion of internal ribosomal entry sites (IRES) or 2A sequences between the single open reading frames allows for the co-expression of individual proteins encoded by a single RNA. An IRES is a RNA element, which promotes internal initiation of RNA translation as it enables ribosome

binding in the absence of the 5' cap (Ngoi et al., 2004). In contrast, the small viral 2A sequences, e.g. derived from thosea asigna virus (T2A) or foot-and-mouth disease virus (F2A), mediate co-translational "cleavage" of polyproteins at their own C-termini by a ribosomal skip mechanism (Donnelly et al., 2001). (4) Last but not least, there is generally no pre-existing immunity against LVs to be expected which is important for *in vivo* applications. Moreover, LVs themselves are characterized by low immunogenicity (Abordo-Adesida et al., 2005). However, as true for all gene delivery systems, the transgene can potentially provide antigenic epitopes and therefore induce immunity (Follenzi et al., 2004).

Besides efficient transfer of foreign genes, retro- and lentiviral particles are also capable to transfer cargo proteins into transduced cells when the cargo is genetically fused to the structural proteins of the vector (Voelkel et al., 2010; Aoki et al., 2011). Thereby, these particles also enable immediate (no delay caused by *de novo* protein synthesis) and completely transient cell modification (protein degradation). Initially, HIV-1 Gag was tagged with the marker protein GFP in order to study its cellular localization (Perrin-Tricaud et al., 1999; Hermida-Matsumoto and Resh, 2000). As no adverse effects of a GFP-fusion were observed for cellular routing and localization (Perrin-Tricaud et al., 1999), fluorescently labeled Gag (MA-GFP) was later on also used to track HIV-1 particles (Müller et al., 2004; Hübner et al., 2007; Lampe et al., 2007). Recently, the approach has been shown to be highly promising also for the transfer of heterologous proteins exerting enzymatic functions, e.g. Flp recombinase or β-lactamase, by retro- and lentiviral particles (Voelkel et al., 2010; Aoki et al., 2011). Quite commonly, the cargo protein encoding sequences are inserted 3' of *matrix* (Müller et al., 2004; Voelkel et al., 2012) although fusion to the N-terminus of Gag has also been described (Aoki et al., 2011). Fusion to the N-terminally myristylated matrix results in membrane-association of the cargo protein and might be exploited, if membrane-proximity is of interest. Alternatively, engineered recognition sites for the viral protease can be introduced between cargo and structural protein to ensure free release of the heterologous protein from Gag and Gag/Pol precursors into the target cells' cytosol (Voelkel et al., 2010). A particularity for the generation of functional protein-transferring particles is the potential requirement of wild-type Gag/Pol co-assembly which is likely due to steric requirements of the cargo proteins. However, both assembly of mixed particles composed of cargo-fused and wild-type Gag/Pol (Larson et al., 2005; Voelkel et al., 2010) as well as particles made up of cargo-tagged Gag/Pol alone (Aoki et al., 2011; Voelkel et al., 2012) have been reported.

Concluding, lentiviral particles can be used as efficient vehicles for gene transfer, combined gene and protein transfer, or protein transfer alone (as virus-like particles), rendering them highly flexible tools for stable and/or transient cell modification.

1.2. Altering the vector tropism

Efforts have been made to improve safety and efficacy of LVs by restricting the vector tropism to the cell or tissue type of interest. Confining transgene expression to target cells can amongst others be achieved by the use of cell- or tissue-specific promoters (transcriptional targeting), or by introduction of microRNA target sites into vector genomes abolishing transgene expression in off-target cells or tissues ("detargeting") (Frecha et al., 2008b). However, these methods have several drawbacks, e.g. limited availability of truly cell-specific promoters and microRNAs or potential leakiness of promoters, which might cause anti-transgene immunity, if the transgene is unwantedly expressed in antigen presenting cells (Frecha et al., 2008b). Moreover, there is a need for threshold microRNA-expression levels ensuring RNA silencing, and, most importantly, broad transduction and transgene insertion in both target and non-target cells, which may be associated with a higher risk of insertional mutagenesis due to genetic alterations of more cells than required for therapy (Frecha et al., 2008b). A promising alternative is transductional targeting. This strategy is based on surface modified vectors, either incorporating heterologous glycoproteins with natural restricted tropism (pseudotyping, see 1.2.1) or engineered, ligand-displaying glycoproteins which determine the vector's specificity (see 1.2.3). Here, the modification of cells is already restricted at the stage of cell entry, thus preserving non-target cells from transduction and thereby unwanted side-effects. More details on entry targeting, used in this thesis to generate SLAM- and CD4-specific lentiviral vectors, are provided in the following sections.

1.2.1. Pseudotyping of lentiviral vectors

Cell entry of enveloped viruses and viral vectors is dependent on the interaction of viral surface proteins with the complementary cellular receptors. This interaction determines the host cell range (tropism) of the virus or vector particle. Most lentiviral vectors are derived from HIV-1. Its envelope protein complex, consisting of gp120 and gp41, interacts with CD4 (Dalgleish et al., 1984; Klatzmann et al., 1984) and commonly either one or both of the main co-receptors CXCR4 (Feng et al., 1996) or CCR5 (Alkhatib et al., 1996; Deng et al., 1996; Dragic et al., 1996). These surface proteins are found on T helper cells, dendritic cells, monocytes, macrophages, and microglia (Shieh et al., 1998; Lee et al., 1999) and thus enable HIV-1 infection of the named cell types.

In order to change the vector tropism, HIV-1 envelope proteins can be substituted by envelope glycoproteins of other viruses as first shown in 1990 by Page *et al.* using amphotropic murine leukemia virus (MLV) glycoproteins (Page et al., 1990). The process of equipping vectors with heterologous envelope glycoproteins, which then determine the vector's specificity, is called pseudotyping. Commonly used for this purpose is the G protein of the vesicular stomatitis virus (VSV-G), resulting in stable particles which can be concentrated by ultracentrifugation to high titer vector stocks (Burns et al., 1993). VSV-G binds to the widespread expressed low-density lipoprotein receptor (LDL-R) and its family members (Finkelshtein et al., 2013), accounting for the broad tropism

of VSV-G pseudotyped vectors. Due to their stability and target cell spectrum, VSV-G pseudotyped vectors are currently used as gold standard to evaluate the performance of other pseudotypes. Besides VSV-G, also a wide variety of glycoproteins derived from other enveloped viruses have been functionally incorporated into lentiviral particles (Cronin et al., 2005). Examples are the envelope proteins of ebola virus (Kobinger et al., 2001), lymphocytic choriomeningitis virus (Beyer et al., 2002), and measles virus (Frecha et al., 2008a). As expected, also here the resulting particles possessed the tissue specificity of the virus the glycoproteins originated from, e.g. a tropism for airway epithelia in case of ebola virus pseudotypes (Kobinger et al., 2001). However, pseudotyping with heterologous glycoproteins does only allow targeting of tissues or cells, if viral envelope proteins with the tropism of interest do exist, at all. Moreover, the expression of the used cellular receptor might not be restricted to the target tissue or target cell type, but also cover other tissues or cell populations, whose alteration might be not desirable. To allow highly selective transduction of distinct target cell populations, attempts have been made lately to genetically modify viral Env proteins to incorporate peptide ligands, growth factors or single-chain antibodies targeting a protein of choice (Froelich et al., 2010). Among these strategies, a targeting system based on engineered measles virus glycoproteins proved to be extraordinary promising (Funke et al., 2008) which is presented in detail in section 1.2.3.

1.2.2. Measles virus glycoproteins and their receptors

Measles virus (MV), the causative agent for the highly contagious measles disease, is a representative of the genus *Morbillivirus* within the family *Paramyxoviridae*. As all other enveloped viruses, it enters its target cells by binding to its cellular receptors followed by fusion of viral and target cell membrane. For several enveloped viruses, for instance the family *Rhabdoviridae* exemplified by the well-known vesicular stomatitis virus, one glycoprotein mediates receptor binding and membrane fusion. In contrast, receptor attachment and fusion function are separated onto two proteins in the family of *Paramyxoviridae* (Iorio et al., 2009). As its name implies, the Fusion protein F initiates the fusion of viral and cellular membranes. Receptor binding of *Paramyxoviridae* is mediated by hemagglutinin-neuraminidase (HN), hemagglutinin (H) or glycoprotein (G), which also exert fusion-helper functions (Ader et al., 2012).

H protein is a type II transmembrane glycoprotein with a molecular weight of approximately 75 kDa. It exists as tetramer formed of two disulfide-linked dimers. Each H protein possesses an amino-terminal cytoplasmic tail, a transmembrane segment, and a long, extracellular stalk region which is connected to a cuboidal head with six-blade β-propeller structure (Navaratnarajah et al., 2011) (Figure 2). The well-characterized binding sites for the MV receptors are located at one site of the β-propeller (Vongpunsawad et al., 2004; Santiago et al., 2010; Hashiguchi et al., 2011b). The second MV envelope protein, the 55 kDa F protein, is a type I glycoprotein, which assembles into trimers (Figure 2). It is synthesized as nonfusogenic F_0 precursor protein, which is activated by furin-mediated proteolytic cleavage into the disulfide-bond-linked subunits F_1 and F_2 in the Golgi apparatus (Bolt and

Pedersen, 1998). H tetramers are associated with F trimers in hetero-oligomeric complexes, which already form in the endoplasmatic reticulum (ER) (Plemper et al., 2001). The stalk region of H interacts with the globular head of the F glycoprotein (Paal et al., 2009) (Figure 2). Receptor binding of H therefore locates F at an appropriate distance to reach the target cell membrane (Buchholz et al., 1996). Moreover, receptor attachment of H leads to rearrangements in its stalk region, which in turn initiate conformational changes in F (Plemper et al., 2011; Ader et al., 2012), exposing a hydrophobic fusion peptide. Subsequent insertion of the fusion peptide into the host cell membrane and refolding of F into a highly stable six-helix-bundle drives membrane fusion. Fusion of viral and cellular membrane is pH-independent (Plemper, 2011).

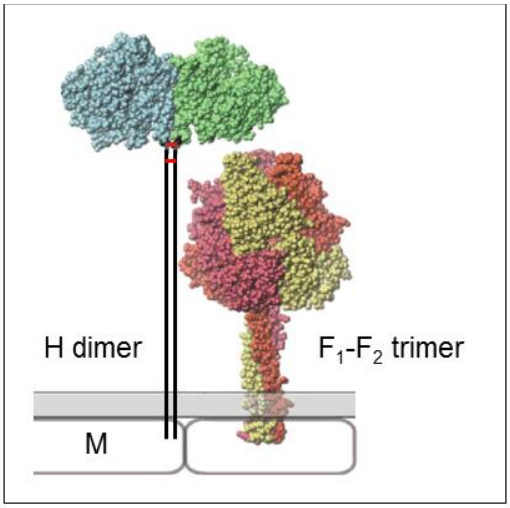

Figure 2: Schematic depiction of MV envelope proteins. Space-filling representation of the crystal structure of a MV H dimer and parainfluenza virus 5 (PIV5) F trimer. PIV5 is a paramyxovirus closely related to MV. Stalk, transmembrane domain, and cytoplasmic tail of H are depicted as vertical lines, disulfide-bonds stabilizing H dimers are indicated as red horizontal lines. Each H or F monomer, respectively, is depicted in a different color. Membrane-associated matrix proteins (M) interact with the cytoplasmic tails of H and F. Figure modified after Griffin and Oldstone, 2008.

MV can be divided into wild-type strains and vaccine strains with distinct receptor usage. Wild-type strains, like IC-B, the strain molecular clone MV_{wt323} is derived from (Takeda et al., 2000), use CD150/ Signaling Lymphocyte Activation Molecule (SLAM) as cell entry receptor (Tatsuo et al., 2000). In humans, SLAM is expressed on activated B and T cells, thymocytes, mature dendritic cells, monocytes, macrophages, and platelets (Sidorenko and Clark, 1993; Cocks et al., 1995; Kruse et al., 2001; Farina et al., 2004). Its predominant expression on immune cells explains the immune cell tropism and concomitant immunosuppressive properties of measles viruses. The extracellular domain of SLAM is composed of two immunoglobulin-like domains, V and C2 (Figure 3A). The binding site of H was mapped to the V domain (Ono et al., 2001b; Hashiguchi et al., 2011b).

Many vaccine strains are derived from an isolate from a measles patient with family name Edmonston. The blood and throat washings of the boy were used to infect primary human kidney cells and the live-attenuated MV Edmonston strain was developed by several passages in chicken eggs and chicken embryo cells (Enders and Peebles, 1954; Enders et al., 1960). In addition to SLAM, these vaccine strains and also the laboratory strains derived thereof use CD46 as cell entry receptor (Dörig et al., 1993; Naniche et al., 1993). CD46 is a type I transmembrane protein with four extracellular short consensus repeats (SCR 1-4), which is expressed on all nucleated, human cells (Hashiguchi et al.,

2011a). The protein exhibits co-factor activity for the degradation of the complement components C3b and C4b by Factor I and is thus involved in prevention of complement-mediated lysis of self-tissue. The binding site of MV H was shown to be located on SCR1 and SRC2 (Figure 3B) (Buchholz et al., 1997; Hsu et al., 1997; Casasnovas et al., 1999).

Besides SLAM and CD46, the existence of a third, epithelial cell receptor (EpR) for MV has been proposed. Epithelial cells do not express SLAM but have been shown repeatedly to be infectable by MV_{wt} *in vitro* and *in vivo* (Sakaguchi et al., 1986; Takeuchi et al., 2003; Takeda et al., 2007). Since MV infects only epithelial cell connected by the apical adhesion complex, involvement of the EpR in the formation of epithelial intracellular junctions has been assumed (Leonard, V.H.J. et al., 2008).

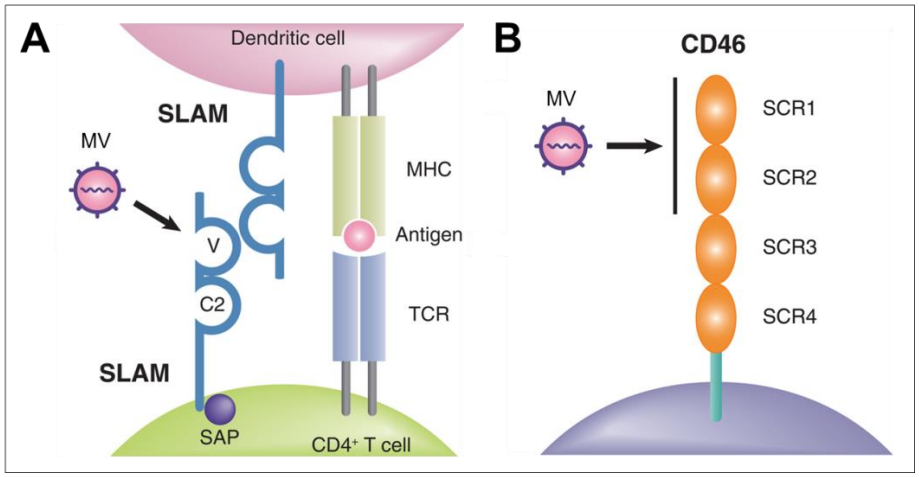

Figure 3: Measles virus receptors. (A) Schematic structure of SLAM. The ectodomain of SLAM is composed of two immunoglobulin-like domains, termed V (variable) and C2 (constant). Binding of MV wild-type, vaccine or laboratory strains has been mapped to the V domain. SAP, SLAM-associated protein; MHC, Major histocompartibility complex; TCR, T cell receptor. **(B)** Schematic structure of CD46. The N-terminal extracellular domain of CD46 consists of four short consensus repeats (SCR). MV vaccine and laboratory strains bind to SCR1 and SCR2 whereas an interaction of SCR3 and SCR4 with the complement proteins C3b and C4b is described. Figure modified after Sato et al., 2012.

1.2.3. Engineering of measles virus glycoproteins

As already mentioned, targeting approaches based on pseudotyping are restricted by the availability of viral glycoproteins with the tropism of interest and their capacity to effectively pseudotype the respective particles. This constraint prompted the development of glycoprotein engineering strategies in order to enable specific targeting of any receptor of choice. These efforts included insertion of single-chain antibodies (scFv), i.e. antigen-binding variable heavy (V_H) and light (V_L) chains of an IgG antibody, which are stably connected via a polypeptide linker (Figure 4), or growth factors in viral glycoproteins. Albeit specific binding of most ligand-displaying envelope glycoproteins to the corresponding receptors was reported, no or only inefficient transduction of target cells has been observed (Verhoeyen and Cosset, 2004). These data indicated the inability of retargeted envelope proteins to induce fusion activity upon receptor binding via the added targeting domain (Sandrin et al.,

2003) and initiated attempts to use membrane fusion protein complexes in which receptor attachment and membrane fusion functions are separated onto two glycoproteins, as for example found in MV. Indeed, in 2005 Nakamura *et al.* reported successful rescue and propagation of fully retargeted measles viruses (Nakamura et al., 2005). Here, four point mutations in the *hemagglutinin* gene, defined before to be critical for interaction with the respective receptors (Vongpunsawad et al., 2004), ablated fusion induction via the natural receptors SLAM (mutation R533A) and CD46 (mutations Y481A, S548L, and F549S). The coding sequences of one of the single-chain antibodies binding to CD38, EGFR, or EGFRvIII, respectively, were genetically fused to the C-terminus of mutated H and cloned into the MV genome. The resulting viruses were shown to specifically and efficiently interact with cells expressing the corresponding target antigens *in vitro* and *in vivo*, mediating receptor-dependent anti-tumor activity, whilst being blind for SLAM and CD46.

In 2008, Funke *et al.* successfully translated this targeting approach based on engineered MV glycoproteins (MV-GPs) into a flexible pseudotyping system for HIV-1 derived lentiviral particles (Funke et al., 2008). In addition to the mutations described by Nakamura *et al.* (Nakamura et al., 2005), efficient incorporation of genetically modified MV-GPs into LV particles required cytoplasmic truncation of H and F proteins by 18 or 30 amino acid residues, respectively. Blinded hemagglutinin was fused to a scFv binding CD20. The specificity of the resulting CD20-LV vector was demonstrated in mixed cell populations and primary human lymphocytes (Funke et al., 2008). Since this proof of principle the system has demonstrated its applicability for a broad variety of target receptors of human and murine origin, including GluR (Anliker et al., 2010), CD105 (Anliker et al., 2010; Abel et al., 2013), CD133 (Anliker et al., 2010), MHC II (Ageichik et al., 2011), CD8 (Zhou et al., 2012) and CD19 (Kneissl et al., 2013). As an alternative to scFv, also DARPins can be used as binding moieties (Münch et al., 2011).

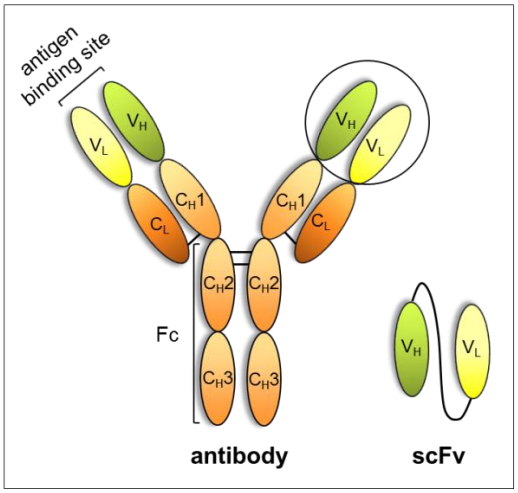

Figure 4: Schematic depiction of an antibody and a thereof derived single-chain antibody. Each IgG antibody consists of two heavy chains (H) and two light chains (L) which are connected via disulfide bonds. The variable domains of heavy and light chains (V_H and V_L, respectively) form the antigen binding site. The constant regions (C_H1-3 and C_L) are responsible for the effector functions of the antibody. A single-chain variable fragment (scFv) or single-chain antibody consists of the variable regions of heavy and light chain, connected via a linker.

DARPins, acronym for **D**esigned **A**nkyrin **R**epeat **P**rote**ins**, are synthetic proteins derived from natural ankyrin repeat (AR) proteins. AR proteins are found in bacteria, archaea, eukarya, as well as in certain

viruses, and are commonly involved in protein-protein interactions (Mosavi et al., 2004). Indeed, besides immunoglobulins they are the most abundant protein class involved in binding (Wetzel et al., 2008). They are characterized by the eponymous ankyrin repeats, which stack together to form protein domains of variable length with a continuous target-binding surface typically established by several adjacent repeats (Binz et al., 2003). Each of these repeat modules is commonly composed of 33 amino acids, which form two antiparallel helices, linked by a loop, and is connected with the following repeat unit via a β-turn (Binz et al., 2003) (Figure 5A). The resulting domains resemble a cupped hand with β-hairpin-fingers and a palm made up of α-helices (Sedgwick and Smerdon, 1999) (Figure 5B). Amino acids involved in binding are located in the ankyrin groove (Figure 5B).

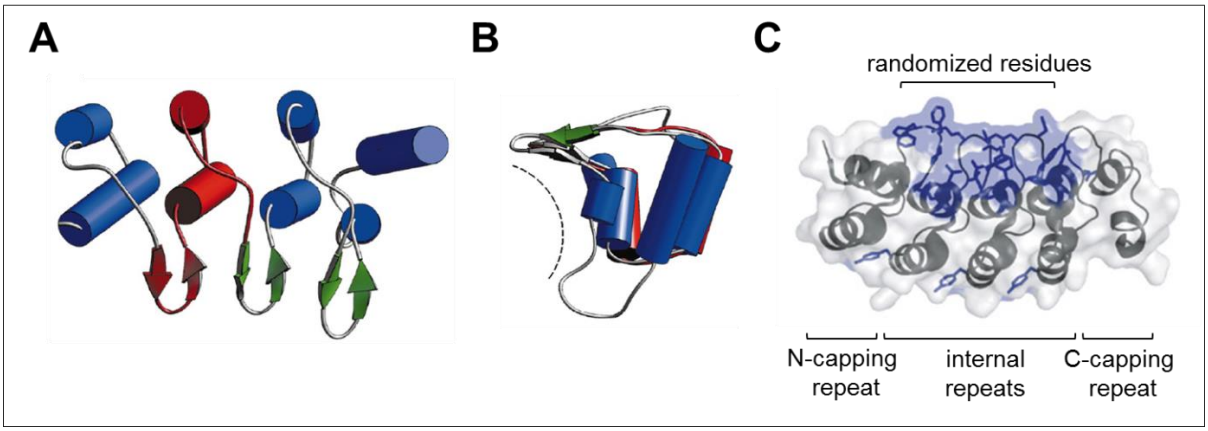

Figure 5: Schematic depiction of secondary structure elements of an ankyrin repeat domain and DARPin. **(A)** Top view of an ankyrin repeat domain. An ankyrin repeat domain is formed by several ankyrin repeats, which are composed of two α-helices (cylinders) and a β-turn (arrow), respectively. A single repeat is indicated in red. **(B)** Side view of an ankyrin repeat domain. The dotted arc indicates the ankyrin groove where residues involved in binding are located. **(C)** Three dimentional representation of a N3C DARPin. Designed ankyrin repeat proteins (DARPins) consist of an N-capping repeat, internal repeats of a freely selectable number (here three), and a C-capping repeat. Randomized residues, mediating binding to the target protein of choice, are depicted in blue. Panels A and B derived from Sedgwick and Smerdon, 1999; panel C modified after Stumpp et al., 2008.

By an *in silico* consensus design approach considering approximately 2,500 different natural AR sequences, Binz *et al*. identified a consensus sequence of an AR domain (Binz et al., 2003). 26 of the 33 amino acids building an ankyrin repeat were characterized as conserved framework residues while the remaining seven surface-exposed residues (Figure 5C) were non-conserved ones which might potentially mediate interaction with a given binding partner (Binz et al., 2003). Based on the identified consensus sequence, combinatorial DARPin libraries with defined repeat numbers were generated where non-conserved positions were randomized (Plückthun, 2015). Using these libraries, high affinity binders to a target structure of choice can be selected *in vitro* by phage display (Smith and Petrenko, 1997) or ribosome display (Hanes and Plückthun, 1997). Similar to the parental AR proteins, the resulting DARPins are composed of stacked repeat units, usually up to six, forming a hydrophobic core. This hydrophobic core is shielded by N- and C- capping ankyrin repeats (Figure 5C), which increase folding yield and prevent aggregation of DARPins (Forrer et al., 2003). Due to their structure,

DARPins show low tendency to aggregate, even when highly concentrated, and are characterized by tremendous thermodynamic stability against denaturation induced by heat or chemicals which increases with the number of repeats (from Tm = 60°C for N1C, i.e. a DARPin consisting of one full-consensus repeat and N- and C-capping repeats, to Tm > 100°C for N3C) (Wetzel et al., 2008). Moreover, they are small, e.g. 14 kDa for a N3C DARPin, which equals approximately one tenth the size of a conventional IgG antibody (Stumpp et al., 2008), bind with affinities in low nanomolar or even picomolar range (Binz et al., 2003; Steiner et al., 2008) and are cost-efficiently producible (Stumpp et al., 2008). The named features render them attractive as an alternative binding motive to single-chain antibodies.

Of particular interest for this thesis is DARPin D29.2 which interacts specifically with domain D1 of human CD4 (Schweizer et al., 2008). With a dissociation constant in the subnanomolar range (K_D = 1.49 x 10^{-9} M), D29.2 is a high affinity binder (Schweizer et al., 2008). It showed no effects on cell viability or activation, $CD4^+$ memory cell function, or CD4 receptor surface density (Schweizer et al., 2008).

1.3. Immune cells as targets for gene and immunotherapy

Bacteria, viruses, and other microorganisms are constantly dispersed in the environment. In view of this, catching an infection is rather a rare event. This is due to the presence of the immune system, which defends the body from invading pathogens. Thus, immune dysfunctions can have profound consequences for the health of respective patients, exemplified by inherited diseases such as X-SCID (X-linked severe combined immunodeficiency). X-SCID is caused by mutation of the gene encoding the interleukin (IL)-receptor common γ chain, which ablates the development of functional natural killer (NK) and T cells, the latter also entailing defects in humoral immunity (Noguchi et al., 1993). Affected persons are easily infected by microorganisms and without treatment rapidly succumb to disease. Besides inherited diseases, also pathogens targeting immune cells themselves can account for serious immune disorders. The most prominent example here is HIV-1 infection of $CD4^+$ immune cells, i.e. T cells, dendritic cells (DCs), monocytes, and macrophages, which finally results in the acquired immune deficiency syndrome (AIDS). Due to the vital function of the immune system, immune cells represent important targets for gene and immunotherapy. Thereby, specific modification of distinct immune cell subpopulations is highly desirable, e.g. genetic alteration of $CD4^+$ cells in HIV-1 infected patients. Moreover, also stimulating the immune system by prophylactic or therapeutic vaccination to recognize and destroy particular microorganisms or altered (cancerous) body cells is of great interest.

1.3.1. The adaptive immune system

In vertebrates, the immune system is comprised of two arms, namely the innate and the adaptive immunity. Innate immunity is also referred to as non-specific immunity and is the first line of defense as it detects and suppresses pathogens instantly (Medzhitov and Janeway, 2000). However, it does not confer long-term memory against invading microorganisms. In contrast, the adaptive immune system has a gradual onset over a few days but is highly specific for single pathogens and additionally provides a memory (Janeway et al., 2008). Adaptive immunity can be further divided into humoral immunity, i.e. antibody-mediated immunity, which involves B cells, and cellular immunity, dependent on (effector) T cells. Essential for the induction of adaptive immune responses are antigen presenting cells (APCs), which serve as a link between innate and adaptive immune response.

The most potent APCs known are myeloid dendritic cells (mDCs) (Gaspari and Tyring, 2008). As such, the main function of DCs is uptake, processing and presentation of antigens to T cells and their subsequent activation. Immature dendritic cells, residing in the tissues, take up extracellular antigens via receptor-mediated endocytosis, phagocytosis or macropinocytosis (Caux and Dubois, 2001). Moreover, also cytosolic pathogens, such as viruses, are processed by DCs after becoming infected, and respective antigens are presented. While taking up pathogens, DCs are activated by their pathogen recognition receptors (PRRs), such as Toll like receptors, as a response to pathogen-associated molecular patterns (PAMPs), like lipopolysaccharides (LPS) (Dearman et al., 2009), or so-called danger-associated molecular patterns (DAMPs), like cytokines released in the context of infection or extracellularly dislocated heat shock proteins (Shurin and Salter, 2009). During their subsequent maturation, DCs upregulate different surface molecules including the chemokine receptor CCR7, the dendritic-cell-specific adhesion molecule DC-SIGN, high levels of major histocompatibility complex (MHC) class II molecules as well as co-stimulatory molecules like B7.1/CD80 and B7.2/CD86 (Janeway et al., 2008). Mature dendritic cells are no longer phagocytic, but are characterized by enhanced antigen processing and presentation (Banchereau et al., 2000). These activated dendritic cells migrate into the peripheral lymphoid organs (lymph nodes, spleen, and mucosa-associated lymphoid tissues, like the Peyer's patches in the gut), where they trigger T cell responses.

Naïve T cells, i.e. T cells that have not yet encountered the antigen their T cell receptor (TCR) is specific for, roam through the lymphoid tissues, transiently bind to DCs, and test the peptides presented on the DC's surface by MHC complexes. Thereby, peptide presentation on MHC molecules is indispensable for recognition by the TCR-complexes of respective T lymphocytes (Alberts, 2002). There are two different MHC classes, namely MHC I and MHC II. MHC I molecules are expressed by all nucleated cells of the body, whereas MHC II expression is restricted to APCs. Accordingly, peptides bound to MHC I molecules are usually derived from proteasomally degraded cytosolic proteins (Rock et al., 2002) (Figure 6A). In contrast, MHC II associated peptides originate from endocytic protein uptake, i.e. from internalized extracellular proteins, or from pathogens residing intracellularly within the vesicular system (Janeway et al., 2008). Here, proteins are degraded in

acidified late endosomes by proteases, such as cathepsin S, prior loading onto MHC II molecules (Villadangos and Ploegh, 2000) (Figure 6A). However, also exogenous antigens can be presented on MHC I molecules, a process called cross-presentation or cross-priming (Bevan, 1976). Loaded MHC I complexes interact with specific TCRs and the co-receptor CD8 on $CD8^+$ T cells, while $CD4^+$ T lymphocytes specifically recognize MHC II-peptide complexes via TCR and CD4 (Coico and Sunshine, 2009) (Figure 6B). The presence of either the co-receptor CD8 or CD4 characterizes two main T cell subsets, which can be further divided into naïve, effector, and memory cells.

However, priming, i.e. initial activation and differentiation of naïve T cells into effector T cells does not only require the interaction of TCR/CD3-complex and CD4 or CD8 with the peptide-MHC complex (Figure 6B). Instead, an activated APC simultaneously needs to provide so-called "co-stimulation" to T cells, achieved by binding of co-stimulatory molecules, upregulated on activated APCs, to their respective receptors on T cells, e.g. interaction of the B7 family members CD80 or CD86 (on APCs) with CD28 (on T cells) (Janeway et al., 2008). This engagement provides a critical co-stimulus necessary for clonal expansion of T cells. Moreover, the differentiation of particularly $CD4^+$ T cells (into the subsets discussed below) is commonly influenced by cytokines, which may be seen as a third signal indispensable for development of distinct effector cell subsets (Janeway et al., 2008). Significance of co-stimulation is illustrated by functional inactivation, so-called anergy, of naïve T cells recognizing "their" antigen without receiving the appropriate co-stimulation (Schwartz, 2003).

Upon encounter of their antigen and appropriate co-stimulation, naïve T cells differentiate into effector T cells. T cells expressing the co-receptor CD8 kill degenerated or pathogen-infected cells (Barry and Bleackley, 2002) and therefore counteract tumor formation and growth or eliminate sources of new viruses or intracellular bacteria (Figure 6B). Hence, they are also termed cytotoxic T lymphocytes (CTLs). In contrast, $CD4^+$ T cells either provide additional signals for the activation or dampening of other immune cells by cell-cell contact or cytokine secretion (Beverley, 2002). $CD4^+$ T cells can be further divided into subsets with distinct functions, amongst others in T helper type 1 cells (Th1), T helper type 2 cells (Th2), T helper type 17 cells (Th17) or regulatory T cells (Treg) (Figure 6B). Th1 cells are involved in the elimination of intracellular infections, as they activate the microbiocidal functions of infected macrophages, stimulate the proliferation of $CD8^+$ cytotoxic T cells and the generation of $CD8^+$ memory cells and activate B cells to produce strongly opsonizing antibodies, i.e. antibodies that bind to the surface of pathogens to stimulate Fc receptor-mediated ingestion by phagocytes (Janeway et al., 2008; Luckheeram et al., 2012). In contrast, Th2 lymphocytes provide essential help for antibody production by B cells and activation of eosinophils and therefore the fight against extracellular pathogens (Geginat et al., 2013). Th17 cells stimulate the production of chemokines by fibroblasts, epithelial cells, and keratinocytes, leading to the recruitment of neutrophils and macrophages, which then ingest and destroy microorganisms at the site of infection (Nijkamp and

Parnham, 2011), whereas Treg cells suppress the activity of other lymphocytes and thus limit immune responses and prevent autoimmunity (Vignali et al., 2008).

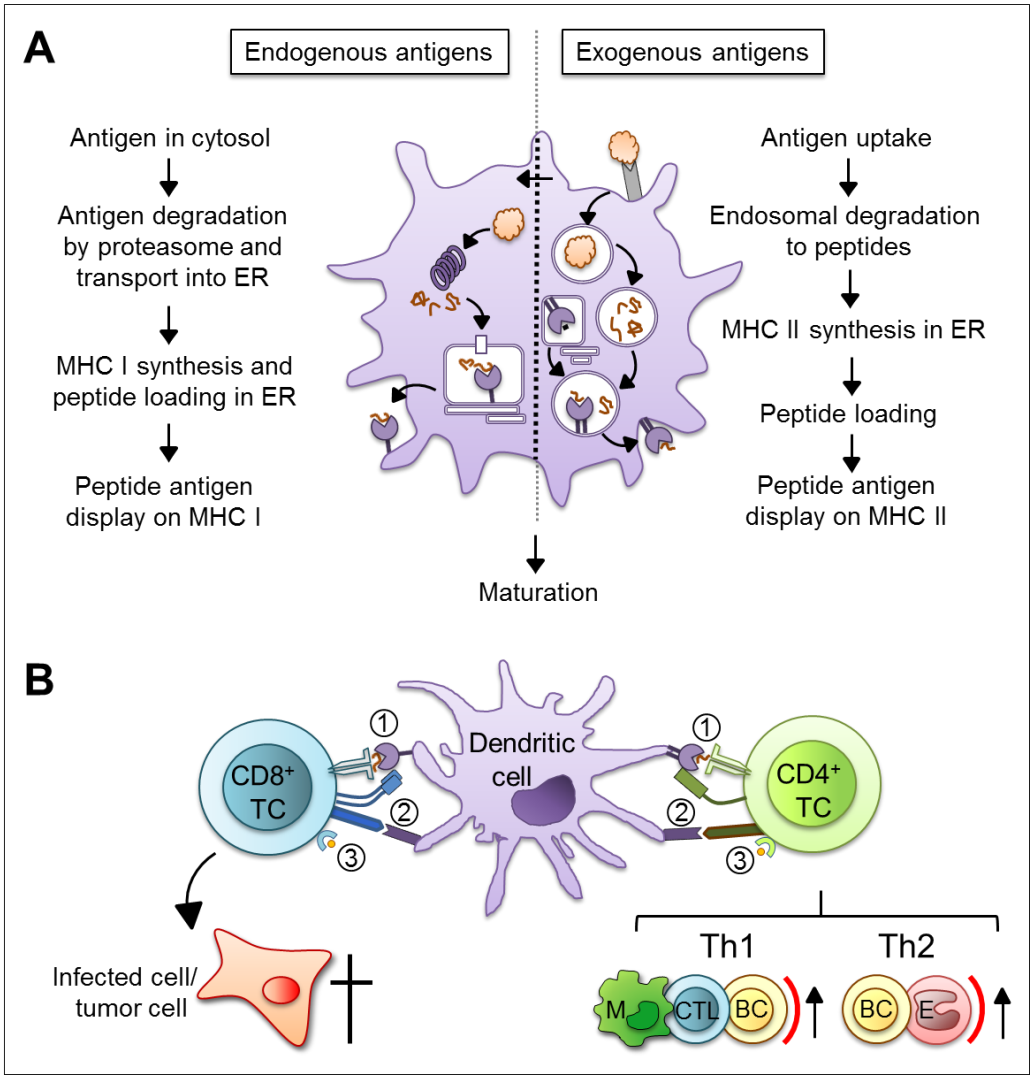

Figure 6: Antigen processing and presentation by APCs and activation of naïve T cells. (A) Antigen processing and presentation by APCs. The arrow pointing from the exogenous to the endogenous pathway indicates cross-presentation, i.e. presentation of extracellular antigen-derived peptides on MHC I molecules. ER, endoplasmatic reticulum. Panel A is modified after Beverley, P C L, 2002. **(B)** Activation of naïve T cells by mature APCs to become effector cells. Activation of naïve T cells requires three kinds of signals provided by activated APCs: (1) Interaction of antigen peptide-MHC complexes on APCs with the TCR/CD3-complex and the respective co-receptor (CD4 or CD8) on T cells. (2) Simultaneous co-stimulation of the naïve T cell by the APC, e.g. by interaction of a B7 family molecule (on APC) with CD28 (on T cell), leading to augmented proliferation and survival of the respective T cell. (3) Signal three, commonly cytokines, influences the differentiation of the naïve T cell, especially of $CD4^+$ T cells. Only T cells which have received all three signals develop into effector cells. $CD8^+$ T cells kill pathogen-infected cells or tumor cells, whereas $CD4^+$ T cells regulate the activity of other immune cells like macrophages (M), $CD8^+$ cytotoxic T cells (CTL), B cells (B) or eosinophils (E). The figure depicts only a selection of $CD4^+$ effector T cell subsets.

When the respective pathogen is cleared, long-lived, antigen-specific lymphocytes persist, so-called memory cells. They are antigen-experienced and able to quickly initiate an immune response upon re-encounter of the respective antigens. Memory T cells are characterized by the expression of several

surface molecules, which are not found in the naïve T cell population, e.g. CD45RO (Dutton et al., 1998). They can be classified into effector memory T cells (T_{EM}) with high immunomodulatory or cytotoxic potential, and central memory T cells (T_{CM}) with low immunomodulatory or cytotoxic but high proliferative potential (Sallusto et al., 1999). T_{EM} patrol through non-lymphoid organs and immediately fulfill effector functions, whereas T_{CM} roam through secondary lymphoid organs and undergo massive proliferation upon encounter of their antigens presented by activated DCs, yielding large amounts of effector cells after this amplification loop.

Besides their essential role in the activation of naïve T cells, DCs are also crucial to orchestrate the humoral immune response. As aforementioned, DCs indirectly trigger T cell-dependent B cell responses via activation of $CD4^+$ T helper cells, which provide essential stimuli for B cells to become antibody-secreting plasma cells. Furthermore, T cell help is crucial for class switching, i.e. change of antibody heavy chains, which determine the effector functions of the antibody species. Moreover, DCs can directly induce specific antibody responses by transferring unprocessed antigens to naïve B cells and additionally provide cell-bound signals to B cells for survival and class switching (Wykes et al., 1998; Wykes and MacPherson, 2000). Antibodies or immunoglobulins (Ig) are soluble forms of B cell receptors (BCRs) with the same specificity, released into extracellular space and fluids such as blood. They play a crucial role in opsonization of pathogens, complement activation (resulting in the lysis of marked pathogens) and antibody-dependent cellular cytotoxicity (i.e. killing of antibody-coated cells by cytotoxic effector cells) (Janeway et al., 2008). Besides, they are involved in neutralization of toxins and of pathogens by binding to critical areas on the pathogens' surface, thereby e.g. sterically blocking receptor binding domains necessary for viral cell entry (Janeway et al., 2008).
Similar to T_{EM} and T_{CM}, also long-lived plasma cells and B memory cells persist after the primary infection has resolved. Plasma cells, residing in bone marrow niches, produce antibodies in an antigen-independent manner, leading to constant levels of specific antibodies in blood and therefore ensure imminent protection (Radbruch et al., 2006). In contrast, B memory cells do not secrete antibodies until antigen re-encounter by their antigen-specific BCR complex. This induces their rapid differentiation into plasma cells, which subsequently produce large amounts of high-affinity antibodies, enabling strong and accelerated immune responses upon a secondary infection with the same pathogen (Plotkin et al., 2012).

Taken together, lymphocytes efficiently combat pathogens in the extracellular space by the production of antibodies and intracellularly by killing of infected cells, after initiation of antigen-specific responses by activated antigen presenting cells.

1.3.2. Immunology of vaccination

The term vaccination describes the administration of single or multiple immunogenic antigens (the so-called vaccine) into individuals to artificially induce antigen-specific adaptive immunity. Vaccination can either serve prophylactic or therapeutic purposes, i.e. aiming at disease prevention or treatment, respectively. As already described in chapter 1.3.1, adaptive immune responses are triggered by APCs, which have been activated by PRR signaling in response to PAMPs and/or DAMPs and present a processed form of the antigen on MHC complexes. Without danger signals, APCs like DCs undergo no maturation and interaction of immature DCs with naïve T cells will either induce apoptosis of T cells, T cell anergy or development of regulatory $CD4^+$ T cells (Mahnke et al., 2002). Thus, it is of utmost importance that a vaccine is composed of an antigen and, in order to induce immunity rather than tolerance, an activation signal for APCs (Kreutz et al., 2013).

Based on their ability to replicate, vaccines can be categorized into two major groups (Plotkin et al., 2012). The first group comprises live-attenuated, replicating vaccines, whereas the second group includes non-replicating vaccines, like inactivated vaccines, subunit vaccines, DNA vaccines, or recombinant vector vaccines (Clem, 2011). Live-attenuated vaccines, such as the measles vaccine (Hilleman et al., 1968), are attenuated strains of the respective pathogens, eliciting comparable cellular and humoral immune responses like the wild-type microorganism (Pulendran and Ahmed, 2011), but causing no disease, any longer. Thus, live-attenuated vaccines trigger strong, broad, and long-lasting immune responses, presumably by efficient activation of APCs following engagement of their PRRs with the vaccine's PAMPs and activation of APCs at multiple sites due to the vaccine's replication and dissemination (Plotkin et al., 2012). However, as exemplified for the Sabin polio vaccine strain (Cann et al., 1984), live-attenuated microorganisms may revert back to their pathogenic wild-type form in immunized patients. Besides, live-attenuated vaccines may still cause disease in immunocompromised individuals (Centers for Disease Control and Prevention, 1996).

There are no such safety concerns for vaccines devoid of living organisms. These vaccines are significantly less efficient in inducing immunity though they may still contain PAMPs. This is due to the lack of replication and spread in the organism, which restricts the activation of immune responses to the limited time frame of antigen persistence and the site of vaccine injection (Plotkin et al., 2012). Therefore, most dead vaccines contain adjuvants, which are defined as any substances that potentiate immunogenicity of antigens *in vivo*, by either activating APCs (immunomodulators, e.g. PAMPs), or enhancing antigen presentation (depot formulation and delivery systems, e.g. antigen-targeting to APCs) (Pashine et al., 2005; Plotkin et al., 2012). In humans, the most frequently used adjuvants are aluminum salts, such as aluminium potassium sulphate (alum). Alum, thought to act via depot formation (Petrovsky and Aguilar, 2004), preferentially induces Th2 responses. In contrast, the adjuvant AS04, composed of the considerably detoxified LPS-derivate monophosphoryl lipid A formulated on alum, favors Th1 responses (Coffman et al., 2010). Thus, different adjuvants can be

used to tailor the relevant immune reaction. Also packaging of antigen-encoding sequences or antigens into/onto liposomes or cationic polylactide co-glycolide (PLG) microparticles (O'Hagan et al., 2004; Fan et al., 2015), or presentation of antigens on the surface of virus-like particles (McBurney et al., 2007) have been shown to elicit beneficial effects on immunogenicity (adjuvanted delivery system).

However, although adjuvants improve immunogenicity of dead vaccines, these vaccines are commonly not capable to confer life-long immunity (Pulendran and Ahmed, 2011) and therefore require booster immunizations to reactivate immune memory. A prime-boost scheme of vaccination can be either homologous (readminsitration of the same vaccine) or heterologous (administration of the same antigen by different delivery systems). Thereby, it has been shown that multiple administrations of an identical vaccine can efficiently boost humoral, but hardly any cellular immunity, whereas heterologous prime-boost regimes have been demonstrated to be highly promising at boosting the latter (Woodland, 2004).

Which kind of adaptive immune responses are mainly required for success of a given vaccine depends on the respective pathogen (e.g. extracellular versus intracellular localization, etc.) and the type of intended vaccine use (prophylactic or therapeutic vaccine). Most classical vaccines are assumed to act primarily by induction of antigen-specific antibodies (Plotkin et al., 2012). However, triggering of strong $CD4^+$ T cell and $CD8^+$ CTL responses is favorable for the development of therapeutic vaccines applied to treat chronic infections and cancer (Bachmann and Jennings, 2010). DCs are the most potent inducers of T cell responses. Thus, the efficiency of a vaccine can be enhanced by targeting it to DCs (Kastenmüller et al., 2014), thereby not only inducing CTL, but also B cell responses, as both require adequate $CD4^+$ T cell help. For this purpose, DC-targeted recombinant vaccine vectors are attractive vaccine candidates. Here, an attenuated vector, e.g. a lentiviral vector (see 1.1), transfers antigen-encoding sequences of a pathogen of choice into DCs, while simultaneously stimulating DCs which recognize the PAMPs of the vector backbone. The antigen is subsequently expressed by the transduced DCs, processed, and antigenic peptides are presented on MHC I or MHC II molecules. Thereby, antigen-specific $CD4^+$ and $CD8^+$ T cells are activated and antibody production is induced. Lentiviral vectors pseudotyped with, e.g. Sindbis virus Env (targeting DC-SIGN) (Yang et al., 2008; Dai et al., 2009), measles virus Env (targeting SLAM) (Humbert et al., 2012) or engineered MV-GPs displaying a single chain antibody fragment directed against MHC II (Ageichik et al., 2011; Ciré et al., 2014) have been successfully used for DC-targeting *in vitro* and in animal models *in vivo*.

In general, the antigen delivery system accounts for the route of antigen cell entry and thus for presentation on MHC I or MHC II molecules, resulting in activation of $CD8^+$ and $CD4^+$ T cells, respectively. Cytosolic delivery results in predominant MHC I presentation, whereas endocytotic uptake favors loading onto MHC II molecules, although some antigens can also gain access to MHC I presentation by cross-presentation (Figure 6A).

However, not only vaccine type, adjuvant, vaccination schedule or route of antigen uptake, but also amount, persistence, and chemical nature of the antigen influence vaccination success. A hallmark of

vaccine-induced immunity is long-term protection, achieved by the generation of memory cells. Memory B cells are exclusively generated during T cell-dependent B cell responses, triggered by proteinaceous antigens, and not during T cell-independent responses to lipopolysaccharides, polysaccharides or polymeric proteins (Janeway et al., 2008). Moreover, whereas the linear T cell epitopes can be generated from basically any region of an antigen and their recognition by antigen peptide-specific TCRs is only further limited by MHC restriction, B cells do exclusively recognize linear or conformational epitopes located at the surface of antigens (Janeway et al., 2008). Additionally, also the antigen dose has an impact on the triggered immune responses. In general, higher doses of priming-antigen preferably induce plasma cells, whereas lower doses predominantly induce B memory cells (Plotkin et al., 2012). Similarly, also the development of Th1 (essentially induced by low antigen doses) or Th2 (essentially induced by high antigen doses) $CD4^+$ T cells is biased by antigen dose (Plotkin et al., 2012).

Concluding, vaccination is an efficient method to induce protective immunity against pathogens. However, its success and the nature of elicited immune responses are influenced by multiple parameters, including (1) the type of vaccine, (2) adjuvants, (3) vaccination schedule, (4) antigen uptake route, (5) chemical nature of the antigen and (6) antigen dose (Plotkin et al., 2012), making vaccine development a challenging endeavor.

1.4. Objectives

The aim of this thesis was the generation and characterization of entry-targeted lentiviral vectors for specific and efficient protein or gene transfer into SLAM- or CD4-positive immune cells, respectively. Both targeting approaches should be realized by pseudotyping LVs with measles virus glycoproteins, either exploiting the natural tropism of MV_{wt}-GPs or using engineered MV-GPs.

In the first part of this thesis, MV_{wt}-GP pseudotyped, SLAM-targeted lentiviral vectors should be generated to mediate protein transfer into SLAM-expressing APCs, such as DCs, and their potential to induce antigen-specific vaccination responses should be assessed. In order to define the entirety of MV_{wt}-LV target cells, the postulated but hitherto unknown epithelial MV receptor had to be initially identified. Since myeloid cells like DCs are described as somewhat resistant to genetic modification by LVs (Pion et al., 2006), it was hypothesized that antigen protein transfer might be an attractive alternative to circumvent post-entry blocks to gene transfer, furthermore avoiding its potentially genotoxic effects. Protein transfer should be achieved by fusion of cargo protein encoding sequences to *matrix* as already described for HIV-1-derived or retroviral vectors (Müller et al., 2004; Voelkel et al., 2010). For that purpose, an optimal protocol to generate protein transfer vectors (PTVs) had to be established. Next, the suitability of MV_{wt}-GPs pseudotyped PVTs to mediate SLAM-specific cytoplasmic protein transfer should be analyzed by GFP, Cre, and Ova protein transfer into receptor

transgenic (indicator) or naturally SLAM-expressing cell lines. The potential of PTVs to induce model antigen (Ova)-specific cellular immune responses should be determined in co-cultures of *ex vivo* transduced myeloid dendritic cells and Ova-specific primary T cells before *in vivo* applicability of Ova-PTVs as vaccines should be assessed in huSLAM-knock in mice.

In the second part of the present thesis, a CD4-specific lentiviral vector should be generated based on the highly flexible targeting system introduced by Funke *et al*. (Funke et al., 2008). Here, the CD4-specific DARPin 29.2 served as binding domain fused to mutated H. First of all, the specificity of CD4-LV should be determined on receptor-positive and -negative cell lines and primary peripheral blood mononuclear cells (PBMC). Special focus was given to the potential of CD4-LV to transduce also resting $CD4^+$ T lymphocytes, which are described to be particularly resistant to gene transfer by commonly used VSV-LV (Maurice et al., 2002; Frecha et al., 2009). Moreover, it should be determined whether transduction success is restricted to $CD4^+$ lymphoid immune cells or also extends to CD4-expressing cells of the myeloid lineage. This question was tackled for macrophages.
Finally, in case of highly CD4-specific and efficient transduction, the potential of CD4-LV to mediate *in vivo* gene transfer upon systemic administration should be evaluated. Therefore, a humanized mouse model had to be established in our working group. Biodistribution of CD4-LV should be assessed by *in vivo* imaging, whereas cell-specificity had to be confirmed by flow cytometry.

Both SLAM-targeted PTVs and CD4-LV generated in this thesis will be powerful tools for various applications in basic research and gene and immunotherapy, relying on the specific modification of SLAM- and CD4-positive immune cell subtypes, respectively.

2. Material and Methods

2.1. Material

2.1.1. Chemicals

Table 1: List of used chemicals.

Name	Source of supply
2-Log DNA Ladder	New England Biolabs
2-Mercaptoethanol	Sigma-Aldrich
Acetic acid	Carl Roth
Acrylamide/ Bis-Acrylamide solution (Rotiphorese® Gel 30)	Carl Roth
Agarose (electrophoresis grade)	Biozym
Ammonium persulfate (APS)	Carl Roth
Ampicillin	Serva
Bovine serum albumin fraction V (BSA)	AppliChem
Bromophenol blue	Sigma-Aldrich
Citric acid	Fluka
Deoxyribonucleotide Mix (10 mM each)	5Prime
Dimethylsulfoxide (DMSO)	Calbiochem, Merck Millipore
Dithiothreitol (DTT)	Sigma-Aldrich
D-Luciferin Potassium Salt	Caliper
D(+)-Saccharose	Carl Roth
Ethidium bromide (10 mg/ml)	Sigma-Aldrich
Ethylenediaminetetraacetic acid (EDTA, 1 M)	Paul-Ehrlich-Institut
Fetal calf serum (FCS)	PAA and Biochrome (standard cell culture) Sigma (dendritic cell culture)
Geneticin (G418)	Gibco, Life Technologies
Glutaraldehyde	Sigma-Aldrich
Glycerin	AppliChem
Glycine	Merck
HCl	Carl Roth
HEPES (1 M, pH 7.4)	Paul-Ehrlich-Institut
Histopaque® -1077	Sigma-Aldrich
Horse serum	Gibco, Life Technologies
L-Glutamine	Biochrom, Merck Millipore
Lipofectamine® 2000	Invitrogen, Life Technologies
Lipopolysaccaride	Sigma
Lysing Buffer (BD Pharm Lyse™)	BD Biosciences
Milk powder	Carl Roth
NaOH	Carl Roth
N,N,N',N'-Tetramethylethylendiamin (TEMED)	Carl Roth
Non-essential amino acids (NEA)	Biochrom, Merck Millipore
NP-40	Biochemika
Paraformaldehyde	Merck
Penicillin-streptomycin solution	Paul-Ehrlich-Institut

Name	Source of supply
Polyethyleneimine (PEI), branched, 25 kDa	Sigma-Aldrich
Potassium chloride	Carl Roth
Precision Plus Protein™ Kaleidoscope™ Standard	Bio-Rad
Protamine sulfate	Sigma-Aldrich
Protease Inhibitor Cocktail complete	Roche
Restore™ PLUS Western Blot Stripping Buffer	Thermo Scientific
Sodium azide	Merck
Sodium carbonate	Merck
Sodium chloride	Carl Roth
Sodium dodecyl sulfate (SDS), 10% solution	Paul-Ehrlich-Institut
Sodium hydrogen carbonate	Biochrom (cell culture) or Merck
Sodium pyruvate	Sigma-Aldrich
TMB ELISA Substrate	BD Biosciences or eBioscience
Tris(hydroxymethyl)aminomethane (Tris)	Carl Roth
Triton® X-100	Serva
Trypan Blue Solution	Sigma-Aldrich
Tween® 20	Carl Roth
Ultrapure Water	Paul-Ehrlich-Institut
Urea	Carl Roth
Western Blotting Substrate (Pierce® ECL 2)	Thermo Scientific
Western Blotting Substrate (Amersham™ ECL™ Prime)	GE Healthcare

2.1.2. Consumables

Table 2: List of used consumables.

Name	Source of supply
Amersham Hybond™-P PVDF Membrane	GE Healthcare
Blood collection tubes (Microtainer lithium-heparin tubes)	Becton Dickinson
Blood collection tubes (Coagulation 9NC/10ml Monovette®, citrate)	Sarstedt
C-Chip Hemocytometer	Digital Bio
Cell culture dishes (15 cm)	TPP
Cell culture multidish plates (96-well, 48-well, 24-well, 12-well, 6-well)	Nunc
Cell scraper	TPP
Cell star® cell culture flasks (T25, T75, T175)	Greiner Bio-One
Cell star® tubes (15 ml, 50 ml)	Greiner Bio-One
Cell strainer (70 µm)	BD Biosciences
Centrifuge tubes (225 ml)	Corning Life Sciences
Chemiluminescence detection film (Amersham Hyperfilm™)	GE Healthcare
Combitips (10 ml)	Eppendorf
Cryo-tubes (Cryo.s ™, 2 ml)	Greiner Bio-One
ELISpot Foil (Eli.Foil)	A.EL.VIS
ELISpot MultiScreen®-IP Filtration Plate	Merck Millipore
Flow cytometry round-bottom tubes (5 ml)	BD Biosciences
Flow cytometry U-bottom tubes (1.4 ml)	Micronic
Insulin syringe (30 G)	B. Braun
LS Columns for MACS Separation	Miltenyi Biotec

Name	Source of supply
Microtubes (low binding, 1.5 ml)	Axygen
Minisart® syringe filter (0.45 µm, 0.2 µm)	Sartorius
Omnifix® disposable syringe (1 ml, 2 ml, 5 ml)	B. Braun
Pasteur pipette glass (150 mm)	VWR International
Pipette tips (10 µl)	Eppendorf
Pipette tips (100 µl, 1000 µl)	Sarstedt
Pipette filter tips (10 µl, 100 µl, 1000 µl)	4titude
Reaction tube (1.5 ml, 2 ml)	Sarstedt
Reagent reservoir (50 ml)	Corning Life Sciences
Serological pipettes, sterile (2 ml, 5 ml, 10 ml, 25 ml)	Greiner Bio-One
Sterican ® disposable cannulas (20 G, 25 G, 30 G)	B. Braun
Stericup ® & Steritop ™ vacuum-driven filtration systems (0.45 µm, 0.2 µm)	Millipore
Tissue	Tork
Ultracentrifuge tubes (36 ml)	Beckmann Coulter
Western Blotting Filter Paper	Bio-Rad

2.1.3. Instruments and software

Table 3: List of used instruments.

Name	Type	Manufacturer
Cell separator	AutoMACS Pro	Miltenyi Biotec
Centrifuge	Heraeus Pico 17 Centrifuge Heraeus Multifuge 3SR+ Avanti® J-26 XP Centrifuge	Thermo Scientific Thermo Scientific Beckman Coulter
Cryo freezing container	Qualifreeze	Qualilab®
Ear punch pliers	KN 293	Bioscape
ELISpot Punching Tool	Eli.Punch	A.EL.VIS
ELISpot Scanner	Eli.Scan	A.EL.VIS
Exposure cassette	BioMax	Kodak
Film processor	Curix 60	Agfa
Flow cytometer	LSRII	Becton Dickinson
Fluorescence microscope and camera	Axiovert 200 with AxioCam	Carl Zeiss
Gel documentation station	UVstar	Biometra
Gel-electrophoresis chamber ▪ Agarose gels ▪ SDS-PAGE	 DNA Sub Cell™ Mini-Protean® Tetra System	 Bio-Rad Bio-Rad
Incubator	BBD 6220	Heraeus
Incubator Shaker	Innova 4000/ 4200/ 4230	New Brunswick Scientific
In vivo bioluminescence detection and gas anesthesia system	Ivis Spectrum XGI-8 Gas Anesthesia System	Caliper, Perkin Elmer
Isoflurane anesthesia unit Vaporizer	Matrx™ VMR VIP 3000	Midmark
Laminar Flow Cabinet ▪ Cell culture ▪ Bacteria culture	 SterilGARD® III Advance HLB 2448 BS	 The Baker Company Heraeus
Laser Scanning Microscope	LSM 7 Live	Carl Zeiss
Magnetic stirrer	RCT basic	IKA

Name	Type	Manufacturer
Microplate reader	SpectraMax 340PC	Molecular Devices
Microplate washer	ELx405	Bio-Tek
Microscope	Axiovert 25	Carl Zeiss
pH electrode	inoLAb	WTW
Pipettes	Reference	Eppendorf
Pipetting Aid	Accu-jet®	Brand
Platform Shaker	Polymax 2040	Heidolph
Power supply unit	Power Pac 200 Standard Power Pack P25	Bio-Rad Biometra
Roller mixer	SRT6	Stuart®
Scales	LP 4200 S	Sartorius
Semi-dry blotter	Trans-Blot® SD Semi-Dry Transfer Cell	Bio-Rad
Stepper	Multipette® plus	Eppendorf
Thermocycler	DNA Engine® PTC 200	Bio-Rad MJ Research
Thermomixer	ThermoStat plus	Eppendorf
Transmission electron microscope	EM109	Carl Zeiss
Ultracentrifuge and rotor	Optima™ L-70K Ultracentrifuge and rotor SW28	Beckman Coulter
UV-VIS spectrophotometer	NanoDrop 2000c	peQlab Biotechnologie GmbH
Vacuum pump	VacuSafe comfort	IBS Integra Biosciences
Vortex mixer	Vortex Genie2™	Bender & Hobein

Table 4: List of used software.

Name	Version	Manufacturer
Axio Vision	4.8	Carl Zeiss
BD FACSDiva	6.1.3	Becton Dickinson
Citavi	4.4.0.28	Swiss Academic Software
Eli.Analyse	5.0	A.EL.VIS
FCS Express	4	De Novo Software
GraphPad Prism	5.4	Graph Pad Software
Living Image	4.2	Caliper, Perkin Elmer
Microsoft Office	2010	Microsoft®
Vector NTI	9	InforMax
ZEN microscope software (LSM)	ZEN black 2012	Carl Zeiss

2.1.4. Buffers, solutions and media

Table 5: List of used buffers and solutions.

Name	Composition
Ammonim chloride buffer	0.86% (w/v) NH_4Cl H_20

Name	Composition
Citric acid buffer	40 mM citcic acid 135 mM NaCl 10 mM KCl H_20 adjust pH of 3.0 with NaOH
DNA Loading buffer (6x)	10% (v/v) Glycerin 20% (v/v) 6x Gel Loading Dye, blue (by NEB) H_20
ELISA Blocking Buffer	10% (v/v) Fetal Calf Serum PBS w/o Ca^{2+}/Mg^{2+}
ELISA/ ELISpot Wash Buffer	0.05% (v/v) Tween 20 PBS w/o Ca^{2+}/Mg^{2+}
FACS-wash	2 % (v/v) Fetal Calf Serum 0.1% (v/v) NaN_3 PBS w/o Ca^{2+}/Mg^{2+}
FACS-fix	1% (w/v) paraformaldehyde PBS w/o Ca^{2+}/Mg^{2+}
MACS Buffer	2 mM EDTA 0.5% (w/v) BSA PBS w/o Ca^{2+}/Mg^{2+} pH 7.2
Phosphate buffered saline (PBS) w/o Ca^{2+}/Mg^{2+}	137 mM NaCl 2.7 mM KCl 8.1 mM Na_2HPO_4 1.47 mM KH_2PO_4 adjust pH of 7.1 with HCl
Red Blood Cell Lysis Buffer	155 mM NH_4Cl 10 mM Tris H_20 adjust pH of 7.5 with HCl
RIPA buffer	50 mM Tris-HCl pH 8.0 150 mM NaCl 1% (w/v) NP-40 0.5% (w/v) Sodium Desoxycholate 0.1% SDS H_20 Supplemented with Roche Protease Inhibitor Cocktail Complete before usage
SDS running buffer	25 mM Tris 200 mM Glycine 1% (w/v) SDS H_2O
Sucrose 20%	20% (w/v) Sucrose PBS w/o Ca^{2+}/Mg^{2+}
TAE buffer	40 mM Tris 20 mM Acetic acid 1 mM EDTA H_20

Name	Composition
TBS-T buffer	50 mM Tris 150 mM NaCl H_20 adjust pH of 7.4 with HCl 0.1% (v/v) Tween 20
Triton® X-100 lysis buffer (10x)	5% (v/v) Triton® X-100 PBS w/o Ca^{2+}/Mg^{2+}
Urea sample buffer (2x)	200 mM Tris-HCL pH 6.8 8 M Urea 5% (w/v) SDS 0.1 mM EDTA 0.03% (w/v) Bromophenol blue 1.5% (w/v) DTT
Western Blot Blocking Buffer	5% milk powder (w/v) or horse serum (v/v) TBS-T
Western Blot Blotting buffer	60 mM Tris 40 mM Glycerin 20% (v/v) Methanol H_2O

Table 6: List of used media.

Name	Composition
Dendritic cell culture medium	RPMI-1640 10% (v/v) Fetal Calf Serum 2 mM L-Glutamine 1% (v/v) Penicillin-streptomycin stock solution 10 mM HEPES 1 mM Sodium Pyruvate 0.1 mM 2-Mercaptoethanol
Dulbecco's Modified Eagle Medium (DMEM)	obtained from Lonza, supplemented with 10% FCS and 2 mM L-Glutamine before use
Eagle's Minimum Essential Medium (EMEM)	obtained from Invitrogen, Life technologies supplemented with 10% FCS and 2 mM L-Glutamine before use
Freezing Medium	90% (v/v) FCS 10% (v/v) DMSO
Lysogeny broth (LB)-ampicillin Agar	4% (w/v) LB-Agar 100 µg/ml ampicillin H_2O
Lysogeny broth (LB)-ampicillin X-gal Agar	4% (w/v) LB-Agar 100 µg/ml ampicillin 0.009% (w/v) X-Gal 2 mM IPTG H_2O
Lysogeny broth (LB) Medium	1% (w/v) Tryptone 0.5% (w/v) Yeast extract 1% (w/v) NaCl H_2O pH 7.0

Name	Composition
Opti-MEM® (1x) + GlutaMAX™	Gibco, Life Technologies
Macrophage medium	RPMI-1640 10% (v/v) Fetal Calf Serum 2 mM L-Glutamine 1% (v/v) Penicillin-streptomycin stock solution 10 mM HEPES 0.25 mM 2-Mercaptoethanol
McCoy's 5A modified medium	obtained from Biochrom, Merck Millipore supplemented with 10% FCS and 2 mM L-Glutamine before use
MEM-α	obtained from Life technologies, supplemented with 20% (v/v) Fetal Calf Serum, 2 mM L-Glutamine, 1 mM Sodium Pyruvate and 5 ng/ml GM-CSF before use
Roswell Park Memorial Institute (RPMI) 1640 Medium	obtained from Biowest, supplemented with 10% FCS and 2 mM L-Glutamine before use
S.O.C.-Medium	2% (w/v) Tryptone 0.5% (w/v) Yeast extract 8.6 mM NaCl 2.5 mM KCl 10 mM $MgCl_2$ 20 mM Glucose H_2O pH 7.0
T cell culture medium	RPMI-1640 10% (v/v) Fetal Calf Serum 2 mM L-Glutamine 0.4% (v/v) Penicillin-streptomycin stock solution 25 mM HEPES (pH 7.4) freshly supplemented with 100 IU/ml IL-2 for activated T cells (but not for resting PBMC)

2.1.5. Antibodies

Table 7: List of used antibodies.

Name	Clone	Application	Dilution/ Concentration[a]	Source of supply
FcR Blocking Reagent (human FcR Block)		Flow cytometry	1:100	Miltenyi Biotec
Purified rat anti-mouse CD16/CD32 (mouse FcR Block)	2.4G2	Flow cytometry	1:100	BD Biosciences
Purified NA/LE mouse anti-human CD3	UCT1	Coating	1 µg/ml or 3 µg/ml	BD Biosciences
Purified NA/LE mouse anti-human CD28	CD28.2	Coating	1 µg/ml or 3 µg/ml	BD Biosciences
mouse IgG1, κ Isotype Control/pure	X40	Flow cytometry	1:50	BD Biosciences

Name	Clone	Application	Dilution/ Concentration[a]	Source of supply
mouse IgG1, κ Isotype Control/ APC/ Pacific Blue™/ PE	MOPC-21	Flow cytometry	1:100	BD Biosciences
mouse IgG2a, κ Isotype Control/ Pacific Blue ™	G155-178	Flow cytometry	1:100	BD Biosciences
rat anti-mouse IgG1/ APC	A85-1	Flow cytometry	1:100	BD Biosciences
rat IgG2b, κ Isotype Control/ FITC	A95-1	Flow cytometry	1:100	BD Biosciences
mouse anti-human CD3/ APC/ Pacific Blue ™	UCHT1	Flow cytometry	1:100	BD Biosciences
mouse anti-human CD4/ APC/ PE	RPA-T4	Flow cytometry	1:100	BD Biosciences
mouse anti-human CD8/ APC/ Pacific Blue ™	RPA-T8	Flow cytometry	1:100	BD Biosciences
mouse anti-human CD14/ Pacific Blue ™	M5E2	Flow cytometry	1:100	BD Biosciences
mouse anti-human CD25/ PE	M-A251	Flow cytometry	1:100	BD Biosciences
mouse anti-human CD45/ PE	HI30	Flow cytometry	1:100	BD Biosciences
mouse anti-human Nectin-1/pure	R1.302	Flow cytometry	1:32	M. Lopez (Cocchi et al., 1998)
mouse anti-human Nectin-2/pure	R2.477	Flow cytometry	1:67	M. Lopez (Lopez et al., 1998)
mouse anti-human PVR/pure	PV.404	Flow cytometry	1:220	M. Lopez (Lopez et al., 1998)
mouse anti-human Nectin-4/pure	N.4.40	Flow cytometry	1:200	M. Lopez (Fabre et al., 2002)
mouse anti-human PVR4	-	Flow cytometry	1:1,000	LifeSpan BioSciences
armenian hamster anti-mouse CD11c/ APC	HL3	Flow cytometry	1:500	BD Biosciences
rat anti-mouse CD45/ FITC	30-F11	Flow cytometry	1:100	BD Biosciences
armenian hamster anti-mouse CD69/ PE-Cy7	H1.2F3	Flow cytometry	1:100	BioLegend
rat anti-mouse CD86/ Pacific Blue ™	GL-1	Flow cytometry	1:100	BioLegend
anti-His/ PE	GG11-8F3.5.1	Flow cytometry	1:11	Miltenyi Biotec
rabbit anti human Ron/MST1R/pure	EP1132Y	Flow cytometry	1:20	Abcam
goat anti-mouse Ig/PE	polyclonal	Flow cytometry	1:50	BD Biosciences
rabbit anti-Cre	polyclonal	Western Blot	1:20,000	Novagen
rabbit anti-chicken ovalbumin	polyclonal	Western Blot	1:40,000	Novus Biologicals

Name	Clone	Application	Dilution/ Concentration[a]	Source of supply
rabbit anti-GFP	polyclonal	Western Blot	1:2,000	Life technologies
rabbit anti-H [H606]	polyclonal	Western Blot	1:2,000	Eurogentec
mouse anti-HIV-1 p24	38/8.7.47	Western Blot	1:1,000	ZeptoMetrix
rabbit anti-F [F1034]	polyclonal	Western Blot	1:4,000	Eurogentec
mouse anti-α Tubulin	B-5-1-2	Western Blot	1:50,000	Sigma-Aldrich
donkey anti-rabbit IgG (H&L)/HRP	polyclonal	Western Blot	1:10,000	Rockland
rabbit anti-mouse IgG+A+M (H&L)/HRP	polyclonal	Western Blot	1:10,000	Invitrogen, Life technologies

[a] Isotype controls were applied in the same concentration as the respective antibody.

2.1.6. Recombinant proteins and peptides

Table 8: List of used recombinant proteins and peptides.

Name	Source of supply
Antigens	
Concanavalin A	Sigma-Aldrich
Ovalbumin	S. Schülke, Paul-Ehrlich-Institut (Schülke et al., 2010)
$Ova_{257-264}$ (SIINFEKL)	InvivoGen
$Ova_{323-339}$ (ISQAVHAAHAEINEAGR)	InvivoGen
Cytokines	
human Interleukin-2	Roche or R&D
Mouse GM-CSF	R&D
Enzymes	
KOD Hot Start Polymerase	Merck Millipore
Restriction endonucleases	New England Biolabs
Taq DNA polymerase	5Prime
T4-Ligase (Rapid ligation Kit)	Roche
Trypsin 2.5% (Sigma)	Paul-Ehrlich-Institut
Inhibitors	
Fusion Inhibiting Peptide (FIP, 2-D-Phe-Phe-Gly-OH)	Bachem

2.1.7. Plasmids

Table 9: List of used plasmids.

Name	Characterization	Origin
pcDNA3.gpGFP.4xCTE	HIV-1 MA-GFP packaging plasmid	A. Schambach, MH Hannover
pCG-1	empty eukaryotic expression plasmid	R. Cattaneo, Mayo Clinic (Cathomen et al., 1995)

Name	Characterization	Origin
pCG-FcΔ30	encodes MV_{NSe} F with a truncated cytoplasmic tail of 30 amino acids under control of the CMV promoter	A. Maisner, Phillips-Universität Marburg (Moll et al., 2002)
pCG-Fwt323Δ30	encodes MV_{wt} F with a truncated cytoplasmic tail of 30 amino acids under control of the CMV promoter	S. Kneissl, Paul-Ehrlich-Institut (Funke et al., 2009)
pCG-H-αCD4	encodes MV_{NSe} H with the four point mutations Y481A, R533A, S548L and F549S, a truncated cytoplasmic tail of 18 amino acids and the CD4-specific DARPin 29.2 fused to its C-terminus	C. Osterburg, Paul-Ehrlich-Institut
pCG-Hwt323Δ18	encodes MV_{wt} H with a truncated cytoplasmic tail of 18 amino acids under control of the CMV promoter	S. Kneissl, Paul-Ehrlich-Institut (Funke et al., 2009)
pcHIV1_MA_P_Cre	HIV-1 MA-Cre packaging plasmid, with HIV-1 protease recognition site between MA and Cre	J. Reusch, Paul-Ehrlich-Institut (Reusch, 2013)
pcHIV1_MA_P_GFP	HIV-1 MA-GFP packaging plasmid, with HIV-1 protease recognition site between MA and GFP	generated within this thesis
pcHIV1_MA_P_Ova	HIV-1 MA-Ova packaging plasmid, with HIV-1 protease recognition site between MA and Ova	generated within this thesis
pCMVΔR8.9	HIV-1 packaging plasmid	U. Blömer, University Hospital Kiel (Zufferey et al., 1997)
pET15b-Ova	expression plasmid coding for ovalbumin	S. Schülke, Paul-Ehrlich-Institut (Schülke et al., 2010)
pS-luc2-GFP-W	HIV-1 packagable vector encoding firefly luciferase and sfGFP under control of the SFFV promoter	T. Abel, Paul-Ehrlich-Institut (Abel et al., 2013)
pSEW	HIV-1 packagable vector encoding GFP under control of the SFFV promoter	M. Gretz, Georg-Speyer-Haus (Demaison et al., 2002)
pSEW-Cre	HIV-1 packagable vector encoding Cre recombinase under control of the SFFV promoter	J. Bryzna, Paul-Ehrlich-Institut (Anliker et al., 2010)
pSEW-TurboFP635	HIV-1 packagable vector encoding the red-fluorescing Katushka protein under control of the SFFV promoter	T. Abel, Paul-Ehrlich-Institut (Bach et al., 2013)
pMD.G2	encodes VSV-G	D. Trono, École Polytechnique Fédérale De Lausanne

2.1.8. Oligonucleotides

Table 10: List of used oligonucleotides.

Name	Sequence 5'→ 3'[a]
CA-Prot-Ova(-)	GCACTATAGGGTAATTTTGGCTGACGCCCCCAGGGGAAACACATCTGCCAAA GAAGAG

HIVgag-BaeI(-)	GCTGAAAACATGGGTATCACTTCTGG
HIVgag-ClaI(+)	CGGGGGAGAATTAGATCGATGGG
MA-Prot(-)	ATTCTGGACGATGGGGTAGTTCTGGGACACCTGATTGCTGTGTCCTGTGTCAG CTGC
MA-Prot-GFP(+)	CAGGACACAGCAATCAGGTGTCCCAGAACTACCCCATCGTCCAGAATGGCGG GATGGTGAGCAAGGGCGAGG
MA-Prot-Ova(+)	CAGGACACAGCAATCAGGTGTCCCAGAACTACCCCATCGTCCAGAATGGCGG GATGGGCTCCATCGGCGCAG
Prot-CA(+)	GGGGGCGTCAGCCAAAATTACCCTATAGTGC

[a] Nucleotides encoding the HIV-1 protease motif (amino-acid sequence VSQNY↓PIVQN) are underlined.

2.1.9. Kits

Table 11: List of used kits.

Name	Source of supply
BD OptEIA™ Set Mouse IL-2	BD Biosciences
BD OptEIA™ Set Mouse IFN-γ	BD Biosciences
Chicken Egg Ovalbumin ELISA Kit	Alpha Diagnostic International
CD4 MicroBeads, human	Miltenyi Biotec
$CD4^+$ T Cell Isolation Kit II, mouse	Miltenyi Biotec
$CD8a^+$ T Cell Isolation Kit, mouse	Miltenyi Biotec
EndoFree® Plasmid Maxi Kit	Qiagen
Expand High Fidelity^{PLUS} PCR System	Roche
Geneclean ® Turbo Kit	MP Biomedicals
HIV-1 p24 Antigen ELISA	Gentaur
Jetstar 2.0 Endotoxin-free Plasmid Giga Kit	Genomed
Mouse IFN gamma ELISPOT Ready-Set-Go!®	eBioscience
Pan T Cell Isolation Kit II, mouse	Miltenyi Biotec
QIAprep ® Spin Miniprep Kit	Qiagen
QIAquick ® PCR Purification Kit	Qiagen
Rapid DNA Ligation Kit	Roche
Topo® TA Cloning® Kit	Invitrogen, Life technologies

2.1.10. Cell lines and bacteria

Table 12: List of used cell lines.

Name	Characterisation	Medium	Split ratio	Origin
B95a	Marmoset lymphoblastoid cell line transformed with Epstein-Barr-Virus	DMEM	1:7	(Kobune et al., 1990)
CHO-CD46	Chinese hamster ovary cell line genetically engineered to express human CD46	DMEM + 1.2 mg/ml G418	1:20	(Nakamura et al., 2004)

Name	Characterisation	Medium	Split ratio	Origin
CHO-hSLAM	Chinese hamster ovary cell line genetically engineered to express human SLAM	RPMI + 0.5 mg/ml G418	1:20	Y. Yanagi, Kyushu University (Tatsuo et al., 2000)
CHO-hSLAM-blue	Chinese hamster ovary cell line genetically engineered to express human SLAM with integrated expression cassette for floxed cerulean	RPMI + 0.5 mg/ml G418	1:20	S. Kugelmann, Paul-Ehrlich-Institut (Kugelmann, 2013)
CHO-K1	Chinese hamster ovary cell line	DMEM	1:20	ATCC, CCL-61
CHO-K1-blue	Chinese hamster ovary cell line with integrated expression cassette for floxed cerulean	DMEM	1:20	S. Kugelmann, Paul-Ehrlich-Institut (Kugelmann, 2013)
CHO-Nectin-1	Chinese hamster ovary cell line genetically engineered to express human Nectin-1	DMEM + 0.5 mg/ml G418	1:12	M. Lopez, INSERM (Reymond et al., 2004)
CHO-Nectin-2	Chinese hamster ovary cell line genetically engineered to express human Nectin-2	DMEM + 0.5 mg/ml G418	1:12	M. Lopez, INSERM (Reymond et al., 2004)
CHO-Nectin-4	Chinese hamster ovary cell line genetically engineered to express human Nectin-4	DMEM + 0.5 mg/ml G418	1:12	M. Lopez, INSERM (Fabre-Lafay et al., 2005)
CHO-PVR	Chinese hamster ovary cell line genetically engineered to express human PVR	DMEM + 0.5 mg/ml G418	1:12	M. Lopez, INSERM (Reymond et al., 2004)
H23	Human lung cell line	RPMI	1:3	ATCC, CRL-5800
H358	Human lung cell line	RPMI	1:3	ATCC, CRL-5807
H441	Human lung cell line	RPMI	1:3	ATCC, HTB-174
H522	Human lung cell line	RPMI	1:3	ATCC, CRL-5810
HEK-293T	Human embryonic kidney cell line genetically engineered to express the large T antigen	DMEM	1:12	ATCC, CRL-11268
HT1080	Human fibrosarcoma cell line	DMEM	1:12	ATCC, CCL-121
HT1080-Cre	Human fibrosarcoma cell line with integrated loxP gene cassette (loxP-*RFP*-loxP-*eGFP*)	DMEM	1:12	(Galla et al., 2004)
HT-1376	Human bladder cell line	EMEM	1:3	ATCC, CRL-1472
JAWSII	Murine, immature dendritic cell line from C57BL/6 mice	MEM-α	1:10 (weekly)	ATCC, CRL-11904
JAWSII-Ova	Murine, immature dendritic cell line from C57BL/6 mice, genetically engineered to express Ovalbumin	MEM-α	1:10 (weekly)	B. Bodmer, Paul-Ehrlich-Institut (Bodmer, 2015)
Molt4.8	Human T cell leukemia cell line	RPMI	1:10	I. Schneider, Paul-Ehrlich-Institut
Raji	Human Burkitt's lymphoma cell line	RPMI	1:20	ATCC, CCL-86

Name	Characterisation	Medium	Split ratio	Origin
Raji-blue	Human Burkitt's lymphoma cell line with integrated expression cassette for floxed cerulean	RPMI	1:20	S. Kugelmann, Paul-Ehrlich-Institut (Kugelmann, 2013)
SCaBER	Human bladder cell line	EMEM + 1.5 g/l $NaHCO_3$ + 0.1 mM NEA + 1 mM sodium pyruvate	1:3	ATCC, HTB-3
T24	Human bladder cell line	McCoy's 5A	1:3	ATCC, HTB-4
Vero-hSLAM	African green monkey kidney cell line genetically engineered to express human SLAM	DMEM + 0.5 mg/ml G418	1:10	Y. Yanagi, Kyushu University (Ono et al., 2001a)

Table 13: List of used bacterial strains.

Strain	Genotype	Origin
E. coli GM2163	F^-, *ara*-14, *leu*B6, *fhu*A31, *lac*Y1, *tsx*78, *sup*E44, *gal*K2, *gal*T22, *his*G4, *rps*L136(Str^R), *xyl*A5, *mtl*-1, *thi*-1, *dam*13*::*Tn9(Cam^R), *dcm*-6, *hsd*R2, *mcr*A, *mcr*B1, *rfb*D1)	New England Biolabs
E. coli Top10	F^-, *mcr*A, Δ(*mrr-hsd*RMS*mcr*BC), Φ80*lacZ*ΔM15, *lac*224, *deo*R, *rec*A1, *ara*D139, Δ(*ara-leu*)7697, *gal*U, *gal*K, *rps*L (Str^R), *end*A1, *nup*G	Invitrogen, Life Technologies

2.1.11. Mice

Table 14: List of mouse strains used in this thesis.

Strain	Characterization[a]	Origin
C57BL/6	Widely used inbred strain	(Murray and Little, 1935)
$IFNAR^{-/-}$ N20 C57BL/6	Interferon Type I Receptor knockout	(Gerlach et al., 2006)
$IFNAR^{-/-}$ $SLAM^{ki}$ C57BL/6	Interferon Type I Receptor knockout and SLAM knock in (replacement of V domain of mouse SLAM by that of human SLAM)	(Ohno et al., 2007)
NOD-scid $IL2R\gamma^{-/-}$	Immunodeficient, lack of B cells, T cells and NK cells	(Shultz et al., 2005)
OT-I C57BL/6	MHC I-restricted, $ovalbumin_{257-264}$ -specific $CD8^+$ T cells	(Hogquist et al., 1994)
OT-II C57BL/6	MHC II-restricted, $ovalbumin_{323-339}$-specific $CD4^+$ T cells	(Barnden et al., 1998)

[a] All animals were bred in-house.

2.2. Methods

2.2.1. Methods of molecular biology

2.2.1.1. Transformation of plasmids in competent *E. coli*

An aliquot of chemically competent *E. coli* Top 10 (highly transformable *E. coli* strain) or *E. coli* GM2163 (*E. coli* strain lacking dam methylation) was thawed on ice and 1 µl of DNA (re-transformation) or 2 µl of newly ligated plasmid was added. After 20 minutes incubation on ice, bacteria were heat-shocked for 30 seconds at 42°C. Then, *E. coli* were placed on ice for further 2 minutes before addition of 250 µl S.O.C. medium without any antibiotics. The bacteria were subsequently shaken at 650 rpm at 25°C or 37°C for 1 hour to allow the expression of plasmid-encoded resistance genes. Finally, 10 µl – 100 µl of the suspension were plated on LB-agar plates with a selection antibiotic, here ampicillin (50 µg/ml), and incubated at 25°C for 48 to 72 hours or 37°C overnight until single colonies could be detected. In general, the incubation temperature depended on the size and kind of plasmid: for large plasmids, low-copy-number plasmids, and for lentiviral transfer vectors containing LTRs 25°C was recommended, in the last case to avoid unwanted recombination of the LTRs. Bacteria containing other plasmids could be grown at 37°C.

2.2.1.2. Amplification and preparation of plasmids

To amplify plasmid-DNA, single colonies of the previously transformed and plated bacteria were picked and inoculated into 5 ml LB medium containing 50 µg/ml ampicillin ("Mini-prep" scale). Bacterial cultures were shaken at 25°C for 72 hours or 37°C overnight (see 2.2.1.1) at 180 rpm. Then, 500 µl retained sample were taken off and stored in the fridge. The remaining culture was pelleted at 3000 rpm for 10 min. The isolation of "Mini-prep" plasmid-DNA was performed using the QIAprep® Spin Miniprep kit following the manufacturer's instructions. The DNA was subsequently subjected to a restriction digest (see 2.2.1.4) and electrophoretically separated on an agarose gel (see 2.2.1.7). Two positive clones were selected and the respective retained samples were inoculated into 200 ml LB-ampicillin medium for a "Maxi-prep". Again, bacteria were grown at 25°C for 72 hours or at 37°C overnight at 180 rpm. For DNA-preparation, bacteria were pelleted for 15 min at 6000 rpm and 4°C and processed using the EndoFree® Plasmid Maxi Kit (Qiagen) according to the protocol. However, the neutralized cell lysate was not directly added to the "QIAfilter Cartridge" but centrifuged for 10 min at 3000 rpm to clear it from cell debris with less fluid loss maximizing DNA-yield. DNA was eluted from the column with an appropriate volume of elution buffer (50 µl – 200 µl, depending on the DNA pellet size and thus the expected amount of DNA). For Giga-prep scale plasmid isolation, a single colony was picked from a LB-ampicillin plate and inoculated into 5 ml LB-ampicillin medium. 6-8 hours later, this starter culture was used to inoculate the 2.4 l main culture, which was grown as

aforementioned. To pre-analyze the DNA, 5 ml of the main culture were removed for a "Mini-prep" with subsequent restriction digest and agarose gel-electrophoresis. If the result was satisfying, plasmid isolation from the main culture was conducted with the Jetstar 2.0 Endotoxin-free Plasmid Giga Kit as described in the manual. Giga-DNA was resuspended in TE-buffer. After DNA isolation, the amount of DNA was quantified (see 2.2.1.3) and DNA was aliquoted and stored at -20°C.

2.2.1.3. Quantification of DNA

DNA was quantified measuring the absorbance at 260 nm (A_{260}) by means of the UV-VIS spectrophotometer NanoDrop 2000c. The absorbance at 260 nm is caused by the π-electrons of the purine and pyrimidine rings of nucleotides and thus correlates with the DNA or RNA content of a given solution. Thereby, an A_{260} of one equals 50 µg/ml double-stranded DNA or 40 µg/ml RNA. For qualitative statements, also A_{280} was determined as aromatic amino acids have an absorbance maximum at 280 nm. Therefore, the ratio of the absorbance at 260 nm and 280 nm ($A_{260/280}$) is an indicator for the purity of the sample and should optimally be 1.8 (pure DNA). $A_{260/280} < 1.8$ corresponds to a protein contamination whereas $A_{260/280} > 1.8$ points at the presence of RNA.

2.2.1.4. Restriction of plasmid DNA

To confirm the identity of a certain plasmid or to isolate a desired subfragment, plasmid DNA was subjected to a restriction digest. Thereby, the DNA was cut by restriction enzymes in characteristic fragments, which were then electrophoretically separated (2.2.1.7) and extracted from the gel (2.2.1.8), if applicable. A restriction reaction composed the chemicals listed in Table 15. If a double digest was performed, the buffer ensuring the maximal activity for both enzymes was chosen. The applied volume of enzymes did never exceed 10% of the total reaction volume. For analytic purposes, the mixture was incubated for 1 hour at the temperature recommended by the manufacturer. Using time saver endonucleases, digestion time could be reduced to 30 minutes. Preparative digests took place at the temperature optimum of the restriction endonuclease(s) for at least 3 hours or overnight. For partial digests, 20 µg DNA were digested in a total volume of 100 µl. 1 min, 2 min, 5 min and 10 min after starting the digest, 25 µl were removed and the reaction was instantly stopped on ice with ice-cold 6x loading buffer.

Table 15: Composition of analytic, preparative or partial digestion reactions.

Chemical	Analytic digest	Preparative digest	Partial digest
DNA	1 µg or 5 µl Miniprep DNA	5 µg	20 µg
10x buffer	2 µl	5 µl	10 µl
10x BSA (if required)	2 µl	5 µl	10 µl
Enzyme(s)	0.5 µl - 1 µl each	up to 5 µl	0.5 µl
H_2O	ad 20 µl	ad 50 µl	ad 100 µl

2.2.1.5. Polymerase chain reaction (PCR)

The polymerase chain reaction, short PCR, allows the amplification (and modification) of specific DNA sequences defined by the used primers. In the present thesis the Expand High Fidelity^{PLUS} PCR System by Roche was applied according to the manufacturer's instructions. The composition of the reaction mix is given in Table 16, the used primers are listed in Table 10.

Table 16: Composition of a PCR.

Chemical	Amount
Template DNA	50 ng
Forward primer (10 pM)	2 µl
Reverse primer (10 pM)	2 µl
Reaction buffer (5x)	10 µl
dNTP-Mix (10 mM each)	1 µl
Polymerase (5 U/ µl)	0.5 µl
H_2O	ad 50 µl

The thermal cycling is depicted in Table 17. A typical PCR cycle started with a denaturation step at 94°C to separate the double stranded DNA. Then, a temperature reduction followed to allow the hybridization of primers and complementary single stranded DNA. The temperature was chosen depending on the melting temperature of the respective primers specified by the producer company Eurofins MWG Operon. During the last step, the elongation phase performed at 72°C, the thermostable blend of *Taq* DNA Polymerase amplified the DNA sequence flanked by forward and reverse primer using the provided dNTPs. The described cycle was repeated up to 20 times to amplify the desired DNA sequence exponentially.

Table 17: Thermal cycles used for PCR.

Step	Temperature [°C]	Time	Cycles
Initial denaturation	94	2 min	1x
Denaturation	94	30 sec	20x
Annealing	52 - 68 (depending on Tm primers)	30 sec	
Elongation	72	1 min/kb	
Final elongation	72	7 min	1x
Cooling	4	∞	

2.2.1.6. Dephosphorylation and ligation of DNA

Dephosphorylation of DNA

Plasmids harboring two compatible ends, e.g. after linearization with one enzyme or digest with blunt end cutters, tend to religate. To prevent this event, these backbones were dephosphorylated at their

5'ends using Antarctic phosphatase. For that purpose, 10x reaction buffer (1/10 of the total reaction volume) and 1 µl Antarctic phosphatase were added to the DNA and incubated for 15 min at 37°C before heat inactivation of the enzyme at 65°C (5 min) was performed. Afterwards, the dephosphorylated DNA was directly purified with the QIAquick® PCR Purification Kit according to the provided protocol.

Ligation of DNA with T4 DNA ligase

To ligate previously digested DNA, the Rapid DNA Ligation Kit by Roche was employed as instructed by the manufacturer. The insert was added in a molar ratio of 3:1 to the backbone. Ligation was performed for 5 - 20 min at room temperature or, in more difficult cases, at 16°C overnight. To assess if religation of backbone occurred, a ligation reaction containing only the backbone but no insert was prepared in parallel. Finally, 2 µl of the ligation reaction or the religation control were used to transform chemically competent *E. coli* (2.2.1.1).

TOPO-TA-Ligation

PCR products which were previously amplified by *Taq* polymerase (2.2.1.5) can be directly inserted into the linearized plasmid backbone pCR2.1-TOPO provided in the TOPO® TA Cloning® Kit (Invitrogen, Life technologies) in a Topoisomerase I-dependent reaction. The reaction was conducted as instructed by the manufacturer using 4 µl gel-purified PCR product (2.2.1.7. and 2.2.1.8). 2 µl of the ligation were transformed into chemically competent *E. coli* (2.2.1.1). Successful transformation could be visualized by blue-white screening on LB-ampicillin-X-gal agar plates as pCR2.1-TOPO harbors a lacZ-operon, which is disrupted by inserted PCR products. The insertion site of the PCR product in pCR2.1-TOPO is flanked by a multiple cloning site and complementary sequences for standard primers like T7 or M13, facilitating sequencing of the PCR product.

2.2.1.7. Agarose gel electrophoresis

To separate DNA fragments according to their size, agarose gel electrophoresis was performed. Thereby, the agarose matrix functions as a sieve for the negatively charged DNA, which migrates through the gel when an electric current is applied. This migration is dependent on the size of the fragments: larger nucleic acids move more slowly than shorter ones resulting in a separation. Additionally, the migration of the fragments is affected by the agarose content which influences the density of the matrix. For the separation of large DNA pieces high percentage agarose gels were used whereas low percentage gels have a better resolution for small DNA fragments.

To generate an agarose gel, an appropriate amount of agarose powder was solved in TAE buffer resulting in a 0.7% - 1.5% (w/v) solution. This agarose-TAE-solution was heated up in a microwave until the agarose was completely dissolved and then slightly cooled down before ethidium bromide solution was added to a final concentration of 50 µg/ml. The melted agarose was then poured into a

casting tray and a comb was inserted to create wells for sample-loading. After approximately 20 minutes, when the gel was completely polymerized, it was transferred to an electrophoresis chamber filled with TAE buffer. Then, the samples were premixed with 6x DNA-loading buffer and subsequently loaded onto the agarose gel. Additionally, 10 µl 2-log-DNA ladder were pipetted into one well as a marker. For analytic gels, electrophoretic separation took place at 120 V for approximately 60 minutes. The DNA was afterwards visualized by fluorescence of DNA-intercalating ethidium bromide excited by UV light at the gel documentation station. For preparative purposes, only 80 V were applied for several hours. DNA was isolated from the gel as described below (see 2.2.1.8).

2.2.1.8. Isolation of DNA from agarose gels

Ethidium bromide stained DNA was visualized under UV-light at the gel documentation station. Agarose, containing the desired DNA-fragment, was cut out of the gel by a scalpel. The piece of agarose was then transferred to a 1.5 ml reaction tube and DNA was subsequently isolated with the Geneclean® Turbo Kit following the manufacturer's instructions.

2.2.1.9. Sequencing of DNA

DNA sequencing was performed at Eurofins MWG Operon. For this purpose, 15 µl plasmid DNA with a concentration of 50-100 ng/µl was sent to the company. Suitable primers could be chosen from a catalog of available standard primers as done so for pCR2.1-TOPO plasmids sequenced with T7 forward and M13 reverse primer. If no applicable primer was present at Eurofins MWG Operon, 15 µl primer with a concentration of 10 pmol/µl were posted. The obtained sequences were analyzed with the ContigExpress software and compared to an *in silico* reference sequence.

2.2.2. Methods of protein biochemistry

2.2.2.1. Preparation of cell lysates

Cell lysates from transfected cells were prepared approximately 48 hours post transfection, as gene expression is at its maximum at that point of time. In contrast to that, cells were lysed 4 hours after transduction with Ova-PTV at MOI 1 to assess ovalbumin protein transfer. In order to inhibit protease activity when preparing cell lysates, all following described procedures took place on ice using ice-cold buffers which were, in case of the lysis buffer, additionally supplemented with protease inhibitors. At the beginning, the culture medium was taken off and cells were briefly washed with PBS before being incubated with cold PBS for 5 min on ice. Then, ice-cold lysis buffer was added, e.g. 500 µl per cavity of a 6-well plate. After 10 min incubation a suspension was generated by pipetting up and down thoroughly. This suspension was subsequently transferred to a 1.5 ml reaction tube. To remove cell

debris, lysates were centrifuged at 13,000 rpm for 15 min at 4°C (Heraeus Pico 17 Centrifuge). The supernatants were transferred to a new reaction tube and either directly used or stored at -80°C.

2.2.2.2. SDS-polyacrylamide gel electrophoresis (SDS-PAGE)

The sodium dodecyl sulfate-polyacrylamide gel electrophoresis, short SDS-PAGE, is a technique to separate proteins in an electric field according to their molecular weight. The method was performed according to Laemmli, 1970. The anionic tenside SDS masks the intrinsic charge of the proteins and, together with the denaturation caused by boiling, leads to their linearization. Therefore, the evenly negatively charged polypeptide chains migrate to the anode independent of their original charge and conformation. As larger proteins are stronger retained within the gel than shorter ones, separation depending on the chain length is achieved which is proportional to the molecular mass of the protein.
Previously prepared cell lysates (2.2.2.1) or vector particles (2.2.4.3) were mixed with 2x Urea Sample Buffer and denatured for 10 min at 95°C. For vector particles, 1 µl concentrated vector stock (undiluted or up to 1:10 pre-diluted) was added to 14 µl RIPA buffer before subjoining 15 µl 2x Urea Sample Buffer. Subsequently, samples and 10 µl Precision Plus Protein™ Kaleidoscope™ Standard (Bio-Rad) were loaded on polyacrylamide gels in a gel-electrophoresis chamber filled with SDS running buffer. The 1.0 mm or 1.5 mm thick 10% SDS polyacrylamide gels were produced beforehand as specified in Table 18. If not all wells were loaded with sample, remaining slots were filled up with equal volumes of 1:1 mixed RIPA/2x Urea Buffer. Initially, electrophoresis was conducted at 80 V. As soon as the samples entered the resolving gel, 120 V were applied by means of the Bio-Rad Power Pac 200. After the dye front had left the resolving gel, electrophoresis was terminated.

Table 18: Composition of resolving and stacking gel.

Chemical	Resolving gel (10%)	Stacking gel (5%)
30% acrylamide solution (Rotiphorese® Gel 30)	3.33 ml	825 µl
1M Tris pH 6.8	-	625 µl
1M Tris pH 8.8	3.9 ml	-
10% SDS	110 µl	25 µl
50% glycerin	820 µl	-
TEMED	13 µl	10 µl
20% APS	26 µl	20 µl
H_2O	1.84 ml	3.5 ml

2.2.2.3. Western blot analysis and immunostaining

Proteins separated by SDS-PAGE (2.2.2.2) can be transferred to a membrane (Western Blot) for antibody-based detection (immunostaining). Here, proteins were immobilized on a PVDF membrane using the Trans-Blot® SD Semi-Dry Transfer Cell by Bio-Rad. For that purpose, the membrane was

briefly activated in methanol, rinsed in transfer buffer and then placed underneath the polyacrylamide gel between two layers of thick filter paper soaked with transfer buffer. Blotting was performed at 180 mA per gel for 45 min and 25 V maximum. The successful transfer of proteins to the membrane was visualized by the colored protein marker. After blotting, unspecific protein binding sites on the membrane were blocked with 5% milk powder or 5% horse serum in TBS-T for 1 hour at room temperature. Then, the membrane was transferred in a 50 ml tube with 5 ml primary antibody in blocking buffer, recognizing the protein to be detected. The antibody incubation took place overnight at 4°C on a roller mixer. The next day, the membrane was washed three times for 10 min each in TBS-T at room temperature. 10 ml HRP (horseradish peroxidase)-conjugated secondary antibody in blocking buffer were subsequently added and incubated with the membrane for 1 hour at room temperature. All primary and secondary antibodies used in this thesis are listed in Table 7. The membrane was washed again three times for 10 min in TBS-T buffer at room temperature. Afterwards, Western Blotting Substrate (Pierce® ECL 2 or Amersham™ ECL™ Prime) was prepared according to the manufacturer's instructions and pipetted onto the membrane. While the horseradish peroxidase converted its substrate into a product, light was emitted which exposed a chemiluminescence detection film (Amersham Hyperfilm™) by GE Healthcare. Exposure times varied from 1 sec to 1 hour depending on the signal intensity. After development of the film, the molecular weight of the detected proteins could be determined in relation to the protein marker. To reprobe the membrane for other proteins, the bound antibody was removed with Restore™ PLUS Western Blot Stripping Buffer by Thermo Scientific for 20 min at room temperature. Subsequently, the membrane was washed three times for 10 min in TBS-T at room temperature and then blocked as described above before starting a new detection circle.

2.2.2.4. Enzyme-linked immunosorbent assay (ELISA)

The enzyme-linked immunosorbent assay, short ELISA, is an antibody-based immunological method to detect and quantify antigens or antibodies in a given sample. Thereby, antigens are captured by a specific antibody bound to the ELISA plate whereas antibodies can be enriched by antigen-coated well-plates. The immobilized proteins are then recognized by an enzyme-coupled (secondary) antibody. The addition of the substrate and the following enzymatic reaction finally lead to a measurable signal and visualize the presence of the protein of interest. The amount of the protein can be quantified in relation to a standard with known protein concentrations. In the present thesis, ELISA was used to characterize vector particles for the amount of HIV-1 p24 and chicken ovalbumin. Moreover, the activation of T cells co-cultured with transduced mDCs was analyzed by determining the levels of IL-2 and IFN-γ secreted in the culture supernatant.

Anti HIV-1 p24 ELISA

HIV-1 p24 was quantified by the Gentauer HIV-1 p24 Antigen ELISA Kit following the provided protocol. The vectors were diluted in 1:5 steps from 1:50 to a 1: 97,656,250 dilution.

Anti Ova-ELISA

To determine the Ova content of Ova-PTV preparations, the Ova-concentration of PTV particles was estimated by a semi-quantitative Western Blot analysis prior performing the Chicken Egg Ovalbumin ELISA with the kit by Alpha Diagnostic International. Based on that estimation, all samples were pre-diluted to an assumed final concentration of 0.5 ng/ml and 1.5 ng/ml as these values lie well within the measurement range of the assay. In a first step, 5 ng/ml or 15 ng/ml vector particles in PBS w/o Ca^{2+}/Mg^{2+} were lysed with a final concentration of 0.5% Triton® X-100 for 15 min at room temperature to ensure the accessibility of Ova in PTVs. Then, the particles were further 1:10 diluted in sample diluent to reduce the amount of Triton® X-100 in the assay. Triton® X-100 was also added to standards, positive control and blanks resulting in the same end concentration of the detergent. All measurements were performed in duplicates.

Anti mouse IL-2 and IFN-γ ELISA

Murine IL-2 and IFN-γ were quantified using the respective BD OptEIA™ Sets according to the manufacturer's instructions. To measure the IL-2 concentration the supernatants were 1:8 prediluted, to determine the IFN-γ concentration supernatants were diluted in a 1:20 ratio.

2.2.3. Cell culture methods

2.2.3.1. Cultivation of cells

Cells were cultivated in the appropriate medium (see Table 12) in an incubator (BBD 6220, Heraeus) at 37°C with 6% CO2 and 96% humidity. All media were supplemented with 10% decomplemented fetal calf serum (decomplementation for 30 min at 56°C) and 2 mM L-glutamine but did not contain penicillin/streptomycin to prevent masking of contaminations. The cells were regularly checked under the microscope for morphology and density as well as the absence of contaminations. When reaching a confluence of about 90%, cells were splitted twice a week in the indicated ratios (see Table 12) under sterile conditions. Therefore, adherent cells were washed with 10 ml PBS w/o Ca^{2+}/Mg^{2+} and incubated with 2 ml trypsin/EDTA (T75 flask) or 5 ml trypsin/EDTA (T175 flask) until cells were detached. Then, new culture medium was added and the desired part of the suspension remained in the flask whereas the other portion was discarded. For T75 flasks, medium was filled up to 12.5 ml, for T175 flasks to 20 ml. Suspension cells were cultivated in 20 ml medium in upright standing T75 flasks.

All cells were passaged less than 30 times or three months after thawing. After that period of time, cells were replaced by newly thawed ones.

Primary cells were cultured as described above with the respective media (Table 5) supplemented with penicillin/streptomycin and cytokines, if applicable. To enable long-term cultivation, T cells needed to be activated (see 2.2.3.4) and new TCM blended with 100 IU/ml IL-2 had to be added every three days. Human macrophage cultures were maintained with medium exchange every three days. However, these cells did not require regular splitting but could survive without singularization for at least 14 days without any problems.

2.2.3.2. Freezing and thawing of cultured cells

For freezing, cells were expanded to four T175 flasks and cultured until they reached a confluency of 60% - 80%. At this point of time, cells are in a logarithmic growth phase and best suited for freezing. First, 250 µl culture medium was sampled from each T175, pooled and spun down for 1 min at 2000 rpm (Heraeus Pico 17 Centrifuge). The supernatant was stored at -80°C until used for mycoplasma testing. Then, the remaining culture medium was taken off, the cells were washed with 10 ml PBS w/o Ca^{2+}/Mg^{2+} and were detached by addition of 5 ml trypsin/EDTA per flask. Trypsin was inactivated by subjoining of 7 ml fresh culture medium per T175 and the resulting suspension from all four flasks was combined. The cells were pelleted for 5 min at 1200 rpm, 4°C (Heraeus Multifuge $3SR^{+}$) and solved in 20 ml cold freezing medium (Table 5). The suspension was subsequently aliquoted at 1 ml into pre-cooled cryo-tubes. The aliquots were placed into a 4°C cold isopropanol-filled freezing container in a -80°C freezer. The employed freezing container guaranteed a defined cooling rate of 1°C per minute until reaching -80°C. After 24 hours the cryo-tubes were transferred from the freezing container to a liquid nitrogen tank where they were stored in the gas phase. To assess if the frozen cells can be successfully thawed and cultured again, one aliquot of the frozen cells was initially subjected to a test thawing.

For thawing of cells, one cryo-tube of the desired cell line was taken out of the liquid nitrogen tank and thawed at room temperature until only a fraction of the cell-suspension remained frozen. Then, the cells were put into 25 ml pre-warmed, fresh culture medium without antibiotics. The suspension was centrifuged for 5 min at 1200 rpm, 4°C (Heraeus Multifuge $3SR^{+}$) and the DMSO-containing supernatant was discarded. The cell pellet was subsequently solved in 13 ml (adherent cells) or 20 ml (suspension cells) pre-warmed, fresh culture medium without antibiotics and transferred to a T75 cell culture flask. After cultivating the cells for 24 hours at 37°C, the medium was exchanged to remove residual DMSO and cell debris. The medium used now was normal culture medium also containing selection antibiotics, if necessary.

2.2.3.3. Transfection of adherent cells

Plasmid DNA was introduced into adherent cells by Lipofectamine® 2000 or polyethylenimine. Lipofectamine® 2000 was used for transfection of up to 1 x 10^6 cells in a 6-well format whereas the low-cost polyethylenimine-transfection was conducted for higher numbers of HEK-293T cells. Maximum gene expression was reached 48 – 72 hours after transfection.

Transfection of cells using Lipofectamine 2000

One day prior transfection, 7 x 10^5 HEK-293T cells were seeded per cavity of a 6-well plate. The next day, when the cells were about 75% - 90% confluent, 5 µg plasmid DNA were diluted in 250 µl cold Opti-MEM®. In another reaction tube 10 µl Lipofectamine® 2000 were mixed with 250 µl cold Opti-MEM® and subsequently incubated for 5 min at room temperature. Then, the Lipofectamine® 2000 solution was transferred to the DNA mix. After thorough vortexing, the mixture was incubated for another 20 min at room temperature to allow the formation of DNA-Lipofectamine® 2000 complexes. In the meantime, the culture medium of the cells was replaced by 1.5 ml pre-warmed Opti-MEM®. Finally, the transfection mix was gently dripped onto the cells. Medium exchange to 2 ml normal growth medium was performed after 4 hours incubation at 37°C. Transfection efficiency was assessed by transfecting a separate HEK-293T well with an expression plasmid encoding a fluorescing protein, e.g. pSEW-TurboFP635.

Transfection of cells using polyethylenimine

For large-scale vector productions in T175 flasks, HEK-293T cells were transfected with polyethylenimine (PEI, 18 mM stock). One day before transduction, 1.85 x 10^7 cells were seeded per T175 flask. The flasks were placed carefully balanced into the incubator to ensure even distribution of the cells. The following day, the confluency of the cells was checked under the microscope. For transfection it should optimally be between 75% and 90%. In a first step, the culture medium of the cells was exchanged to 10 ml DMEM with 15% FCS and 2 mM L-glutamine. Then, 35 µg DNA were united with 2.3 ml DMEM (with 2 mM L-glutamine, w/o FCS). In another reaction tube, 140 µl PEI reagent (18 mM) were diluted in 2.2 ml DMEM (with 2 mM L-glutamine, w/o FCS) and both tubes were mixed thoroughly. The PEI-DMEM solution was then transferred to the DNA-mix and rigorously vortexed. The transfection mixture was incubated for 20 min at room temperature and subsequently added to the prepared cells resulting now in 10% FCS-containing medium. The next day, the medium was replaced by 16 ml new culture medium. Successful transfection was visualized by fluorescence of cells transfected with the transfer vector plasmid, which was usually encoding a fluorescing protein.

2.2.3.4. Isolation and activation of human peripheral blood mononuclear cells (PBMC)

Human peripheral blood mononuclear cells (PBMC) were isolated from buffy coats obtained from the German Red Cross Blood Donor Service Frankfurt or fresh in-house donor blood by density centrifugation with Histopaque-1077®. First of all, the blood was mixed with the same volume of room temperature PBS w/o Ca^{2+}/Mg^{2+}. Subsequently, 15 ml cold Histopaque-1077® were carefully overlain with 25 ml diluted blood in a 50 ml tube and centrifuged at 1800 rpm for 30 min at room temperature without break (Heraeus Multifuge $3SR^{+}$). The blood was separated into a top layer of plasma, the PBMC-containing "lymphocyte ring" (lymphocytes, monocytes, and macrophages) and pelleted erythrocytes and polymorphonuclear cells (granulocytes). The PBMC-fraction was aspirated cautiously and collected in a new 50 ml tube. The cells were washed twice with 45 ml room temperature PBS w/o Ca^{2+}/Mg^{2+} per 5 ml PBMC and pelleted in the course thereof for 10 min at 1500 rpm and then at 1200 rpm. All cells were subsequently combined and blended with PBS w/o Ca^{2+}/Mg^{2+} once again. After centrifugation at 1200 rpm for 10 min (Heraeus Multifuge $3SR^{+}$), the pellet was resuspended in 10 ml 0.86% ammonium chloride buffer and incubated 20 min at 37°C to lyse remained erythrocytes. Following, PBMC were washed twice as previously described. The cells were counted and either directly used for further experiments or activated.

Activation of PBMC was accomplished by addition of anti-CD3 and anti-CD28 antibodies, and IL-2. In a first step, cell culture plates were coated with the aforementioned antibodies. Thereby, 1 ml pre-warmed PBS w/o Ca^{2+}/Mg^{2+} with 3 µg/µl of each antibody (6-well) or 500 µl PBS w/o Ca^{2+}/Mg^{2+} containing 1 µg/µl anti-CD3 and anti-CD28 antibody (24-well, 48-well) were added to a tissue culture-treated well-plate. The plate coated at 37°C for 2 hours or at 4°C overnight. Afterwards, the PBS-antibody solution was replaced by 2% BSA in water and the plate was incubated for at least 30 min at 37°C. Then, the wells were washed twice with 3 ml PBS w/o Ca^{2+}/Mg^{2+} (6-well) or 1 ml PBS w/o Ca^{2+}/Mg^{2+} (24-well, 48-well) before the cells were added. Up to 1 x 10^7 cells in 3 ml T cell culture medium (TCM) could be stimulated in a 6-well. A 24-well was suited for the activation of up to 1 x 10^6 PBMC in 1 ml TCM and a 48-well for 5 x 10^5 PBMC in 1 ml TCM. The medium was supplemented with 100 IU/ml IL-2. The cells were cultivated in the antibody-coated stimulation plates for 3 days before being used for experiments.

2.2.3.5. Magnetic cell sorting (MACS)

Pan T cells, $CD4^{+}$ or $CD8^{+}$ cells were isolated from murine splenocytes (extracted from mouse spleen as described in 2.2.5.7) or human PBMC (2.2.3.4) using MACS cell separation kits from Miltenyi Biotech (see Table 11) according to the manufacturer's instructions. This method allows the separation of cell populations depending on the expression of surface molecules. Antibodies directed against an antigen of interest are coupled to magnetic beads which retain the so-labeled cells within a column surrounded by a strong magnetic field. In contrast to that, unlabeled cells are washed away. After

removal of the magnetic field, the retained cells are eluted. The target cells can either be the beads-conjugated fraction (positive selection) or found in the flow through (depletion of unwanted cells or untouched isolation). Positive selection was applied to remove human $CD4^+$ cells from PBMC whereas murine $CD4^+$ and $CD8^+$ cells as well as pan T cells were isolated untouched. Separation took place using the AutoMACS Pro Separator (Miltenyi Biotech) or was performed manually.

2.2.3.6. Generation and co-culture of transduced myeloid dendritic cells with T cells

Myeloid dendritic cells (mDCs) were generated by cultivation of bone marrow cells in the presence of the cytokine GM-CSF (Schülke et al., 2010). Bone marrow cells were isolated from two $IFNAR^{-/-}$ N20 C57BL/6 and two $IFNAR^{-/-}$ $SLAM^{ki}$ C57BL/6 mice, respectively, as described in 2.2.5.7. Usually, 3 - 5 x 10^7 cells were obtained from of one animal. For differentiation of myeloid dendritic cells 1.5 x 10^7 cells were seeded in 15 ml dendritic cell medium supplemented with 100 ng/ml GM-CSF per T75 flask. The cells were cultivated for 8 days with partial medium exchange every 2 – 3 days. After that period of time, the bone marrow cells developed into a mixed population of macrophages and myeloid dendritic cells. mDCs could be detached by rinsing the cell culture flask with medium, whereas the strongly adherent macrophages sticked to the bottom of the T75. The so harvested mDCs of one donor were pooled, pelleted at 1200 rpm for 5 min (Heraeus Multifuge $3SR^+$) and resuspended in 10 ml DC medium. 3.2 x 10^5 cells were seeded in 0.5 ml or 1 ml DC medium supplemented with 100 ng/ml lipopolysaccharide (LPS) in a 24-well plate. LPS was added in order to upregulate SLAM, the main cell entry receptor for MV_{wt} H, in mDCs generated from $IFNAR^{-/-}$ $SLAM^{ki}$ C57BL/6 mice (Ohno et al., 2007). mDCs derived from $IFNAR^{-/-}$ N20 C57BL/6 animals were treated likewise. The next morning, mDCs were transduced with protein transfer vectors at MOI 1 or 3. For this purpose, a master mix was prepared: at first, PTVs were prediluted in the solvent Opti-MEM® resulting in the same volume Opti-MEM® per volume vector solution to be added to one well. Secondly, the required volume DC medium was subjoined. Then, the culture medium was removed from the cells and replaced by 250 µl of the prepared transduction mixture. If transduction in the presence of the fusion-inhibitor FIP (Richardson et al., 1980) was contemplated, 200 µM FIP-containing medium was added at least 30 min before transduction with PTVs. Besides, inhibitor-supplemented medium was used for all further steps of the experimental procedure. After incubating mDCs with PTVs for 4 hours, PTV-containing medium was replaced by 8 x 10^5 primary T cells solved in 1 ml DC medium. These T cells had been previously isolated by untouched magnetic cell separation (see 2.2.3.5) from the spleens of OT-I C57BL/6 or OT-II C57BL/6 mice. OT-I C57BL/6 mice are characterized by $CD8^+$ ovalbumin-specific T cells whereas OT-II C57BL/6 possess $CD4^+$ ovalbumin-specific T cells (Hogquist et al., 1994; Barnden et al., 1998). 24 hours after addition of T cells, 100 µl co-culture supernatant were sampled for the quantification of secreted IL-2 by ELISA (2.2.2.4). The collected supernatant was incubated with 0.2% (v/v) Tween-20 for 10 min - 20 min at room temperature to inactivate vector particles. Then, the samples were stored at -20°C for further analysis. 72 hours after starting the co-

culture, the remaining supernatant was harvested for IFN-γ ELISA (2.2.2.4). Vector particles were inactivated as aforementioned and samples were stored at -20°C.

2.2.3.7. Enzyme-linked immuno spot assay (ELISpot)

The enzyme-linked immuno spot assay (ELISpot) is a method to determine the number of single, stimulated immune cells. It is based on the detection of cytokines secreted upon activation, which then become immobilized to a membrane.

In this thesis, the IFN-γ-secretion of splenocytes obtained from PTV-vaccinated mice upon addition of appropriate stimulants was analyzed using the Mouse IFN gamma ELISPOT Ready-Set-Go!®-Kit from eBioscience. One day prior to the assay, MultiScreen filter plates with hydrophobic Immobilon-P PVDF membrane were activated with 50 µl 70% ethanol per well. Immediately, 200 µl sterile water were added to the wells and the fluid was decanted. The plate was washed twice more with sterile water and then once with sterile PBS w/o Ca^{2+}/Mg^{2+} before proceeding following the manufacturer's instructions. Splenocytes were isolated as described (2.2.5.7). 5 x 10^5 splenocytes solved in 100 µl RPMI-1640 (with 10% FCS, 2 mM L-glutamine, and 1% penicillin/streptomycin) were aliquoted per well of a 96-U-well plate. Then, 100 µl of stimulatory peptides, proteins or controls diluted in complete RPMI-1640 medium were added to each well. 10 µg/ml concanavalin A served as a positive control, plain medium as a negative control. Cells were specifically restimulated by addition of 10 µg/ml recombinant Ova, 5 µg/ml $Ova_{257-264}$ (MHC I-restricted immunodominant peptide epitope of ovalbumin) or 5 µg/ml $Ova_{323-339}$ (MHC II-restricted immunodominant peptide epitope of ovalbumin). The experiment was performed in triplicates. The prepared mixture of stimulants and cells was subsequently transferred to blocked MultiScreen-IP filter plates and incubated for 36 hours at 37°C in an 5% CO_2 humidified incubator avoiding any further movements. IFN-γ secreting cells were detected following the manufacturer's instructions. The spots were counted with an ELISpot Reader (Eli.Scan; software ELI. Analyse). Wells with too many spots to be reliably counted were set to a maximum value of 1500 spots, which represents the maximum spot count reliably determined by the software in the used settings.

2.2.3.8. Flow cytometry

Flow cytometry is a method to characterize single cells for their size, granularity, and fluorescence. It enables the detection of surface proteins as well as intracellular antigens by labeling with fluorophore-conjugated antibodies directed against the marker of interest. It is based on the detection of scattered light and fluorescence signals emitted by cells passing a laser beam.

A prerequisite for the staining procedure and the subsequent measurement is a single-cell suspension. To obtain this, adherent cell lines were detached using trypsin/EDTA, unhitched by vigorous pipetting (dendritic cells) or scraped off (macrophages). Trypsin/EDTA could be used as no trypsin-sensitive

epitopes were examined. If surface markers on primary cells, e.g. mouse splenocytes or human lymphocytes, should be analyzed, erythrocytes were lysed with 0.86% ammonium chloride solution prior staining. For murine blood, lysis was performed right after staining (see below). To stain cell surface antigens, approximately 1 - 5 x 10^5 suspension or previously detached adherent cells were aliquoted per flow cytometry U-bottom tube and washed thoroughly with FACS-wash to remove the culture medium. Alternatively, 20 µl previously collected, fresh murine blood (2.2.5.2) were pipetted into a 1.4 ml flow cytometry tube and filled up with 500 µl FACS-wash. The cells were spun down at 1200 rpm, 4°C for 5 minutes (Heraeus Multifuge $3SR^+$) and the supernatant was discarded except for 50 µl - 100 µl in which the cells were resuspended in again. In case of MST1R detection, however, cells were initially incubated in 100 µl ice-cold methanol for 5 min at -20°C, washed twice with PBS w/o Ca^{2+}/Mg^{2+} containing 1% (w/v) BSA and blocked with PBS w/o Ca^{2+}/Mg^{2+} containing 10% (v/v) FCS and 300 mM glycine before proceeding with the staining procedure. When staining whole blood or immune cells, an FcR-blocking reagent was applied for 15 minutes at room temperature in order to block the unspecific binding of Fc receptor expressing cells to the antibodies. Then, antibody/antibodies were added in the required dilution (Table 7). Antibodies conjugated with different fluorochromes and diverse specificities could be used to stain the same sample (multicolor staining). Moreover, every staining approach included an unstained sample (mock), single-stained samples, if applicable, and the respective isotype controls. Isotype controls are antibodies of the same isotype as the primary antibody, which are conjugated to the same fluorophore but without specificity for the antigen of interest. They were applied in the same concentration as the corresponding antibodies. Subsequently, the samples were incubated for 20 min – 1 hour at 4°C in the dark. If the used antibody was not directly conjugated to a fluorophore, cells were washed thoroughly with FACS-wash and followingly incubated with a labelled secondary antibody (1 hour, 4°C, in the dark). Whenever such a two-step staining procedure was conducted, a secondary antibody only control was performed as well. In case of murine blood, red blood cells were lysed with 700 µl 1x FACS Lysing Solution by Becton Dickinson (15 min, RT) and lymphocytes were pelleted as aforementioned. After staining, all cells were washed twice with FACS-wash before fixation with 100 µl – 300 µl FACS-fix (Table 5) took place. Cells expressing fluorophores, e.g. after transfection or transduction, did not necessarily have to be stained but could be subjected to flow cytometry analysis after being washed thoroughly and fixed with FACS-fix. All samples were either directly analyzed or stored in the fridge until measured in the LSRII SORP cytometer by Becton Dickinson. Lymphocytes should be measured within 24 hours, all other samples could be stored up to one week at 4°C in the dark. Normally, 10.000 cells were read in the FSC-SSC gate. However, organ-derived samples from humanized NSG mice injected with CD4-LV required measurement of 1 million events in the FSC-SSC gate to ensure appropriate GFP detection. Compensation of multicolor stained samples was performed directly at the LSRII SORP cytometer (FACSDiva software) or later using FCS Express. For homogeneous cell

populations, doublet exclusion was performed. The obtained data were analyzed using the FACSDiva or FCS Express software.

2.2.4. Virological methods

2.2.4.1. Amplification of recombinant measles virus

To amplify MV_{wt323}-GFP(N), Vero-hSLAM cells were seeded into four 15 cm dishes at 5 x 10^6 cells per dish and cultivated for 4 hours at 37°C. Then, cells were infected with passage 3 MV_{wt323}-GFP(N) at MOI 0.03. To assure even infection of cells, the culture medium was removed, mixed with virus suspension and pipetted back onto the cells. Infected cells were cultured for 2-3 days at 37°C until nearly all cells were infected. Then, cell-associated virus was harvested. For that purpose, the culture medium was removed and replaced by 0.5 ml Opti-MEM. Cells were detached using a cell scraper and the suspension was subsequently transferred into a 15 ml reaction tube and quick-frozen in liquid nitrogen for approximately 3 minutes. The freezing step leads to cell disruption and thus release of cell-associated virus. The suspension was either stored at -80°C or directly thawed (but not heated) at 37°C in a water bath. Cell debris was subsequently removed by centrifugation for 5 min at 3,000 rpm and 4°C (Heraeus Multifuge $3SR^+$). The virus-containing supernatant was then aliquoted at 300 µl in Cryo-tubes and stored at -80°C.

2.2.4.2. Titration of recombinant measles virus

For titration of each MV_{wt323}-GFP(N) virus stock, Vero-hSLAM cells were seeded into 2 96-well plates at 1 x 10^4 cells per well three hours before titration. The viruses were diluted from 10^{-1} to 10^{-12} in duplicates by initially mixing 270 µl DMEM without FCS with 30 µl virus suspension followed by a serial 1:10 dilution. Cells were infected by transferring 30 µl of virus-dilution in 8 replicates to the cells. The cells were cultivated for 4 days at 37°C and infection of each replicate was determined by microscopic analysis of GFP fluorescence. Virus titers were calculated by the $TCID_{50}$ method according to Spearman and Kärber (Spearman, 1908; Kärber, 1931) and the final titer was determined by averaging the duplicate values. The $TCID_{50}$/ml gives the dilution of 1 ml virus, which has a probability of 50% to infect susceptible cells. The detection limit of this method is defined with 1 x 10^2 $TCID_{50}$/ml.

2.2.4.3. Production and concentration of lentiviral vectors

HIV-1 derived lentiviral vectors were produced in HEK-293T packaging cells. For that purpose, the cells were transiently transfected with transfer vector, packaging plasmid and Env expression construct(s) using polyethylenimine as described in 2.2.3.3. The amount and kind of plasmid DNA

needed for the production of the different gene and protein transfer vectors deployed in the present thesis are listed in Table 19. 24 hours after transfection the medium was carefully exchanged to 16 ml new DMEM (+15% FCS and 2 mM L-glutamine) per T175 flask. The next day, vector-containing supernatant was harvested and filtered using a 0.45 µm Minisart® syringe filter or, for larger volumes, the 0.45 µm Stericup® & Steritop™ vacuum-driven filtration system. For titer determination of un-concentrated vector, 1 ml of the filtered supernatant was aliquoted and stored at -80°C. The remaining medium was filled into 36 ml ultracentrifuge tubes at 32 ml per tube. Then, 4.5 ml 20% sucrose solution were cautiously layered below and vectors were pelleted at 28,000 rpm, 4°C for 3 hours using a SW28 rotor in an Optima™ L-70K ultracentrifuge. Alternatively, pelletizing was achieved by low-speed centrifugation in a Heraeus Multifuge 3SR$^+$ bench-top centrifuge (50 ml or 250 ml tubes with sucrose cushion, centrifugation at 4,300 rpm, 4°C, 25 hours). The supernatant was discarded and the tubes were carefully wiped with fuzz-free cloth to remove residual fluid. Subsequently, the vector pellets were solved in prechilled PBS w/o Ca^{2+}/Mg^{2+} or Opti-MEM® (120 µl for VSV-G pseudotyped vectors, 85 µl for MV H+F pseudotyped ones). The tubes were placed on ice on a shaking device for 1-2 hours. Afterwards, vectors were resuspended by pipetting approximately 60 times up and down and pooled, if more than one ultracentrifugation tube containing a certain vector type was present. In a last step, vectors were aliquoted into 1.5 ml (low binding) tubes and stored at -80°C.

For VSV-G or MV_{wt} H and F-pseudotyped vectors, harvest and concentration could be repeated the next day if new medium was added to the packaging cells right after the first harvest. In contrast to that, CD4-LV and CD8-LV only allowed for a single harvest due to stronger syncytia formation.

Table 19: Transfection scheme for lentiviral vector production.

	Plasmid [µg]	Gene transfer vectors[a]			Protein transfer vectors[a]			
		VSV-LV	MV_{wt}-LV	CD4-LV	VSV-Cargo-LV	MV_{wt}-Cargo-LV	Bald-Cargo-LV	VSV/MV_{wt}-Cre-LV[b]
Env	pMD.G2	6.13	-	-	3.98	-	-	3.98
	pCG-Hwt323Δ18	-	4.04	-	-	1.49	-	1.49
	pCG-H-αCD4	-	-	0.9	-	-	-	-
	pCG-Fwt323Δ30	-	6.73	-	-	2.49	-	2.49
	pCG-FcΔ30	-	-	4.49	-	-	-	-
packagable vectors	transfer vector:	17.5	15.17	15.17	12.73	12.73	14.36	12.73
	pSEW	+	+	-	-	-	-	-
	pSEW-Cre	+	+	-	-	-	-	-
	pSEW-TurboFP635	+	+	-	+	+	+	+
	pS-luc2-GFP-W	-	+	+	-	-	-	-
packaging plasmids	pCMVΔR8.9	11.38	9.06	14.44	9.15	9.15	10.32	12.2
	packaging plasmid with cargo:	-	-	-	9.15	9.15	10.32	6.1
	pcDNA3.gpGFP.4xCTE	-	-	-	+	+	+	-
	pcHIV1_MA_P_GFP	-	-	-	+	+	+	-
	pcHIV1_MA_P_Ova	-	-	-	+	+	+	-
	pcHIV1_MA_P_Cre	-	-	-	+	+	-	+

[a] +/-, indicate if a certain plasmid was generally used for the generation of the specified vector type. [b] brackets, either VSV-G or MV_{wt}-GP encoding expression constructs were used.

2.2.4.4. Titration of vectors

All PTVs were titrated on adherent CHO-hSLAM cells whereas CD4-LV and was titrated on Molt4.8 suspension cells. The titer of VSV-LV_{Cre} was determined on HT1080-Cre cells and MV_{wt}-LV was either titrated on Raji or CHO-hSLAM cells. One day before titration, adherent cells were seeded resulting in 70% - 80% confluency at the time point of transduction, e.g. 2 x 10^4 CHO-hSLAM cells per 96-well or 9 x 10^4 CHO-hSLAM cells per 48-well. Suspension cells were seeded likewise right before titration, e.g. 3 x 10^4 Molt4.8 cells in 50 µl medium per 96-well. To determine the number of adherent cells at the time point of titration, the cells of one previously seeded well were detached with Trypsin/EDTA and subsequently counted. For titration, vectors were serially diluted 1:10 in culture medium in 6 steps and either directly added to suspension cells or, in case of adherent cells, right after the old medium was removed. Titration took place in 150 µl medium per 96-well with no further medium addition or 250 µl medium per 48-well with subjoining of 500 µl culture medium approximately 5 hours after transduction. 3 days after transduction, transduction efficiency was analyzed by flow cytometry (2.2.3.8). The titers were calculated according to the formula below, including only dilutions where 1% - 20% of cells were transduced.

$$\text{Titer [t.u./ml]} = \frac{(\%\ \text{transduced cells}) \times (\text{number of cells at time point of transduction})}{(\text{Applied volume of vector [µl]})} \times 1000$$

2.2.4.5. Transduction of adherent or suspension cells

Adherent cells were seeded one day before transduction in 6 - 96-well plates so that cells would be ~70% - 80% confluent at the time of transduction, e.g. 6 x 10^4 CHO-K1 cells per well of a 48-well-plate. The cells of one well were counted right before transduction. For suspension cells, the cell number was determined and cells were seeded into a well plate just before transduction using as little medium as possible, e.g. 50 µl per 48-well or 100 µl per 24-well. In order to transduce the cells with a specific multiplicity of infection (MOI), the volume of vector to be applied to the given number of cells was calculated according to the following formula:

$$\text{Volume (ml)} = \frac{\text{MOI x cell number}}{\text{titer}}$$

Transduction was conducted in as little medium as possible, but as much as necessary to reliably cover the cells, e.g. 150 µl per 48-well or 300 µl per 24-well. Vector stocks were freshly thawed before transduction and mixed by pipetting up and down. The vector was premixed with fresh culture medium by pipetting and the cells were subsequently incubated with the vector mix for approximately 4 hours. As a matter of course, the culture medium was removed from adherent cells before addition of vector. Then, the vector-containing medium was replaced by normal growth medium or normal growth medium was added up to the volume usually used for cultivation. Protein transfer was

analyzed 4 hours after transduction by flow cytometry (2.2.3.8) or Western Blot (2.2.2.3). As robust transgene expression is reached 48 - 72 hours post transduction, gene transfer was assessed by flow cytometry 3 days after transduction.

Transduction of primary unstimulated PBMC and thereof derived activated T cells with CD4-LV was conducted in presence of 4 µg/ml protamine sulfate. Protamine sulfate is a polycation that should minimize the charge repulsion between vector particles and cell surface and thus increase transduction efficiency (Cornetta and Anderson, 1989). Moreover, a spin occulation was performed. Therefore, the vector was added to the cells and the culture plate was immediately centrifuged at 1,200 rpm, 32°C (Heraeus Multifuge $3SR^{+}$) for approximately 90 minutes. Then, the plate was either transferred to the incubator for 3 hours before addition of new T cell medium or medium was instantly subjoined. Transgene expression was analyzed 3 days after transduction as described above.

2.2.5. *In vivo* mouse experiments

All animal experiments were performed in compliance with the German animal protection law and following the recommendations of the Federation of European Laboratory Animal Science Associations (FELASA). Mice were bred in-house under specified pathogen-free (SPF) conditions and housed in individually ventilated cages (IVC). All animals used in experiments were about 6 to 12 weeks old. The health status of the mice was checked regularly.

2.2.5.1. Isoflurane gas anesthesia of mice

Mice were anesthetized using isoflurane gas anesthesia in a special isoflurane anesthesia unit. Isoflurane was the narcotic of choice as it is only minimally metabolized by the liver and is therefore less toxic for the animals (Fish, 2008). Initially, the induction chamber was flushed with 5% (v/v) isoflurane. Then, mice were placed in the chamber and the isoflurane content was reduced to 2.5% (v/v). The animals were left in the unit until entirely narcotized. Mice were usually awake and alert a few minutes after being taken out of the induction chamber.

2.2.5.2. Blood collection from the orbital sinus

Mice were anesthetized using isoflurane (2.2.5.1) and laid on their sides on a table. The loose skin in the neck of the animals was tightened with thumb and index finger. The grasp should be strong enough to accumulate the blood and immobilize the mice but not result in occlusion of the trachea. When the eyeballs were protruding out of the eye sockets, the tip of a thin Pasteur pipette was inserted in the medial canthus of one eye under the eyeball, directed in a 45° angle towards the middle of the eye socket. The pipette was gently rotated until blood was entering it and then slightly moved backwards. When the desired amount of blood was withdrawn, mice were released and blood flow was stopped by

briefly applying light pressure on the eye with a gauze swab, if necessary. The blood was collected in lithium-heparin Microtainer tubes purchased from BD.

2.2.5.3. Xenograft transplantation

To generate so-called "humanized mice", immunodeficient NOD-scid IL2Rγ$^{-/-}$ (NSG) mice were repopulated with human peripheral blood mononuclear cells (PBMC). Human PBMC were isolated and, if applicable, activated as previously described (see 2.2.3.4). The cells were subsequently washed with PBS w/o Ca^{2+}/Mg^{2+} and counted. Then, the desired cell number was solved in PBS w/o Ca^{2+}/Mg^{2+} and well resuspended before administration. Cells were injected intravenously (2.2.5.4) in a total volume of 200 µl into 6-8 weeks old NSG mice. In case of unstimulated PBMC 5 x 10^7 cells, in case of activated T cells 1.5 x 10^7 cells were injected per mouse. Repopulation was monitored by analyzing the percentage of human $CD45^+$ cells in the peripheral blood of the animals. Usually, 10% - 20% human $CD45^+$ lymphocytes were detected 3 days after injection of cells. PBMC-repopulated NSG mice were closely monitored for signs of graft versus host disease (GvHD), e.g. loss of weight, rough fur, apathy, abnormal/ unphysiological posture and isolation from the group. If GvHD set in during the course of an experiment, animals were euthanized to prevent suffering.

2.2.5.4. Intravenous or intraperitoneal vector injection

For intravenous vector injection, mice were placed under a heat-lamp in order to dilate the veins by warming of the animals. Then, the mice were transferred to a mouse-restrainer and vector or solvent was injected with a 30 G cannula in one of the lateral tail veins. The solution was pre-warmed to room temperature and free from air bubbles. The maximal volume applied was 200 µl. To perform intraperitoneal vector injection, mice were manually restrained and held with their heads pointing downwards. This position ensured a cranial shift of the inner organs and thus the formation of an empty cavity in the lower abdominal region. Vector or solvent were injected with a 30 G cannula in the lower right or left quadrant of the abdomen to avoid injury of inner organs. The injected volume did not exceed 200 µl. After both, intravenous and intraperitoneal injection, mice were put back in their cage and their state of health was observed for several minutes.

2.2.5.5. *In vivo* imaging

For *in vivo* imaging, mice were injected intraperitoneally with 150 µg D-luciferin/ g body weight (see 2.2.5.4). 4 min after injection of the substrate, mice were transferred into a pre-floated anesthesia chamber with 2.5% (v/v) isoflurane for 3 min - 4 min. The animals were subsequently placed into the IVIS Spectrum imaging device where anesthesia was maintained individually by nose-cone masks also delivering 2.5% (v/v) isoflurane. The mice were imaged in ventral position first, then turned to dorsal

position. Luminescence acquisition took place at approximately 8 min – 18 min after substrate injection when the substrate distribution was at steady state.

In case of final imaging, the animals were recorded as described above (common parameters: 60 sec exposure time, F-Stop 1, binning 8, subject height 1.5) and subsequently sacrificed. Ventral, the skin was detached from the body and pinned to a polystyrene board with cannulas. After imaging again (subject height 4), axillary and submandibular lymph node like structures as well as spleen, thymus and, if applicable, other luminescing organs were removed (2.2.5.7) and the gut was arranged in a circular manner around the mice. The organs as well as the in such a way prepared animals were imaged one last time (organs: subject height 0.3, mice: subject height 4).

2.2.5.6. Vaccination with protein transfer vectors

6 to 8 weeks old IFNAR$^{-/-}$ and SLAM^{ki} mice were intraperitoneally injected (2.2.5.4) with 1 µg recombinant ovalbumin or Bald-Ova-LV$_{Katushka}$, MV$_{wt}$-Ova-LV$_{Katushka}$ or VSV-Ova-LV$_{Katushka}$ adjusted to contain 1 µg ovalbumin. The amount of MV$_{wt}$-GFP-LV$_{Katushka}$ was normalized to capsid protein content of MV$_{wt}$-Ova-LV$_{Katushka}$. Opti-MEM injected animals served as mock controls. Mice were primed, and boosted 4 weeks later as described. The animals were sacrificed on day 32, i.e. four days after boosting, their spleens were harvested and splenocytes were isolated (2.2.5.7). The number of IFN-γ secreting, antigen-specific T cells among splenocytes was determined by an ELISpot assay (2.2.3.7).

2.2.5.7. Removal of organs and preparation of single-cell suspensions

Prior to removal of organs, mice were sacrificed by cervical dislocation. Then, the animals were disinfected using 70% ethanol and placed on their backs. The ventral midline was incised and the skin was retracted and pinned to a polystyrene board with cannulas. Axillary and inguinal lymph node like structures were spotted and removed. The intestinal cavity was opened up and thymus, spleen, and further lymph node like structures were harvested and placed in medium until processing (on ice, if no further cultivation but flow cytometry analysis was intended). The location of lymphatic organs in the mouse is depicted in Figure 7. If desired, femur and tibia of the animals were removed for bone marrow preparation.

To isolate splenocytes, the spleen was put in a dish with RPMI-1640 medium and its capsule was slightly scarified with a 100 µl pipette tip. Then, a 2 ml pipette was used to crush the spleen and with this extract the cells. The suspension was subsequently passed through a 70 µm cell strainer which was rinsed once with 15 ml medium to collect remaining cells. Alternatively, the entire spleen was placed on the 70 µm cell strainer, mashed with the plunger end of a syringe and pushed through the strainer. The cells were centrifuged for 5 minutes at 1200 rpm (Heraeus Multifuge 3SR^{+}) and the pellet was resuspended in 2 ml Red Blood Cell Lysis Buffer (5 min, room temperature) to lyse erythrocytes.

Then, ≥ 5 ml of PBS w/o Ca^{2+}/Mg^{2+} or medium were added and the splenocytes were spun down again as described above. The cells were resuspended in the desired volume of FACS-wash for flow cytometry analysis (2.2.3.8), MACS buffer for magnetic cell separation (2.2.3.5) or RPMI-1640 medium supplemented with 10% FCS and 1% penicillin/streptomycin/L-glutamine for cultivation purposes.

To gain bone marrow cells, femur and tibia of the animals were removed, thoroughly cleaned from muscle tissue and briefly sterilized in 70% ethanol. The ends of the bones were cut off and the bones were flushed with 5 ml medium per bone, e.g. dendritic cell medium (see Table 5), using a syringe and a 25 G needle. A single cell suspension was obtained by vigorous pipetting. The cells from one leg were pooled and pelleted at 1200 rpm for 5 min (Heraeus Multifuge 3SR^{+}). The cell pellet was then solved in 1.5 ml Red Blood Cell Lysis Buffer and incubated for 1 min at room temperature. After washing with 10 ml medium or FACS-wash, the cells isolated from one mouse were resuspended in 10 ml medium for further cultivation or FACS-wash for immediate flow cytometry analysis.

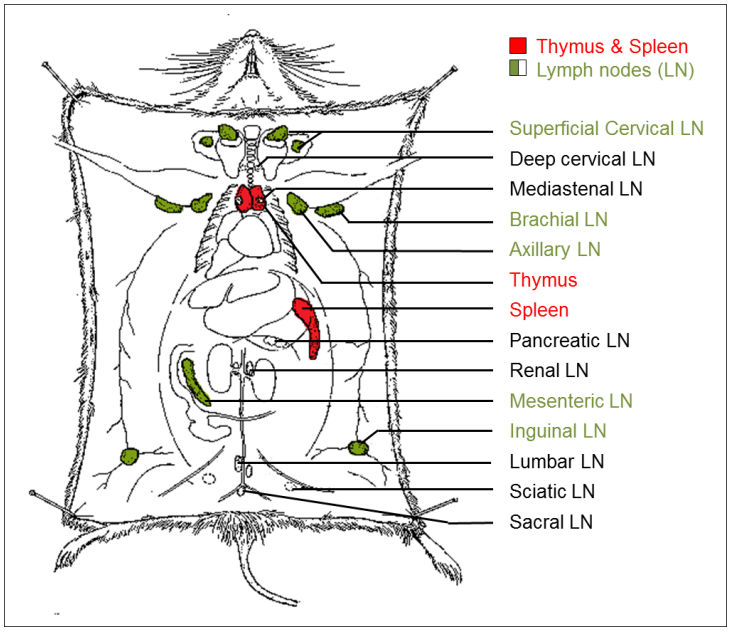

Figure 7: Location of lymph nodes, thymus and spleen in the mouse. Lymph node like structures in green were removed during final imaging of the animals. Figure modified after Dunn, 1954.

3. Results

This thesis describes the generation and characterization of lentiviral vectors (LVs) engineered to enable selective protein or gene transfer into signaling lymphocyte activation molecule (SLAM)-positive antigen presenting cells (APCs) or CD4-positive T lymphocytes, respectively. Targeting of these vectors is based on pseudotyping with measles virus (MV) glycoproteins (GPs), either exploiting the natural tropism of wild-type hemagglutinin (H) for SLAM, or displaying a designed ankyrin repeat protein (DARPin) specific for human CD4 on receptor blind H. After assessment of receptor-specificity, SLAM-targeted vectors were shown to stimulate cellular immune responses upon model antigen ovalbumin (Ova) protein transfer into APCs *in vitro* and *in vivo*. Similarly, CD4-targeted vectors were demonstrated to enable specific and efficient gene delivery into $CD4^+$ cells *in vitro* and as the first lentiviral vector also *in vivo* upon systemic application.

3.1. Targeted protein transfer into $SLAM^+$ cell lines and antigen presenting cells

3.1.1. MV H_{wt} tropism – identification of Nectin-4 as EpR

As outlined above, signaling lymphocyte activation molecule (SLAM)-targeted lentiviral vectors should be generated enabling specific modification of $SLAM^+$ antigen presenting cells (APCs). The desired specificity for SLAM should be achieved by pseudotyping lentiviral vectors with MV_{wt} glycoproteins (GPs), which use SLAM (CD150) as the main cell entry receptor (Tatsuo et al., 2000). However, besides CD150 an epithelial receptor (EpR) for MV_{wt} hemagglutinin was predicted (see 1.2.2). To define all target cell receptors and thus target cell populations for MV_{wt}-GPs and assess potential SLAM-independent off-target effects, identification of the unknown EpR had been crucial. All experiments associated with the search for the EpR were performed using recombinant wild-type IC-B strain derived measles virus expressing GFP in pre N position (MV_{wt323}-GFP(N)) which was amplified and titrated as described in 2.2.4.1 and 2.2.4.2.

Potential receptor proteins had already been spotted by a mRNA-based, genome-wide expression analysis comparing MV_{wt323} permissive epithelial cell lines (H358, H441, HT-1376) with non-permissive ones (H23, H522, T24, SCaBER). The underlying data had been derived from an microarray by Dr. Mühlebach, Paul-Ehrlich-Institut (Mühlebach et al., 2011). Then, receptor-negative and therefore non-permissive Chinese hamster ovary (CHO) cells were transfected by S. Prüfer, Paul-Ehrlich-Institut, with expression plasmids encoding 30 EpR candidates (cloned by A. Schnoor Cancio and S. Prüfer). These 30 selected EpR candidates were surface-exposed proteins, preferentially expressed in the permissive cell lines or with interesting biological properties. 48 hours after transfection, cells were infected with GFP-expressing MV_{wt323} at MOI 1 by S. Prüfer. Out of these 30

transmembrane proteins 29 did not confer susceptibility to MV_{wt323} infection. The same was true for 22 proteins tried in a previous screen (by Dr. Leonard, Mayo Clinic, USA) based on an already published mRNA-microarray (Wagner et al., 2007). Only upon transfection of a Nectin-4 expression plasmid, infection with MV_{wt323} and syncytia formation was observed by. S. Prüfer (Figure 9A). All other transfected CHO cells expressing the respective proteins, confirmed within this thesis for MST1R as an example by flow cytometry, remained resistant.

To clearly attribute the observed susceptibility to MV_{wt323} infection to Nectin-4 expression, Nectin-4 should be detected in transfected cells. However, in initial attempts, testing four different anti-Nectin-4 antibodies in Western Blot analysis (antibodies GTX116900 by GeneTex, ab57873 by abcam, H00081607-M01A and H00081607-B01P, both by Abnova), no specific signals were detected (data not shown). As an alternative, Nectin-4 expression should be confirmed by flow cytometric analysis. For that purpose, the performance of two primary antibodies recognizing Nectin-4 (N.4.40 kindly provided by Dr. Lopez; Fabre et al., 2002 and LS-C37483 purchased from LifeSpan BioSciences) was evaluated by flow cytometry (2.2.3.8). Both antibodies were specific for Nectin-4 expressed by MV_{wt323} permissive H358 cells while no binding to MV_{wt323} non-permissive H23 cells was observed (Figure 8). However, a higher percentage of H358 cells stained positive with the anti-Nectin-4 antibody obtained from LifeSpan BioSciences than with N.4.40 from Dr. Lopez despite ten-times lower concentration of the former antibody. Moreover, cells incubated with the anti-Nectin-4 antibody from LifeSpan BioSciences were characterized by a higher mean fluorescent intensity (MFI) than cells stained by N.4.40. Therefore, the antibody purchased from LifeSpan BioSciences was used for all further analyses.

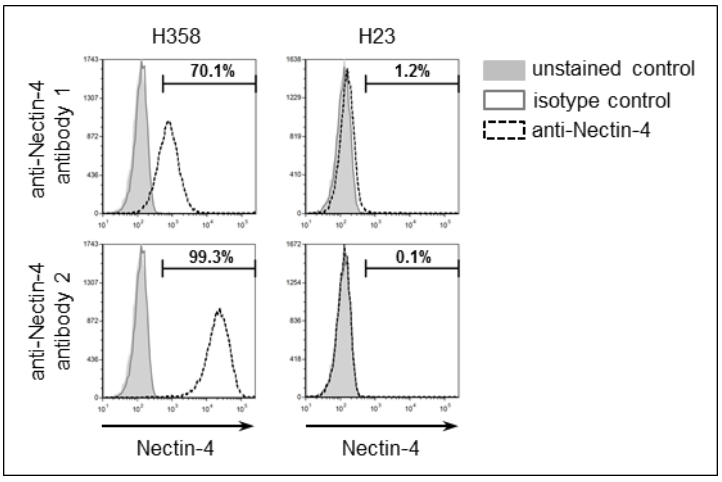

Figure 8: Detection of Nectin-4 by flow cytometry. MV_{wt323} permissive (H358) or none-permissive (H23) epithelial cells were stained with two different primary antibodies against human Nectin-4 to establish a detection protocol. Antibody 1: N.4.40 (10 µg/ml) kindly provided by Dr. Lopez; antibody 2: LS-C37483 (1 µg/ml) purchased from LifeSpan BioSciences. Secondary antibody: PE-conjugated goat anti-mouse Ig.

Using the established staining protocol, Nectin-4 expression in transfected CHO cells susceptible to MV_{wt323} infection was confirmed by flow cytometry analysis (Figure 9A, lower panel).

As this finding pointed at Nectin-4 as putative EpR, Nectin-4 expression was also examined in the seven epithelial cell lines used in the mRNA expression screen for receptor candidates. Indeed, the

permissive cell lines H358, H441, and HT-1376 all stained positive for Nectin-4 whereas the non-permissive cell lines did not express Nectin-4 at all (H23, H522, and T24) or on a considerably lower level than the permissive ones (SCaBER) (Figure 9B). The hypothesis of Nectin-4 being the EpR was further supported by transfection of H358 cells with an siRNA specific for the *nectin-4* mRNA and infection with MV_{wt323} (MOI 0.5) 48 hours after transfection by S. Prüfer. The knock-down of Nectin-4 by approximately 90%, as confirmed in the framework of this thesis by flow cytometric analysis of siRNA transfected cells, nearly ablated the subsequent viral infection (Figure 9C).

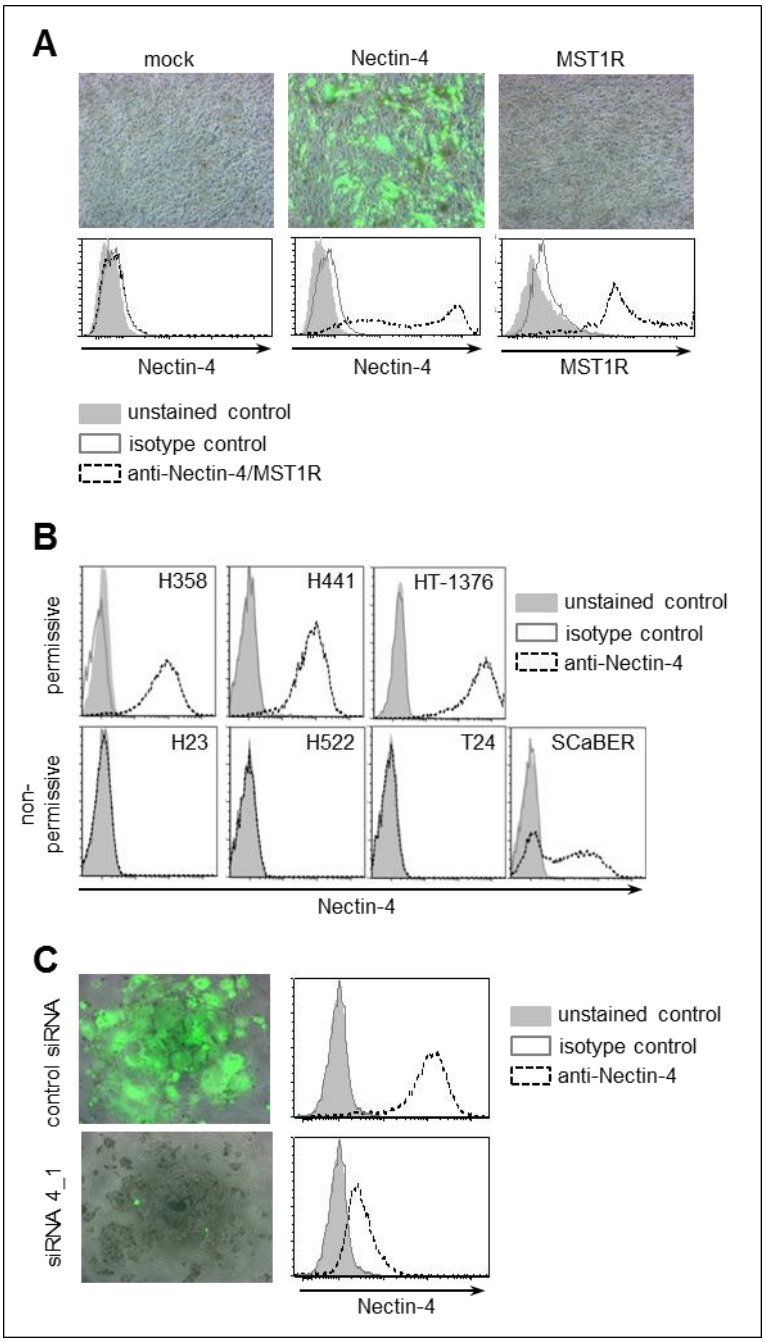

Figure 9: Identification of Nectin-4 as putative EpR. (A) Nectin-4 serves as MV entry receptor. CHO-K1 cells were not transfected (mock) or transfected with expression plasmids for Nectin-4 and macrophage stimulating 1 receptor (MST1R). Cells were infected with MV_{wt323}-GFP(N) at MOI 1 (top). The expression of Nectin-4 and MST1R was confirmed by flow cytometry (bottom). **(B)** Flow cytometric analysis of Nectin-4 expression in epithelial cell lines. H358, H441, and HT-1376 are permissive for MV infection, whereas H23, H522, T24, and SCaBER are non-permissive. **(C)** Knockdown of Nectin-4 expression impedes MV infection. H358 cells were mock transfected (control) or transfected with Nectin-4-specific siRNA 4_1. 48 h after transfection, H358 cells were infected with MV_{wt323}-GFP(N) at MOI 0.5. Flow cytometry analysis confirmed down-regulation of Nectin-4 (right panel). Figure modified after Mühlebach et al., 2011.

Nectin-1, Nectin-2, and PVR (polio virus receptor), all belonging to the PVR/ nectin family which also comprises Nectin-4, are used as receptors by alpha-herpesviruses (Nectin-1 and Nectin-2), and poliovirus (PVR) (Mendelsohn et al., 1989; Campadelli-Fiume et al., 2000). As it is, moreover, not uncommon that related proteins interact with the same virus, the question arose whether also other PVR/ nectin family members could serve as MV receptors. To address this issue, CHO-derived cell lines stably expressing Nectin-1, Nectin-2, Nectin-4 or PVR were received by a collaboration laboratory (Dr. Lopez, INSERM, France) and the respective transgene expression was confirmed by flow cytometry analysis (2.2.3.8). CHO-Nectin-3 were not included as Nectin-3 had already been tested in a previous screen and did not confer permissiveness to MV infection (Mühlebach et al., 2011). All transgenic cell lines expressed the respective nectin at similar or higher density than CHO-Nectin-4 (Figure 10, lower panel). When these cells were infected by S. Prüfer with MV_{wt323}-GFP(N), green fluorescing cells and syncytia formation were only observed in CHO-Nectin-4 cells (Figure 10, upper panel). Thus, none of the other nectins did enable MV_{wt323} infection meaning that only Nectin-4 has receptor properties.

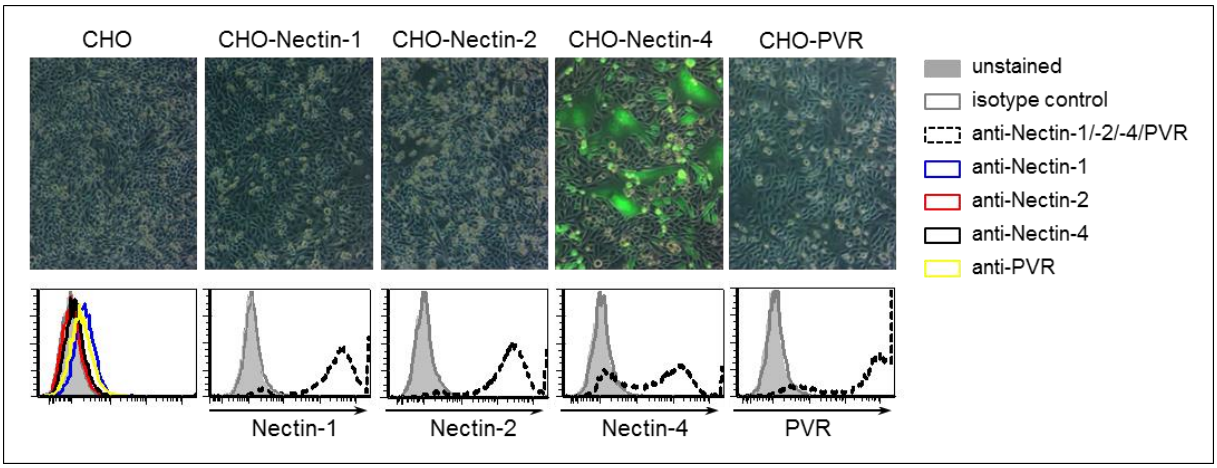

Figure 10: Nectin-4 is the only PVR/ nectin family member which serves as MV receptor. Chinese hamster ovary (CHO) cells stably expressing different PVR/ nectin family members were infected with MV_{wt323}-GFP(N) (top row). Transgene expression of cells was confirmed by flow cytometry (bottom row). Figure modified after Mühlebach et al., 2011.

An often observed phenomenon upon virus infection is the down-regulation of the respective cellular receptor in infected cells. Therefore, to analyze if also Nectin-4 is down-regulated upon infection with MV_{wt323}, the bladder epithelial cell line HT1376 and the lung epithelial cell line H358 were infected with MV_{wt323} at MOI 1. Two hours later, the fusion inhibiting peptide FIP [200 µM] (Richardson et al., 1980) was added to prevent syncytia formation which would hamper flow cytometric analysis of surface protein expression levels. 48 hours after infection, Nectin-4 expression was analyzed by flow cytometry (2.2.3.8). MV_{wt323} infection indeed induced an approximately 5-fold reduction of the median Nectin-4 surface expression compared to uninfected control cells (Figure 11). This finding further strengthened the evidence of Nectin-4 being the EpR.

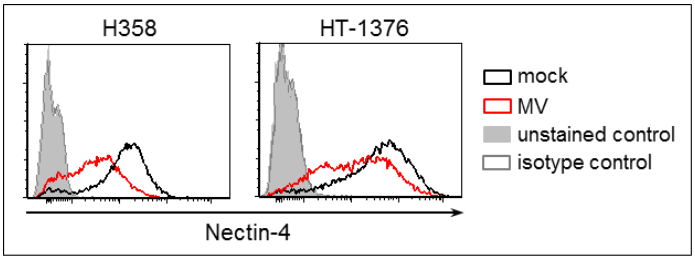

Figure 11: Downregulation of Nectin-4 after MV infection. H358 lung epithelial cells or HT-1376 bladder epithelial cells were infected with MV_{wt323}-GFP(N) at MOI 1. 2 h later, fusion inhibiting peptide FIP [200 µM] was added. Nectin-4 expression levels were determined 48 h after infection by flow cytometry. Figure modified after Mühlebach et al., 2011.

Taken together, the obtained data strongly suggested adherens junction protein Nectin-4 as the epithelial receptor for MV_{wt323}. Besides, further experiments confirmed Nectin-4 as the epithelial receptor for MV wild-type and vaccine strains (Mühlebach et al., 2011).

3.1.2. Optimizing the production of GFP-PTVs

After identification of Nectin-4 as secondary receptor for MV_{wt323}, this thesis concentrated on production of lentiviral vectors as protein carriers in the next step.

Retroviral vectors have not only been shown to transfer their genome, but also heterologous cargo proteins into transduced cells if those are genetically fused to the structural proteins of the respective vector particles (Voelkel et al., 2010). Thereby, a promising novel concept of protein delivery for transient cell modification was introduced. Here, protein transfer vectors (PTVs) derived from HIV-1 should be used for targeted antigen-transfer into antigen presenting cells (APC), allowing vaccination with a new platform technology. First, a protocol for the generation of cargo protein transferring particles needed to be set up to establish the production of LV particles allowing maximum protein and gene delivery into transduced cells. To this end, HEK-293T cells were transfected (2.2.3.3, Lipofectamine® 2000 transfection) with varying ratios of unmodified packaging plasmids to packaging plasmids additionally encoding GFP fused to matrix within the Gag polyprotein, together with constant amounts of VSV-G expression plasmid and transfer vector comprising the *turboFP635* marker gene sequence, which codes for the red-fluorescent Katushka protein (Figure 12). Subsequently, HT1080 cells were transduced with the resulting vector-containing supernatants and PTV-mediated protein or gene delivery into HT1080 cells were visualized by flow cytometric analysis of GFP or Katushka fluorescence, respectively (2.2.3.8).

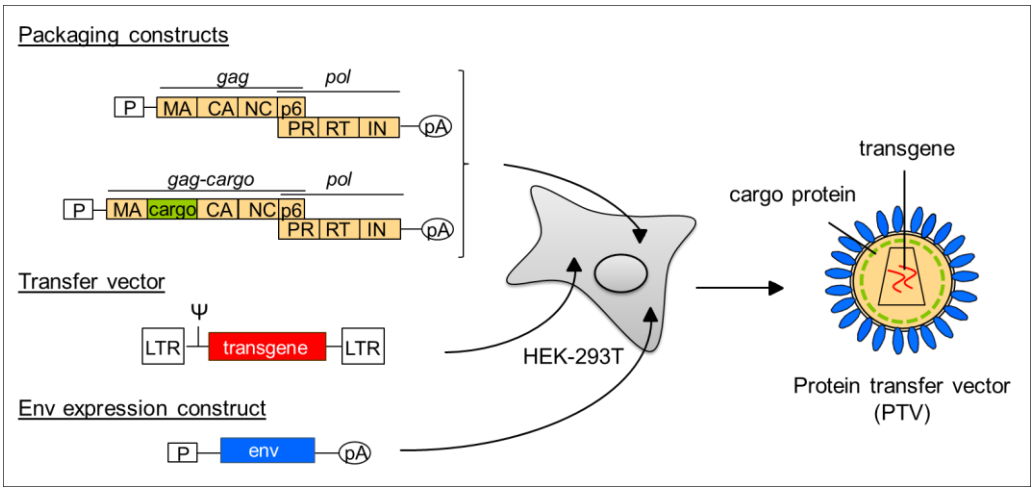

Figure 12: Generation of lentiviral protein transfer vectors. Lentiviral protein transfer vectors (PTVs) were generated by transient transfection of HEK-293T cells with packaging plasmids (encoding the structural proteins of the vector) with or without cargo protein encoding sequence, transfer vector (harboring the transgene) and env expression plasmid, coding for the envelope protein. 2 d after transfection, vector-containing supernatant was harvested and particles were either directly used or concentrated by ultracentrifugation through a 20% sucrose cushion. CA, capsid; IN, integrase; LTR, long terminal repeat; MA, matrix; NC, nucleocapsid; P, promoter; pA, polyadenylation signal; PR, protease, RT, reverse transcriptase; Ψ, packaging signal.

Increasing the relative amounts of cargo-encoding *gag-gfp/pol* compared to *gag/pol* for vector production positively correlated with GFP transfer into transduced target cells, and reciprocally correlated with *turboFP635* marker gene delivery (Figure 13). However, when no wild-type *gag/pol* was supplemented for particle generation, i.e. the vectors were composed of Gag-GFP/Pol only, GFP transfer into HT1080 cells was significantly limited and gene transfer was not observed at all (Figure 13), indicating absence of functional particles. The optimal ratio of GFP protein and *turboFP635* gene transfer was obtained for PTV particles produced in HEK-293T cells transfected with equal amounts of Gag-GFP/Pol and Gag/Pol encoding packaging plasmids (Figure 13). Thus, this 1:1 ratio was further used for PTV generation. The only exception were PTVs transferring Cre recombinase. For such vectors, the optimum was determined at a ratio of 2:1 for *gag/pol* to *gag-cre/pol* within the Bachelor thesis of Johannes Reusch (Reusch, 2013).

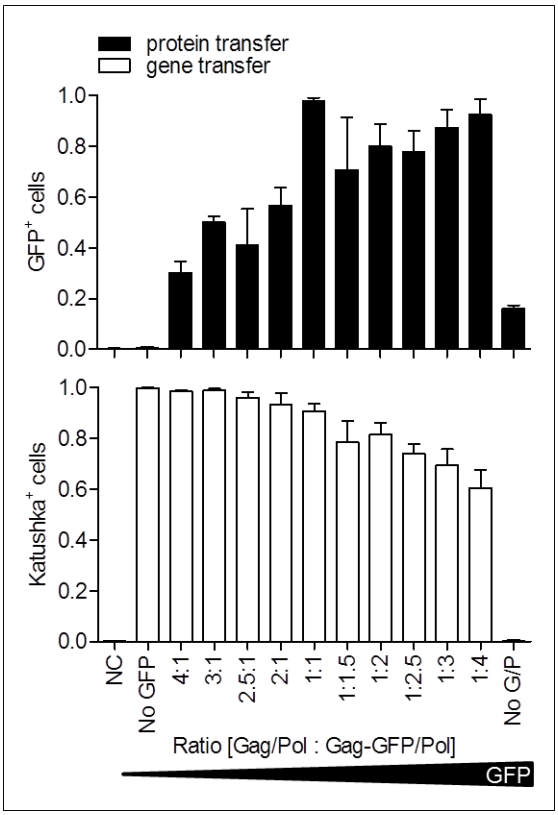

Figure 13: Impact of the ratio of untagged *gag/pol* to *gag-gfp/pol* for PTV generation on protein and gene transfer into transduced target cells. Vector particles were produced with the indicated ratios of *gag/pol* to *gag-gfp/pol*, *gag/pol* (No GFP) or *gag-gfp/pol* (no G/P) packaging plasmids. The total amount of DNA used for transfection of packaging cells was kept constant for all ratios. 72 h after transfection of packaging cells, unconcentrated, vector-containing supernatant was cleared and immediately used to transduce HT1080 cells. HT1080 cells incubated with vector-free cell culture medium served as negative control (NC). 4 h after transduction, protein transfer was assessed by flow cytometric analysis of GFP fluorescence. Transfer of the *turboFP635* marker gene was quantified 72 h after transduction by flow cytometric detection of red-fluorescing Katushka marker protein. Maximum protein or gene transfer (% transduced of all cells) of three independent experiments was set to 1, all other transduction rates were calculated accordingly. Results are depicted as mean ± SEM (n = 3). Figure modified after Uhlig et al., 2015.

To assess if the decreasing infectivity of particles produced with increasing amounts of *gag-gfp/pol* (Figure 13) may be due to altered steric needs of the Gag-GFP polyprotein entailing changes in particle structure, a set of vectors should be generated and morphologically analyzed. For that purpose, HEK-293T cells were transfected (2.2.4.3) with VSV-G expression plasmid, transfer vector pSEW-TurboFP635 and either only *gag/pol*, equal amounts of *gag-gfp/pol* and *gag/pol* or only *gag-gfp/pol* packaging plasmid(s). Then, vector-producing packaging cells were fixed with 10% glutaraldehyde and handed to Anke Muth and Regina Eberle, both Paul-Ehrlich-Institut, who kindly performed electron microscopic (EM) analysis of ultrathin sections of those. The fixed packaging cells were expected to be associated with a high density of assembling and budding particles.

Whereas lentiviral gene transfer vectors and PTVs generated using equal amounts of *gag-gfp/pol* and *gag/pol* were phenotypically indistinguishable from each other by EM and present in similar quantities (Figure 14 and data not shown), notably less PTV particles were detected when produced in packaging cells transfected with only *gag-gfp/pol* (data not shown). The particles exclusively composed of GFP-tagged Gag were further characterized by an aberrant morphology, including gaps in the particles' Gag layer and were only pseudotyped by moderate amounts of irregularly arranged VSV-G envelope glycoproteins (Figure 14).

Taken together, EM clearly demonstrated an impact of the relative amount of *gag-gfp/pol* used for transfection of HEK-293T packaging cells and hence the amount of heterologous cargo protein incorporated into vector particles on the morphology of originating PTVs. Particles exclusively

composed of GFP-tagged Gag showed morphological abnormalities. The data strengthen the 1:1 ratio of *gag-gfp/pol* to *gag/pol* identified as most suitable for PTV production.

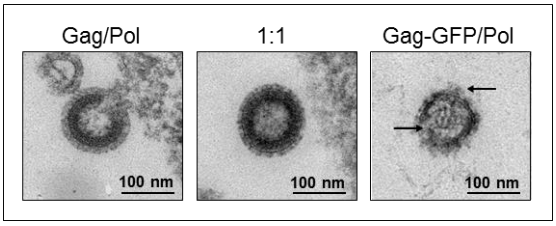

Figure 14: Electron microscopy of ultrathin slices of packaging cells releasing PTVs. HEK-293T cells were transfected with all plasmids necessary to produce VSV-G pseudotyped PTVs. The structure of released particles produced with an equal amount of *gag/pol* to *gag-gfp/pol* (1:1) was compared to particles produced with only *gag-gfp/pol* (Gag-GFP/Pol) and conventional gene transfer vectors (Gag/Pol) devoid of GFP. Arrows point at gaps in matrix layer and irregularly arranged VSV-G envelope glycoproteins. Figure modified after Uhlig et al., 2015.

To analyze whether titers and protein transfer efficiencies of PTVs could be further improved, HEK-293T cells were transfected (2.2.3.3) with varying ratios of packaging plasmids to transfer vector and expression construct (here encoding VSV-G). Vector-containing supernatants were harvested from packaging cells, and CHO-hSLAM cells were transduced (2.2.4.5) with similar volumes of unconcentrated vector suspension or concentrated vector stock after ultracentrifugation through a 20% sucrose cushion. Transduction was followed by flow cytometric analysis (2.2.3.8) of GFP delivery (four hours after transduction) or Katushka expression (three days after transduction) indicating protein or gene transfer, respectively.

Particles produced in packaging cells transfected with a relative ratio of 0.87 (VSV-G expression plasmid) to 1.62 (sum of Gag-(GFP)/Pol expression plasmids) to 2.5 (transfer vector) delivered GFP protein and *turboFP635* marker gene into 11.0 ± 2.8% and 74.9 ± 34.1% of target cells, respectively (Figure 15, ratio A). Increasing the relative amount of Gag-(GFP)/Pol expression constructs while reducing envelope expression plasmid and transfer vector amount, both protein and gene transfer efficiencies could be further improved, as demonstrated by detection of 31.7 ± 11.6% and 92.6 ± 6.4% (Figure 15, ratio B) or 55.2 ± 25.5% and 95.5 ± 3.8% (Figure 15, ratio C) GFP^+ and $Katushka^+$ HT1080 cells, respectively. Thus, the amount of *gag(-gfp)/pol* packaging plasmids transfected into HEK-293T cells in the course of vector production positively correlated with the ability of the resulting PTV particles to mediate GFP protein transfer into target cells.

Since vector particles assembled in packaging cells transfected with the ratio of 2.3 (packaging plasmids) to 0.5 (env expression plasmid) to 1.6 (transfer vector) mediated highest protein and gene delivery into transduced target cells (Figure 15, ratio C), this relative plasmid ratio was kept for further particle productions. MV_{wt}-GP pseudotyped PTVs were generated likewise, only the amount of plasmid-DNA encoding VSV-G was distributed between H (37.5%) and F (62.5%) expression constructs as previously described (Funke et al., 2009).

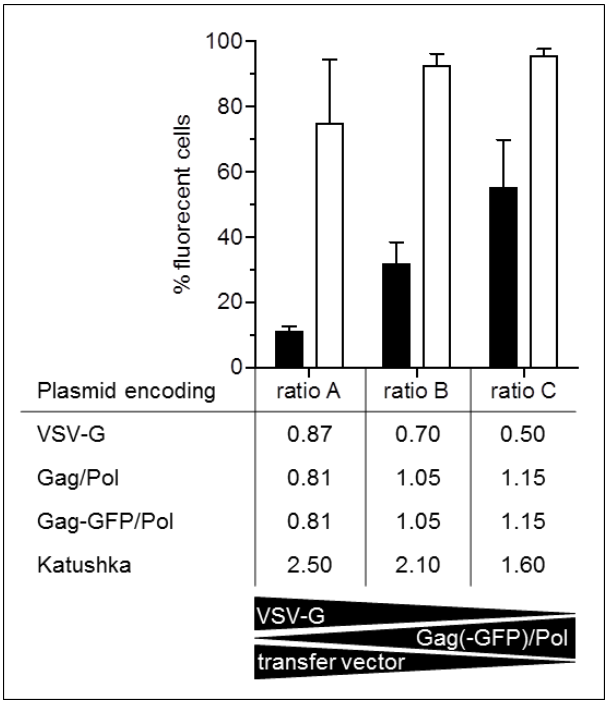

Figure 15: Improvement of plasmid ratios for PTV production. HEK-293T cells were transfected with the indicated relative plasmid amounts and vector containing supernatant was harvested 2 d later. Vector particles were either directly used for transduction or further concentrated by ultracentrifugation through a 20% sucrose cushion. Then, CHO-hSLAM cells were transduced by similar volumes of each vector. Transduction efficiency was determined by flow cytometric analysis of GFP fluorescence (4 h after transduction) and Katushka fluorescence (72 h after transduction). Black bars, GFP protein transfer; white bars, *turboFP635* gene transfer. Mean ± SEM of n = 3 experiments performed in triplicates are shown. Figure modified after Uhlig et al., 2015.

3.1.3. Generation of HIV-1 packaging plasmids encoding different cargo proteins

The production of PTVs was established using the reporter protein GFP (3.1.2). As presented in the preceding chapter, GFP provides an appropriate tool for the initial characterization of PTVs and their generation since it allows easy visualization of successful protein transfer. However, GFP does not allow discrimination between surface adhesion of vectors and incorporated cargo proteins to the cells and cytoplasmic protein transfer. Moreover, it is not designed for immunological studies. For those purposes, the use of either the recombinase Cre, which requires nuclear localization to exert its function and therefore can act as indicator for intracellular protein transfer, or the model antigen Ova was intended. Fusion of the cargo nucleotide sequence to *matrix* ensures packaging into PTVs as part of the Gag/Pol precursor but also sequesters the matrix-cargo fusion protein at the target cell membrane. However, free release of cargo proteins into the target cell's cytosol is preferable for the named applications, i.e. transfer of Cre recombinases being active in the nucleus or model antigen ovalbumin requiring processing as cytoplasmic cellular content. As Gag/Pol is posttranslationally cleaved by the HIV-1 protease during maturation of budding particles, separation of cargo from matrix protein can be achieved by inserting an additional HIV-1 protease recognition site between the sequence of the antigen gene and *matrix*. This should result in free cytosolic release of the cargo protein without impairing packaging into the vector particles. Initially, the functionality of such an inserted artificial HIV-1 protease motif was tested for the marker protein GFP, again for reasons of easy visualization of unaffected cargo protein function and transfer into transduced target cells.

For that purpose, a HIV-1 packaging plasmid encoding matrix and GFP separated by a HIV-1 protease site was cloned based on the plasmid pcDNA3.gpGFP.4xCTE used before, coding for the matrix-GFP fusion protein within the *gag* open reading frame (ORF) (Figure 16). First, the 3' end of *matrix* and a second fragment composed of the *gfp* gene and the 5' end of *capsid* were amplified by PCR (2.2.1.5) using the primer pairs HIVgag-ClaI(+) / MA-Prot(-) and MA-Prot-GFP(+) / HIVgag-BaeI(-), respectively (see Table 10). Thereby, the oligonucleotides MA-Prot(-) and Prot-Ca(+) (Table 10) introduced the sequence of the additional HIV-1 protease site 3' of *matrix* and 5' of *gfp*. In a primer-extension PCR (Horton et al., 1989) with the flanking primers HIVgag-ClaI(+) and HIVgag-BaeI(-) and both PCR fragments amplified in the first round serving as templates the entire cassette consisting of the 3' end of *matrix*, the additional protease recognition site, *gfp* and the 5' end of *capsid* was assembled. The PCR product was directly ligated into pCR2.1-TOPO (2.2.1.6) and the insert of the resulting plasmid pCR2.1HIV1_Ma_P_GFP was sequenced (2.2.1.9), confirming the absence of mutations. Then, pcDNA3.gpGFP.4xCTE and pCR2.1HIV1_Ma_P_GFP, both amplified in Dam methylation deficient *E. coli* GM2163, were digested with *Cla*I/*Pfo*I and the insert of pCR2.1HIV1_Ma_P_GFP was cloned into the backbone of pcDNA3.gpGFP.4xCTE. The newly generated plasmid was named pcHIV1_MA_P_GFP.

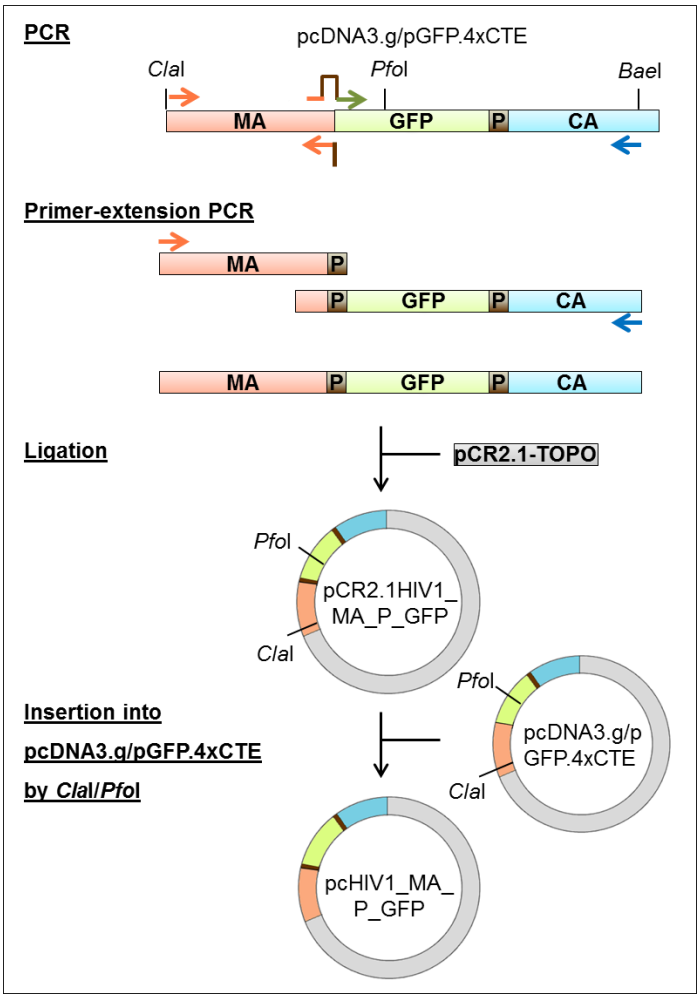

Figure 16: Schematic overview - generation of pcHIV1_MA_P_GFP. To obtain pcHIV1_MA_P_GFP, an additional HIV-1 protease cleavage site (P) was introduced between *matrix* (MA) and *gfp* in the *gag* ORF of the packaging plasmid pcDNA3.g/pGFP.4xCTE. CA, *capsid*. Color code: blue, *capsid*; brown, HIV-1 protease cleavage site; green, *gfp*; gray, plasmid backbone; salmon, *matrix*. For the sake of simplicity, the scheme shows only relevant cleavage sites of the enzymes, even if they are multiple cutters.

To enable examination of PTVs' immunostimulatory properties, the coding sequence for model antigen *ovalbumin* was cloned within the *gag* ORF flanked by two HIV-1 protease recognition sites. For that purpose, the 3' end of *matrix* and the 5' end of *capsid* were amplified by PCR (2.2.1.5) using the template pcMVΔR8.9 and the primer pairs HIVgag-ClaI(+) / MA-Prot(-) and Prot-ClaI(+) / HIVgag-BaeI(-), respectively. The plasmid pET15b-Ova served as template for the PCR-amplification of the *ovalbumin* gene (using the primers pair MA-Prot-Ova(+) / CA-Prot-Ova(-), see Table 10), those 3' and 5' end were elongated by the coding sequence of a HIV-1 protease cleavage site (introduced by primers). All three DNA fragments were subsequently fused by a primer-extension PCR (Horton et al., 1989) using the flanking primers HIVgag-ClaI(+) / CA-Prot-Ova(-). The PCR product was ligated into pCR2.1-TOPO (2.2.1.6) and the resulting plasmid pCR2.1HIV1_MA_P_Ova was sequenced (2.2.1.9), confirming the absence of mutations. To allow directed subcloning, pCR2.1HIV1_MA_P_Ova was linearized with *Nsi*I, dephosphorylated using Antarctic phosphatase (2.2.1.6) and elongated at its 3' end by a 1.64 kb *gag* sequence derived from *Nsi*I cleaved pcDNA3.gpGFP.4xCTE. The insert orientation of the resulting plasmid pCR2.1-gag-Ova.NsiI was determined by an analytical restriction with *Cla*I and *Sbf*I (2.2.1.4). Plasmids with the desired insert orientation were digested with *Cla*I/*Sbf*I and the excised sequence was transferred into pcDNA3.gpGFP.4xCTE to generate pcHIV1_MA_P_Ova. The complete cloning strategy is depicted in Figure 17.

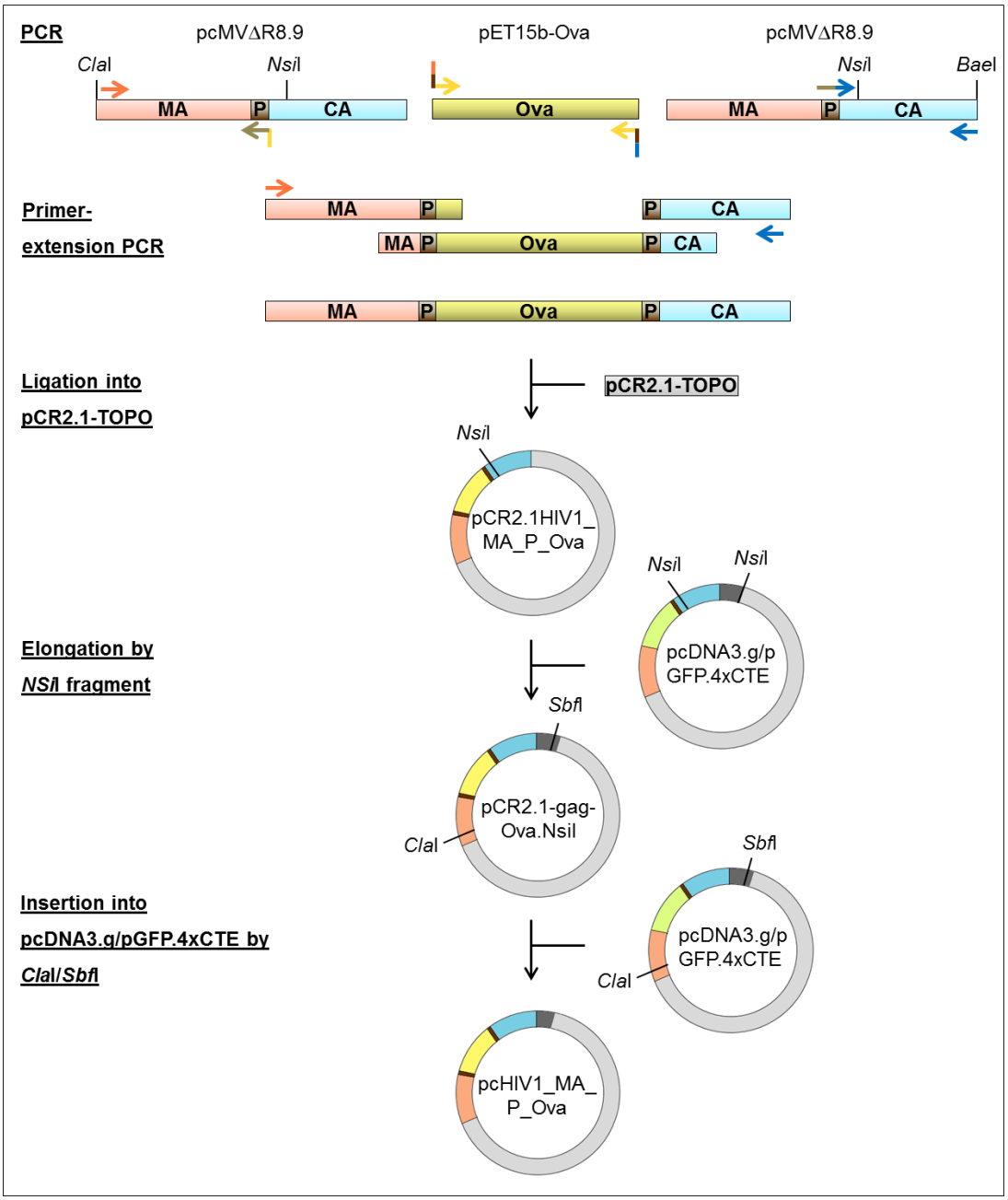

Figure 17: Schematic overview - generation of pcHIV1_MA_P_Ova. pcHIV1_MA_P_Ova encodes matrix (MA)-fused Ova within the *gag* ORF. Ova is flanked by HIV-1 protease cleavage sites (P). CA, *capsid*. Color code: brown, HIV-1 protease cleavage site; dark gray, *gag* fragment; green, *gfp*; gray, plasmid backbone; light blue, *capsid*; salmon, *matrix*; yellow, *ovalbumin*. For the sake of simplicity, the scheme shows only relevant cleavage sites of the enzymes, even if they are multiple cutters.

pcHIV1_MA_P_Cre, the expression plasmid encoding Gag-Cre/Pol with HIV-1 protease recognition sites flanking Cre, was generated by Johannes Reusch within his bachelor thesis at Paul-Ehrlich-Institut, as described in his thesis (Reusch, 2013)

To evaluate cargo protein expression by the newly cloned lentiviral packaging plasmids, the respective plasmids were transfected into HEK-293T cells (2.2.3.3, transfection with Lipofectamine® 2000). 48 hours after transfection, cells were lysed (2.2.2.1) and lysates were subjected to Western Blot

analysis (2.2.2.3). Lysates of non-transfected cells and cells transfected with unmodified HIV-1 *gag/pol* packaging plasmid served as negative controls whereas the lysate of HEK-293T transfected with a Cre expression plasmid represents a positive control.

Figure 18 shows efficient expression of all cargo proteins encoded within the *gag* ORF by HEK-293T packaging cells. Thereby, GFP, Cre, and Ova were detected at the expected molecular weight of the cargo protein, i.e. 27 kDa, 38 kDa or 43 kDa, respectively, and as fusion with 55 kDa Gag-polyprotein or 17 kDa matrix, precisely as Gag-GFP (82 kDa) and matrix-GFP (44 kDa) (Figure 18A), Gag-Cre (93 kDa) and matrix-Cre (55 kDa) (Figure 18B) or Gag-Ova (98 kDa) (Figure 18C). Moreover, also degradation products of Cre were observed at approximately 30 kDa (Figure 18B). Of note, whereas in lysates of HEK-293T cells transfected with pcHIV1_MA_P_GFP free GFP was present, essentially no free GFP was detected in lysates of HEK-293T cells transfected with pcDNA3.g/p.4xCTE, not encoding the artificial HIV-1 protease motif between matrix and cargo.

Thus, Western Blot analysis revealed efficient expression of GFP, Cre, and Ova cargo proteins by the packaging plasmids and functionality of the HIV-1 protease site introduced between MA and cargo.

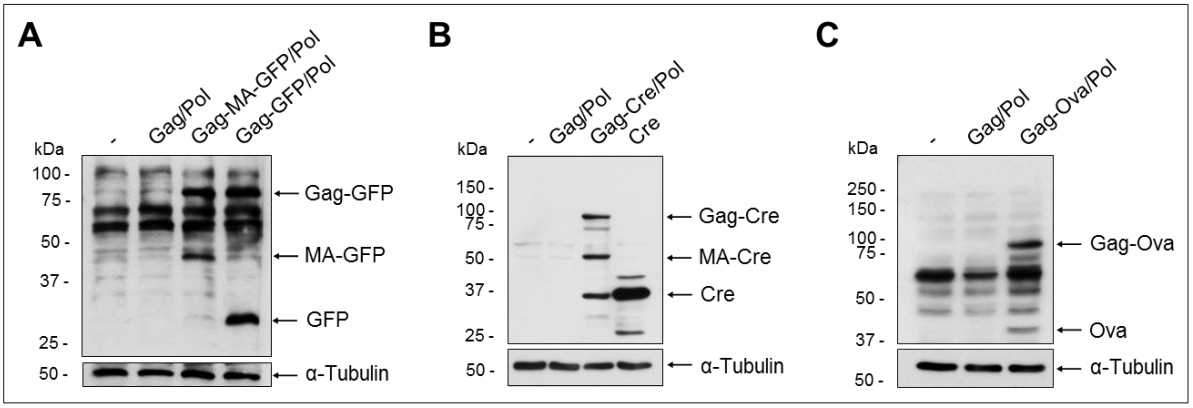

Figure 18: Expression of cargo proteins encoded within the *gag* ORF of HIV-1 packaging plasmids. HEK-293T cells were left untransfected (-) or transfected with HIV-1 packaging plasmids encoding the indicated Gag(-Cargo)/Pol proteins. 48 h after transfection, cells were lysed and lysates were subjected to anti-GFP **(A)**, anti-Cre **(B)** or anti-Ova **(C)** Western Blot analysis (upper panels) after normalization to total protein content visualized by anti-α-Tubulin Western Blot analysis (lower panels). Figure modified after Uhlig et al., 2015.

3.1.4. Characterization of PTVs for antigen content, morphology and titers

The previously cloned (3.1.3) *gag-cargo/pol* expression plasmids were used for production of MV_{wt}-GP- or VSV-G-pseudotyped PTVs or PTVs devoid of envelope glycoproteins (2.2.4.3). Concentrated vector particles, purified by ultracentrifugation through a 20% sucrose cushion, were subsequently analyzed for cargo protein incorporation, cargo content, morphology, and infectious titers.

To assess if cargo proteins were packaged into PTV particles, purified PTV preparations were subjected to Western Blot analysis (2.2.2.3). As controls, respective *turboFP635* gene transfer vectors, delivering no cargo proteins, were generated and analyzed in parallel.

Matrix-GFP (44 kDa), GFP (27 kDa), Cre (38 kDa) or Ova (43 kDa) were detected in lysates of the respective PTVs in agreement with the expected molecular weights (Figure 19). Additionally, in lysates of Cre-transferring particles, degradation products of the recombinase were observed (Figure 19C). The data demonstrate efficient particle-incorporation of cargo proteins and successful release of GFP, Cre or Ova by the HIV-1 protease in particles including the artificial HIV-1 protease motif between matrix and cargo (Figure 19B-D), but not of MA-GFP in particles lacking this motif (Figure 19A).

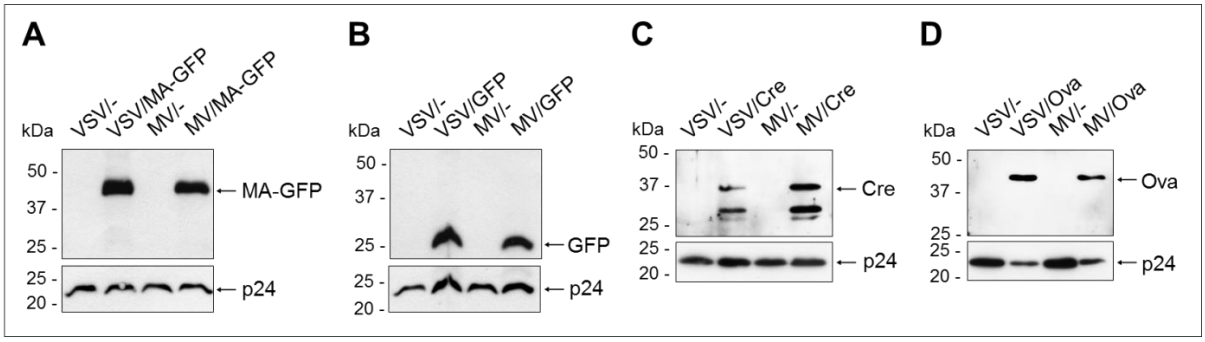

Figure 19: Efficient incorporation of cargo proteins into protein transfer vector particles. Concentrated PTVs were subjected to Western Blot analysis to detect incorporation of matrix-fused GFP (MA-GFP) **(A)**, GFP **(B)**, Cre **(C)** and Ova **(D)** into vector particles (upper panels) after normalization to p24 content (lower panels). Vectors were pseudotyped with VSV-G (VSV) or MV_{wt}-GPs (MV), transferred cargo proteins are indicated after the slash. Gene transfer vectors (VSV/- and MV/-), delivering no cargo proteins, served as negative controls. Figure modified after Uhlig et al., 2015.

Having shown incorporation of cargo proteins into PTV particles, in principle, we next aimed to quantify the amount of incorporated cargo protein. As cargo protein content was especially interesting for Ova-PTVs, enabling direct comparison of immune-stimulatory efficiencies of Ova-PTVs and particle-free, recombinant Ova protein, antigen content was assessed semiquantitatively for these PTV particles by Western Blot analysis (2.2.2.3) or by ELISA (2.2.2.4). When comparing equal volumes of vector lysates by Western Blot analysis, incorporation of different amounts of Ova in various PTVs was observed (Figure 20). VSV-G pseudotyped PTVs were characterized by a significantly lower Ova content than MV_{wt}-GP pseudotyped or bald ones, i.e. particles possessing no envelope glycoproteins (Figure 20).

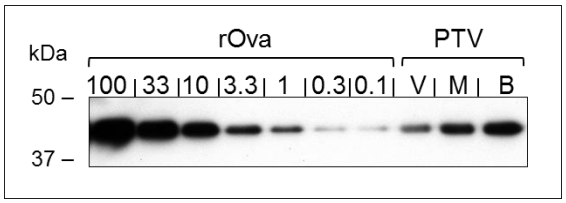

Figure 20: Determination of Ova content in PTV preparations by Western Blot analysis. PTVs devoid of envelope glycoproteins (bald, B) or pseudotyped with VSV-G (V) or MV_{wt}-GPs (M) were produced, harvested, concentrated and purified by ultracentrifugation through a 20% sucrose cushion. Ova content of vectors was assessed by Western Blot analysis, comparing 0.2 µl PTV stocks to a decreasing concentration of recombinant Ova [ng].

The findings of Western Blot analysis were confirmed by ELISA revealing the Ova content of VSV-Ova-$LV_{Katushka}$ to be approximately 1.8 or 2.3 times less than of MV_{wt}-Ova-$LV_{Katushka}$ or Bald-Ova-$LV_{Katushka}$ particles, respectively (Table 20, first column). Interestingly, whereas Bald-Ova-$LV_{Katushka}$ and VSV-Ova-$LV_{Katushka}$ particles were characterized by a similar Ova content when related to p24 content (Table 20, fourth column), the cargo content of MV_{wt}-Ova-$LV_{Katushka}$ was about 1.8-fold lower. In contrast, when the Ova content was related to transducing units (t.u.) of the vectors, MV_{wt}-Ova-$LV_{Katushka}$ contained approximately 34 times more Ova than VSV-Ova-$LV_{Katushka}$ (Table 20, last column). Taken together, these data show that 1 ml vector stock contains some microgram Ova. Moreover, they indicate that the amount of cargo protein which can be transferred by a given PTV pseudotype is influenced by the selected normalization method (e.g. normalization by volume, p24 content or transducing units).

Table 20: Determination of Ova content in PTV preparations by ELISA.

Vector	µg Ova/ ml	µg p24/ ml	t.u./ ml[c]	ng Ova/ µg p24	fg Ova/ t.u.[c]
Bald-Ova-$LV_{Katushka}$ [a]	67	395	-	169	-
MV_{wt}-Ova-$LV_{Katushka}$ [a]	52	549	7.2×10^7	95	723
VSV-Ova-$LV_{Katushka}$ [b]	29	172	1.4×10^9	169	21

[a] Mean value of two independent vector stocks. [b] Mean value of first and second harvest of one vector stock. [c] t.u., transducing unit.

To analyze next whether incorporation of cargo proteins into lentiviral particles or introduction of a protease site between cargo and matrix affects particle morphology, HEK-293T cells were transfected to produce PTVs (2.2.4.3), fixed with 10% glutaraldehyde and handed to Anke Muth and Regina Eberle (Paul-Ehrlich-Institut), who performed EM analysis of ultrathin sections of PTVs produced by these cells. All particles were round, approximately 120 nm in diameter and characterized by a consistent core. Interestingly, MA-GFP-PTVs, GFP-PTVs, and the corresponding lentiviral gene transfer vectors were morphologically indistinguishable (Figure 21) and could also not be discriminated from Ova-transferring particles (data not shown). However, bald particles or particles

pseudotyped with VSV-G or MV_{wt}-GPs, respectively, could be easily distinguished. As expected, no envelope glycoproteins were observed for bald particles (Figure 21 A), whereas a dense layer of regularly arranged spikes, presumably VSV-G, surrounded VSV-G pseudotyped particles (Figure 21B, presumed glycoproteins marked by arrows) and several, but compared to VSV-G pseudotyped particles significantly less, envelope protein complexes were detected for MV_{wt}-GP pseudotyped particles (Figure 21C, surface proteins marked by arrows).

Thus, EM revealed particle morphology to be independent from incorporation of cargo proteins or the presence of a HIV-1 protease motif between matrix and cargo but modulated by envelope glycoproteins.

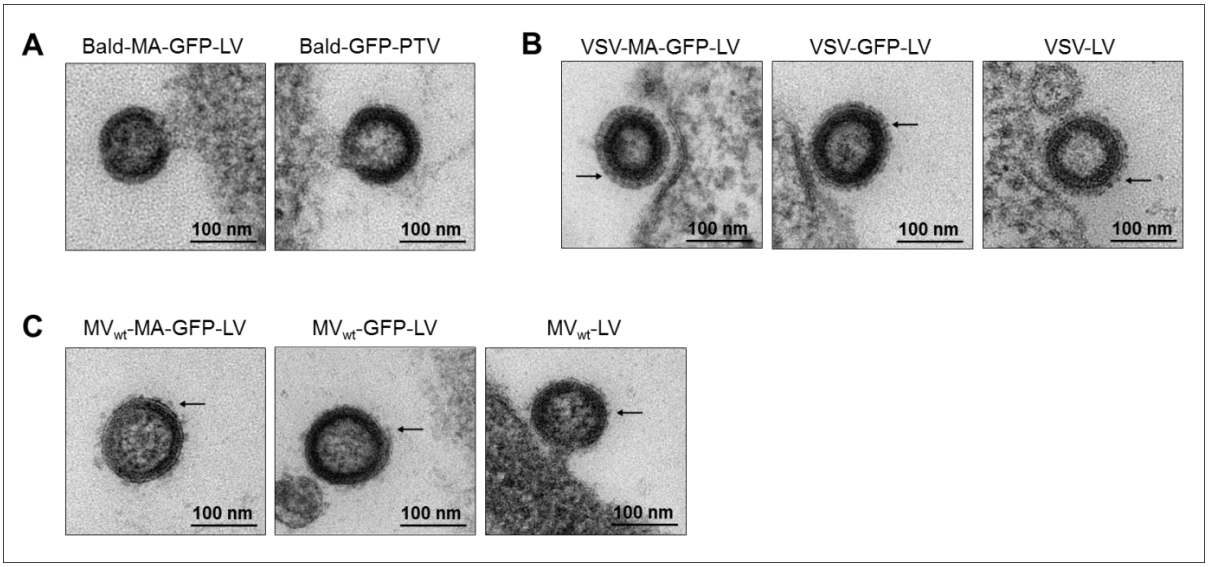

Figure 21: Electron microscopy of ultrathin sections of PTVs released by HEK-293T packaging cells. EM analysis of HEK-293T cell transfected with the respective expression plasmids to produce MA-GFP or GFP protein transfer vectors or lentiviral gene transfer vectors where no additional cargo protein was encoded within the *gag* ORF. Particles are either devoid of envelope proteins (bald, **A**) or pseudotyped by VSV-G (VSV, **B**) or MV_{wt} H and F (MV_{wt}, **C**). Arrows exemplarily mark envelope proteins or envelope protein complexes protruding from the particles' surface. Scale bar, 100 nm (as indicated). Figure modified after Uhlig et al., 2015.

As incorporation of cargo proteins into lentiviral vectors was shown to modulate the infectivity of vector preparations (Figure 13), titers of concentrated protein transfer vectors were determined and analyzed for cargo protein-specific differences. Vectors were titrated on CHO-hSLAM (2.2.4.4). As depicted in Figure 22, determined mean titers were similar within the pseudotypes for MV_{wt}-pseudotyped (MV_{wt}-MA-GFP-$LV_{Katushka}$: 6.6 x 10^7 t.u./ml, MV_{wt}-GFP-$LV_{Katushka}$: 7.4 x 10^7 t.u./ml, MV_{wt}-Ova-$LV_{Katushka}$: 8.1 x 10^7 t.u./ml) or VSV-pseudotyped PTVs (VSV-MA-GFP-$LV_{Katushka}$: 4.0 x 10^9 t.u./ml, VSV-GFP-$LV_{Katushka}$: 4.5 x 10^9 t.u./ml, VSV-Ova-$LV_{Katushka}$: 3.3 x 10^9 t.u./ml), respectively. Thus, GFP or Ova cargo proteins did not affect the vectors' infectivity.

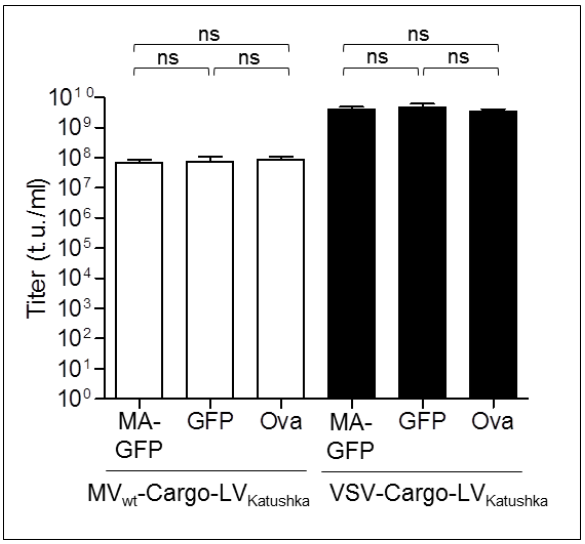

Figure 22: PTV titers. Lentiviral vectors transferring matrix-GFP fusion proteins (MA-GFP) or GFP and Ova proteins proteolytically separated from matrix, respectively, were generated by transient transfection of HEK-293T packaging cells. Vectors were concentrated by ultracentrifugation through a 20% sucrose cushion and CHO-hSLAM cells were transduced with serial dilutions of the first vector harvest. Gene transfer was assessed 72 hours after transduction by flow cytometric determination of Katushka expression. Titers were calculated according to the number of transduced cells. Mean ± SD of MV_{wt}-Cargo-$LV_{Katushka}$ (n = 4) or VSV-Cargo-$LV_{Katushka}$ (n = 3) preparations (first harvest) is shown. Statistical analysis by unpaired Student's t-test. Ns, not significant.

3.1.5. Targeted protein transfer of GFP into cell lines

After identification of the optimal conditions to generate PTVs and their biochemical characterization, receptor-specificity of PTVs pseudotyped by MV_{wt}-GPs or VSV-G should be analyzed. Similar to respective gene transfer vectors (Funke et al., 2009), PTVs pseudotyped by truncated MV_{wt}-GPs should enter only cells expressing the main MV_{wt} cell entry receptor SLAM or the newly identified EpR protein Nectin-4 (3.1.1). In contrast, VSV-G pseudotyped particles should be characterized by a broad tropism and allow "unspecific" protein transfer into nearly all mammalian cell types as they use the widely expressed LDL-R as receptor for cell entry (Finkelshtein et al., 2013).

Receptor-specificity was determined on MV-receptor transgenic CHO cell lines, positive for either MV_{wt} receptors SLAM or Nectin-4, MV_{vac} receptor CD46 or no MV receptor in case of parental CHO-K1. Furthermore, vector preparations were tested on naturally SLAM expressing B95a and Raji B cell lines. Cells were transduced with MV_{wt}-MA-GFP-$LV_{Katushka}$ or VSV-MA-GFP-$LV_{Katushka}$ at MOI 1 (titrated by gene transfer, see 2.2.4.4). MA-GFP protein and *turboFP635* gene transfer, i.e. expression of the encoded Katushka protein, were analyzed by flow cytometry (2.2.3.8) four hours or 72 hours after transduction, respectively.

MV_{wt}-MA-GFP-$LV_{Katushka}$ particles mediated parallel protein and gene transfer specifically into SLAM and Nectin-4 expressing cells, i.e. CHO-hSLAM, CHO-Nectin-4, B95a, and Raji cells, but not into CHO-K1 cells (Figure 23). Of note, despite efficient MA-GFP delivery, gene transfer was rather inefficient in CHO-Nectin-4 and B95a cells. Although CHO-CD46 remained Katushka-negative after transduction with MV_{wt}-MA-GFP-$LV_{Katushka}$, some minor background protein transfer was observed into this cell line. In contrast, VSV-MA-GFP-$LV_{Katushka}$ revealed an opposing pattern of transduction. Whereas the vector efficiently delivered the *turboFP635* marker gene into CHO and Raji cells, as expected, hardly any MA-GFP transfer was detected upon transduction with the VSV-G pseudotyped vector particles at MOI 1 (Figure 23). In analogy with the results for MV_{wt}-MA-GFP-$LV_{Katushka}$, the

cotton-top tamarin cell line B95a was resistant to lentiviral gene transfer by VSV-MA-GFP-$LV_{Katushka}$. Similar results were obtained using PTVs transferring released GFP instead of the MA-GFP fusion protein (data not shown).

Concluding, protein and gene transfer mediated by MV_{wt}-MA-GFP-$LV_{Katushka}$ particles depended mainly on the expression of the respective receptors SLAM and Nectin-4, whereas VSV-MA-GFP-$LV_{Katushka}$ broadly transduced the cells irrespective of the presence of SLAM or Nectin-4.

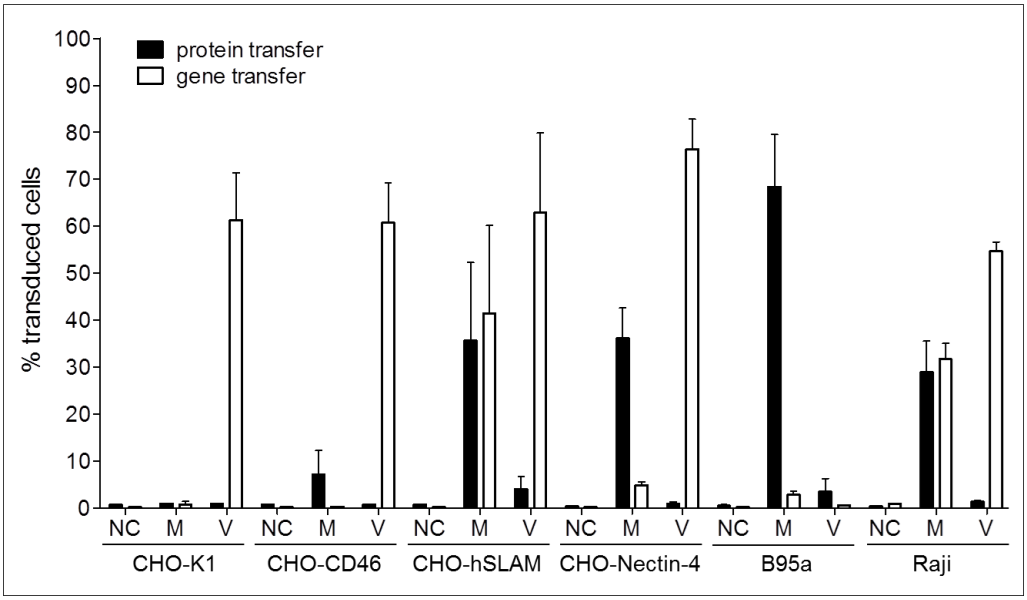

Figure 23: Assessment of PTVs' receptor-specificity. Percentage of marker protein positive cells of a CHO cell panel expressing either no MV receptor (CHO-K1), MV vaccine strain receptor CD46 (CHO-CD46) or MV_{wt} receptors (CHO-hSLAM and CHO-Nectin-4) or naturally SLAM-positive B95a and Raji cells after mock transduction (negative control, NC) or transduction with concentrated matrix-GFP protein transfer vectors at MOI 1 (titrated by gene transfer). PTVs were pseudotyped with MV_{wt}-GPs (M) or VSV-G (V). MA-GFP protein and *turboFP635* gene transfer were analyzed by flow cytometry 4 h or 72 h after transduction, respectively. Mean ± SEM of n = 3 experiments shown. Figure modified after Uhlig et al., 2015.

As just shown, transduction with VSV-MA-GFP-$LV_{Katushka}$ barley resulted in any protein transfer whereas MV_{wt}-MA-GFP-$LV_{Katushka}$ efficiently delivered cargo proteins (Figure 23). Due to the higher infectious titers of VSV-G pseudotyped vectors (Figure 22), less VSV-MA-GFP-$LV_{Katushka}$ than MV_{wt}-MA-GFP-$LV_{Katushka}$ particles were needed for transduction at MOI 1. Therefore, the question arose whether both pseudotypes possess the same ability to transfer proteins into their target cells when adapted to the same particle number. To tackle this question, MV_{wt} receptor-negative CHO-K1 and SLAM-positive CHO-hSLAM or B95a cells were transduced with vector stocks normalized to 80 ng p24 and subsequently analyzed for protein and gene transfer by flow cytometry as described above. Under these conditions, remarkable MA-GFP protein transfer was also observed for VSV-G pseudotypes, which even outperformed SLAM-targeted transfer into CHO-hSLAM cells (Figure 24). However, protein transfer into B95a cells was still more efficient with MV_{wt}-MA-GFP-LVs than using VSV-MA-GFP-LVs. This data set demonstrates the ability of VSV-G pseudotyped PTVs to efficiently transfer cargo proteins into transduced cells, given sufficient particles are supplied.

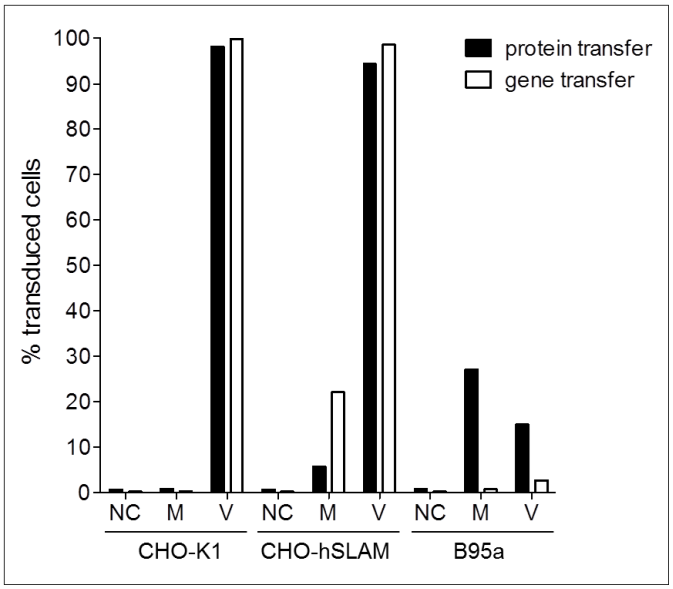

Figure 24: Assessment of protein transfer by PTVs normalized to p24 content. CHO cells expressing no MV receptor (CHO-K1) or MV_{wt} receptor SLAM (CHO-hSLAM) and naturally $SLAM^+$ B95a were mock transduced (negative control, NC) or transduced with concentrated matrix-GFP PTVs. Vectors were normalized to particle count (80 ng p24). PTVs were pseudotyped with MV_{wt}-GPs (M) or VSV-G (V). MA-GFP protein and *turboFP635* gene transfer were analyzed by flow cytometry 4 h or 72 h after transduction, respectively. N = 1 experiment.

3.1.6. Demonstration of cytoplasmic protein transfer

Protein delivery mediated by MA-GFP-PTVs was assessed by GFP-fluorescence of target cells (3.1.5). However, this experimental setting did not discriminate between protein in MA-GFP-delivering particles attached to the cells' surface or actual cytoplasmic protein transfer into the respective target cells. For this reason, intracellular protein delivery should be demonstrated by transduction of Cre indicator cell lines with PTVs transferring Cre recombinase.

Cre recombinase recognizes so-called loxP sites, i.e. specific sequence stretches in double stranded DNA, and excises or inverts genetic information between a pair of these recognition sites depending their orientation (Sternberg and Hamilton, 1981; Hamilton and Abremski, 1984). Its activity can be visualized in indicator cells with expression cassettes for fluorescent proteins in between a pair of loxP sites within the cells' genomes. If active Cre is present in these cells, the expression cassette is excised and the particular fluorescence is lost. However, Cre has to be active within the cells' nucleus to excise the cassettes, thus Cre activity in transduced indicator cells demonstrates transfer of the recombinase by PTV particles into the cytosol of transduced cells and its subsequent nuclear translocation.

A HIV-1 derived packaging plasmid encoding Cre recombinase within the Gag polyprotein was cloned within the Bachelor thesis of Johannes Reusch at Paul-Ehrlich-Institut (Reusch, 2013). The optimal ratio of *gag/pol* to *gag-cre/pol* to generate VSV-G pseudotyped Cre protein transfer vectors was identified with that work to be 2:1. Moreover, initial Cre protein transfer into HT1080-Cre cells had also been demonstrated with VSV-G pseudotyped vectors. However, HT1080-Cre cells do not express MV_{wt} receptors.

Therefore, another Bachelor thesis (Stefanie Kugelmann, Paul-Ehrlich-Institut; Kugelmann, 2013) focused on the generation of a Cre-indicator cell line panel derived from CHO-K1 ($SLAM^-$),

CHO-hSLAM or Raji (both $SLAM^+$). The parental cell lines of interest were transduced by a lentiviral gene transfer vector transferring a loxP-flanked expression cassette for cerulean blue-fluorescing protein (Figure 25A), a stabilized version of CFP (Rizzo et al., 2004). The resulting CHO-K1-blue, CHO-hSLAM-blue or Raji-blue single cell clones are fluorescing blue, but after activity of Cre recombinase in these cells, they lose their blue fluorescence.

In the present thesis, CHO-K1-blue, CHO-hSLAM-blue or Raji-blue cells were transduced with MV_{wt}-Cre-$LV_{Katushka}$ and VSV-Cre-$LV_{Katushka}$ PTVs transferring Cre at MOI 15 (titrated by gene transfer, see 2.2.4.4), respectively, or the *cre* gene transfer vector VSV-LV_{Cre}. High amounts of Cre itself are cytotoxic (Silver and Livingston, 2001). Therefore, the control vector was applied at MOI 10, only, as already with this vector dose cytotoxic effects could be observed (data not shown). Reduction of cerulean fluorescence was assessed by flow cytometry (2.2.3.8) two weeks after transduction, which was previously determined to be a suitable time point since it allowed metabolic degradation of cerulean protein produced before excision of the *cerulean* ORF (data not shown).

Indeed, CHO-K1-blue and CHO-hSLAM-blue cells transduced with VSV-LV_{Cre} had nearly lost all blue fluorescence 14 days after transduction. Also the vast majority of Raji-blue cells (77.4%) were detected to be cerulean-negative 14 days after transduction with VSV-LV_{Cre} (Figure 25B). Transduction with VSV-Cre-$LV_{Katushka}$ induced cerulean-deficiency in a fraction of CHO-K1-blue, CHO-hSLAM-blue, and Raji-blue cells, whereas loss of cerulean fluorescence was confined to a fraction of the $SLAM^+$ cell lines CHO-hSLAM-blue and Raji-blue following transduction with MV_{wt}-Cre-$LV_{Katushka}$ (Figure 25B). No fading of blue fluorescence was observed for MV-receptor negative CHO-K1-blue cells incubated with MV_{wt}-Cre-$LV_{Katushka}$ (Figure 25B). Interestingly, a higher percentage of CHO-hSLAM-blue and Raji-blue indicator cells lost their cerulean fluorescence after transduction with MV_{wt}-Cre-$LV_{Katushka}$ than with VSV-Cre-$LV_{Katushka}$ at the same MOI (Figure 25B), precisely 13.0% versus 3.0% of transduced CHO-hSLAM-blue cells, and 1.9% versus 0.8% of transduced Raji-blue cells (after subtraction of background seen in mock transduced cells), respectively.

Concluding, the observed loss of blue fluorescence indicates excision of loxP-flanked *cerulean* OFR, which is catalyzed by Cre recombinase in the nucleus. Thus, the data argue for successful PTV mediated transfer of Cre into the cytosol of receptor-positive target cells, followed by its nuclear translocation. They prove the enzymatic activity of Cre to be conserved after release from viral particles.

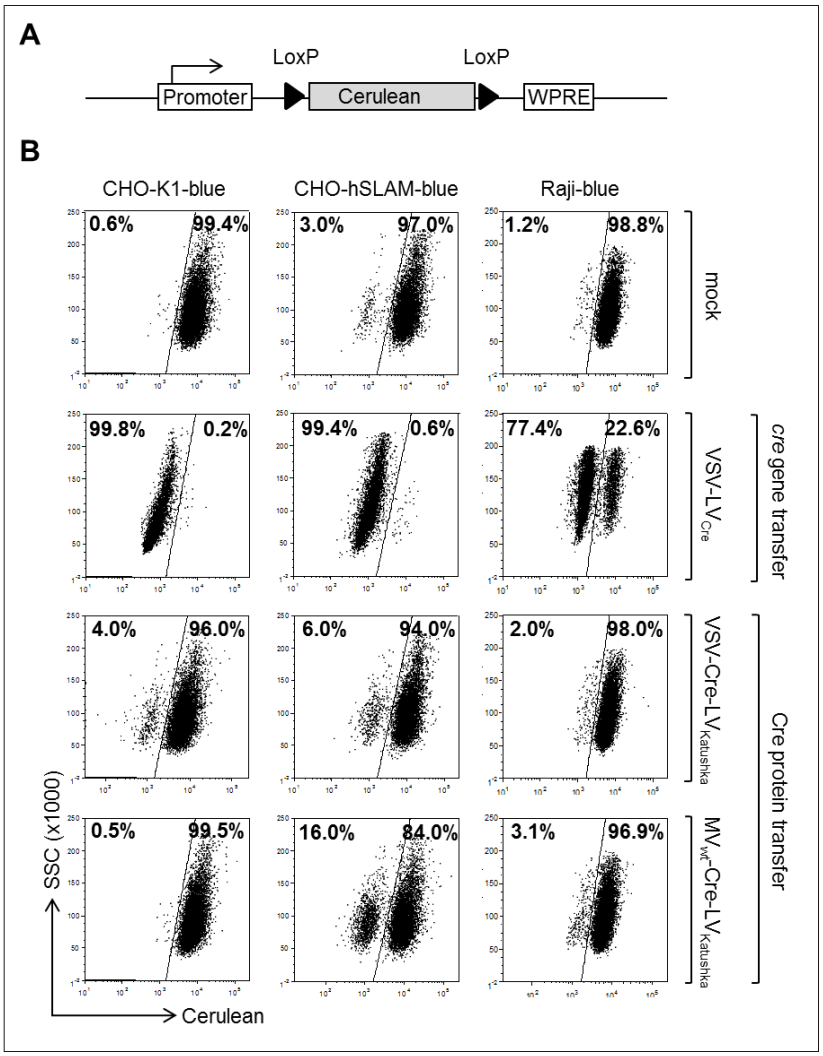

Figure 25: Cytoplasmic Cre protein transfer into indicator cell lines. (A) Schematic representation of the cerulean expression cassette in the genome of Cre indicator cell lines. The ORF encoding blue-fluorescing cerulean marker protein is flanked by Cre recombinase recognition sequences (loxP), enabling specific excision of *cerulean*. WPRE, woodchuck hepatitis virus posttranscriptional regulatory element. **(B)** Cre protein delivery into indicator cell lines. The cerulean-expressing Cre indicator cell lines CHO-K1-blue ($SLAM^-$), CHO-hSLAM-blue ($SLAM^+$), and Raji-blue ($SLAM^+$) were transduced with Cre-PTVs at MOI 15. 14 d after transduction, cerulean expression was analyzed by flow cytometry. Mock transduced cells (mock) or cells transduced with a Cre gene transfer vector (MOI 10) served as controls. One experiment out of n = 3 is shown. Figure modified after Uhlig et al., 2015.

3.1.7. SLAM-dependent transfer of ovalbumin by PTVs

One major aim of this thesis was the evaluation of PTVs' suitability for vaccination purposes. To this end, the chicken egg white protein ovalbumin was chosen as model antigen. Similar as for MA-GFP- (3.1.5) or Cre-PTVs (3.1.6), ovalbumin-PTVs' ability to strictly transduce MV receptor-positive cells should initially be analyzed using receptor-transgenic CHO and naturally SLAM-expressing B cell lines, again. Despite the small quantities of transferred protein (Figure 20B), detection of Ova in lysates of transduced target cells was attempted by Western Blot analysis (2.2.2.3).

For this purpose, cells were transduced with Ova-PTVs at MOI 1 (titrated by gene transfer, 2.2.4.4). Three hours after transduction lysates were prepared (2.2.2.1.). In addition, some MV_{wt}-Ova-$LV_{Katushka}$ transduced cells were washed with PBS and subsequently incubated with citric acid buffer for two minutes to remove potential surface-bound vector particles prior lysis. Beside Western Blot analysis to monitor protein delivery, transfer of the *turboFP635* marker gene was assessed by flow cytometric detection of Katushka fluorescence 72 hours after transduction in cultures transduced in parallel (2.2.3.8).

Ova was detected in lysates of the SLAM-positive CHO-hSLAM, B95a or Raji cells transduced with MV_{wt}-Ova-$LV_{Katushka}$ PTVs, irrespective of citric acid buffer treatment prior lysis, whereas only background Ova signals were observed in CHO-K1 or CHO-CD46 cells (Figure 26A). Accordingly, flow cytometry revealed *turboFP635* gene transfer into SLAM-expressing cells in parallel, whereas no transduction of SLAM-negative cell lines was observed, as expected (Figure 26B). Gene transfer efficiency, though, varied between the cell lines. As described also before, especially B95a cells revealed a certain degree of resistance to gene transfer, independent of the pseudotype used for transduction. In contrast, no Ova became detectable in lysates of cells transduced with the same MOI of VSV-Ova-$LV_{Katushka}$ particles (Figure 26A), although successful *turboFP635* marker gene delivery was observed into all VSV-Ova-$LV_{Katushka}$ transduced cells, except B95a (Figure 26B).

Taken together, the data show receptor-dependent protein and gene delivery by MV_{wt}-Ova-$LV_{Katushka}$ particles. Since citric acid buffer treatment prior lysis did not reduce the quantity of Ova detected in respective cell lysates, cytoplasmic protein transfer must have occurred, confirming the results of the Cre-transfer experiments (Figure 25B). VSV-Ova-$LV_{Katushka}$ mediated efficient gene transfer into transduced cells but Ova protein delivery was below the detection limit.

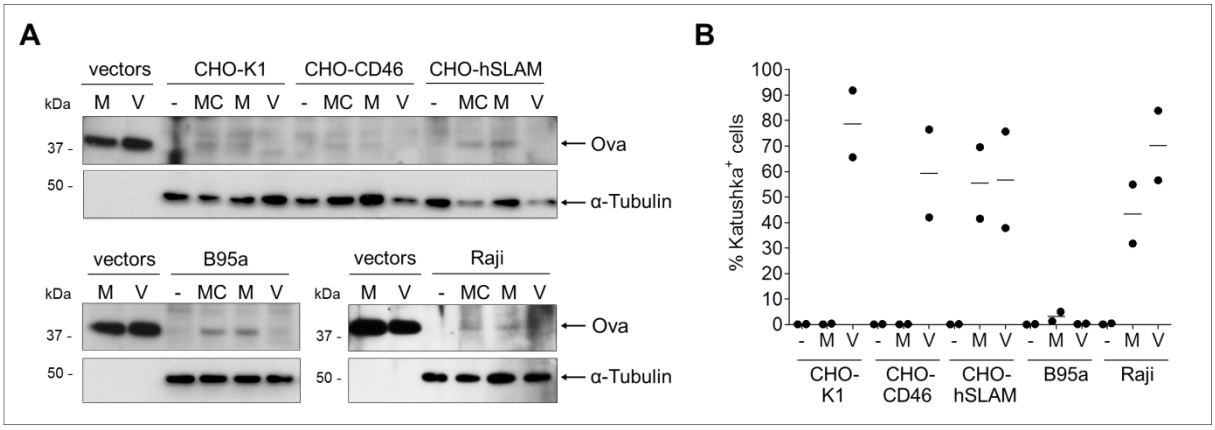

Figure 26: Receptor-dependent ovalbumin transfer into cell lines. (A) Anti-OvaWestern Blot analysis of receptor-transgenic CHO cells or naturally SLAM-expressing B95a and Raji cells 3 h after mock transduction (-) or transduction with concentrated Ova-PTVs pseudotyped with VSV-G (V) or MV_{wt} H and F (M) at MOI 1. MC, incubation of MV_{wt}-Ova-$LV_{Katushka}$ transduced cells with citric acid buffer prior lysis to remove unspecifically surface-bound particles. **(B)** Gene transfer in cultures transduced in parallel to (A) and analyzed 72 h post transduction for Katushka expression. N = 2 independent experiments. Figure derived from Uhlig et al., 2015.

3.1.8. Immunostimulatory properties of Ova-PTV-transduced mDCs *ex vivo*

Ovalbumin protein transfer vectors were shown to successfully mediate receptor-dependent transfer of their cargo protein into transduced target cells *in vitro* (Figure 26). In a next step, the ability of Ova-PTVs to stimulate antigen-specific $CD4^+$ and $CD8^+$ T lymphocytes by directed Ova transfer into APCs should be assessed *ex vivo*. For that purpose, myeloid dendritic cells (mDCs) were generated from bone marrow of $IFNAR^{-/-}$ N20 C57BL/6 (short $IFNAR^{-/-}$) and $IFNAR^{-/-}$ $SLAM^{ki}$ C57BL/6 ($SLAM^{ki}$)

mice as described in 2.2.3.6. Thereby, IFNAR$^{-/-}$ mice do not express any functional MV-receptors on immune cells such as APCs. In contrast, SLAM^{ki} mice are characterized by a replacement of the V domain of murine SLAM by the V domain of human SLAM, which renders the chimeric protein a functional receptor for MV_{wt} H (Ohno et al., 2007). mDCs were transduced with Ova-transferring PTVs and subsequently co-cultured with CD8$^+$ (OT-I) or CD4$^+$ (OT-II) Ova-specific T cells (2.2.3.6), obtained from TCR-transgenic mice (see 2.2.5.7 and 2.2.3.5). Later, co-culture supernatants were sampled and release of IL-2 and IFN-γ, amongst others secreted by CD4$^+$ and CD8$^+$ T cells upon activation (Schoenborn and Wilson, 2007; Boyman and Sprent, 2012), was quantified by ELISA (2.2.2.4). The experimental design is schematically depicted in Figure 27.

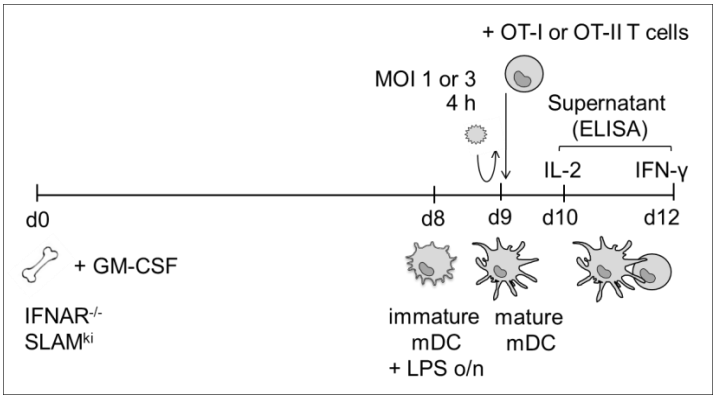

Figure 27: Schematic depiction of the experimental set-up to determine the immunostimulatory properties of Ova-PTVs *ex vivo*. Bone marrow from IFNAR$^{-/-}$ or SLAM^{ki} mice was isolated and used for generation of myeloid dendritic cells (mDCs). mDCs were activated by addition of 100 ng/ml LPS overnight (o/n), and then incubated with PTVs at MOI 1 or 3. After 4 h, the vectors were removed and Ova-specific CD8$^+$ OT-I or CD4$^+$ OT-II T cells were added to the mDCs. 24 h or 72 h later, co-culture supernatants were sampled for the quantification of IL-2 and IFN-γ by ELISA. Figure modified after Uhlig et al., 2015.

3.1.8.1. Analysis of APC co-stimulation by Ova-PTVs

Viral components are known to provide "danger signals" to antigen presenting cells (Mak and Saunders, 2006) which are a prerequisite for the activation of APCs and thus the induction of immune responses. To assess the co-stimulatory capacity of Ova-PTVs (which are, structurally, viral particles) on APCs, mDCs were transduced with PTVs at MOI 3 and expression of CD69 and CD86, described to be upregulated on activated dendritic cells (Schülke et al., 2010), was analyzed by flow cytometry (2.2.3.8) 24 hours after transduction. Transduction of mDCs with PTVs neither led to upregulation of CD69 nor CD86 on the cells' surfaces (Figure 28). In contrast, addition of LPS, a strong maturation stimulus, induced CD86 expression on mDCs (Figure 28), as expected. This effect was also not enhanced by presence of PTVs. Thus, no indication of a co-stimulatory effect of Ova-PTVs on APCs was found when analyzing CD69 and CD86 expression on mDCs.

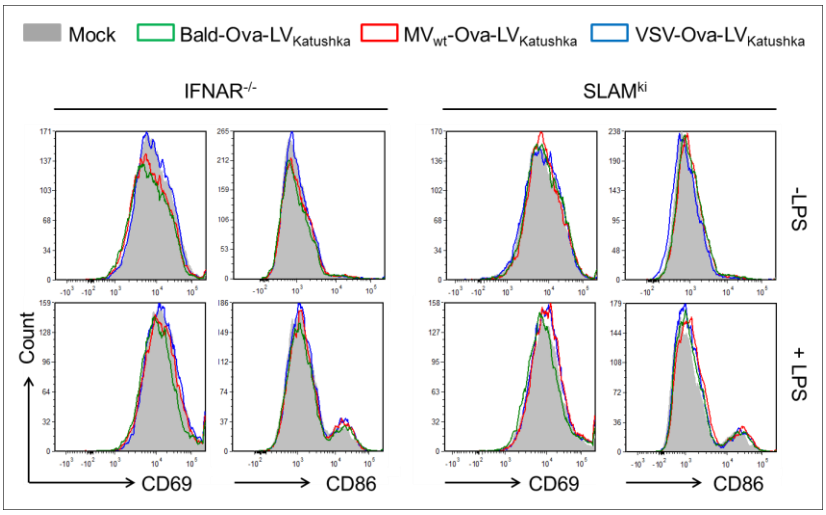

Figure 28: Absence of DC co-stimulation by Ova-PTVs. Bone marrow-derived mDCs (pretreated with 100 ng/ml LPS prior transduction where indicated) were incubated with PTVs at MOI 3 for 4 h. 24 h post transduction, expression of CD69 and CD86 in the CD11c^{+} dendritic cells population were analyzed by flow cytometry. One representative donor out of n = 5 (IFNAR$^{-/-}$) or n = 6 (SLAM^{ki}) is shown. Figure modified after Uhlig et al., 2015.

3.1.8.2. Activation of Ova-specific CD8^{+} OT-I T cells by Ova-PTV transduced mDCs

To determine whether Ova-PTV-transduced mDCs stimulate Ova-specific CD8^{+} T cells, the co-culture experiment outlined before (3.1.8) was performed with T lymphocytes isolated from OT-I C57BL/6 mice. As already mentioned, these mice are TCR-transgenic; all CD8^{+} T cells recognize the SIINFEKL-peptide of ovalbumin (Ova$_{257-264}$) when presented via MHC I. Upon activation T cells secrete IL-2 and IFN-γ.

IL-2 and IFN-γ release by CD8^{+} T cells was exclusively induced by IFNAR$^{-/-}$ mDCs which had been preincubated with recombinant Ova protein or transduced with VSV-Ova-LV$_{Katushka}$, but not with Bald-Ova-LV$_{Katushka}$, MV$_{wt}$-Ova-LV$_{Katushka}$, or the GFP-transferring vectors VSV-GFP-LV$_{Katushka}$ or MV$_{wt}$-GFP-LV$_{Katushka}$ (Figure 29A and B). Also SLAM^{ki} mDCs stimulated secretion of IL-2 and IFN-γ by OT-I T cells following preincubation with recombinant Ova protein or after transduction with VSV-Ova-LV$_{Katushka}$ (Figure 29A and B). Besides, activation of CD8^{+} Ova-specific T cells was triggered by MV$_{wt}$-Ova-LV$_{Katushka}$-transduced SLAM^{ki} mDCs in a MOI-dependent manner (Figure 29B). Fusion inhibiting peptide FIP (Richardson et al., 1980) abolished IL-2 secretion in this setting (Figure 29C). Of note, SLAM^{ki} mDCs transduced with MV$_{wt}$-Ova-LV$_{Katushka}$ induced similar IL-2 and IFN-γ secretion by CD8^{+} T cells as mDCs preincubated with 50 µg recombinant Ova protein, although only approximately 230 ng Ova were delivered by MV$_{wt}$-Ova-LV$_{Katushka}$ at MOI 1 (Figure 29A and B). Moreover, IL-2 and IFN-γ production detected in co-cultures of IFNAR$^{-/-}$ or SLAM^{ki} mDCs transduced with VSV-Ova-LV$_{Katushka}$ (corresponding to approximately 7 ng Ova) even exceeded the amounts of secreted cytokines in protein-stimulated cultures (Figure 29A and B).

Taken together, these data argue for highly receptor-dependent transduction and glycoprotein-mediated transfer of antigens into the cytosol of mDCs by targeted PTVs, followed by proteasomal processing and MHC I presentation via the endogenous antigen presentation pathway. Thereby, pseudotyped Ova-PTV particles were able to induce similarly strong stimulation of $CD8^+$ Ova-specific T cells as triggered by 50 µg recombinant ovalbumin in the same setting, although delivering approximately 220- (MV_{wt}-Ova-$LV_{Katushka}$) to 7150-times (VSV-Ova-$LV_{Katushka}$) less Ova protein. Bald particles, where the antigen is supposed to be absorbed via the endosomal route and presented on MHC II molecules, did not cause activation of $CD8^+$ OT-I T lymphocytes, as expected.

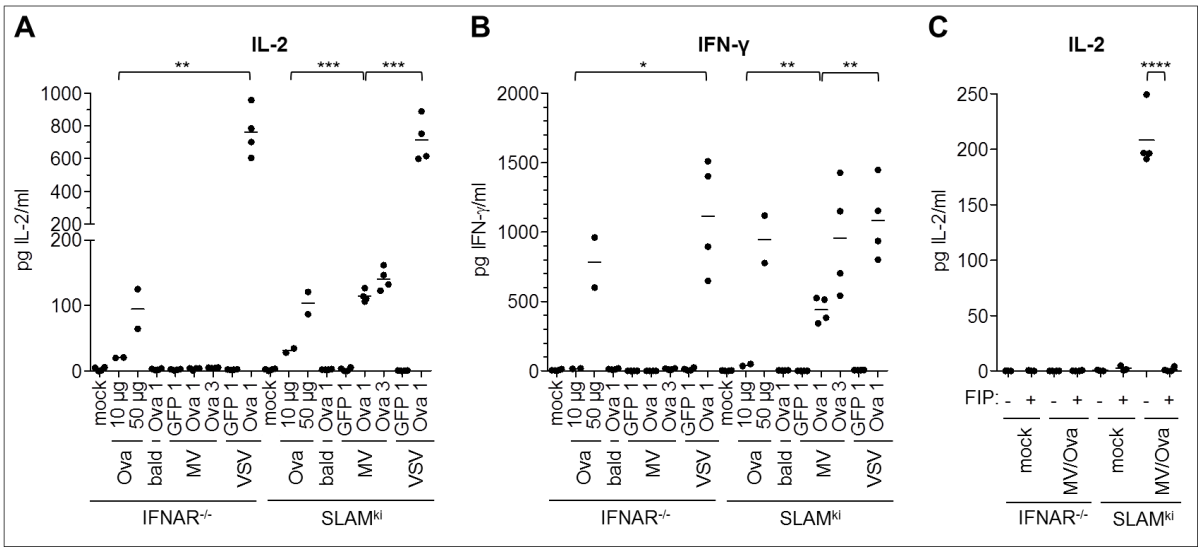

Figure 29: IL-2 and IFN-γ secretion by ovalbumin-specific $CD8^+$ OT-I T cells after incubation with *ex vivo* transduced mDCs or untransduced mDCs in the presence of recombinant Ova. mDCs were transduced with GFP- or Ova-PTVs pseudotyped with MV_{wt}-GPs (MV) or VSV-G (VSV) at MOI 1 or 3 (indicated by numbers 1 and 3). Alternatively, mDCs were incubated with particles harboring no envelope glycoproteins (bald), which were adjusted to MV_{wt}-Ova-$LV_{Katushka}$ by p24 values, or recombinant Ova (Ova). Secretion of IL-2 **(A** and **C)** or IFN-γ (**B**) by $CD8^+$ Ova-specific T cells in co-culture with these mDCs was determined by ELISA. One representative experiment out of four (A and B) or two (C) is shown. Experiments was performed in triplicates or quadruplicates with each technical replicate depicted as a single dot. **(C)** IL-2 secretion by $CD8^+$ T cells in co-culture with mDCs transduced by MV_{wt}-Ova-$LV_{Katushka}$ (MV/Ova) in normal culture medium, - or medium supplemented with Fusion inhibiting peptide (FIP), +. Statistical analysis by two-tailed unpaired Student's t-test. *, **, ***, **** indicate P<0.05, P<0.01, P<0.001, and P<0.0001, respectively. Panels A and B modified after Uhlig et al., 2015.

3.1.8.3. Activation of Ova-specific $CD4^+$ OT-II T cells by Ova-PTV transduced mDCs

Next, the potency of Ova-PTV-transduced mDCs to activate Ova-specific $CD4^+$ T cells was evaluated in the experimental system outlined before (3.1.8). Here, IL-2 and IFN-γ secretion by Ova-specific $CD4^+$ T cells was most vigorously induced by $IFNAR^{-/-}$ and $SLAM^{ki}$ mDCs incubated with soluble, recombinant Ova or Bald-Ova-$LV_{Katushka}$ particles devoid of envelope glycoproteins (Figure 30). Also MV_{wt}-Ova-$LV_{Katushka}$-transduced mDCs stimulated cytokine secretion by Ova-specific $CD4^+$ T cells. This effect was particularly strong when MV-receptor-negative $IFNAR^{-/-}$ mDCs were incubated with

MV_{wt}-Ova-$LV_{Katushka}$ vector particles before co-cultivation with OT-II T cells (Figure 30). However, in contrast to $CD8^+$ T cell activation by mDCs transduced with VSV-Ova-$LV_{Katushka}$ (Figure 29A and B), $CD4^+$ T cells in co-culture with $IFNAR^{-/-}$ or $SLAM^{ki}$ mDCs transduced with VSV-Ova-$LV_{Katushka}$ did not secrete detectable levels of IL-2 or IFN-γ (Figure 30).

Thus, $CD4^+$ T cells are mainly stimulated by mDCs which have internalized Ova in a receptor-independent manner. When no cell entry receptors are present, PTV-associated Ova is presumably taken up by mDCs via the endosomal route, leading to MHC-II presentation via the exogenous antigen presenting pathway which enables antigen-recognition by Ova-specific $CD4^+$ T cells.

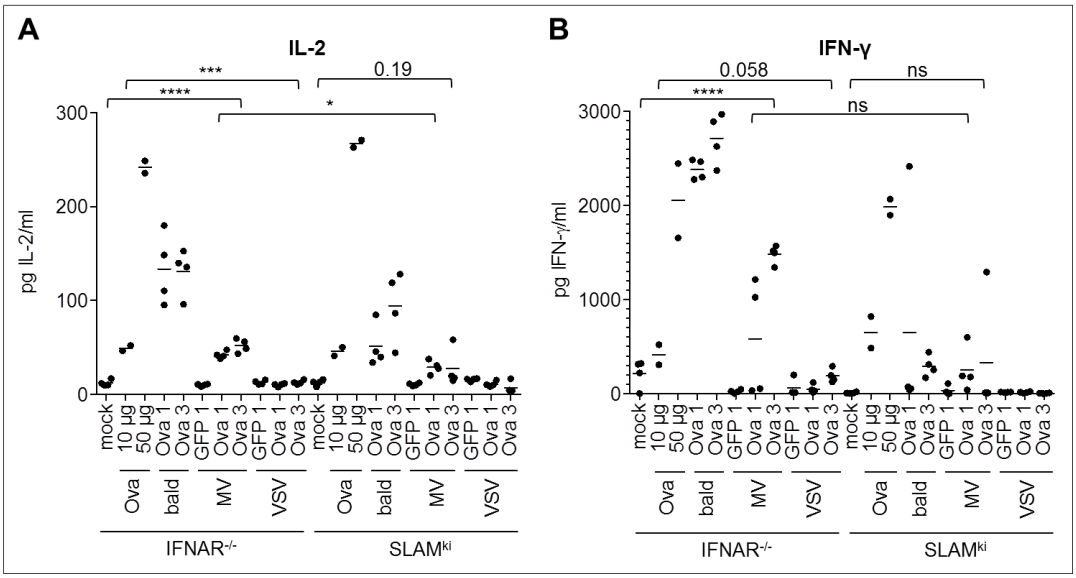

Figure 30: Activation of $CD4^+$ Ova-specific OT-II T cells after incubation with *ex vivo* transduced mDCs or untransduced mDCs in the presence of recombinant Ova. mDCs were transduced with GFP- or Ova-PTVs pseudotyped with MV_{wt}-GPs (MV) or VSV-G (VSV) at MOI 1 or 3 (indicated by numbers 1 and 3). Alternatively, mDCs were incubated with particles harboring no envelope glycoproteins (bald), which were adjusted to MV_{wt}-Ova-$LV_{Katushka}$ by p24 values, or recombinant Ova (Ova). Activation of $CD4^+$ T cells was measured as secretion of IL-2 (**A)** or IFN-γ (**B**) by ELISA. One representative experiment out of two is shown (n = 2). Experiments was performed in triplicates or quadruplicates with each technical replicate depicted as a single dot. Statistical analysis by two-tailed unpaired Student's t-test. Ns, *, ***, **** indicate not significant, $P<0.05$, $P<0.001$, and $P<0.0001$, respectively. Figure modified after Uhlig et al., 2015.

3.1.9. Vaccination with Ova-PTVs

mDCs transduced with Ova-PTVs were shown to be potent activators of Ova-specific $CD8^+$ T lymphocytes in *ex vivo* co-culture experiments (Figure 29A and B). Next, Ova-PTVs' ability to stimulate antigen-specific, cytotoxic T cells should be assessed also *in vivo*. For this purpose, 6-8 weeks old $IFNAR^{-/-}$ and $SLAM^{ki}$ mice were vaccinated (2.2.5.6), following the scheme depicted in Figure 31. Briefly, the animals were intraperitoneally inoculated with medium (mock), 1 µg recombinant Ova or vector stocks normalized to a content of 1 µg ovalbumin at day 0 (prime) and day 28 (boost). Control vector MV_{wt}-GFP-$LV_{Katushka}$, not transferring Ova but GFP, was adjusted to p24

content of MV_{wt}-Ova-$LV_{Katushka}$. After sacrificing the animals four days after boosting, spleens were harvested and splenocytes isolated (2.2.5.7). IFN-γ secretion of Ova-specific T cells was quantified by ELISpot (2.2.3.7) after recall using recombinant Ova, $Ova_{257-264}$ or $Ova_{323-339}$, the MHC I and MHC II-restricted immunodominant peptide epitopes of ovalbumin, respectively.

Figure 31: Experimental immunization scheme. Mice were intraperitoneally injected with different experimental vaccines and boosted 28 d after priming. 4 d after boosting, mice were sacrificed and splenocytes were isolated. The number of antigen-specific T cells among splenocytes of vaccinated mice was determined by IFN-γ ELISpot analysis. Figure modified after Uhlig et al., 2015.

Splenocytes from $IFNAR^{-/-}$ mice immunized with VSV-Ova-$LV_{Katushka}$ contained a significant number of activated, IFN-γ releasing cells (685.9 ± 750.8 reactive T cells/ 10^6 splenocytes after restimulation with Ova), but no or hardly any IFN-γ secreting splenocytes were obtained from $IFNAR^{-/-}$ mice injected with Opti-MEM (mock), recombinant Ova, Bald-Ova-$LV_{Katushka}$, MV_{wt}-GFP-$LV_{Katushka}$ or MV_{wt}-Ova-$LV_{Katushka}$ (Figure 32A). In splenocytes isolated from $SLAM^{ki}$ mice vaccinated with Bald-Ova-$LV_{Katushka}$ (101.0 ± 118.0 reactive T cells/ 10^6 splenocytes after restimulation with Ova), MV_{wt}-Ova-$LV_{Katushka}$ (212.8 ± 288.2 reactive T cells), or VSV-Ova-$LV_{Katushka}$ (121.4 ± 134.9 reactive T cells) IFN-γ secreting T cells were abundant, whereas no IFN-γ producing T cells were found in splenocytes from the other experimental $SLAM^{ki}$ mouse cohorts (Figure 32B). Of particular note, IFN-γ secretion of splenocytes derived from both vaccinated $IFNAR^{-/-}$ and $SLAM^{ki}$ mice was not influenced by the stimuli used for antigen-specific recall (Figure 32).

To assess why T cell reactivity was unaffected by the stimuli used for recall, frozen splenocytes from vaccinated mice were thawed, pooled according to vaccine and separated into untouched pan T cells and the APC-containing retentate by magnetic cell sorting (MACS, see 2.2.3.5). The purified T cells were incubated in medium lacking IL-2 overnight to tranquilize the potentially activated cells. Then, T lymphocytes were co-cultured with syngeneic mDCs, which had been generated from bone marrow cells of previously untreated $IFNAR^{-/-}$ or $SLAM^{ki}$ mice (2.2.3.6), in the presence of recombinant Ova, $Ova_{257-264}$ or $Ova_{323-339,}$ or murine JAWSII cells, transgenic for ovalbumin (JAWSII-Ova) (Bodmer, 2015), or not (JAWSII). Ova-specific T cells activation was assessed by IFN-γ-ELISpot analysis (2.2.3.7).

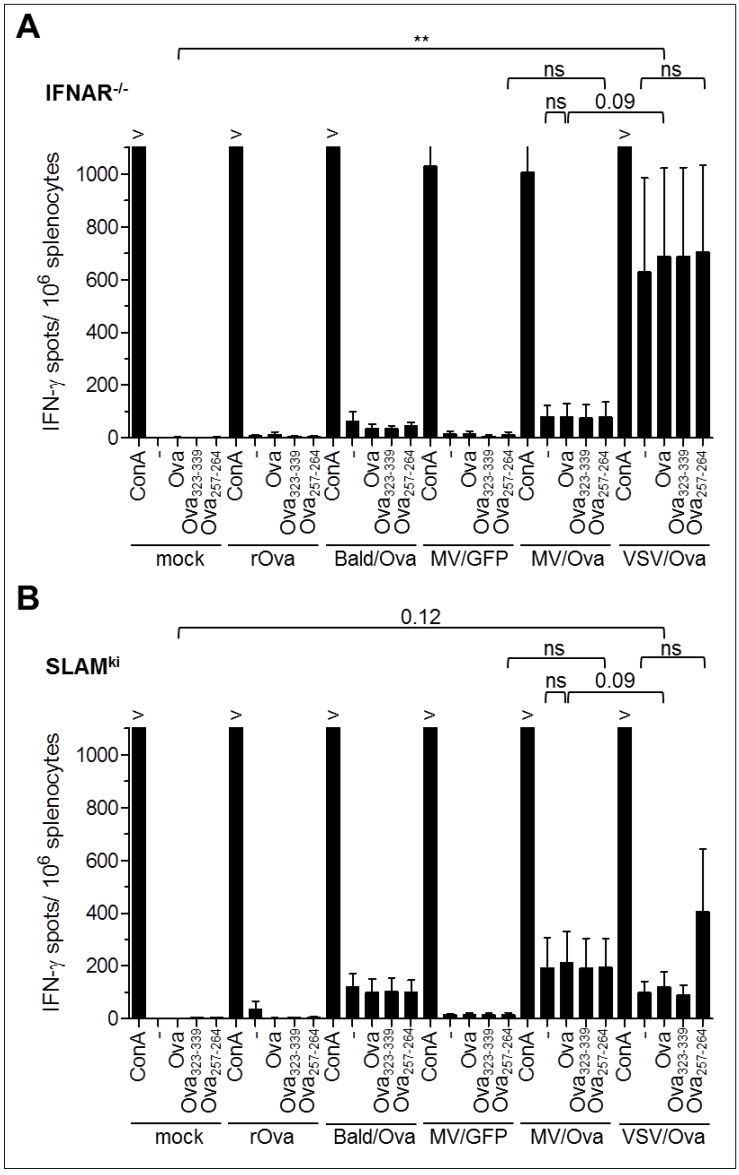

Figure 32: IFN-γ secretion by splenocytes from PTV-vaccinated mice. IFNAR$^{-/-}$ **(A)** or SLAM^{ki} **(B)** mice were injected with Opti-MEM (mock), recombinant ovalbumin (rOva), Bald-Ova-LV$_{Katushka}$ (Bald/Ova), MV$_{wt}$-GFP-LV$_{Katushka}$ (MV/GFP), MV$_{wt}$-Ova-LV$_{Katushka}$ (MV/Ova) or VSV-Ova-LV$_{Katushka}$ (VSV/Ova) according to the immunization scheme depicted in Figure 31. Splenocytes were freshly isolated from vaccinated animals and subjected to ELISpot analysis to determine the number of IFN-γ secreting, stimulated T cells among splenocytes. For antigen-specific recall, recombinant Ova protein (Ova) or immunodominant Ova-peptides for induction of CD4$^+$ or CD8$^+$ T cell responses, Ova$_{323-339}$ or Ova$_{257-264}$, respectively, were added. Plain medium (negative control, -) and Concanavalin A (positive control, ConA) served as controls. > indicates a spot count > 1100. Results are expressed as mean ± SEM of 5-6 individual animals (n = 5-6) measured in triplicates. Statistical analysis by Mann-Whitney-test (unpaired values between different animal groups) or Wilcoxen-test (paired values of one animal group). Ns, not significant; **, P<0.01. Figure derived from Uhlig et al., 2015.

Similarly to freshly isolated splenocytes (Figure 32A), purified T cells from IFNAR$^{-/-}$ mice immunized with VSV-Ova-LV$_{Katushka}$ secreted IFN-γ in co-culture with pulsed, syngeneic mDCs. Of note, the pronounced IFN-γ release by these T cells was triggered by syngeneic mDCs pulsed with Ova (303.3 ± 187.7 reactive T cells/ 10^6 T cells) and Ova$_{257-264}$ (446.7 ± 156.3 reactive T cells/ 10^6 T cells), but was not evoked when recall was performed with Ova$_{323-339}$-loaded mDCs (Figure 33A, compare to IFN-γ secretion of T cells co-cultured with syngeneic mDCs in the absence of antigen). In contrast, no or hardly any IFN-γ releasing T cells were detected in co-cultures of pulsed, syngeneic mDCs with T lymphocytes from the other experimental groups, i.e. IFNAR$^{-/-}$ mice injected with Opti-MEM (mock), recombinant Ova, Bald-Ova-LV$_{Katushka}$, MV$_{wt}$-GFP-LV$_{Katushka}$ or MV$_{wt}$-Ova-LV$_{Katushka}$ (Figure 33A). Also purified T cells obtained from vaccinated SLAM^{ki} mice injected with Opti-MEM, recombinant Ova, Bald-Ova-LV$_{Katushka}$, and MV$_{wt}$-GFP-LV$_{Katushka}$ did not release IFN-γ when co-incubated with pulsed, syngeneic mDCs (Figure 33B). Interestingly, pulsed, syngeneic mDCs induced IFN-γ secretion by T cells derived from MV$_{wt}$-Ova-LV$_{Katushka}$-vaccinated SLAM^{ki} mice but, again, no

correlation between T cell activation and the stimuli used for recall was observed (Figure 33B). In contrast, T cells from VSV-Ova-$LV_{Katushka}$-vaccinated $SLAM^{ki}$ mice were clearly stimulated by $Ova_{257-264}$-loaded mDCs (276.7 ± 20.8 reactive T cells/ 10^6 T cells) but not by mDCs pulsed with recombinant Ova or $Ova_{323-339}$ (Figure 33B).

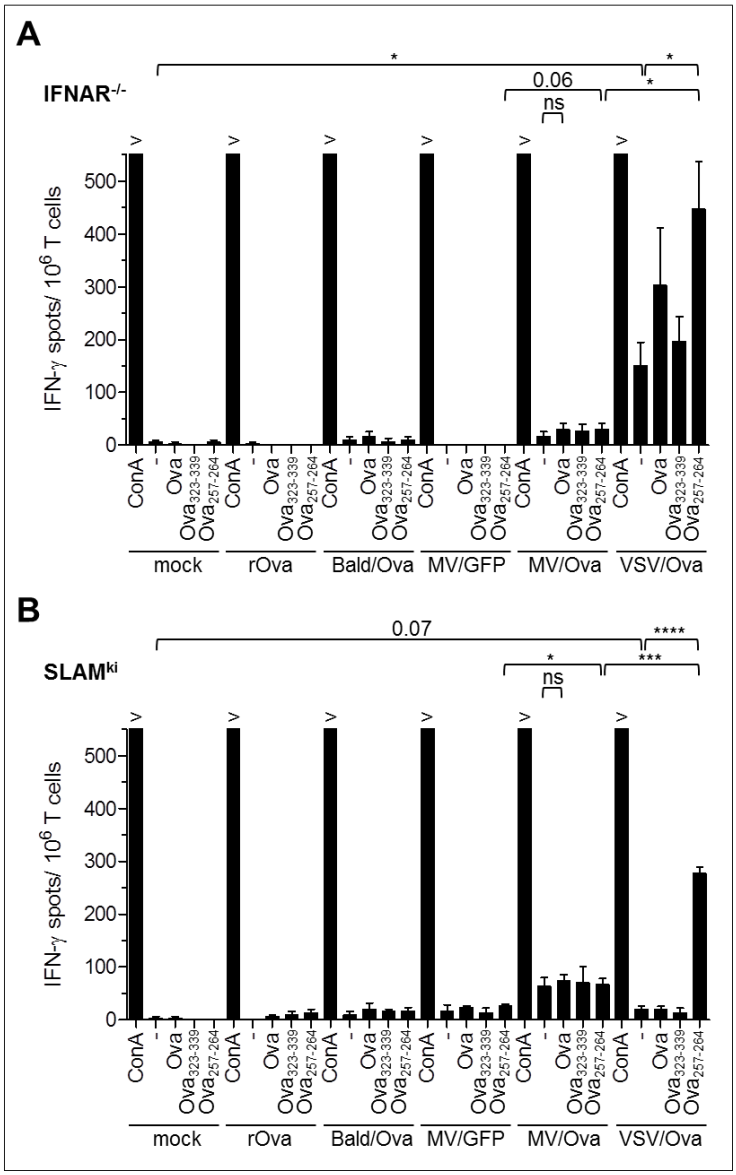

Figure 33: IFN-γ secretion by purified T cells in co-culture with antigen-pulsed syngeneic mDCs. $IFNAR^{-/-}$ **(A)** or $SLAM^{ki}$ **(B)** mice were injected with Opti-MEM (mock), recombinant ovalbumin (rOva), Bald-Ova-$LV_{Katushka}$ (Bald/Ova), MV_{wt}-GFP-$LV_{Katushka}$ (MV/GFP), MV_{wt}-Ova-$LV_{Katushka}$ (MV/Ova) or VSV-Ova-$LV_{Katushka}$ (VSV/Ova) according to the immunization scheme depicted in Figure 31**.** Splenocytes were harvested, pooled and untouched T cells were isolated by magnetic cell separation using a Pan T cell isolation Kit. The next day, T cells were co-incubated with mDCs generated from non-vaccinated syngeneic mice pulsed with recombinant Ova protein (Ova) or immunodominant Ova-peptides for induction of $CD4^+$ or $CD8^+$ T cell responses, $Ova_{323-339}$ or $Ova_{257-264}$, respectively. mDCs incubated with plain medium (negative control, -) and Concanavalin A (positive control, ConA) served as controls. The number of IFN-γ secreting, stimulated T cells was determined by IFN-γ ELISpot. > indicates a spot count > 550. Mean ± SEM of triplicate values shown. Statistical analysis by unpaired Student's t-test. Ns, *, **, ***, **** indicate not significant, $P<0.05$, $P<0.01$, $P<0.001$, and $P<0.0001$, respectively. Figure modified after Uhlig et al., 2015.

Incubation of purified T cells from vaccinated $IFNAR^{-/-}$ or $SLAM^{ki}$ mice with unmodified JAWSII dendritic cells did not induce IFN-γ secretion by T cells (Figure 34). Similar to Ova-pulsed syngeneic mDCs (Figure 33A), also transgenic JAWSII-Ova cells triggered only activation of T cells from $IFNAR^{-/-}$ mice injected with VSV-Ova-$LV_{Katushka}$ (Figure 34A). For most vaccine groups, this pattern was also found for T cells from vaccinated $SLAM^{ki}$ mice incubated with JAWSII-Ova cells (Figure 34B). However, in addition to VSV-Ova-$LV_{Katushka}$-treated animals, also T cells from MV_{wt}-Ova-$LV_{Katushka}$-injected $SLAM^{ki}$ mice seemed to be activated in co-culture with JAWSII-Ova (Figure 34B), although statistical significance was not reached.

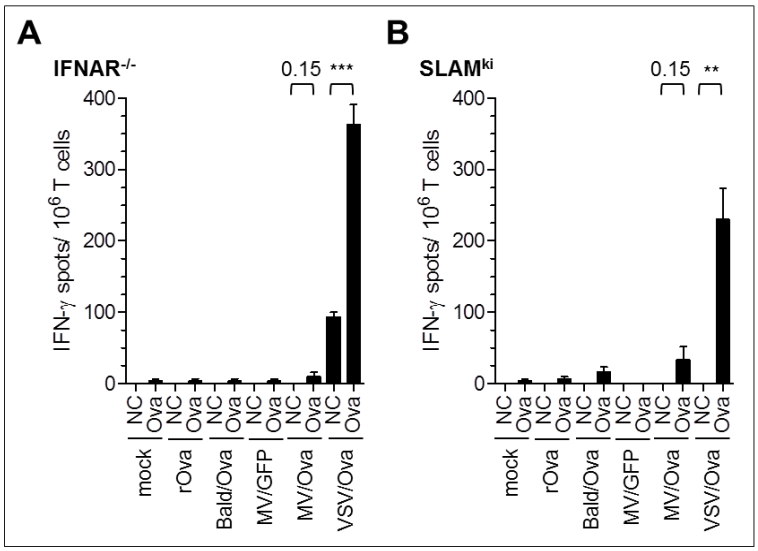

Figure 34: IFN-γ secretion by murine T cells in co-culture with antigen presenting dendritic cells. Splenocytes of IFNAR$^{-/-}$ **(A)** or SLAM^{ki} **(B)** mice injected with Opti-MEM (mock), recombinant ovalbumin (rOva), Bald-Ova-LV$_{Katushka}$ (Bald/Ova), MVwt-GFP-LV$_{Katushka}$ (MV/GFP), MVwt-Ova-LV$_{Katushka}$ (MV/Ova) or VSV-Ova-LV$_{Katushka}$ (VSV/Ova) were harvested, pooled and untouched T cells were isolated using a Pan T cell isolation Kit. The following day, T cells were co-incubated with JAWSII dendritic cells (NC) or JAWSII dendritic cells genetically engineered to express ovalbumin (JAWSII-Ova; Ova). IFN-γ secreting, stimulated T cells were determined by IFN-γ ELISpot. Mean ± SEM of triplicates shown. Statistical analysis by two-tailed unpaired Student's t-test. **, P<0.01; ***, P<0.001. Figure modified after Uhlig et al., 2015.

After investigating if the observed recall-independent IFN-γ secretion by splenocytes derived from certain groups of PTV-vaccinated mice (Figure 32) was a result of persistent T cell activation, it should be assessed if also long-lasting antigen-presentation by APCs might have played a role.
For this purpose, the APC-containing retentate fraction of splenocytes after MACS separation was co-cultured with freshly isolated splenocytes from C57BL/6 mice (no Ova-specific T cells), OT-I mice (CD8$^+$ Ova-specific T cells) or OT-II mice (CD4$^+$ Ova-specific T cells). OT-I and OT-II T cells' Ova-specific reactivities were confirmed in co-culture with JAWSII-Ova cells, in parallel (data not shown). IFN-γ-ELISpot analysis revealed activation of at least OT-I splenocytes incubated with the APC-containing retentate from VSV-Ova-LV$_{Katushka}$-immunized IFNAR$^{-/-}$ mice (Figure 35A).

Taken together, vaccine experiments indicate preferential induction of antigen-specific, cytotoxic T cell responses by APCs transduced with Ova-transferring PTVs in a receptor-dependent manner. APCs seem to present PTV-delivered Ova over several days, which favoured persistent stimulation of T cells, accounting for the initially observed stimulation-independent IFN-γ secretion by freshly isolated splenocytes from IFNAR$^{-/-}$ mice injected with VSV-Ova-LV$_{Katushka}$ and SLAM^{ki} mice immunized with VSV-Ova-LV$_{Katushka}$, MV$_{wt}$-Ova-LV$_{Katushka}$ or Bald-Ova-LV$_{Katushka}$.

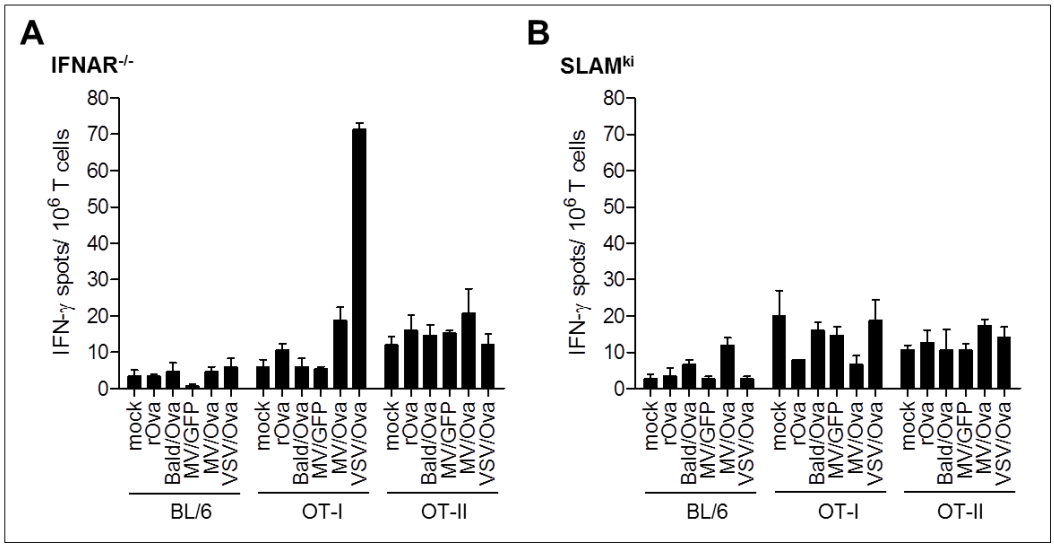

Figure 35: IFN-γ secretion by splenocytes co-cultivated with APCs isolated from PTV-vaccinated mice. Splenocytes of IFNAR$^{-/-}$ **(A)** or SLAM^{ki} **(B)** mice injected with Opti-MEM (mock), recombinant ovalbumin (rOva), Bald-Ova-LV$_{Katushka}$ (Bald/Ova), MV$_{wt}$-GFP-LV$_{Katushka}$ (MV/GFP), MV$_{wt}$-Ova-LV$_{Katushka}$ (MV/Ova) or VSV-Ova-LV$_{Katushka}$ (VSV/Ova) were harvested, pooled and fractioned into pan T cells and the APC-containing retentate by magnetic cell sorting. The APC-containing retentate was then co-cultured with splenocytes derived from C57BL/6 (BL/6) or OT-I or OT-II mice, characterized by no, CD8$^+$ or CD4$^+$ Ova-specific T cells, respectively. The number of stimulated T cells was determined by IFN-γ ELISpot. The experiment was performed in triplicates, mean ± SEM are shown. Figure modified after Uhlig et al., 2015.

3.2. Targeted gene transfer into CD4$^+$ T lymphocytes

3.2.1. Generation of a CD4-targeted vector

In this thesis, a CD4-specific targeting vector should be generated based on the highly flexible targeting system introduced by Funke *et al*. (Funke et al., 2008). Here, the CD4-specific DARPin 29.2, which was kindly provided by Prof. Trkola, University of Zurich, was employed as binding domain. The protein was described to specifically interact with human CD4 without provoking detectable effects on cell viability and stimulation (Schweizer et al., 2008). In the course of an internship in the Buchholz lab at Paul-Ehrlich-Institut, Christian Osterburg PCR-amplified the coding sequence of the CD4-specific DARPin 29.2 and cloned it into the pCG-Hmut backbone (encoding the cytoplasmic tail-truncated Hmut protein Funke et al., 2008) via *Sfi*I/*Not*I. The resulting plasmid pCG-H-αCD4, encoding MV$_{Nse}$-derived HmutΔ18 fused to the DARPin 29.2 (Figure 36A), was used in this thesis for the generation of CD4-LV.

Surface expression of envelope glycoproteins on packaging cells is required to ensure their incorporation into lentiviral particles. To assess the surface expression of H-αCD4, HEK-293T cells were seeded in 6-well plates and transfected with 5 µg pCG-H-αCD4 or 5 µg pCG-1, the empty expression plasmid, which served as negative control. 48 hours later, cells were subjected to flow

cytometric analysis. 77.9% of transfected HEK-293T cells stained positive for histidine-tagged H-αCD4, demonstrating strong surface expression of H-αCD4 in packaging cells (Figure 36B).

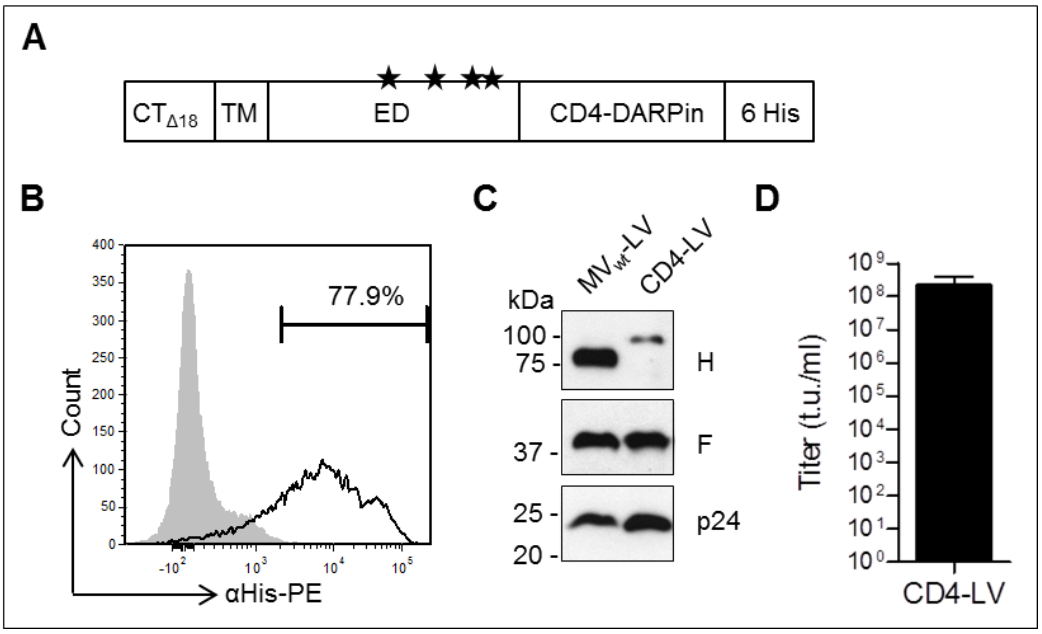

Figure 36: Characterization of CD4-LV. (A) Schematic depiction H-αCD4. The natural receptor tropism of MV_{Nse} hemagglutinin (H) is ablated by four point mutations in the ectodomain (ED), as indicated by asterisks, and the CD4-specific Designed Ankyrin Repeat Protein 29.2 (CD4-DARPin) is fused to the C-terminus of Hmut. A histidine tag (6 His) is located at the DARPin's C-terminus. N-terminal truncation of the cytoplasmic tail of Hmut by 18 amino acids ($CT_{\Delta 18}$) allows stable incorporation into lentiviral particles. TM indicates the transmembrane domain. **(B)** Surface expression of H-αCD4. HEK-293T cells were transfected with pCG-H-αCD4 (black line) or the empty expression plasmid pCG-1 (gray area). 48 h after transfection, cells were stained with anti-His-PE antibody and subsequently analyzed by flow cytometry. One representative experiment out of n = 3 shown. **(C)** Incorporation of H-αCD4 and F into lentiviral particles. To assess the incorporation of H-αCD4 and F into lentiviral particles, concentrated CD4-LV was subjected to Western Blot analysis using antibodies against H, F and p24. MV_{wt}-LV, displaying no additional binding domain, was used as control. **(D)** Average titer of concentrated CD4-LV. CD4-LV containing supernatant of HEK-293T packaging cells was harvested, concentrated and titers were determined on Molt4.8 cells (n = 11). Error bars represent mean ± SD. Panels A-C derived from Zhou et al., 2015.

Incorporation of the engineered MV envelope glycoproteins H-αCD4 and F into LV particles was examined by Western Blot analysis. To generate the resulting CD4-LV particles, HEK-293T cells were transfected with pCMVΔR8.9 (packaging plasmid), pS-luc2-GFP-W (transfer vector encoding firefly luciferase and sfGFP), pCG-FcΔ30 and pCG-H-αCD4 (MV Env encoding plasmids) as described in 2.2.4.3. H and F expression plasmids were employed in the ratio of 1:5, which resulted in high titer stocks (data not shown). Vector-containing supernatant was concentrated by ultracentrifugation through a 20% sucrose-cushion and concentrated CD4-LV was loaded on a SDS-polyacrylamide gel. MV_{wt}-LV served as a positive control. The membrane was probed for H, F and HIV-1 p24. $H_{wt}\Delta 18$ was detected at approximately 75 kDa according to its expected molecular weight (Funke et al., 2008), whereas H-αCD4 resulted in a signal at about 90 kDa, reflecting the fusion of HmutΔ18 with the CD4-specific DARPin 29.2 (Figure 36C). MV-GPs were efficiently incorporated into MV_{wt}-LV and CD4-LV particles, respectively. However, albeit detecting similar amounts of F,

CD4-LV was reproducibly characterized by a lower H and higher p24 content than MV_{wt}-LV. This might either reflect less incorporation of H-αCD4 into vector particles compared to H_{wt} or be due to a steric blocking effect of the DARPin on the antibody epitope.
Finally, the titer of concentrated CD4-LV was assessed on Molt4.8 leukemia cells. The mean titer of 11 concentrated preparations was $2.3 \pm 1.8 \times 10^8$ t.u./ml (Figure 36D).

3.2.2. Specificity of CD4-LV

As the biochemical characterization of H-αCD4 expression in HEK-293T packaging cells and its incorporation into CD4-LV provided satisfactory results (3.2.1), the specificity of CD4-LV for its target receptor was tested on cell lines in the next step. To this end, Molt4.8 and Raji cells were separately transduced with CD4-$LV_{Luc,GFP}$ at MOI 1. Molt4.8 is a human T cell line, expressing both CD4 and CD8. In contrast to that, the human Burkitt's lymphoma cell line Raji is negative for CD4. Three days after transduction, the percentage of transduced, GFP-expressing cells was measured by means of flow cytometry. Flow cytometry revealed exclusive transduction of $CD4^+$ but sparing of $CD4^-$ cells (Figure 37A). This speaks for the high specificity of CD4-LV for its target receptor CD4 on cell lines.
Moreover, the specificity of CD4-LV was assessed in human PBMC consisting of a naturally mixed population of $CD4^+$ and $CD4^-$ primary human T lymphocytes. For that purpose, human PBMC were isolated from buffy coats by density centrifugation using Histopaque®-1077 and T cells were subsequently activated by anti-CD3 and anti-CD28 antibodies and 100 IU/ml IL-2 (2.2.3.4). Using this stimulation approach, the vast majority of PBMC is composed of $CD3^+$ T cells after three days of incubation. These cells were then transduced with CD4-$LV_{Luc,GFP}$ at MOI 1. Three days later, the percentage of $GFP^+/CD4^+$ and $GFP^+/CD4^-$ cells was evaluated by flow cytometry. As shown in Figure 37B, CD4-LV exclusively transduced $CD4^+$ but not $CD4^-$ T cells. Transduction efficiency on $CD4^+$ T cells was determined with $39.0 \pm 11.9\%$ for $n = 6$ donors and was dependent on the respective donor. Concluding, CD4-LV displayed high selectivity for its target receptor also on primary cells.

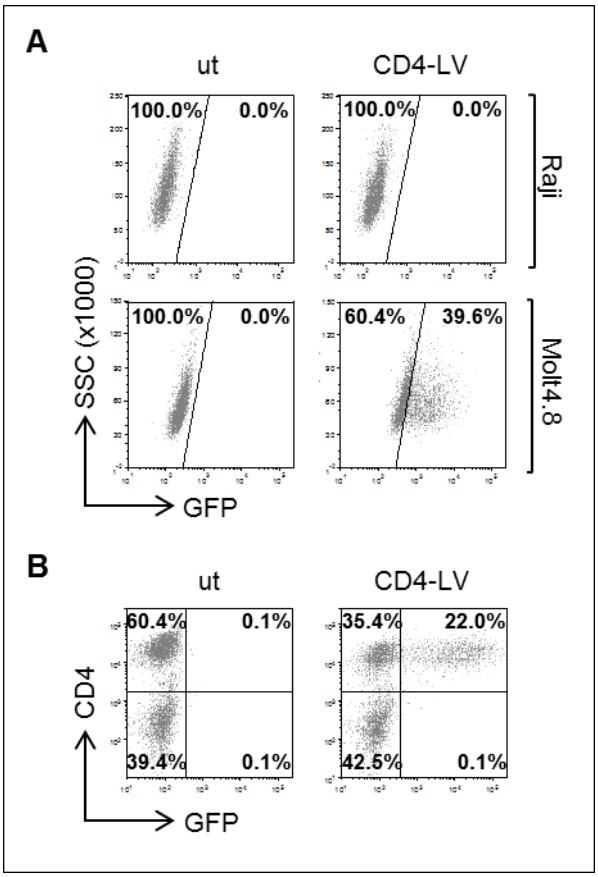

Figure 37: Specificity of CD4-LV. (A) Specificity of CD4-LV on cell lines. $CD4^-$ Raji and $CD4^+$ Molt4.8 cells were separately transduced with CD4-$LV_{Luc,GFP}$ (MOI 1) or left untransduced (ut). The percentage of GFP-expressing cells was determined by flow cytometry 3 d after transduction. **(B)** Specificity of CD4-LV on primary PBMC. Buffy coat-derived human PBMC were stimulated with anti-CD3/CD28 antibodies and recombinant human IL-2 for 3 d before transduction with CD4-$LV_{Luc,GFP}$ (MOI 1). Untransduced cells (ut) represent the negative control. The percentage of GFP^+ cells was determined by flow cytometry 3 d after transduction. Surface expression of CD4 was visualized by staining with an APC-conjugated antibody directed against human CD4. One representative donor out of six (n = 6) is shown. Panel A derived from Zhou et al., 2015.

3.2.3. Transduction of resting T helper cells

Lentiviruses and thereof derived lentiviral vectors are capable of transducing a variety of non-proliferating cells (Weinberg et al., 1991; Lewis et al., 1992; Naldini et al., 1996). Nonetheless, there are a few particularly resting cell types exempted for commonly used vectors like VSV-LV, e.g. quiescent lymphocytes (Amirache et al., 2014). Recently, it has been shown, however, that LVs pseudotyped with MV vaccine strain or wild-type glycoproteins can overcome this block and productively transduce resting lymphocytes (Frecha et al., 2008a; Frecha et al., 2009; Zhou et al., 2011). Moreover, vectors pseudotyped with MV glycoproteins engineered to target CD19 and CD20 surface molecules were able to transduce receptor-positive resting B cells while inducing minimal activation of the cells (Kneissl et al., 2013). Therefore, the question arose whether also CD4-LV is able to transduce resting $CD4^+$ T cells and if so, how efficient resting $CD4^+$ lymphocytes are transduced in comparison to activated ones.

To tackle this question, PBMC were isolated from fresh donor blood by density centrifugation using Histopaque®-1077 (2.2.3.4). Then, PBMC were either left unstimulated and directly transduced by spin occulation with CD4-$LV_{Luc,GFP}$ at MOIs 2 and 10 in T cell medium (TCM) containing no IL-2, or stimulated (see 2.2.3.4) before spin occulation with CD4-$LV_{Luc,GFP}$ (MOIs 2, 10) in TCM supplemented with 100 IU/ml IL-2. The activation state of the lymphocytes at the time point of

transduction was assessed by staining for CD25, the α-chain of the IL-2 receptor which is upregulated upon stimulation of T cells (Janeway et al., 2008). Transduction efficiency was analyzed by quantification of GFP^+ cells in the $CD4^+$ population by flow cytometry. Three days after transduction, unstimulated PBMC were thoroughly washed in PBS and subsequently activated using anti-CD3 and anti-CD28 antibodies, and 100 IU/ml IL-2 in order to enable long-term cultivation.

In the freshly isolated PBMC, only about 1.5% of $CD4^+$ cells stained positive for CD25 (Figure 38A), whereas activation of PBMC by anti-CD3/CD28 antibodies and IL-2 was confirmed by solid CD25 expression (Figure 38B). CD4-LV specifically transduced 8.1% of the unstimulated $CD4^+$ T cells in PBMC at an MOI of 2 (Figure 38C, day 3). Stable transgene expression was confirmed six days after transduction by flow cytometric detection of 7.9% $GFP^+/CD4^+$ lymphocytes. As expected, CD4-LV (MOI 2) transduced stimulated T cells more efficiently than unstimulated ones (approximately 5-fold increased transduction efficiency, see Figure 38C). Interestingly, a temporary down-regulation of the CD4 surface expression was observed following transduction with CD4-LV (Figure 38D). This was especially pronounced for unstimulated cells and the more distinct the more vector particles were applied (compare MOI 2 and 10, Figure 38D). Over time, an increase in CD4 surface expression back to levels observed for untransduced control cells was monitored.

Taken together, the data show the ability of CD4-LV to stably transduce primary resting T cells and exclude pseudotransduction. However, transduction efficiency in resting T lymphocytes was lower than in stimulated ones.

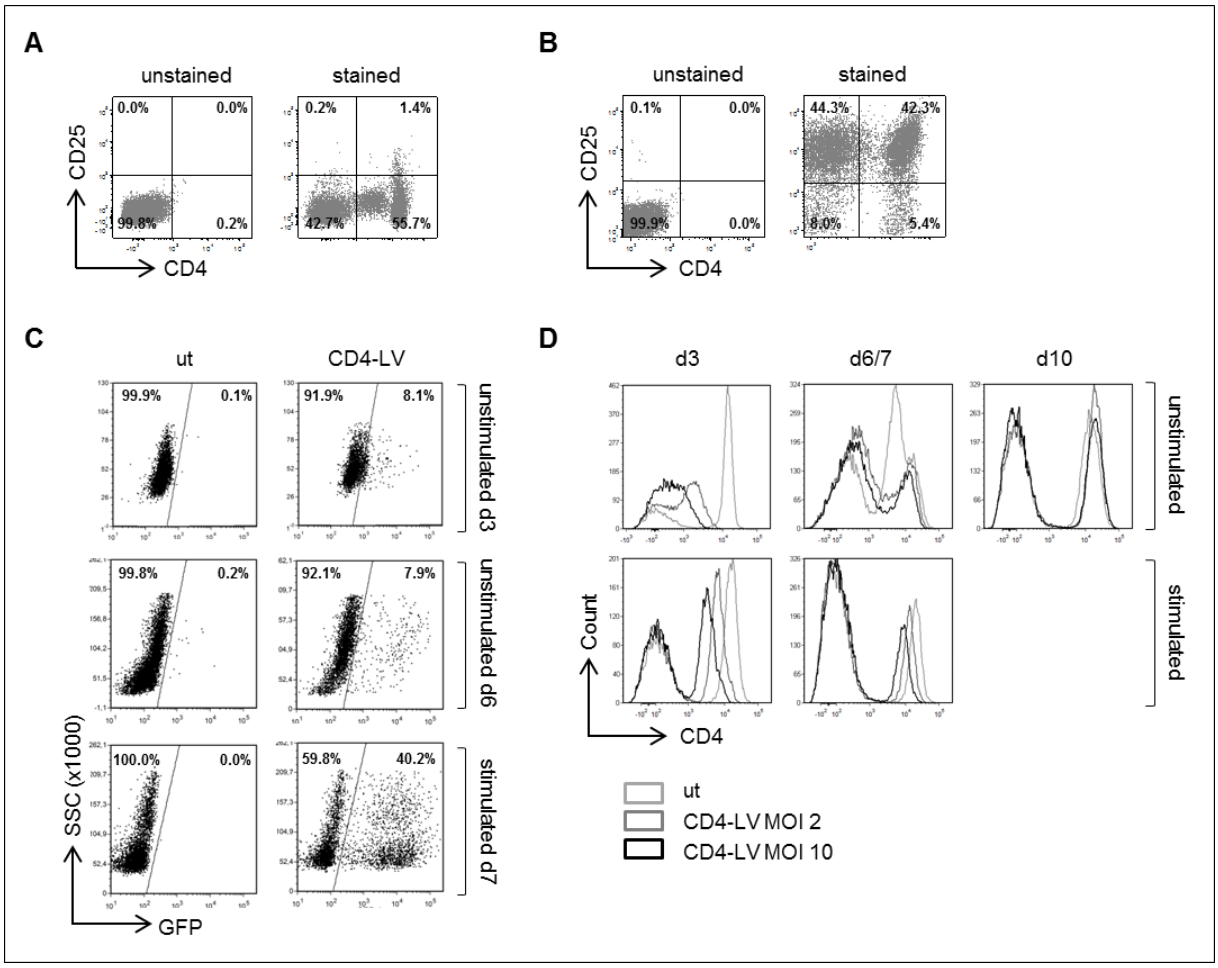

Figure 38: Transduction of resting primary PBMC. (A) Examination of CD25 expression in freshly isolated PBMC. PBMC derived from fresh donor blood were stained for CD4 and CD25 and subjected to flow cytometry analysis. One representative donor out of three is shown (n = 3). **(B)** Examination of CD25 expression in activated PBMC. PBMC were stimulated by anti-CD3/CD28 antibodies and IL-2 for 3 d and subsequently examined for CD4 and CD25 expression by flow cytometry. One representative donor out of three is shown (n = 3). **(C)** Transduction of unstimulated PBMC. To determine the ability of CD4-LV to transduce resting T cells, freshly isolated PBMC were left untransduced (ut) or transduced with CD4-$LV_{Luc,GFP}$ at MOI 2. 3 d after transduction, half of the cells were analyzed by flow cytometry for the percentage of GFP^+ cells in the $CD4^+$ population. The other half was thoroughly washed in PBS and cultured in the presence of anti-CD3/CD28 antibodies and 100 IU/ml IL-2 for three more days. Then, the percentage of GFP^+ cells in the CD4-gated population was determined by flow cytometry again. In parallel, PBMC from the same donor were stimulated for three days and then transduced with CD4-$LV_{Luc,GFP}$ at the same MOI. 7 d after transduction, the percentage of $GFP^+/CD4^+$ cells was determined by flow cytometry. One representative donor out of three is shown (n = 3) **(D)** Surface expression of CD4. Unstimulated and stimulated PBMC were transduced with CD4-$LV_{Luc,GFP}$ at MOI 2. At the indicated time points after transduction, CD4-expression was assessed by flow cytometry. One representative donor out of three is shown (n = 3). Panels C and D modified after Zhou et al., 2015.

3.2.4. Transduction of macrophages

CD4 is not only expressed on T helper cells but also present on monocytes and macrophages (Lee et al., 1999). Therefore, the question arose if also these cell types become transduced by CD4-LV, which was tested in the present thesis for human macrophages.

Two different macrophages types, named M1 and M2 macrophages, were kindly provided by Meike Thomas (van Zandbergen group, Paul-Ehrlich-Institut). M1 or classically activated macrophages are

activated through Toll-like receptors and IFN-γ and are characterized as pro-inflammatory. The more heterogeneous M2 or alternatively activated macrophage population is induced by IL-4 or IL-13 and has anti-inflammatory properties (Mosser and Edwards, 2008; Jetten et al., 2014). The cells were generated from buffy coat-derived PBMC by plastic adherence (incubation of 5 x 10^6 PBMC per T25 flask in the presence of 1% human plasma for 1.5 hours) and subsequent cultivation of adherent cells in the presence of either 10 ng/ml GM-CSF (M1 macrophages) or 30 ng/ml M-CSF (M2 macrophages) for six days.

In a first step, both macrophage types were analyzed for surface expression of the target receptor CD4 as well as the monocyte/macrophage marker CD14 by flow cytometry. Flow cytometry revealed expression of CD4 both in M1 and M2 macrophages (Figure 39). However, M1 macrophages showed considerably lower levels of CD4 than M2 macrophages. This observation is in line with a previous report demonstrating M1 polarization to be associated with a down-regulation of CD4 (Cassol et al., 2009).

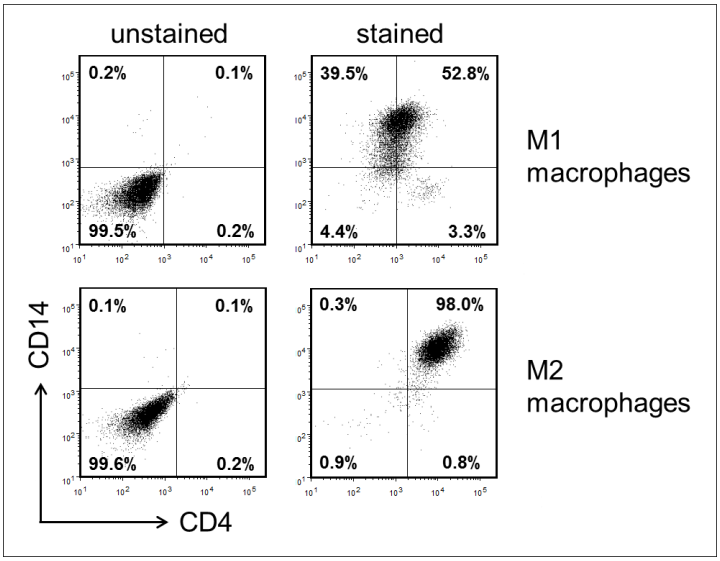

Figure 39: Expression of CD4 and CD14 by M1 and M2 macrophages. Macrophages were generated from PBMC by plastic adherence and subsequent cultivation in the presence of GM-CSF or M-CSF. The cells were stained for the surface markers CD4 and CD14 and analyzed by flow cytometry.

M1 and M2 macrophages were transduced with CD4-$LV_{Luc,GFP}$ at MOIs of 1 and 10, respectively. Additionally, macrophages were pre-incubated with HIV-2 protein Vpx transferring PBj-VLP vpx (kindly provided by Meike Thomas, van Zandbergen group Paul-Ehrlich-Institut) at MOI 1 for two hours before transduction with CD4-$LV_{Luc,GFP}$ MOI 10. PBj-VLP vpx pre-treated cells served as positive controls as Vpx leads to the degradation of the HIV-1 restriction factor SAMHD1, a dNTP triphosphohydrolase that reduces the levels of intracellular dNTPs and therefore hampers HIV-1 reverse transcription (Berger et al., 2011; Laguette et al., 2011). Transduction efficiency was analyzed by laser scanning microscopy (9 days after transduction) and flow cytometry (12 days after transduction).

The data indicate that both, M1 and M2 macrophages, can be transduced by CD4-LV (Figure 40). For M1 macrophages, comparable transduction of about 30% was observed with CD4-LV at MOI 10

independent of the pre-incubation with PBj-VLP vpx. Transduction of M1 macrophages with CD4-LV at MOI 1 resulted in approximately 10-fold lower transduction efficiency compared to CD4-LV at MOI 10. M2 macrophages were found to be considerably more susceptible to CD4-LV upon pre-incubation with PBj-VLP vpx than without Vpx pretreatment (70% versus 2% GFP^+ cells after transduction with CD4-LV MOI 10). Incubation of M2 macrophages with CD4-LV at MOI 1 did barely lead to any transduction.

Taken together, both M1 and M2 macrophages can be transduced by CD4-LV albeit transduction efficiencies strongly varied. Addition of Vpx increased transduction efficiency in M2 but not M1 macrophages.

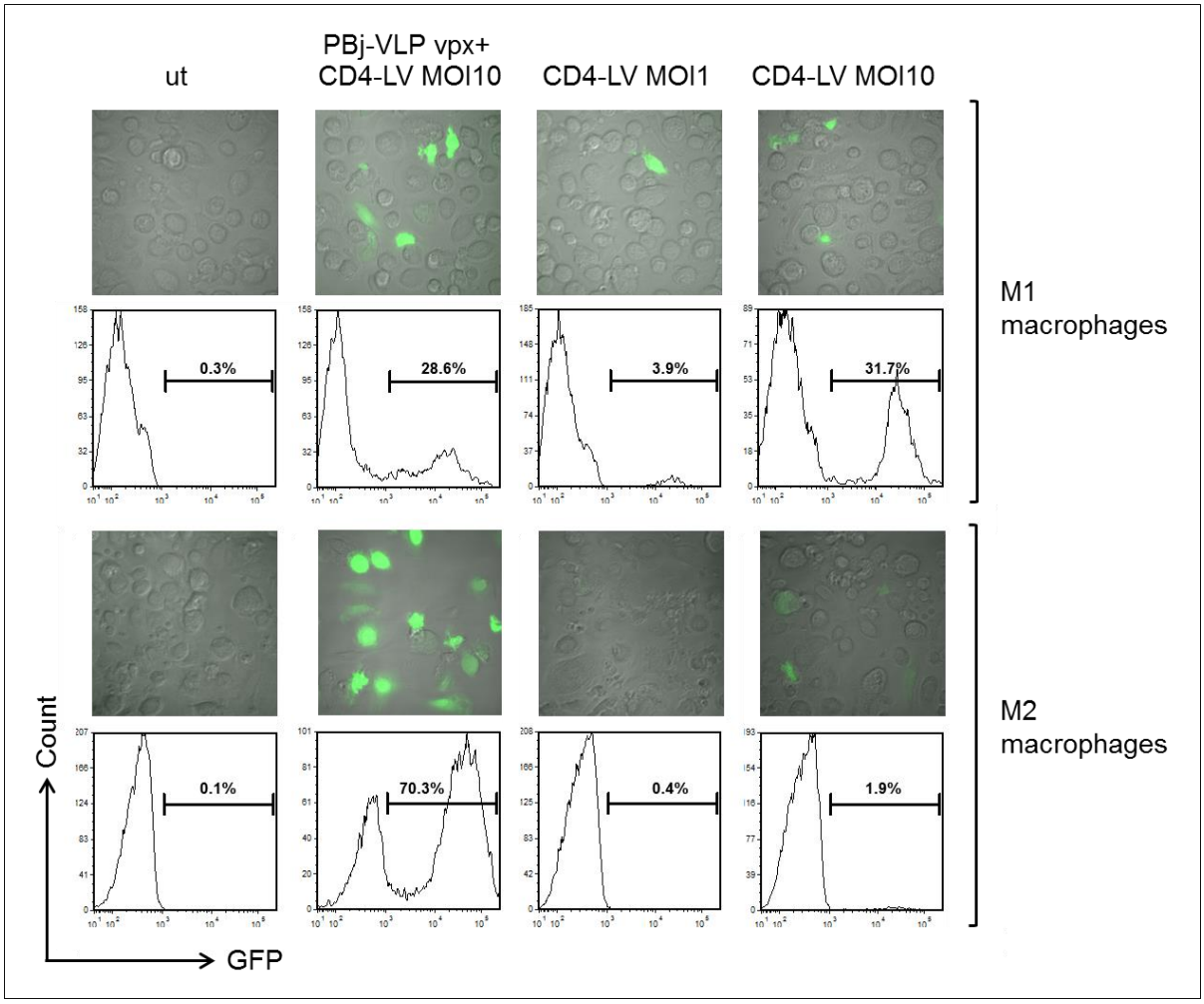

Figure 40: Transduction of M1 and M2 macrophages by CD4-LV. M1 and M2 macrophages were generated from PBMC by plastic adherence and subsequent cultivation in the presence of 10 ng/ml GM-CSF or 30 ng/ml M-CSF, respectively. Macrophages remained untransduced (ut) or were transduced with CD4-$LV_{Luc,GFP}$ at the indicated MOIs with or without preincubation with PBj-VLP vpx (MOI 1) for 2 h. Transduction efficiency was analyzed by microscopy (9 d after transduction) and flow cytometry (12 d after transduction). The percentage of GFP^+ transduced cells is indicated. The experiment was performed once (n = 1).

3.2.5. Systemic application of CD4-LV in PBMC-reconstituted mice

In vitro, the tropism of CD4-LV had been restricted to $CD4^+$ target cells (Figure 37). Additionally, potent CD4-LV stocks could be generated (Figure 36D), characterized by an at least 10-fold higher titer than CD8-LV which mediated successful gene transfer after local administration (Zhou et al., 2012). Meeting these requirements, the *in vivo* targeting potential of systemically injected CD4-LV was examined. As the implemented DARPin 29.2 is highly specific for human CD4 and does not recognize the murine version (Schweizer et al., 2008), specificity could not be assessed in a conventional mouse system. However, immunodeficient NOD-scid $IL2\gamma^{-/-}$ (NSG) mice can be repopulated with human PBMC or human HSC in order to develop a (functional) human immune system within these animals (Shultz et al., 2012). Therefore, these mice represent a suitable *in vivo* model to test the specificity and biodistribution of CD4-LV. To enable both, non-invasive biodistribution studies over time, and simple detection of transduced cells by flow cytometry, CD4-$LV_{Luc,GFP}$ vectors were employed. The bicistronic genome transferred by these particles encoded firefly luciferase and sfGFP (Abel et al., 2013). Both transgenes are under control of a SFFV promoter and were separated by a T2A site (Figure 43A).

3.2.5.1. Establishing the animal model

Before the specificity and biodistribution of CD4-LV in PBMC-repopulated NOD-scid $IL2R\gamma^{-/-}$ mice could be tested, this humanized mouse model had to be established in our laboratory. In order to assess repopulation kinetics dependent on the application route, five immunodeficient NSG mice were intravenously (i.v.) or intraperitoneally (i.p.) injected with 1 x 10^8 PBMC, respectively. The cellular composition of freshly isolated buffy coat-derived PBMC was exemplarily evaluated for one random donor (Figure 41A). At day 5 and 7 post injection of PBMC, peripheral blood was withdrawn (2.2.5.2) and analyzed for the percentage of human $CD45^+$ lymphocytes by flow cytometry (2.2.3.8). Moreover, also the abundance of distinct human cell populations in the blood of PBMC-repopulated NSG mice was assessed by flow cytometry, staining for the T cell marker CD3, the B cell antigen CD19 and CD14, present on the surface of monocytes and macrophages.

As shown in Figure 41B, intravenous cell application proved to be superior to intraperitoneal administration with 2 - 3 fold more human $CD45^+$ cells detectable in the peripheral blood. Besides, flow cytometric analysis revealed the vast majority of engrafted cells to be T cells (Figure 41C) which is in line with literature (Shultz et al., 2012). However, as *in vivo* specificity and biodistribution of the T cell-tropic CD4-LV should be assessed, PBMC-repopulated NSG mice represented a suitable animal model for initial tests.

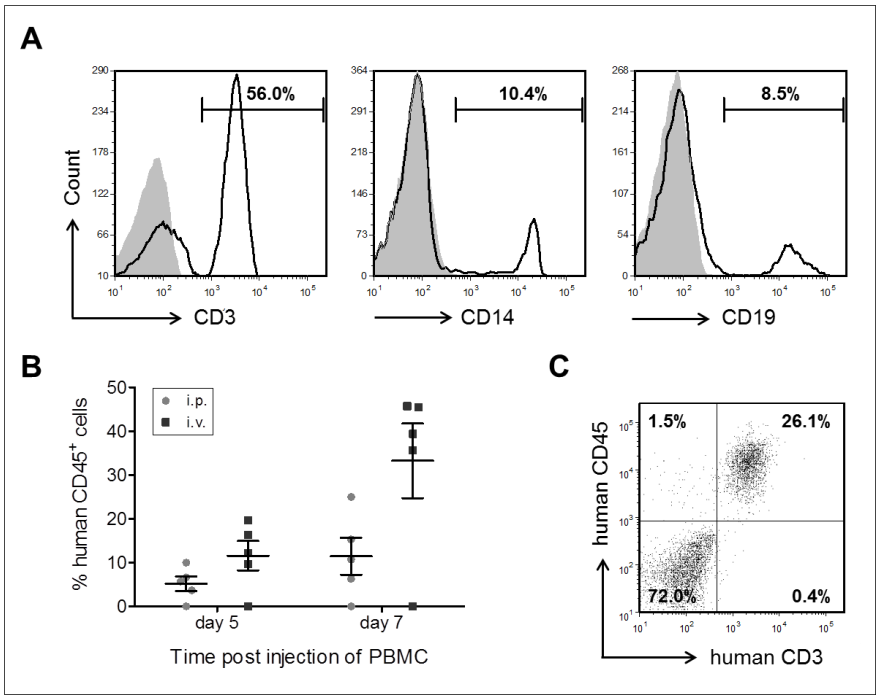

Figure 41: Humanization of NOD-scid IL2Rγ$^{-/-}$ mice with primary human PBMC. (A) Flow cytometric characterization of freshly isolated PBMC from a random donor for the percentage of T cells (CD3$^+$), monocytes and macrophages (CD14$^+$) as well as B cells (CD19$^+$). Gray: unstained control, black lines: antibody staining. **(B)** Determination of the percentage of human CD45$^+$ cells in the peripheral blood of NOD-scid IL2Rγ$^{-/-}$ mice intraperitoneally (i.p.) or intravenously (i.v.) injected with human PBMC. Results are depicted as mean ± SEM. **(C)** Blood of a humanized animal analyzed for the expression of human CD45 and human CD3 9 d after i.p. injection of 1 x 10^8 PBMC.

As expected, the animals succumbed to graft versus host disease (GvHD) when a certain level of human lymphocytes was reached within their bodies. Imminent death was to be expected when approximately 60% human CD45$^+$ cells were present in the peripheral blood (data not shown). Animals injected with 1 x 10^8 PBMC reached nearly 50% human CD45$^+$ cells in the peripheral blood seven days after injection (Figure 41B). Thus, the number of PBMC to be injected had to be reduced in order to extend the observation period in further experiments. However, administering too few PBMC would delay the optimal time point for vector injection (reached for 10% - 20% human CD45$^+$ cells in the peripheral blood according to own experience values). Therefore, the PBMC number was adjusted to 5 x 10^7 unstimulated and 1.5 x 10^7 stimulated PBMC which show faster repopulation kinetics. Successful engraftment was observed for mice of different ages, the oldest animals being 18 weeks old at the time point of cell injection (data not shown).

3.2.5.2. Intravenous administration of CD4-LV

6-8 weeks old immunodeficient NSG mice were i.v. injected with 5 x 10^7 freshly isolated unstimulated PBMC or 1.5 x 10^7 stimulated PBMC solved in 200 µl PBS. Activation of PBMC was performed as described in 2.2.3.4. Some of the stimulated PBMC were depleted for CD4$^+$ T cells before injection (see 2.2.3.5 and Figure 42). When approximately 10% - 20% human CD45$^+$ cells were present in

blood (commonly on day three), animals were injected with 200 µl CD4-$LV_{Luc,GFP}$ the next day or the next two consecutive days (Figure 43A). The administered CD4-$LV_{Luc,GFP}$ dilutions in PBS corresponded to 5 x 10^6 t.u. or 8 x 10^7 t.u. per mouse. Humanized animals injected with PBS or unhumanized animals injected with CD4-$LV_{Luc,GFP}$ served as negative controls. An overview over the different groups and their treatment is given in Figure 43B.

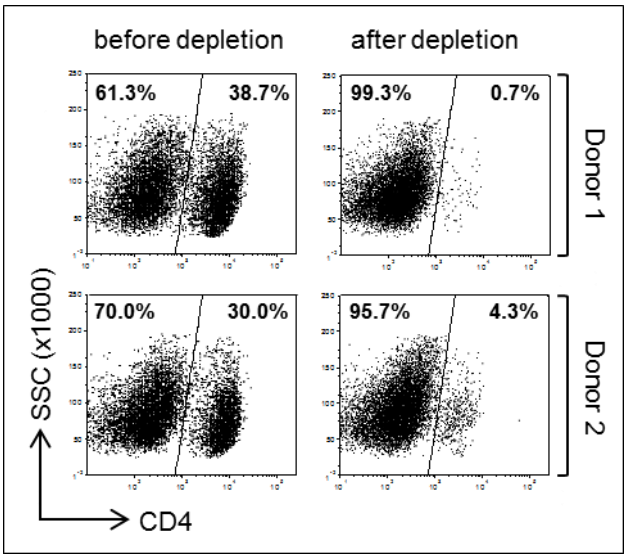

Figure 42: Residual $CD4^+$ T cells after CD4-depletion of activated PBMC. PBMC from two different donors were activated by anti-CD3/CD28 antibodies and IL-2 for 3 d and subsequently depleted for $CD4^+$ cells using microbeads. To determine the percentage of $CD4^+$ T cells before and after depletion, cells were stained with APC-conjugated anti-CD4 antibody and analyzed by flow cytometry. Figure modified after Zhou et al., 2015.

Assessment of *in vivo* distribution of CD4-LV by *in vivo* imaging of luciferase activity

In vivo distribution of CD4-$LV_{Luc,GFP}$ was monitored by imaging luciferase activity. Following vector administration, luciferase activity was detected in both, animals humanized with unstimulated PBMC (Group D and E) and mice engrafted with activated PBMC (Group F) (Figure 43C-F). Strong luciferase activity was found in lymphoid organs like spleen, thymus and lymph node like structures (Figure 43F). Besides, luciferase activity was observed in the skin, liver and lung of the animals (Figure 43E and data not shown) and depended on the state of graft versus host disease (GvHD). Luciferase expression correlated positively with vector dose as stronger luciferase activity was detected in animals repopulated with unstimulated PBMC and injected with 8 x 10^7 t.u. CD4-LV (Group E) than in animals injected with 5 x 10^6 t.u. CD4-LV (Group D) (Figure 43C, D and F). However, as already observed *in vitro* (Figure 38), higher transduction efficiency and therefore luciferase activity was detected in mice which received stimulated PBMC (Group F) compared to animals engrafted with unstimulated PBMC (Group E), when the same vector dose was applied. In mice repopulated with CD4-depleted PBMC and also injected with 8 x 10^7 t.u. CD4-LV (Group C), overall luciferase activity was significantly reduced compared to animals engrafted with unstimulated or stimulated PBMC (Figure 43C-F). In these animals, luciferase activity was present in spleen and spine or buttocks region and positively correlated with the number of residual $CD4^+$ cells in the respective CD4-depleted PBMC-engraftment (left animal in Group C (Figure 43) engrafted with donor 1 (Figure 42); right animal in Group C (Figure 43) engrafted with donor 2 (Figure 42)). In

humanized control animals, which received no vector (Group A), no luciferase activity could be observed upon injection of the substrate luciferin. Also in unhumanized mice injected with CD4-$LV_{Luc,GFP}$ (Group B) only negligible spleen and spine signals just above the detection limit on the logarithmic scale were present (Figure 43C).

Taken together, these data demonstrate *in vivo* transduction with CD4-$LV_{Luc,GFP}$ to be clearly dependent on the presence and activation state of its target cells.

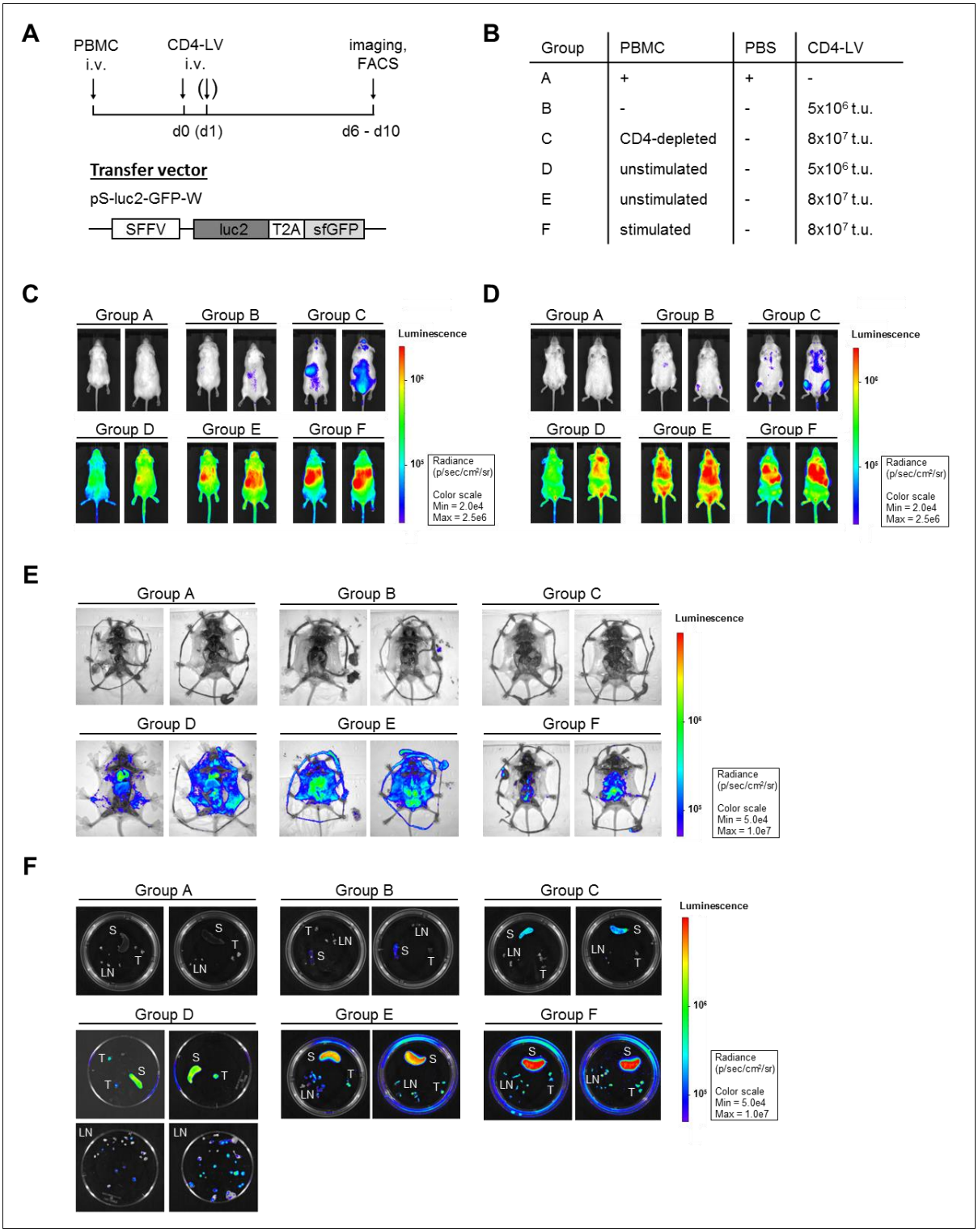

Figure 43: *In vivo* luminescence imaging of PBMC-engrafted mice i.v. injected with CD4-LV$_{Luc,GFP}$. (A) Experimental set-up. NOD-scid IL2Rγ$^{-/-}$ mice were intravenously injected with either 5 x 10^7 unstimulated PBMC or 1.5 x 10^7 PBMC stimulated with anti-CD3/CD28 and IL-2 for 3 d. Stimulated PBMC may additionally have been depleted for CD4$^+$ cells (Group C). One day after flow cytometric detection of 10-20% human CD45$^+$ cells in the peripheral blood of the animals, 200 µl CD4-LV transferring the reporter genes *luciferase* (luc2) and *gfp* (sfGFP) was administered systemically. The two genes are connected via a T2A linker and are expressed under control of the spleen focus-forming virus (SFFV) promoter. 6-10 d after vector injection, luciferase activity was monitored by *in vivo* imaging (C-F) and transduction efficiency was quantified by flow cytometry. Luciferase signal intensity in panels C-F is expressed as photons/second/square centimeter/steradian (p/sec/cm2/sr). **(B)** Legend for the group designations used in subpanels C-F. **(C-D)** Whole body imaging of humanized mice injected with CD4-LV in dorsal (C) and ventral view (D). Mice were imaged 6-10 d after vector administration. Images of two representative animals from each group are shown. **(E)** *In vivo* imaging of mice after dissection. Animals were dissected and spleen, thymus, and lymph node like structures were removed and imaged separately. Additionally, lung, heart, and liver were removed (all groups except Group D). Intestinal tracts were arranged in a circle around the animals. **(F)** Luciferase activity in explanted lymphoid organs. Luminescence of spleen (S), thymus (T), and lymph node like structures (LN) was acquired by *in vivo* imaging. Panels C and F derived from Zhou et al., 2015.

Quantification of transduction events in blood and spleen by flow cytometry

Transduction efficiency of CD4-LV$_{Luc,GFP}$ in blood and spleen was quantified by flow cytometric detection of GFP$^+$ cells. In order to ensure proper read-out of the percentage of GFP$^+$ transduced cells, it was absolutely necessary to analyze as much cells as possible, e.g. 1 million splenocytes. All GFP-expressing cells were characterized as human CD45-positive lymphocytes (Figure 44 and data not shown for Groups C-E).

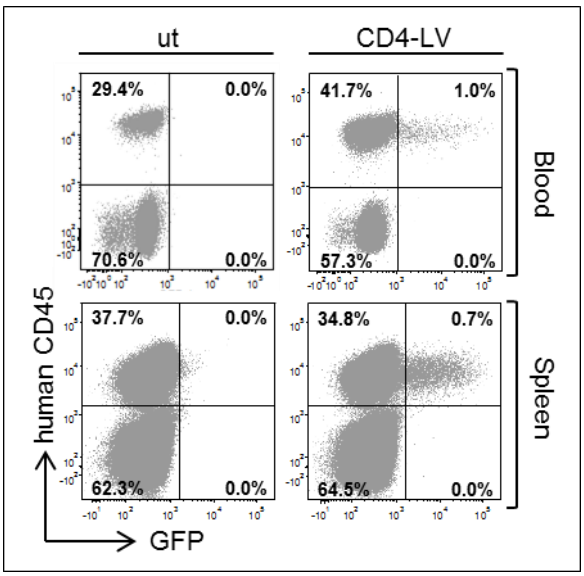

Figure 44: No off-target transduction of murine cells by CD4-LV in PBMC-repopulated animals. Mice were treated as described for Group F in Figure 43A. 7 d after systemic administration of CD4-LV, mice were sacrificed and cells isolated from blood and spleen were stained for human CD45 to distinguish mouse and human cells. The percentage of transduced cells was determined by flow cytometry. One representative data set out of six individual mice shows GFP$^+$ cells in the human and murine cell population.

Within the CD45$^+$ human lymphocyte population, CD4-LV$_{Luc,GFP}$ selectively transduced CD3$^+$/CD4$^+$ human lymphocytes while sparing CD3$^+$/CD4$^-$ human T cells (Figure 45A, and data not shown for Groups C and D). The percentage of transduced cells in blood and spleen of animals repopulated with unstimulated PBMC averaged between approximately 0.5% (Group D) and 1.0% (Group E), and reached up to 16.6% and 9.2% in blood and spleen of mice humanized with stimulated PBMC (Group F), respectively (Figure 45B).

Taken together, also *in vivo* CD4-LV showed clear target cell specificity. It preferentially transduced more activated cells.

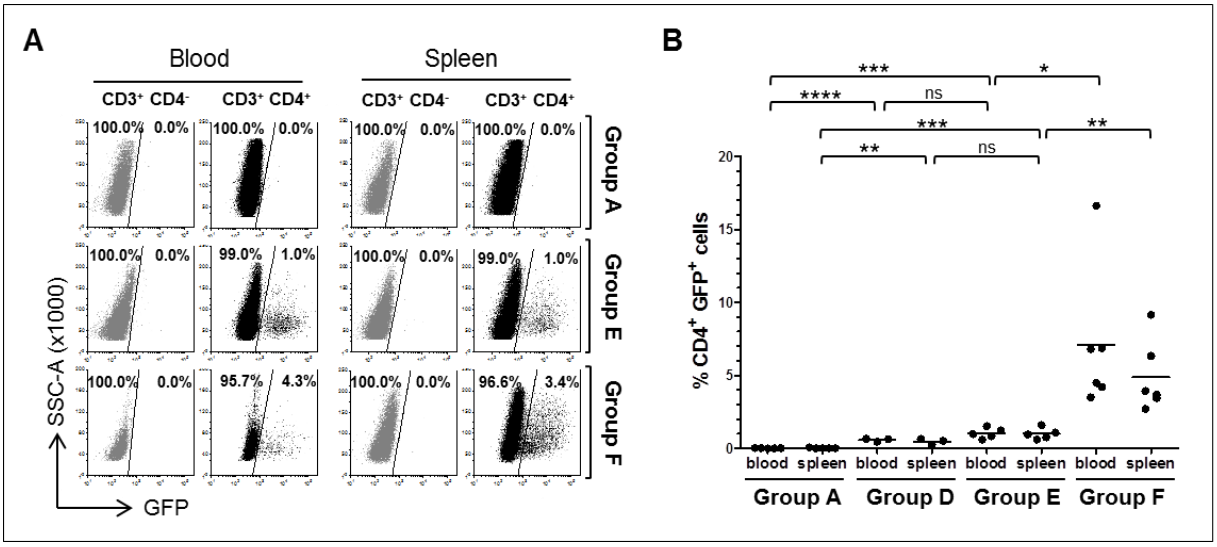

Figure 45: *In vivo* transduction of CD4$^+$ T cells in PBMC-engrafted mice. 6-10 d after intravenous vector injection, animals were sacrificed and cells isolated from blood and spleen were stained for human CD45, human CD3 and human CD4. The percentage of GFP$^+$ cells in the human CD45$^+$/CD3$^+$/CD4$^-$ and CD45$^+$/CD3$^+$/CD4$^+$ population was determined by flow cytometry. **(A)** Quantification of transduction events within the human CD45$^+$/CD3$^+$/CD4$^-$ and CD45$^+$/CD3$^+$/CD4$^+$ population. **(B)** Summary of *in vivo* transduction efficiency. Each mouse is represented by a dot. Results are depicted as mean. *, **, ***, **** and ns indicate P<0.05, P<0.01, P<0.001, P<0.0001 and not significant, respectively. Data were analyzed using the two-tailed unpaired Student's t-test. Figure modified after Zhou et al., 2015.

3.2.6. *In vivo* targeting of CD4$^+$ cells in HSC-reconstituted mice

In the previous experiment PBMC-repopulated animals were used to assess the *in vivo* targeting potential of CD4-LV. However, in these mice mainly T cells developed from unstimulated PBMC or stimulated T cells were injected. Moreover, the observation period was limited due to GvHD. In order to evaluate the targeting properties of CD4-LV in a model better reflecting the natural immune system and its diverse cell types which additionally allows long-term monitoring of transgene expression, animals reconstituted with human hematopoietic stem cells (HSC) were used in the next step.

Systemic administration of CD4-LV$_{Luc,GFP}$ into HSC-reconstituted NSG mice was performed in collaboration with Dr. Udo Hartwig, University of Mainz, according to the experimental set-up shown in Figure 46A. For this purpose, Dr. Hartwig kindly engrafted 5-6 weeks old NSG mice with human CD34$^+$ HSC. Reconstitution of human immune cells was regularly monitored by flow cytometry and mice with 5-15% human CD4$^+$ T cells and 5-35% of human CD19$^+$ B cells in the peripheral blood were included in the experiment (data not shown). As stimulated T cells were shown *in vitro* and *in vivo* to be more prone to CD4-LV transduction than unstimulated ones (see 3.2.3 and 3.2.5.2), T cells were activated by i.v. injection of 10 µg OKT-3 five days prior systemic administration of 1.5 x 10^7 t.u.

CD4-LV$_{Luc,GFP}$. *In vivo* distribution of CD4-LV$_{Luc,GFP}$ was monitored by imaging luciferase activity over the period of 26 days.

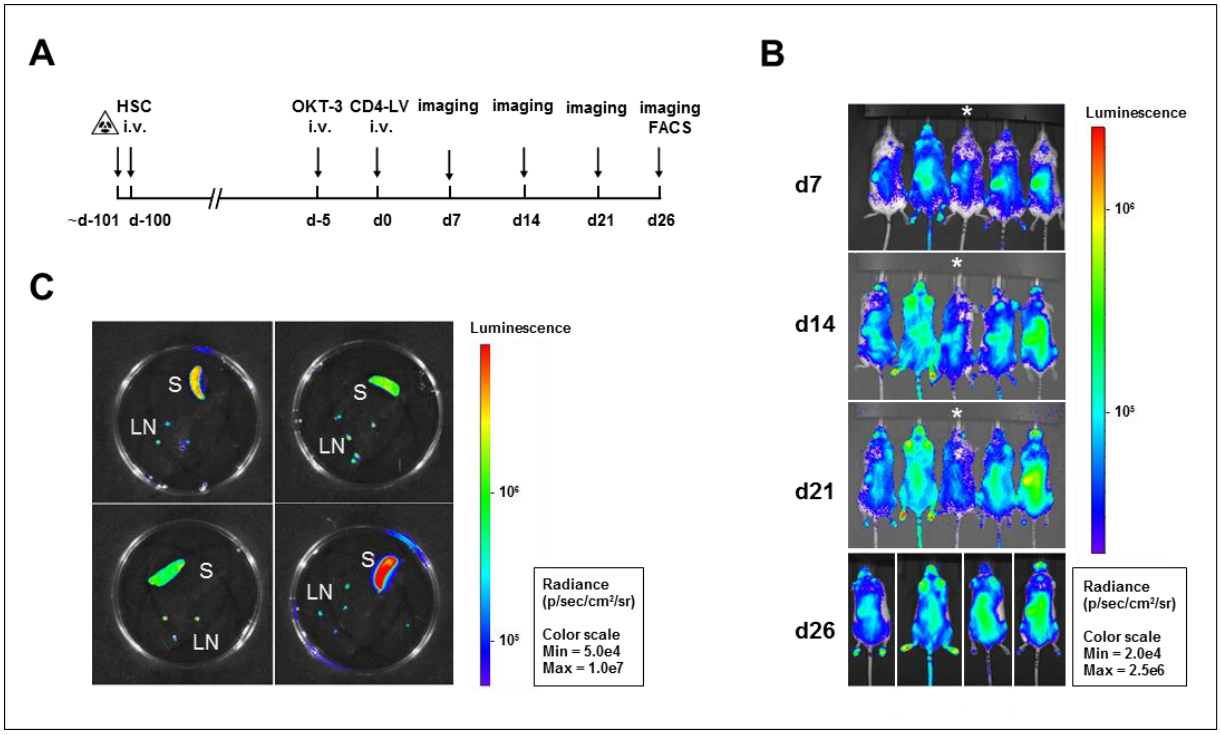

Figure 46: *In vivo* luminescence imaging of HSC-engrafted mice i.v. injected with CD4-LV$_{Luc,GFP}$. (A) Experimental set-up. 5-6 weeks old NOD-scid IL2Rγ$^{-/-}$ mice were irradiated with 150 cGy and intravenously (i.v.) injected with 1 x 10^6 adult CD34$^+$ HCS per mouse the next day. Approximately 95 d after injection of HSC, when stable engraftment of CD45$^+$ cells was demonstrated in the peripheral blood, each animal was i.v. injected with 10 µg OKT-3 to stimulate T cells. Five days later, 1.5 x 10^7 transducing units CD4-LV transferring *luciferase* and *gfp* reporter genes were i.v. injected per mouse. Transgene expression was monitored on day 7, 14 and 21 by luciferase imaging and on day 26 by luciferase imaging and flow cytometric detection of GFP$^+$ cells. **(B)** Whole body *in vivo* luminescence imaging of CD4-LV-injected animals. CD4-LV-injected mice were imaged at the indicated time points. One mouse (labeled by asterisk) had to be sacrificed before the scheduled end of the experiment due to splenic hyperplasia. **(C)** *In vivo* luminescence imaging of organs explanted from CD4-LV-injected mice. Mice were sacrificed 26 d after vector injection and luciferase activity in lymphoid organs was acquired by *in vivo* imaging. Each image shows spleen (S) and lymph node like structures (LN) isolated from an individual mouse. Luciferase signal intensity in panels B and C is expressed as photons/second/square centimeter/steradian (p/sec/cm^2/sr). Panels B and C derived from Zhou et al., 2015.

Luciferase activity was detected in all five animals injected with CD4-LV$_{Luc,GFP}$ (Figure 46B). Overall signal intensity increased within the first 14 days after vector injection and then remained constant to the end of the observation period. One week after vector administration, the strongest luminescence was observed in spleen, whereas at later observation points luciferase activity had spread within the entire torso. However, 26 days after vector injection, strongest luciferase activity was detected in the explanted spleens of dissected mice (Figure 46C). The data demonstrate stable transgene expression over the observation period of 26 days, which was especially pronounced in lymphoid organs.

Transduction events in blood, spleen, and bone marrow were assessed by flow cytometry. The analysis revealed exclusive transduction of up to 570 or 800 single human CD45$^+$ lymphocytes in spleen and

bone marrow (after substraction of negative control), respectively, but no transduction of murine cells (Figure 47).

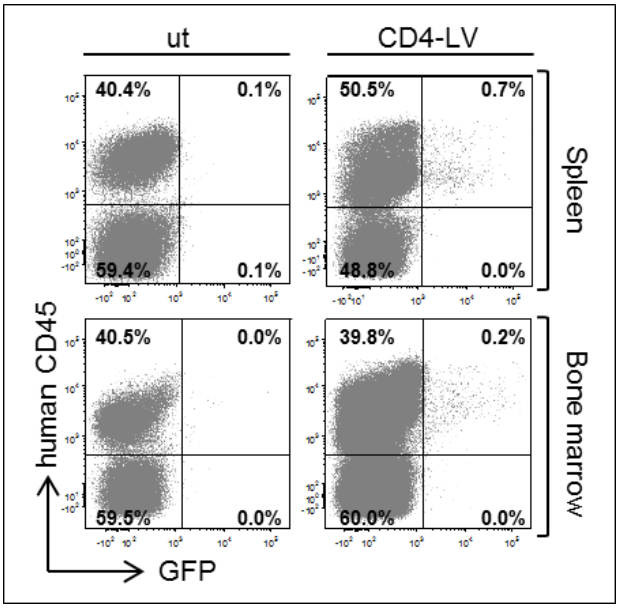

Figure 47: No off-target transduction of murine cells in HSC-repopulated animals. Mice were treated as described in Figure 46A**.** 26 d after systemic administration of CD4-LV, mice were sacrificed and cells isolated from spleen and bone marrow were stained for human CD45 to distinguish mouse and human cells. The percentage of transduced cells was determined by flow cytometry. One data set out of four individual mice shows GFP^+ cells in the human and murine cell population.

In blood, no human lymphocytes could be detected (data not shown). However, in spleen and bone marrow selective transduction of approximately 2% of $CD4^+$ cells but no transduction of $CD4^-$ cells in the human $CD45^+/CD3^+$ population was observed after a single injection of CD4-LV (Figure 48A). To identify the phenotype of transduced T cells, cells were stained for CD45RA (naïve T cells) and CD45RO (memory T cells). Here, a clear preference of CD4-LV for memory T cells was found in both tissues (Figure 48B and C). Concluding, CD4-LV displayed high selectivity for $CD4^+$ human T cells, and predominantly T lymphocytes with memory phenotype, *in vivo*.

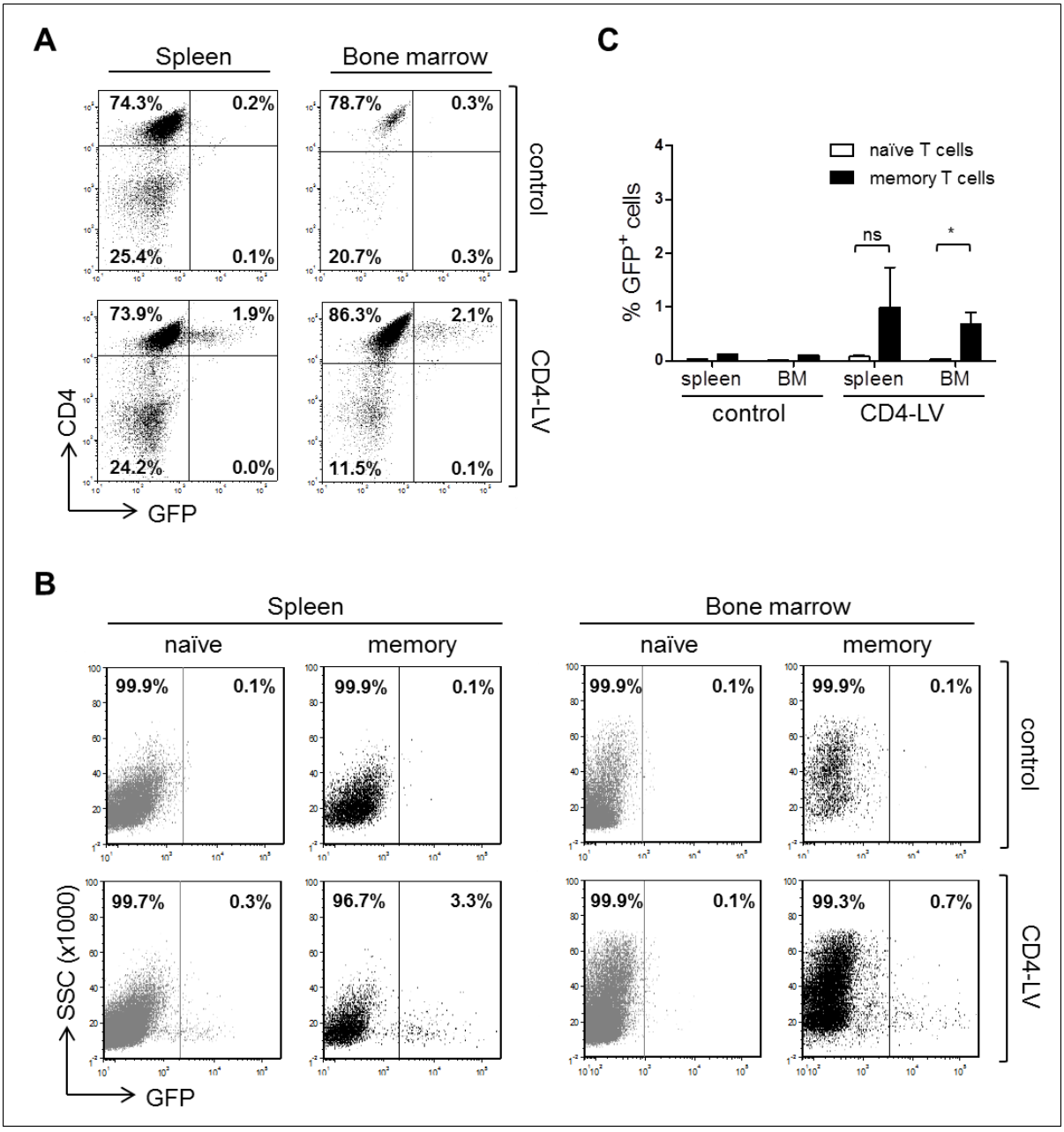

Figure 48: *In vivo* targeting of CD4$^+$ T cells in HSC-engrafted mice. NOD-scid IL2Rγ$^{-/-}$ mice were treated as described in Figure 46A. 26 d after systemic administration of CD4-LV, mice were sacrificed and spleen and bone marrow were removed. The percentage of transduced cells (A) and their phenotypes (B and C) was determined by flow cytometry. Control: humanized animal which received no CD4-LV. **(A)** Quantification of transduction events in spleen and bone marrow. One data set out of four individual mice showing the percentage of CD4$^+$/GFP$^+$ cells in the CD45$^+$/CD3$^+$ gate is depicted. **(B)** Quantification of transduced naïve and memory T cells. The percentage of GFP$^+$ cells in the naïve (CD45RA$^+$) and memory (CD45RO$^+$) T cell subsets was determined by flow cytometry. **(C)** Summary of transduction efficiency in four individual mice (n = 4). Results are depicted as mean ± SEM. * and ns indicate P<0.05 and not significant, respectively. Data were analyzed using the two-tailed unpaired Student's t-test. Figure modified after Zhou et al., 2015.

4. Discussion

Viral vectors have proven to be powerful tools for basic research and medical application, including gene therapy and vaccination. One major achievement concerning the safety and specificity of these vectors is entry-targeting. Entry-targeting is either based on pseudotyping with naturally occurring heterologous envelope proteins with desired narrow receptor specificity or engineered envelope glycoproteins selectively binding to a receptor of choice. In this thesis, both strategies of vector targeting were exploited using modified measles virus glycoproteins pseudotyped lentiviral vectors. Pseudotyping with truncated MV_{wt}-GPs led to a predominant tropism for SLAM-expressing cells and therefore enabled protein transfer into $SLAM^+$ APCs, whereas engineered MV_{NSe}-derived glycoproteins displaying a CD4-specific DARPin on receptor-blind H allowed specific gene delivery into $CD4^+$ immune cells.

4.1. Targeted protein transfer into $SLAM^+$ cells

Dendritic cells are considered the most potent type of APCs (Gaspari and Tyring, 2008). They are powerful inducers of B and T lymphocyte immune responses (Banchereau and Steinman, 1998) and as such attractive targets for vaccination approaches.

Therefore, major effort has been devoted to introduce antigens specifically into DCs. Since DCs are non-dividing, the ability of LVs to transduce mitotically inactive cells is most advantageous and successful lentiviral DC-targeting, exploiting surface molecules like the C-type lectin DC-SIGN (Yang et al., 2008), SLAM (Humbert et al., 2012) or MHC II (Ageichik et al., 2011; Ciré et al., 2014), has already been reported. Of note, all these endeavors focused on lentiviral transfer of antigen-encoding sequences, but not of antigens as such. Hence, transduced DCs have to express the encoded antigen before processing and presenting it on MHC I and MHC II complexes in order to induce T and B cell responses. Despite the principle success of DC-targeting and subsequent triggering of immune responses, a major limitation of these approaches is the relative resistance of DCs to lentiviral gene transfer, requiring high vector doses or co-delivery of Vpx to obtain satisfactory transduction rates (Humbert et al., 2012). Moreover, insertional mutagenesis due to vector genome's integration into host cell chromosomes imposes an inherent risk of such gene transfer for vaccines.

An attractive alternative to circumvent these hurdles might be the exploitation of retroviral particles for protein delivery into target cells, as already successfully shown for fluorescent proteins (GFP, CFP, mRFP, YFP) or enzymes (Flp recombinase, β-lactamase) (Maetzig et al., 2012). Such protein transfer represents a transient cell modification, which does not influence the genomic integrity of the target cell and does not require *de novo* protein synthesis, as complete proteins are delivered. Also blocks to lentiviral gene transfer do not apply, since these blocks act on post-entry replication steps, when the

vector components including the transferred protein have been released into the transduced cell's cytosol.

Due to the constraints of lentiviral gene delivery into DCs, the present thesis aimed to establish lentiviral protein transfer vectors for vaccination and provide proof of concept using model antigen Ova-transferring particles, especially considering APC-targeted, MV_{wt}-GP pseudotyped vectors.

4.1.1. Setting up the vector system

This project intended to examine the potency of lentiviral vectors for targeted delivery of foreign proteins into APCs to induce antigen-specific immune responses. Initially, optimal conditions for the generation of protein transfer vectors exhibiting the desired characteristics needed to be determined, since such vectors had not been published, yet.

DC-targeting should rely on pseudotyping of LVs with MV-GPs, specifically interacting with SLAM, which is expressed on activated immune cells, including mature DCs (Bleharski et al., 2001; Kruse et al., 2001). Humbert and colleagues already demonstrated the suitability of MV vaccine strain glycoprotein-pseudotyped LVs, specifically recognizing CD46 and SLAM, for DC-targeted vaccination approaches (Humbert et al., 2012). Also MV wild-type glycoproteins use SLAM as cell entry receptor, but do not recognize CD46 (Tatsuo et al., 2000), which improves vector specificity (Funke et al., 2009). Of note, titers of MV_{wt}-LV have previously been shown to exceed those of MV_{vac}-LV (Funke et al., 2009), which is another advantage of pseudotyping with MV_{wt}-GPs. However, besides SLAM a third, epithelial receptor for MV had been proposed when this PhD project was started (Leonard, V.H.J. et al., 2008), to whose identification as the adherens junction protein Nectin-4 the present thesis has contributed (Figure 9, Figure 10, Figure 11 and Mühlebach et al., 2011). In parallel, Nectin-4 was also described as epithelial cell receptor for MV vaccine and laboratory strains by Noyce *et al.* (Noyce et al., 2011). Notably, SLAM-transgenic CHO cells were approximately five-fold more efficiently infected with MV_{wt323} than transgenic CHO-Nectin-4 cells, speaking for preferential infection of SLAM-expressing over Nectin-4 expressing cells (Mühlebach et al., 2011). Furthermore, immunological experiments in this thesis were based on human SLAM but not human Nectin-4 transgenic mice and thereof derived mDCs. Although murine Nectin-4 can serve as functional MV receptor, it is used less efficiently than its human homolog (Noyce et al., 2011), and, most importantly, it is not expressed on immune cells. Since SLAM is expressed on immune cells and therefore allows targeting of the respective cell populations, SLAM played the major role in this thesis.

Retroviral vectors have been described as transfer vehicles for heterologous proteins (Voelkel et al., 2010). Prerequisite for such protein delivery is the genetic fusion of cargo proteins to viral structural proteins. Thereby, several positions of the *gag/pol* ORF, e.g. 5' of *matrix* (Aoki et al., 2011) or 3' of *nucleocapsid* or *integrase* (Voelkel et al., 2010), have been shown to tolerate introduction of foreign

protein encoding sequences. Others, such as 3' of *gag*, however, have rather been avoided in order to preserve the frameshift signal indispensable for Gag/Pol production (Aoki et al., 2011). Especially promising results have been obtained by insertion of heterologous protein encoding sequences between *matrix* and *capsid* (Voelkel et al., 2010), prompting the use of this approach also in this thesis' work (Figure 12).

Interestingly, retroviral PTVs did not only transfer heterologous cargo proteins, but also maintained their ability to deliver transgenes (Voelkel et al., 2010). We aimed to generate similar bifunctional LV particles, exploiting marker gene transfer to enable easy titration of vector particles and experimental read-out. In order to yield maximum protein and gene transfer into transduced cells, the optimal ratio of *gag/pol* to *gag-cargo/pol* during PTV-production was determined. Lentiviral PTVs generated in this thesis possessed the fundamental ability to transfer genetic information into transduced target cells (Figure 13), as expected. Here, a clear correlation between particle composition and ability to mediate successful gene transfer was observed (Figure 13, Figure 15). Strikingly, gene transfer was ablated when particles were generated using only *gag-gfp/pol* for particle production. This loss-of-function was associated with evident morphological abnormalities of the particles like reduction and irregular arrangement of envelope glycoproteins and discontinuities in the Gag-shell (Figure 14). However, this was not entirely unexpected, as also other reports indicated phenotypical changes, i.e. similar discontinuities in the Gag-layer, of VLPs produced with only HIV-1 Gag-GFP, which were attributed to the GFP polypeptide (Pornillos et al., 2003; Larson et al., 2005). Moreover, several studies showed beneficial effects or the necessity of wild-type Gag/Pol supplementation for generation of functional, i.e. infective and/or morphologically normal, particles (Sherer et al., 2003; Müller et al., 2004; Larson et al., 2005). It corresponds well to the data acquired here revealing equal amounts of gag-gfp/pol and wild-type gag/pol being optimal for PTV production (Figure 13). This ratio has already been successfully used for generation of γ-retroviral (Voelkel et al., 2010) and lentiviral (Müller et al., 2004) protein delivering particles, the latter in early marking experiments aiming to obtain fluorescently labeled HIV-1 derivatives exhibiting wild-type morphology and infectivity as tools for HIV-1 research.

Besides GFP, also other cargo proteins can be transferred by PTVs (Maetzig et al., 2012). In this thesis, successful incorporation of GFP, Cre recombinase or ovalbumin was demonstrated (Figure 19). Depending on the respective cargo protein, release from its viral fusion partner can be necessary to allow proper function. Especially when the protein of interest exerts its function in membrane-distal compartments of the cell, release from membrane-anchored MA is indispensable. Introduction of an additional retroviral protease recognition site between the cargo and its viral fusion partner releases the heterologous protein from γ-retroviral (Voelkel et al., 2010), and also from lentiviral particles, as also documented for GFP, Cre or Ova in this thesis (Figure 18, Figure 19). Interestingly, GFP-PTVs harboring or lacking an engineered HIV-1 protease site were phenotypically indistinguishable from one another and from the parental lentiviral gene transfer vectors MV_{wt}-LV or VSV-LV if generated in

appropriate *gag/pol* to *gag-cargo/pol* ratios (Figure 21). Thus, particle generation and morphology is not negatively influenced by the artificial HIV-1 protease site separating MA and cargo, as expected, since successful production of functional γ-retroviral particles including an additional retroviral protease site between MA and cargo had been described before (Voelkel et al., 2010).

How many cargo proteins can be transferred by lentiviral particles? An average immature HIV-1 particle is comprised of about 5,000 Gag molecules (Briggs et al., 2004). Thus, particle generation with equal amounts of *gag/pol* and *gag-cargo/pol* should theoretically include 2,500 Gag molecules tagged with a heterologous protein and therefore allow incorporation of 2,500 cargo molecules per single vector particle. To get an idea if the theoretical value of 50% tagged Gag molecules indeed represents payload protein abundance in vector preparations, Ova-transferring PTVs were examined for their Ovalbumin content. On average, MV_{wt}-Ova-$LV_{Katushka}$ preparations contained only 95 ng Ova/ µg p24 (Figure 20B), corresponding to a labeling efficiency of 5.3%, when calculating with a molecular weight of 42.8 kDa for Ova. For VSV-Ova-$LV_{Katushka}$ 169 ng Ova/ µg p24 were measured (Figure 20B), which equals 9.6% Ova-tagged Gag proteins. These data point at augmented incorporation of wild-type Gag/Pol into PTV particles, which might be due to steric constraints of the tagged protein.

Determining the amount of Ova per transducing unit, 723 fg Ova/ t.u. MV_{wt}-Ova-$LV_{Katushka}$ and 21 fg Ova/ t.u. VSV-Ova-$LV_{Katushka}$ were found (Figure 20B). Thereby, 723 fg Ova equal 1.0×10^7 Ova molecules, whereas 21 fg Ova correspond to 3.0×10^5 molecules. Labeling efficiencies of 5.3% and 9.6%, respectively, suggest 1.9×10^8 and 3.1×10^6 Gag molecules per transducing unit in total. These molecule numbers would suffice to yield 3.8×10^4 MV_{wt}-Ova-$LV_{Katushka}$ and 6.3×10^2 VSV-Ova-$LV_{Katushka}$ particles, keeping in mind that one HIV-1 derived particle contains approximately 5,000 Gag molecules (Briggs et al., 2004). Thus, only one in 3.8×10^4 MV_{wt}-Ova-$LV_{Katushka}$ and one in 6.3×10^2 VSV-Ova-$LV_{Katushka}$ particles is active in gene transfer. Therewith, VSV-Ova-$LV_{Katushka}$ meets the expectations of average retroviral infectivity, specified by one infectious retroviral particle in 100 to 1,000 physical particles (Maetzig et al., 2012), while MV_{wt}-Ova-$LV_{Katushka}$ is evidently less infective. VSV-G is very stable and pseudotyping LVs with this glycoprotein gives rise to high titer stocks (Burns et al., 1993), whereas titers of MV_{wt}-GP pseudotyped particles are usually 1-2 log-levels lower (Figure 22) as also previously described (Anliker et al., 2010). Thus, vector titers and infectivity are strongly affected by the envelope glycoproteins used for pseudotyping (Kahl et al., 2004; Steidl, 2004) and differences in the range of log-levels are not uncommon (Kahl et al., 2004), also for protein transfer vector particles.

4.1.2. Mechanistical analysis of targeted PTVs' function

Protein transfer vector particles were pseudotyped with MV_{wt}-GPs to allow specific APC-targeting, and VSV-G, which can be considered the gold standard to evaluate the performance of other vector

pseudotypes. MV_{wt}-GPs recognize the receptors SLAM (Tatsuo et al., 2000) and Nectin-4 (3.1.1; Mühlebach et al., 2011; Noyce et al., 2011) whereas VSV-G specifically interacts with members of the widespread expressed LDL receptor family (Finkelshtein et al., 2013), enabling its broad tropism. Conservation of MV receptor-specificity has already been shown for lentiviral gene transfer vectors pseudotyped with MV_{vac}-GPs (Funke et al., 2008) and MV_{wt}-GPs (Funke et al., 2009). In line with this, dependency of cell-entry on receptor-envelope glycoprotein interactions was also demonstrated for protein and gene delivery by PTVs generated during this thesis' work on MV receptor-transgenic Chinese hamster ovary (CHO) cell lines or naturally SLAM-expressing B95a/ Raji B cell lines (Figure 23, Figure 25, Figure 26). CHO cells themselves do not express any MV receptors and therefore represent a suitable tool to assess the impact of transgenetically expressed, putative receptors on susceptibility to MV infection (Buchholz et al., 1996) or transduction of LVs pseudotyped with engineered MV-GPs (Münch et al., 2011). Of note, although substantial protein transfer was detected for cotton-top tamarin cell line B95a transduced with MV_{wt}-GP pseudotyped particles, these cells were rather resistant to gene transfer at an MOI of 1 (Figure 23, Figure 26B). A plausible explanation is provided by expression of HIV-1 restriction factor Trim5α in cotton-top tamarin cells (Goldschmidt et al., 2008). Trim5α favors species-specific premature disassembly of viral capsids, and thus prevents reverse transcription of viral RNA (Stremlau et al., 2006). Protein transfer, however, is not hampered by Trim5α, and no interaction of the restriction factor with the protein payload is to be expected since cargo proteins are cleaved off the capsid by action of the viral protease during particle maturation. Also for CHO-Nectin-4 only limited gene delivery was observed upon transduction with MV_{wt}-MA-GFP-$LV_{Katushka}$. However, this is in line with the preferential infection of CHO-hSLAM over CHO-Nectin-4 cells by MV_{wt323} (Mühlebach et al., 2011), the virus the glycoproteins used for pseudotyping of LV particles are derived from. The background MA-GFP protein transfer into CHO-CD46 cells by MV_{wt}-MA-GFP-$LV_{Katushka}$ may be explained by the overlap of the binding site of MV vaccine and laboratory strain receptor CD46 on MV hemagglutinin with the one of Nectin-4 (Zhang et al., 2013).

In contrast to considerable protein transfer by MV_{wt}-MA-GFP-$LV_{Katushka}$, protein transfer by VSV-G pseudotyped particles was barely observed upon normalization to MOI 1 (Figure 23). As already mentioned in 4.1.1, VSV-G is very stable and gives rise to highly infectious vector stocks (Burns et al., 1993), whereas titers of MV_{wt}-GP pseudotyped LVs are much lower (Figure 22; Anliker et al., 2010). Thus, overall less VSV-MA-GFP-$LV_{Katushka}$ than MV_{wt}-MA-GFP-$LV_{Katushka}$ particles needed to be applied for transduction at MOI 1. Among the total number of MV_{wt}-GP pseudotyped particles used for transduction, consisting of infectious and non-infectious particles, there may be particles containing no genetic information. Those are hence not included in the calculation of infectious titers (determined by gene transfer). However, if they possess functional glycoprotein complexes, such VLPs are able to transfer cargo proteins into the cytosol of receptor-positive cells, what might account for the high protein delivery capacity of MV_{wt}-GP pseudotypes normalized to MOI 1 (Figure 23).

Moreover, particle composition of VSV-G and MV_{wt}-GP pseudotyped particles may differ, i.e. more cargo proteins might be incorporated into MV_{wt}-GP pseudotyped LV particles than into VSV-G pseudotyped ones. Besides, also the entry pathway may affect PTVs' ability to transfer cargo proteins. In contrast to MV and thereof derived pseudotypes relying on pH-independent fusion of viral and plasma membrane (Plemper, 2011), VSV and thereof derived pseudotypes enter host cells via the endocytic pathway (Matlin et al., 1982). Thus, cargo proteins delivered by VSV-G pseudotyped vectors may be subjected to degradation in late endosomes, resulting in lower protein transfer capacities of VSV-G pseudotyped vector particles.
However, when adjusted to particulated protein (80 ng p24), also VSV-MA-GFP-$LV_{Katushka}$ particles demonstrated the ability to mediate substantial protein transfer (Figure 24) and even outperformed MV_{wt}-GP pseudotyped PTVs in CHO cells under these conditions. This indicates a critical influence of the normalization method on relative protein and gene transfer efficiencies of PTVs.

In accordance with other studies reporting intracellular transfer of native, functional proteins like enzymes and transcription factors (Voelkel et al., 2010; Aoki et al., 2011; Kaczmarczyk et al., 2011; Wu and Roth, 2014), in this thesis cargo proteins were also delivered into target cells and shown to be bioactive. Transfer of Cre recombinase into receptor-positive indicator cell lines led to excision of a loxP-flanked *cerulean* expression cassette (Figure 25B), implying nuclear translocation and catalytic activity of the enzyme. Also the model antigen Ova was delivered into the cytosol of receptor-expressing cells, as indicated by immunoblot analysis detecting similar amounts of Ova in PTV-transduced cells with and without citric acid buffer pretreatment (Figure 26A), which is a common method to remove surface-bound virions (Voelkel et al., 2012).

Interestingly, receptor-positive mDCs transduced with MV_{wt}-Ova-$LV_{Katushka}$ and VSV-Ova-$LV_{Katushka}$ triggered predominantly $CD8^+$ Ova-specific T cells (compare Figure 29A, B with Figure 30A, B). Of note, transduction of mDCs with MV_{wt}-Ova-$LV_{Katushka}$ in the presence of fusion inhibiting peptide FIP, which blocks MV-GP induced membrane fusion (Richardson et al., 1980), completely abolished stimulation of co-cultured $CD8^+$ Ova-specific T cells (Figure 29C). In contrast, mDCs incubated with soluble Ova and Bald-Ova-$LV_{Katushka}$ stimulated mainly $CD4^+$ Ova-specific T lymphocytes (compare Figure 29A, B with Figure 30A, B). Taken together, these data demonstrate receptor-dependent cytosolic uptake of antigens into APCs upon transduction with PTVs harboring envelope glycoproteins. Subsequently, antigens are proteasomally processed and presented on MHC I molecules via the endogenous antigen presentation pathway. Soluble or solely particle-associated Ova, however, is taken up endosomally, processed in acidified late endosomes or lysosomes and presented on MHC II molecules via the exogenous antigen presentation pathway. This proposed mode of action of PTVs is summarized in Figure 49 of the present thesis.

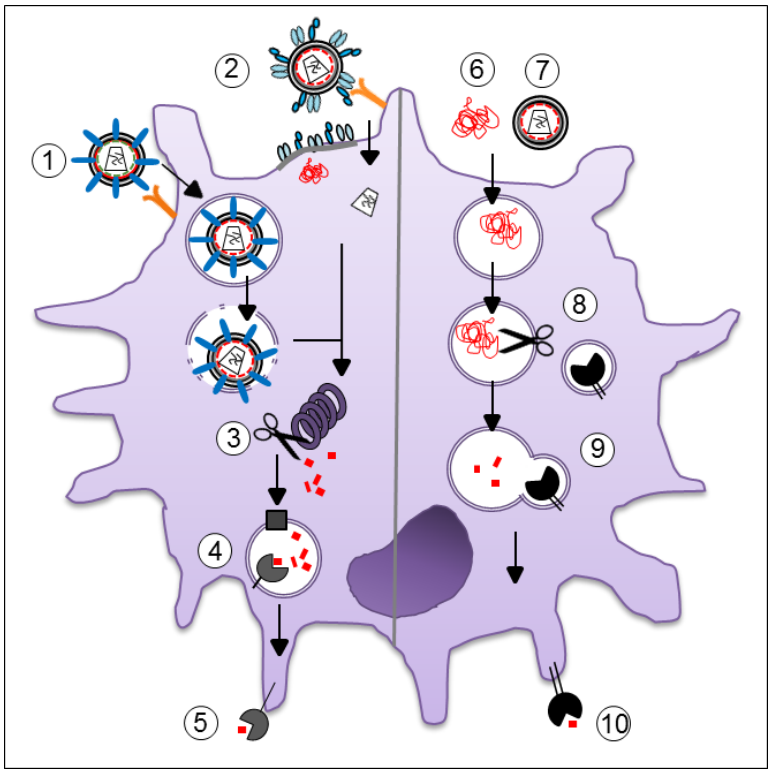

Figure 49: Proposed model for uptake, processing and presentation of soluble and particulate antigens by APCs. Antigens (red) are incorporated into PTV particles as part of the Gag polyprotein and subsequently released by HIV-1 protease mediated cleavage during particle maturation. Interaction of viral Env (blue) with the respective cellular receptors (orange) leads to receptor-mediated endocytosis and pH-dependent membrane fusion (VSV-G pseudotyped particles, (1)) or pH-independent membrane fusion at the cell's surface (MV-GP pseudotyped particles, (2)) followed by cytosolic release of antigens into transduced APCs. Antigens are proteasomally processed (3), loaded onto MHC I molecules (4) and finally presented via the endogenous antigen-presentation pathway (5). Without specific Env-receptor interactions, soluble (6) or particulate antigens (7) are endocytosed, cleaved by proteases in late endosomes (8), loaded onto MHC II molecules (9) and presented via the exogenous antigen presentation pathway (10). Figure modified after Uhlig et al., 2015.

Strikingly, also SLAM$^-$ mDCs incubated with MV$_{wt}$-Ova-LV$_{Katushka}$ were able to stimulate CD4$^+$ T cells (Figure 30, see cytokine secretion by Ova-specific T cells in co-culture with mDCs of IFNAR$^{-/-}$ mice incubated with MV$_{wt}$-Ova-LV$_{Katushka}$). This might be due to target receptor-independent endocytosis of these particles by APCs. These "particulated antigens" are subsequently processed and presented via the exogenous antigen presentation pathway (Figure 49, to the right). Target receptor-independent endosomal uptake of lentiviral and γ-retroviral particles by different human cell lines has been described before, also for MV$_{vac}$-GP pseudotyped LVs (Voelkel et al., 2012). Although in this thesis hardly any protein or gene transfer was observed into receptor-negative cell lines (Figure 23, Figure 25, Figure 26 and data not shown for bald particles), target receptor-independent antigen uptake is conceivable since APCs are known for their high capacity to endocytose antigens. Even though such antigen uptake is primarily attributed to immature APCs, recent work demonstrated also mature DCs being capable of doing so (Platt et al., 2010). Here, uptake was mostly restricted to antigens captured by endocytotic receptors. Interestingly, MV wild-type and vaccine strains (Witte et al., 2006) and MV$_{vac}$-LVs (Humbert et al., 2012) have been reported to attach to the C-type lectin DC-SIGN, but do

not actively enter DC-SIGN-expressing cells. As DC-SIGN is involved in receptor-mediated endocytosis (Engering et al., 2002; Cambi et al., 2009), one could speculate that attachment of MV_{wt}-Ova-$LV_{Katushka}$ to murine DC-SIGN in SLAM-negative APCs might favor endocytotic particle uptake and presentation of Ova peptides via the endogenous antigen presentation pathway (Figure 49, to the right). However, until now it is not known if/how MV or MV-LV particles bind to murine DC-SIGN (Takaki et al., 2014).

4.1.3. Vaccine properties of PTVs

The promising results regarding specificity and immunostimulatory potential of PTVs obtained *in vitro* prompted the assessment of PTV-induced immune stimulation *in vivo*. *In vivo* studies with MV are usually performed in MV receptor-transgenic mice (Mrkic et al., 1998; Ohno et al., 2007) or naturally MV receptor-positive non-human primates (Myers et al., 2007), which are susceptible to MV infection. Thus, immunogenicity of MV_{wt}-GP pseudotyped PTVs was assessed in $SLAM^{ki}$ mice, characterized by replacement of the murine V domain of SLAM against the human one (Ohno et al., 2007), to which MV H can bind (Sato et al., 2012). $IFNAR^{-/-}$ mice, the parental strain to $SLAM^{ki}$ mice, served as MV receptor-negative control animals.

Following vaccination of these mice with MV_{wt}-GP and VSV-G pseudotyped Ova-PTVs, receptor-dependent, but antigen-specific recall-independent activation of splenocytes was observed four days after booster immunization (Figure 32). To elucidate recall-independent activation of antigen-specific T cells, thawed and pooled splenocytes of each vaccinated animals' group were separated into T cells and other cells, containing APCs. T lymphocytes, when incubated overnight in medium containing no IL-2, reacted to antigen recall whereas control T cells did not (Figure 33, Figure 34). This indicates persisting antigen-specific activation of splenocytic T lymphocytes four days after booster immunization. A similar phenomenon has already been reported by Haglund *et al.*, who observed persistent activation of HIV-1 Env-specific $CD8^+$ T cells five days after boosting with recombinant VSV expressing HIV-1 Gag or HIV-1 Gag and Env (Haglund et al., 2002). Moreover, in our study the APC-containing retentate obtained after MACS separation of PTV-vaccinated mice's splenocytes stimulated Ova-specific naïve T cells from TCR-transgenic OT-I mice (Figure 35). The data suggest constant antigen processing and presentation, which might be possible due to intracellular storage of particulate antigens in APCs. Interestingly, lysosome-like antigen storage organelles, different from MHC I and II loading compartments, have been described in mature DCs (van Montfoort et al., 2009). These organelles provide continuous antigen supply and thus enable long-term $CD8^+$ T lymphocyte cross-priming by DCs, as measured by proliferation of antigen-specific T cell for up to 14 days after injection of pulsed DCs *in vivo* (van Montfoort et al., 2009). Presumably, PTV-associated Ova was stored within these organelles. It will be interesting to investigate potential differences in processing and storage of PTV-associated versus proteinaceous antigens in further experiments.

Immunization with VSV-Ova-$LV_{Katushka}$ (Figure 33, Figure 34, Figure 35A) led to predominant stimulation of $CD8^+$ T lymphocytes *in vivo*. A similar trend was also observed for MV_{wt}-Ova-$LV_{Katushka}$ (Figure 34; JAWSII-Ova cells were previously shown to stimulate $CD8^+$ but not $CD4^+$ TCR-transgenic T cells (Bodmer, 2015)). This is in accordance with the *in vitro* data showing induction of Ova-specific $CD8^+$ T cell but hardly any $CD4^+$ T cell responses by receptor-positive mDCs transduced with the pseudotyped PTVs (Figure 29 and Figure 30). Thus, the data indicate cytoplasmic transfer of Ova upon transduction with pseudotyped PTVs, followed by antigen processing and presentation via the endogenous antigen presentation pathway (Figure 49, to the left). The picture is similar to the one found after immunization with lentiviral gene transfer vectors. Here, predominant induction of $CD8^+$ T lymphocyte responses is expected since the particles deliver antigen-encoding sequences into APCs, which provide the template for *de novo* synthesis of proteins in the cytoplasm and subsequent MHC I presentation. Indeed, lentiviral gene transfer vectors induce mainly $CD8^+$ T lymphocyte responses, independent if broadly transducing VSV-G pseudotypes (Esslinger et al., 2002; Palmowski et al., 2004) or APC-specific vectors were employed (Yang et al., 2008; Ageichik et al., 2011).

To allow direct comparison of immunogenicity among differently pseudotyped PTVs and of PTVs with recombinant protein, antigen content of all vector preparations and protein was normalized to 1 µg Ova per injection. Adjusted that way, approximately 34-times more transducing units of VSV-Ova-$LV_{Katushka}$ than MV-Ova-$LV_{Katushka}$ PTVs were administered due to higher infectivity of VSV-G pseudotypes (Figure 20B, right column). This likely explains the stronger stimulation of antigen-specific T cells, and especially $CD8^+$ CTLs, upon injection of VSV-Ova-$LV_{Katushka}$ (Figure 33, Figure 34). Expectedly, both MV_{wt}-GP and VSV-G pseudotyped PTVs induced stronger APC-mediated stimulation of splenocytes/ T cells than recombinant Ova (Figure 32, Figure 33, Figure 34). Similar observations have already been made with other antigens. HIV-1 Env (McBurney et al., 2007) or glycosylphosphatidylinositol-conjugated Her2 (Patel et al., 2015), for example, triggered a more vigorous cellular or cellular and humoral immune response, respectively, when presented on VLPs than the corresponding soluble proteins. Contrary to the assumption that VLPs do cause strong immune stimulation due to the structural and antigenic similarity to the virus they are derived from (Grgacic. and Anderson, 2006), no PTV-mediated upregulation of CD69 or CD86 on murine mDCs was observed (Figure 28). However, CD69 and CD86 are not the only markers for activation of dendritic cells. Since PTVs were able to induce $CD8^+$ T lymphocyte responses *in vitro* and *in vivo* (Figure 29, Figure 33, Figure 34), some activation of DCs must have occurred.

Taken together, PTVs were able to deliver the model antigen Ova into receptor-positive APCs, leading to the stimulation of antigen-specific T cells, and especially $CD8^+$ T lymphocytes, *in vitro* and *in vivo*. Thereby, PTVs showed promise for vaccination approaches requiring the induction of a strong cellular immune response.

4.2. Targeted gene delivery into $CD4^+$ T cells

$CD4^+$ T cells play a key role in coordinating adaptive immune responses, including the support of $CD8^+$ cytotoxic T cell and B cell effector functions. Moreover, they are involved in various diseases like HIV-1 infection/AIDS, cancer or autoimmune disorders (Broux et al., 2012; Kamphorst and Ahmed, 2013). Hence, $CD4^+$ T cells are important target cells for gene therapy and immunotherapy approaches.

State of the art for the genetic modification of $CD4^+$ T lymphocytes by lentiviral vectors is the isolation of these cells from the patient's body, followed by *ex vivo* modification, expansion and reinfusion into the patient (Levine et al., 2006). Thus, genetic manipulation of $CD4^+$ cells is both costly and laborious. Moreover, the procedure can be associated with altered characteristics, e.g. phenotypical and functional changes (Sauce et al., 2002a; Sauce et al., 2002b; Marktel et al., 2003), reduced *in vivo* persistence or proliferation of autologous cells (Naldini, 2011) and may cause poor clinical responses. The exclusive and stable genetic modification of $CD4^+$ cells by LVs *in vivo*, however, would open new therapeutic avenues and is thus highly desirable. Ideally, transduction should not be restricted to activated lymphocytes, which is true for commonly applied LVs (Maurice et al., 2002; Frecha et al., 2009), but also, at least to a certain degree, extend to naïve, resting $CD4^+$ T cells. These lymphocytes, which may persist over years in patients, possess the capacity to respond to new antigens, providing long-lasting immune reconstitution to patients, and are therefore of great interest as gene therapy targets (Verhoeyen et al., 2009).

When this PhD project was initiated, no vector mediating highly selective and efficient *in vivo* gene transfer into $CD4^+$ lymphocytes after systemic administration had been described. Therefore, this thesis aimed to generate a CD4-targeted vector suitable for *in vivo* gene delivery approaches. Since $CD4^+$ T cells are distributed throughout the entire body, an entry-targeted vector was established to allow systemic vector application without modification of non-target cells.

4.2.1. Surface-engineered lentiviral vectors and their targets

At present, there are two flexible entry retargeting systems for LVs available, either based on engineered MV-GPs or engineered Sindbis virus glycoproteins. Whereas the first strategy has shown absolute specificity for a wide range of target receptors of human or murine origin (see Table 21), preferential target cell transduction accompanied by substantial off-target transduction was demonstrated for the latter (Zhang et al., 2010). Due to the leakiness of the mutations introduced in the Sindbis virus E2 protein to abolish the natural receptor binding, these LVs require combination with transcriptional targeting in order to achieve high target specificity (Pariente et al., 2007). Thus, the retargeting system based on MV-GPs, as used in this thesis, can be considered superior to the one using Sindbis virus GPs with respect to selectivity.

With the MV-GP based retargeting system, scFvs, natural protein ligands or DARPins have been fused to blinded MV hemagglutinin to confer specificity of LVs for a receptor of choice (for an overview see Table 21). It has been shown that the biophysical properties of the targeting ligand, including stability, the tendency to aggregate, and its affinity, are pivotal for the successful generation of targeted LVs (Friedel et al., 2015). Hence, DARPins are especially suited as binding domains as they are characterized by tremendous stability, a low tendency to aggregate, and affinities in the low nanomolar or picomolar range (Plückthun, 2015).

Table 21: Characteristics of MV-LV and thereof derived surface-engineered lentiviral vectors.

Targeting domain	**Vector**	**Target receptor**	**Transduction of resting lymphocytes?**	***In vivo* application?**	**Reference**
-	MV_{vac}-LV	huSLAM, huCD46	yes	n.d.[a]	(Frecha et al., 2008a; Frecha et al., 2009; Zhou et al., 2011)
Natural protein ligand	EGF-LV[b]	huEGFR	n.a.[c]	n.d.[a]	(Funke et al., 2008)
	IL-13-LV[b]	huIL-13R	n.d.[a]	s.c.[d], i.c.[e]	(Ou et al., 2012)
scFv	CD20-LV[b]	huCD20	yes	n.d.[a]	(Funke et al., 2008)
	GluA-LV[f]	muGluR	n.a.[c]	intracerebral	(Anliker et al., 2010)
	CD105-LV[b]	huCD105	n.a.[c]	systemic	(Anliker et al., 2010; Abel et al., 2013)
	CD133-LV[b]	huCD133	n.a.[c]	systemic	(Anliker et al., 2010)
	MHC II-LV[b]	muMHC II	n.d.[a]	systemic	(Ageichik et al., 2011)
	CD8-LV[b]	huCD8	no	only local	(Zhou et al., 2012)
	mCD105-LV[b]	muCD105	n.a.[c]	systemic	(Abel et al., 2013)
	CD19ds-LV[b]	huCD19	yes	n.d.[a]	(Kneissl et al., 2013)
	CD30-LV[b]	huCD30	n.a.[c]	n.d.[a]	(Friedel et al., 2015)
DARPin	D9.29-LV[b]	huHer2/neu	n.a.[c]	systemic	(Münch et al., 2011)
	CD4-LV[b]	huCD4	yes	systemic	this thesis

[a] n.d., not determined. [b] Targeting relies on modified MV_{NSe} vaccine strain H. [c] n.a., not applicable. [d] s.c., subcutaneous. [e] i.c., intracranial. [f] Targeting relies on modified MV_{wt} H.

The CD4-specific LV generated in this thesis relied on a CD4-specific DARPin as binding moiety. H-αCD4 was shown to be well expressed in HEK-293T packaging cells (Figure 36B), leading to its efficient incorporation into CD4-LV particles (Figure 36C). Titers of CD4-LV were on average at least 10-fold higher than those of the other lymphocyte-targeted vectors, i.e. CD20-LV, CD19ds-LV, and CD8-LV (Funke et al., 2008; Zhou et al., 2012; Kneissl et al., 2013). Although augmented transduction due to particular properties of the CD4 receptor itself cannot be ruled out, the used

DARPin is the more likely reason. Likewise, higher titers of DARPin-displaying than scFv-incorporating particles have already been reported for Her2/neu-targeted LVs (Münch et al., 2011). Thus, the respective binding domain also influences the *in vivo* performance of a given vector, which critically depends on high vector yields. Recently, a CD8-targeted vector, displaying an OKT3-derived scFv, has been introduced by our laboratory, which is highly selective for its target cells and able to transfer complex genes like tumor antigen-specific TCR sequences into $CD8^+$ T lymphocytes (Zhou et al., 2012). However, although local injection led to specific *in vivo* transduction of $CD8^+$ T cells, vector titers were too low to result in significant numbers of transduced $CD8^+$ cells upon systemic administration (Zhou and Buchholz, unpublished data; and own data not shown). Nonetheless, albeit DARPin-displaying particles are commonly characterized by higher titers, there are also targeted vectors relying on scFv-display, which mediate satisfying *in vivo* gene delivery upon systemic administration, as demonstrated for mCD105-LV (Table 21).

Due to its broad tropism and high stability, LVs are often pseudotyped with VSV-G. However, one major drawback of VSV-LV is its inability to mediate efficient gene transfer into resting lymphocytes, i.e. lymphocytes in the G_0 phase of the cell cycle, which has been attributed to the very low expression of its receptor LDL-R on these cells (Amirache et al., 2014). Thus, transduction with VSV-LV depends on upregulation of LDL-R, which is achieved by pre-activation of lymphocytes.

In contrast, LVs pseudotyped with glycoproteins of the MV_{NSe} variant of the MV vaccine strain Edmonston B were shown to efficiently transduce resting T and B cells, respectively, without inducing cell cycle entry (Frecha et al., 2008a; Frecha et al., 2009). Thereby, interaction with both, CD46 and SLAM, was required for adequate gene transfer into resting lymphocytes (Frecha et al., 2011; Zhou et al., 2011). In line with these findings, MV_{wt}-LV, not recognizing CD46, was not able to transduce resting T cells (Zhou et al., 2012).

Accordingly unexpected at first, also some targeted LVs, where CD46 and SLAM recognition by MV_{NSe} hemagglutinin was abolished, have been reported to enable transduction of resting lymphocytes (see Table 21) (Funke et al., 2008; Kneissl et al., 2013). Of note, transgene expression was detected in about 60% and 20% (two days post transduction) or 30% and 10% (six days post transduction) of unstimulated B lymphocytes after transduction with CD20-LV and CD19ds-LV (both MOI 2), respectively (Kneissl et al., 2013). Also CD4-LV was able to deliver transgenes into resting lymphocytes, as demonstrated by detection of approximately 8% $GFP^+/CD4^+$ T cells three and six days after incubation with vector particles at MOI 2 (Figure 38C). Here, no decline of GFP-positive $CD4^+$ cells was observed over time, indicating stable transduction without pseudotransduction. However, compared to the gene transfer rate by CD20-LV and CD19ds-LV, gene delivery in resting $CD4^+$ T cells was relatively low. This might be due to the action of SAMHD1, a dNTP triphospho-hydrolase abundantly expressed in resting $CD4^+$ T cells, monocytes and dendritic cells, which depletes

the pool of free dNTPs and therefore prevents reverse transcription of viral RNA in these cells (Baldauf et al., 2012).

What is the underlying mechanism enabling transduction of resting lymphocytes by targeted LVs pseudotyped with engineered MV-GPs not recognizing SLAM or CD46? Here, transduction seems to be dependent on activating stimuli induced by targeted LVs. It has been suggested that incorporated scFvs transfer features of their parental antibody to vector particles, e.g. activation of cells upon antibody-antigen interaction (Zhou et al., 2012; Kneissl et al., 2013). Antibodies directed against CD20, for instance, were described to stimulate B lymphocytes and initiate cell cycle progression from G_0 to G_1 (Golay et al., 1985). Similarly, also for CD20-LV minimal activation and transition from G_0 to G_1 phase of cell cycle was observed (Kneissl et al., 2013), which likely enabled efficient transduction of resting cells without the requirement of pre-activation. In contrast, engagement of CD4 on DCs by a CD4-specific DARPin selected in parallel to DARPin D29.2 did not cause activation of these cells, as determined by expression of the co-stimulatory molecule CD80 (Schweizer et al., 2008). Also in our study, no significant difference in the expression of the activation marker CD25 was observed between untransduced and CD4-LV (MOI 2) transduced lymphocytes three days after transduction (data not shown). However, contrary to the data by Schweizer *et al*. reporting no change in CD4 density at the surface of $CD4^+$ T cells upon incubation with DARPin D29.2 (Schweizer et al., 2008), pronounced CD4 down-regulation following transduction with CD4-LV was observed in the present thesis (Figure 38D). CD4 is closely linked to the cell activation pathway (Kornfeld et al., 1988; Pelchen-Matthews et al., 1989) and the observed internalization of CD4 upon CD4-LV transduction strongly suggests cell signaling. Thus, it is likely that CD4-LV, similar to CD20-LV and CD19ds-LV, at least minimally activated the cells, which conferred susceptibility of the resting lymphocytes to lentiviral transduction.

However, transduction efficiency in quiescent lymphocytes was clearly lower than in activated primary human PBMC (Figure 38C). The positive correlation between CD4-LV transduction efficiency and activation state of its target cells was also confirmed *in vivo*, since higher luciferase activity and more transduction events were found in mice engrafted with stimulated than with unstimulated PBMC (Figure 43 C-D, Figure 45). This is likely owed to various post-entry blocks to HIV-1 infection or transduction with thereof derived LVs in resting T lymphocytes (Zack et al., 1990; Yoder et al., 2008; Baldauf et al., 2012), which do not apply in activated T cells, thus allowing their more efficient transduction.

4.2.2. Targeting $CD4^+$ cells with γ-retroviral and lentiviral vectors

Attempts aiming at targeted γ-retroviral or lentiviral transduction of CD4-expressing cells involved transcriptional as well as entry targeting endeavors. Using transcriptional targeting, Marodon and colleges reported transgene expression in primary human $CD4^+$ T cells as well as in $CD4^+$ T cells, dendritic cells and macrophages derived from human HSC, which had been transduced with a LV

transferring GFP under control of *CD4* gene-specific promoter and enhancer sequences (Marodon et al., 2003). Despite being vastly absent in B lymphocytes, transgene expression was not restricted to $CD4^+$ T lymphocytes but also detected in $CD8^+$ T lymphocytes. Here, the percentage of $CD4^+$ and $CD8^+$ GFP-expressing cells was even similar, and addition of the *CD4* gene silencing element to the vector regulatory sequences could only reduce but not completely ablate transgene expression in $CD8^+$ cells.

Entry targeting attempts mostly concentrated on exploiting the natural tropism of HIV-1 Env, which was used to pseudotype MLV-derived γ-retroviral vectors (Mammano et al., 1997; Schnierle et al., 1997) or HIV-1 derived lentiviral vectors (Poznansky et al., 1991; Shimada et al., 1991; Agosto et al., 2009; Geng et al., 2014). Of note, LVs pseudotyped with CXCR4-tropic HIV-1 Env did allow efficient gene transfer into resting $CD4^+$ T lymphocytes while preserving their natural quiescent state (Agosto et al., 2009; Geng et al., 2014). Additionally, also SIVmac Env pseudotyped MLV-derived vectors have been employed to mediate CD4-specific gene transfer (Indraccolo et al., 1998). However, vectors pseudotyped with HIV-1 or SIVmac Env can be neutralized by HIV-1-specific antibodies present in HIV-1 seropositive patients, which would limit their application for HIV-1 gene therapy (Stitz et al., 2000). Therefore, also SIVagm Env pseudotyped MLV-derived vectors, resistant to neutralizing antibodies, have been developed to allow selective genetic modification of $CD4^+$ cells (Stitz et al., 2000). Besides HIV-1 and SIV Env, exhibiting a natural tropism for $CD4^+$ cells, engineered Sindbis virus envelope proteins, conjugated to a CD4-specific antibody, have been used to pseudotype HIV-1 derived vectors (Morizono et al., 2001; Liang et al., 2009). However, transgene expression following transduction with these vectors was enriched in but not limited to $CD4^+$ cells *in vitro*. In contrast, CD4-LV, relying on the MV-GP based retargeting system, did not transduce $CD4^-$ Raji cells or primary human $CD8^+/CD4^-$ lymphocytes in the naturally mixed PBMC population while efficiently transducing $CD4^+$ cells *in vitro* (Figure 37).

Similar to CD4-LV, most CD4-targeted vectors indeed showed target specificity on cell lines and primary T cells. However, transduction efficiencies were rather moderate and *in vivo* gene delivery was not assessed. So far, only one other study reported CD4-specific gene transfer *in vivo* (Schüle et al., 2006). There, gene delivery was mediated by a MLV-derived γ-retroviral vector pseudotyped with CD4/CXCR5-tropic HIV-1 envelope proteins, termed [MLV(HIV)]. Administered intraperitoneally into mice double transgenic for human CD4 and human CCR5, about 0.3% of the $(hu)CD4^+/(hu)CCR5^+$ target cells in the peritoneal cavity were transduced, whereas upon intravenous injection into the same mice only single, sporadic transduction events could be observed in spleen and liver but not in peripheral blood. Interestingly, average titers of 3×10^6 t.u./ml for concentrated [MLV(HIV)] necessitated three to four vector injections in order to infuse 1×10^6 (i.v. administration) or 8×10^6 (i.p. administration) t.u./mouse, respectively.

In contrast, CD4-LV with a concentrated titer of 2.3 ± 1.8 x 10^8 t.u./ml required only a single administration to inject the applied 8 x 10^7 t.u./ NSG mouse engrafted with human PBMC or 1.5 x 10^7 t.u./ NSG mouse engrafted with human HSC, respectively. In both mouse models, CD4-LV showed high specificity for its target cells, as demonstrated by gene transfer into human $CD4^+/CD3^+$ but not into human $CD4^-/CD3^+$ cells or cells of murine origin (Figure 44, Figure 45A, Figure 47, Figure 48A). Systemic application of CD4-LV into PBMC-engrafted NSG mice resulted in up to 16.6% of $GFP^+/CD4^+$ T lymphocytes in the peripheral blood (Figure 45B), and was thus way more effective than injection of [MLV(HIV)]. In this model, strong luciferase activity was detected in lymphoid organs where T lymphocytes are supposed to concentrate (Figure 43 C, D, F). Additionally, luciferase activity was also observed in skin, liver, and lung of the animals (Figure 43 E). This is in line with the literature where the named organs are described as the first targets for infiltrating human lymphocytes in the course of GvHD (Ferrara et al., 1996; Schroeder and DiPersio, 2011). Supporting this hypothesis, in human HSC-engrafted mice, where human T cells are tolerant to the mouse environment, basically no luminescence in skin and liver and only weak signals in lung were observed (data not shown).

Which factors influence transduction efficiency and *in vivo* distribution of CD4-LV? A positive correlation between transduction efficiency and target receptor surface density was previously reported for targeted LVs pseudotyped with engineered MV-GPs (Anliker et al., 2010; Münch et al., 2011; Abel et al., 2013) or engineered Sindbis virus glycoproteins (Liang et al., 2009). In line with this, CD4-LV efficiently transduced $CD4^+$ T cells in spleen, lymph node like structures, and blood of HSC-engrafted NSG mice, which are characterized by a high CD4 density, whereas thymus-derived $CD4^+$ cells with lower CD4 receptor density were hardly transduced (Zhou et al., 2015). The same pattern was observed for naïve and memory $CD4^+$ T cells, with naïve lymphocytes, exhibiting a lower CD4 density (Zhou et al., 2015), less efficiently transduced by CD4-LV (Figure 48B and C and Zhou et al., 2015).

Besides receptor surface density, also blood circulation kinetics are pivotal for *in vivo* transduction and vector biodistribution. Accordingly, low velocity of blood flow in the sinuses of the liver has been suggested as one reason for enhanced gene delivery with a lentiviral vector targeting the endothelial cell marker CD105 (Abel et al., 2013). Also in the capillaries of the bone marrow the blood flow is substantially slowed down, which presumably increased the likelihood of productive interaction between CD4-LV and its receptor. This might have compensated for the lower CD4 density in this organ (Zhou et al., 2015) and accounted for the transduction of bone marrow-derived $CD4^+$ T cells (Figure 48 and Zhou et al., 2015).

Taken together, this thesis describes the first lentiviral vector enabling specific and efficient $CD4^+$ T lymphocyte targeting both *in vitro* and *in vivo*.

However, besides $CD4^+$ T cells, also dendritic cells, monocytes, and macrophages express CD4. Similar to resting $CD4^+$ T lymphocytes, transduction of these cell types with common LVs is known to be rather inefficient due to the presence of HIV-1 restriction factors like APOBEC3 (Peng et al., 2007) or the dNTP triphoshohydrolase SAMHD1 which hinders reverse transcription of viral RNA in resting $CD4^+$ T cells (Baldauf et al., 2012) and human dendritic and myeloid cells (Laguette et al., 2011).
Interestingly, CD4-LV was able to transduce M1 and M2 macrophages generated from human PBMC (Figure 40). M1 macrophages were characterized by lower CD4 receptor density than M2 macrophages (Figure 39), in line with literature describing M1 polarization to be accompanied by CD4 down-regulation (Cassol et al., 2009). Based on the above mentioned experiences with receptor-targeted LVs, which preferentially transduced cells with higher target receptor density (Anliker et al., 2010; Münch et al., 2011; Abel et al., 2013) and also the observations made with CD4-LV on T lymphocytes (Zhou et al., 2015), M2 macrophages would have been expected to be more prone to lentiviral gene transfer than M1 macrophages. However, approximately 30% of M1 macrophages were transduced by CD4-LV at MOI 10, whereas only about 2% gene delivery into M2 macrophages was observed in the same setting (Figure 40). Interestingly, pre-incubation with VLPs delivering the accessory viral protein X (Vpx), naturally encoded by HIV-2 and some SIV strains, which induces proteasomal degradation of SAMHD1, led to increased transduction of M2 (about 70% transduced cells) but not M1 macrophages (Figure 40). This would argue for a SAMHD1 mediated restriction of lentiviral transduction in M2 macrophages. However, no significant differences in SAMHD1 levels between M1 and M2 macrophages, which could explain the experimental data, are described (Cobos Jiménez et al., 2012). Thus, further investigations are needed to elucidate the mechanisms causing different susceptibility of M1 and M2 macrophages to lentiviral transduction.
Concluding, CD4-LV could transduce human macrophages generated from PBMC although gene transfer was less efficient than in $CD4^+$ T lymphocytes, requiring higher MOIs of CD4-LV or pre-treatment with Vpx.

4.3. Lentiviral vectors for immunotherapy

Immunotherapy aims to treat diseases by eliciting, amplifying or suppressing immune reactions. Thereby, immunotherapeutic efforts may address autoimmune disorders, transplant rejection, chronic inflammation, infectious diseases or cancer (Steinman and Mellman, 2004). Since both PTVs and CD4-LV target immune cell subsets with pivotal functions in the orchestration of immune responses, also these vector types may become interesting tools for immunotherapy.

What would adequate indications for PTV- and CD4-LV-based immunotherapy be?
In this proof of principle study, transfer of the model antigen Ova by PTVs triggered stimulation of cellular immunity, and more precisely predominant activation of $CD8^+$ T cells (Figure 29A and B,

Figure 33, Figure 35). Thus, PTV vaccines seem to be especially suited for indications requiring the induction of strong antigen-specific $CD8^+$ cytotoxic T cell responses, like cancer immunotherapy.

Traditionally, the pivotal role of $CD8^+$ T lymphocytes in anti-tumor immunity has been acknowledged. However, mounting evidence underscores the relevance of $CD4^+$ T cell responses in cancer immunotherapy (Muranski and Restifo, 2009). Indeed, $CD4^+$ T cell help has been reported to be indispensable for induction of functional $CD8^+$ CTL effector cells from naïve precursors (Bennett et al., 1998; Ridge et al., 1998; Schoenberger et al., 1998) and generation of $CD8^+$ T memory cells *in vivo* (Janssen et al., 2003; Shedlock and Shen, 2003; Sun and Bevan, 2003). Moreover, $CD4^+$ T lymphocytes themselves can directly kill tumor cells upon recognition of antigen-peptides presented on MHC II molecules (Hunder et al., 2008; Weigand et al., 2012). However, although most tumor cells are MHC I-positive, expression of MHC II molecules is rather rare. To circumvent MHC II restriction, $CD4^+$ T cells have lately been engineered to express chimeric antigen receptors (CARs), in which the antigen-binding moiety of an antibody is fused to intracellular T cell signaling domains. These cells exhibited direct cytotoxicity towards target cancer cells (Hombach et al., 2001; Hombach et al., 2006). Transfer of CAR-encoding genes is clearly also a field of application of CD4-LV. In fact, following transduction with the CD4-LV vector introduced in this thesis, Her2/neu-CAR expressing $CD4^+$ T cells lysed $Her2/neu^+$ tumor cells and produced high amounts of Th1 cytokines in a short-term *in vitro* killing assay (Zhou et al., 2015).

Besides applying the two vector types on their own, it might be interesting to combine APC-targeted PTVs and CD4-LV to cause strong anti-tumor effects. Thereby, immunogenicity of PTVs transferring tumor-associated antigens might be additionally boosted by co-delivery of immunostimulatory nucleic acids, potentially increasing vaccination success. Moreover, further combination with CD8-LV, which has been previously generated in our laboratory (Zhou et al., 2012), might have beneficial effects on anti-tumor immune responses. In line with this, parallel use of TCR-engineered $CD8^+$ and $CD4^+$ for tumor therapy has already been described to be more effective than either cell type alone (Kuball et al., 2005).

In addition to cancer immunotherapy, also HIV-1 gene therapy is well in scope of therapeutic applications of CD4-LV. Accordingly, CD4-LV transduced T cells, engineered to express the membrane-anchored HIV-1 entry inhibitor maC46, were protected against HIV-1 infection *in vitro* (Zhou et al., 2015). Within the plethora of anti-HIV-1 strategies interfering with different steps of HIV-1 life cycle, blocking HIV-1 already at the stage of cell entry is especially desirable. maC46 expression conferred a clear selective advantage upon HIV-1 challenge, which is in line with previous *in vitro* and *in vivo* data (Kimpel et al., 2010) and which will be of prime importance in clinical trials since only a minor fraction of the HIV-1 target cell population in men can be genetically modified.

Moreover, CD4-LV is suitable to induce $CD4^+$ regulatory T cells by transfer of *FoxP3* or *IL-10* genes *in vitro* and *in vivo* (Zhou, Pfeiffer and Buchholz, unpublished data and Zhou et al., 2015). Tregs are major players in the suppression of immune responses and their induction is highly desirable in

diseases like allergies or autoimmune disorders. Also GvHD can be suppressed by Tregs, with implications on organ transplantation in human patients.

However, before the vectors can enter clinical trials, preclinical animal studies have to confirm the suitability of PTVs and CD4-LV for the named therapeutic applications *in vivo*. Moreover, several hurdles, like production of sufficient amounts of high titer stocks, pre-existing MV-specific immunity and dependency of transduction on activation state/ phenotype of the cells, have to be overcome:

1) Production of sufficient amounts of high titer stocks.

Currently, both PTVs and CD4-LV are produced by transient PEI-transfection of adherent HEK-293T packaging cells seeded in single T175 flasks. After harvest, filtrated, vector-containing cell culture supernatant is concentrated by ultracentrifugation through a 20% sucrose cushion. Thus, the procedure is laborious, costly and only limited amounts of vector-containing supernatant can be processed at a given point of time, which restricts final vector yield.

In recent successful gene therapy trials, relying on *ex vivo* correction of autologous cells prior reinfusion, approximately $1 \times 10^9 - 4 \times 10^{10}$ infectious units of vector per patient were applied (Sanber et al., 2015). The antigen content of approved vaccines or vaccines in clinical trials commonly lies between few µg (Johnson et al., 2014) and several µg/few mg (Kim et al., 2014; Zandberg et al., 2015) per injection. Hence, to provide sufficient quantities of vector for clinical trials and commercialization, LV production clearly needs scale-up. Suitability of transiently PEI-transfected, serum-free suspension cultures and ultrafiltration or affinity chromatography purification for large-scale LV production has been described before (Segura et al., 2007) and has to be implemented. Interestingly, titers of various vectors produced by suspension cells were reported to exceed those of adherent-cell culture based ones (Ghani et al., 2006; Durocher et al., 2007), which is highly desirable for clinical application.

If titers should be not sufficiently high, multiple injections at consecutive days, injection of large volumes of vector or local injections, e.g. in tumors, might ensure therapy success. Moreover, also autologous transfer of *ex vivo* modified APCs or $CD4^+$ T lymphocytes might be an option to compensate for lower vector titers. However, *in vivo* application is clearly preferable as *in vitro* cultivation of cells can significantly affect their properties (Marktel et al., 2003) and *in vivo* modification would turn personalized medical products into universally applicable drugs.

2) Pre-existing MV-specific immunity.

Despite the appealing data obtained *in vitro* and in mouse studies, successful clinical application of LVs pseudotyped with (engineered) MV-GPs may be hampered by the pre-existing MV-specific immunity in humans developed in response to natural infection or vaccination. Strengthening these concerns, *in vitro* experiments showed neutralization of MV-LV by human serum (Lévy et al., 2012). Thereby, the human humoral immune response was described to be mainly directed against H, and here primarily against the immunodominant epitopes “Noose” and “NE” (Ertl et al., 2003), while anti-

F antibodies hardly contributed to humoral anti-MV immunity (de Swart, Rik L et al., 2005). Mutating the two immunodominant epitopes of H abolished binding of Noose- and NE-specific antibodies without loss of vector activity but did not suffice to achieve complete escape from polyclonal MV-specific antibodies in human sera (Lévy et al., 2012). Additional introduction of an extra glycosylation site, found in certain emerging MV_{wt} strains, however, also prevented neutralization by polyclonal antibodies in human sera while leaving the transductional potency of the vectors unaffected (Lévy et al., 2012).

Interestingly, also receptor-targeted vectors, where Noose and NE epitopes are unmutated and no additional glycosylation site is inserted, have been reported to partially escape neutralizing antibodies in human plasma (Kneissl et al., 2012). Here, protection from neutralizing antibodies was attributed to the four point mutations introduced to ablate interaction with the natural MV receptors, which most likely destroyed immunogenic epitopes, since antibodies are often directed against the SLAM binding site (Ertl et al., 2003). Moreover, a shielding effect of the displayed binding domain was proposed.

Another possibility to circumvent anti-MV immunity is provided by the transfer of the targeting system to envelope proteins of animal paramyxoviruses, which are non-pathogenic to humans, as recently described for LVs pseudotyped with CD20-targeted *Tupaia paramyxovirus* glycoproteins (Enkirch et al., 2013). Thus, anti-MV immunity can be alleviated by several approaches, paving the way for clinical application of LVs incorporating (engineered) MV-GPs into their envelopes.

3) Transduction of resting lymphocytes.

CD4-LV selectively transduced its target cells *in vitro* and *in vivo* (Figure 37, Figure 44, Figure 45A, Figure 47, Figure 48A). However, a clear preference for transduction of activated or memory $CD4^+$ T cells over naïve, resting $CD4^+$ T cells was observed (Figure 38C, Figure 48B and C). In contrast to memory cells, naïve $CD4^+$ T cells can recognize new antigens and are therefore of great importance to cellular immunity and of pivotal interest to gene therapy. Gene delivery into resting cells might be enhanced by co-transfer of the viral protein X (Vpx) derived from HIV-2 or several SIV strains. Vpx counteracts the HIV-1 restriction factor SAMHD1 in resting $CD4^+$ T cells (Baldauf et al., 2012), monocytes and dendritic cells (Laguette et al., 2011), and therefore likely improves transduction efficiency in resting $CD4^+$ T cells, as already shown by Geng *et al*. (Geng et al., 2014). Thus, it will be interesting to evaluate the effect of Vpx co-delivery by CD4-LV on transduction efficiency in resting $CD4^+$ T cells.

Taken together, despite several drawbacks, this thesis introduced two new and highly promising vectors candidates for immunotherapy. It will be interesting to follow further development of both vector types towards clinical application.

5. Summary

Although pathogens are ubiquitously found in the environment, catching disease is quite scarce. This can be attributed to the action of immune cells, protecting the body from invading microorganisms. A central role in the induction and orchestration of adaptive immune responses is ascribed to antigen presenting cells (APCs), like dendritic cells (DCs), and $CD4^+$ T lymphocytes. Due to their important functions, these cell types gained center stage in immunotherapy. Thereby, their specific modification is highly desirable for several applications, including prophylactic or therapeutic vaccination approaches and the fight against human immunodeficiency virus type 1 (HIV-1) infection. In recent years, especially viral vectors proved to be powerful tools for the modification of target cells. Among them, lentiviral vectors (LVs) are of particular interest as they are not only able to transduce dividing but also non-dividing cells. They can be retargeted to basically any receptor of choice by pseudotyping with (engineered) measles virus (MV) glycoproteins (GPs) hemagglutinin (H) and fusion protein (F). Beside transfer of genetic information, retroviral and lentiviral vectors are able to deliver heterologous proteins into their target cells when the cargo proteins are genetically fused to structural proteins of the vector particle ("protein transfer vectors", PTVs). Taking advantage of this system, the present thesis aimed to employ lentiviral vectors for the specific modification of signaling lymphocyte activation molecule $(SLAM)^+$ APCs and $CD4^+$ T lymphocytes.

Initially, production of PTVs was optimized to allow maximum gene and protein transfer into transduced cells. In order to achieve targeting of SLAM-positive APCs, PTVs were pseudotyped with truncated MV_{wt}-GPs with an established tropism for SLAM. Beside SLAM, a hitherto unknown epithelial MV receptor was postulated, to whose identification as adherens junction protein Nectin-4 the present thesis contributed to characterize $SLAM^-$ target cell populations of MV_{wt}-GPs. Indeed, upon pseudotyping of PTVs with MV_{wt}-GPs, marker gene and GFP, Cre or ovalbumin (Ova) cargo protein delivery was completely restricted to SLAM- and Nectin-4-positive CHO cells and naturally SLAM-expressing B cell lines, whereas broad transduction was observed for VSV-G pseudotyped control vectors. Specific excision of the loxP-flanked *cerulean* open reading frame in receptor-positive indicator cell lines following PTV-mediated transfer of Cre recombinase exemplarily demonstrated cytoplasmic protein transfer and unimpaired functionality of the delivered cargo protein. Finally, transfer of the model antigen Ova by MV_{wt}-GP and VSV-G pseudotyped PTVs into receptor-positive, murine DCs *in vitro* or after administration into human SLAM-transgenic and control mice *in vivo* was shown to stimulate antigen-specific T cells, and here especially $CD8^+$ T lymphocytes.

In contrast to SLAM-targeted PTVs, which relied on MV_{wt}-GPs, specificity of CD4-targeted LV (CD4-LV) was achieved by pseudotyping with engineered MV-GPs, displaying a CD4-specific designed ankyrin repeat domain (DARPin) as binding domain on receptor-blinded H. H-αCD4 was well expressed on the surface of HEK-293T packaging cells allowing its efficient incorporation into CD4-LV particles and giving rise to high titer vector stocks with average yields > 10^8 transducing units/ml after concentration. *In vitro*, CD4-LV demonstrated absolute receptor specificity on cell lines and the naturally mixed population of primary peripheral blood mononuclear cells (PBMC), with transgene expression exclusively detectable in $CD4^+$ but not $CD4^-$ cells. Of particular note, CD4-LV was capable to stably transduce not only activated but also resting primary $CD4^+$ lymphocytes. Beside transduction of $CD4^+$ T lymphocytes, also gene transfer into $CD4^+$ human macrophages could be demonstrated *in vitro*. *In vivo*, following systemic injection of CD4-LV transferring a bicistronic *gfp*/*luciferase* reporter gene, luciferase activity in NOD-scid IL2R$\gamma^{-/-}$ mice reconstituted with human PBMC or hematopoietic stem cells was mainly detected in lymphoid organs. Flow cytometric analyses of GFP-expression in lymphoid organs and blood confirmed the strict receptor-dependency of transduction events found *in vitro* also to apply *in vivo*. Interestingly, a clear preference for transduction of $CD4^+$ T memory cells over naïve $CD4^+$ T lymphocytes was observed.

Concluding, this thesis clearly demonstrated suitability of (engineered) MV-GPs pseudotyped LV for specific protein and gene delivery into distinct subsets of immune cells. By the successful generation of SLAM- and CD4-targeted LVs, which allowed specific modification of $SLAM^+$ APCs and $CD4^+$ T lymphocytes, including even resting T lymphocytes, respectively, the broad applicability of MV-GP based cell entry targeting approaches for diverse cell surface receptors was emphasized. Both PTVs and CD4-LV are promising tools for basic research and gene and immunotherapy, opening up new avenues for a multitude of diverse applications.

6. Zusammenfassung

Obwohl wir permanent von einer Vielzahl von Pathogenen umgeben sind, werden wir nur selten krank. Dieses Phänomen ist auf die Gegenwart des Immunsystems zurückzuführen, das den Körper vor eindringenden Mikroorganismen schützt. Eine zentrale Rolle in der Induktion und Koordination adaptiver Immunantworten wird antigen-präsentierenden Zellen (engl. antigen presenting cells, APCs), wie dendritischen Zellen (engl. dendritic cells, DCs), und $CD4^+$ T Lymphozyten zugeschrieben. Aufgrund ihrer bedeutenden Funktion sind diese Zelltypen in den Fokus der Immuntherapie gerückt. Ihre spezifische Modifikation ist dabei für verschiedene Anwendungen erstrebenswert, unter anderem für prophylaktische und therapeutische Impfung und die Bekämpfung von Infektionen durch das humane Immundefizienzvirus Typ 1 (HIV-1). In den vergangenen Jahren haben sich besonders virale Vektoren als nützliche Hilfsmittel für die genetische Modifikation von Zielzellen erwiesen. Unter ihnen sind vor allem lentivirale Vektoren (LVs) von großem Interesse, da sie nicht nur mitotisch aktive, sondern auch ruhende Zellen transduzieren können. Durch Pseudotypisierung mit den modifizierten Masernvirus (MV) Glykoproteinen (GPs) Hämagglutinin (H) und Fusionsprotein (F) kann ihnen Spezifität für nahezu jeden beliebigen Rezeptor verliehen werden. Zudem können retrovirale und lentivirale Vektoren neben dem Transfer von Genen auch heterologe Proteine in ihre Zielzellen übertragen, insofern diese genetisch mit Strukturproteinen der Vektorpartikel fusioniert wurden („Proteintransfervektoren“, PTVs). Basierend auf diesem System war es das Ziel der vorliegenden Arbeit, lentivirale Vektoren für die zielgerichtete Modifikation von $SLAM^+$ (Akronym für engl. signaling lymphocyte activation molecule) APCs und $CD4^+$ T Lymphozyten zu generieren.

Initial wurde die Herstellung von PTVs optimiert, um maximalen Gen- und Proteintransfer in transduzierte Zellen zu ermöglichen. Um zudem zielgerichtet $SLAM^+$ Zellen modifizieren zu können, wurden PTVs mit zytoplamatisch verkürzten MV_{wt}-GPs pseudotypisiert, die bekanntermaßen einen Tropismus für SLAM aufweisen. Neben SLAM war die Existenz eines bis dato unbekannten epithelialen MV-Rezeptors postuliert worden, zu dessen Identifikation als Adhärenzverbindungsprotein Nectin-4 die vorliegende Arbeit beigetragen hat, um $SLAM^-$ Zielzellpopulationen von MV_{wt}-GPs zu charakterisieren. Tatsächlich waren Markergen- und GFP-, Cre- oder Ovalbumin- (Ova) Cargoproteintransfer komplett auf SLAM- und Nectin-4-positive CHO-Zellen und natürlich SLAM-exprimierende B Zelllinien beschränkt, während VSV-G pseudotypisierte Kontrollvektoren einen breiten Tropismus aufwiesen. Das spezifische Ausschneiden einer loxP-flankierten *cerulean*-Expressionskassette in transduzierten, rezeptorpositiven Indikatorzelllinien, das durch die in PTVs verpackte Rekombinase Cre katalysiert wurde, demonstrierte beispielhaft sowohl den zytoplasmatischen Transfer als auch die unbeeinträchtigte Funktion des übertragenen Cargoproteins. Schlussendlich konnte gezeigt werden, dass der PTV-vermittelte Transfer des Modellantigens Ova in

rezeptorpositive APCs *in vitro* und in für humanes SLAM transgene Mäuse oder Kontrollmäuse *in vivo* zur Stimulation antigen-spezifischer T Lymphozyten, und hier vor allem $CD8^+$ T Lymphozyten, führt.

Im Gegensatz zu SLAM-spezifischen PTVs, deren Tropismus auf MV_{wt}-GPs basierte, wurde die Spezifität eines gezielt $CD4^+$ Zellen transduzierenden LVs (CD4-LV) durch Pseudotypisierung mit modifizierten MV-GPs erreicht, wobei ein CD4-spezifisches DARPin (Akronym für engl. designed ankyrin repeat protein, konzipierte Proteine mit Ankyrinwiederholungseinheiten) als Bindedomäne an rezeptorblindes H fusioniert wurde. Die gute Oberflächenexpression von H-αCD4 in HEK-293T Verpackungszellen ermöglichte den effizienten Einbau in CD4-LV-Partikel und war Grundlage für die mit durchschnittlich > 10^8 transduzierenden Einheiten/ ml hochtitrigen Vektorstocks nach Aufkonzentration. *In vitro* zeigte CD4-LV absolute Spezifität für $CD4^+$ Zelllinien und $CD4^+$ T Lymphozyten in der natürlich gemischten Zellpopulation primärer PBMC (Akronym für engl. peripheral blood mononuclear cells, mononukleäre Zellen des peripheren Blutes), während keine Transgenexpression in $CD4^-$ Zellen detektiert werden konnte. Dabei ist besonders hervorzuheben, dass CD4-LV nicht nur in der Lage war, aktivierte sondern auch ruhende, primäre $CD4^+$ Lymphozyten stabil zu transduzieren. Zudem konnten auch $CD4^+$ Makrophagen *in vitro* mit dem Vektor transduziert werden. Nach systemischer Applikation von *gfp/luciferase* übertragendem CD4-LV wurde Luziferaseaktivität vor allem in den lymphatischen Organen von mit humanen PBMC oder hämatopoetischen Stammzellen repopulierten NOD-scid $IL2R\gamma^{-/-}$ Mäusen detektiert. Durchflusszytometrische Analysen der GFP-Expression in lymphatischen Organen und Blut bestätigten die bereits *in vitro* beobachtete strikte Rezeptorabhängigkeit der Transduktion auch *in vivo*. Interessanterweise konnte eine bevorzugte Transduktion von $CD4^+$ T-Gedächtniszellen gegenüber naiven $CD4^+$ T Lymphozyten beobachtet werden.

Zusammenfassend konnte in der vorliegenden Arbeit die Eignung von mit (modifizierten) MV-GPs pseudotypisierten LVs für den selektiven Protein- und Gentransfer in verschiedene Immunzellsubtypen gezeigt werden. Durch die erfolgreiche Herstellung SLAM- beziehungsweise CD4-spezifischer LVs, die die gezielte Modifikation von $SLAM^+$ APCs oder $CD4^+$ T Lymphozyten, einschließlich ruhender T Lymphozyten, erlaubten, wurde die breite Anwendbarkeit des auf MV-GPs basierenden Zelleintrittstargetings für verschiedene Zelloberflächenrezeptoren unterstrichen. Sowohl PTVs als auch CD4-LV stellen vielversprechende Hilfsmittel für Grundlagenforschung und Gen- und Immuntherapie dar und eröffnen damit neue Möglichkeiten für eine Vielzahl verschiedenster Anwendungen.

7. References

Abel, T., El Filali, E., Waern, J., Schneider, I.C., Yuan, Q., Münch, R.C., Hick, M., Warnecke, G., Madrahimov, N., and Kontermann, R.E., et al. (2013). Specific gene delivery to liver sinusoidal and artery endothelial cells. Blood 122, 2030-2038.

Abordo-Adesida, E., Follenzi, A., Barcia, C., Sciascia, S., Castro, M.G., Naldini, L., and Lowenstein, P.R. (2005). Stability of lentiviral vector-mediated transgene expression in the brain in the presence of systemic antivector immune responses. Human gene therapy 16, 741-751.

Ader, N., Brindley, M.A., Avila, M., Origgi, F.C., Langedijk, Johannes P M, Örvell, C., Vandevelde, M., Zurbriggen, A., Plemper, R.K., and Plattet, P. (2012). Structural rearrangements of the central region of the morbillivirus attachment protein stalk domain trigger F protein refolding for membrane fusion. The Journal of biological chemistry 287, 16324-16334.

Ageichik, A., Buchholz, C.J., and Collins, M.K. (2011). Lentiviral vectors targeted to MHC II are effective in immunization. Hum. Gene Ther. 22, 1249-1254.

Agosto, L.M., Yu, J.J., Liszewski, M.K., Baytop, C., Korokhov, N., Humeau, L.M., and O'Doherty, U. (2009). The CXCR4-tropic human immunodeficiency virus envelope promotes more-efficient gene delivery to resting CD4+ T cells than the vesicular stomatitis virus glycoprotein G envelope. J. Virol. 83, 8153-8162.

Alberts, B. (2002). Molecular biology of the cell (New York: Garland Science).

Alkhatib, G., Combadiere, C., Broder, C.C., Feng, Y., Kennedy, P.E., Murphy, P.M., and Berger, E.A. (1996). CC CKR5: a RANTES, MIP-1alpha, MIP-1beta receptor as a fusion cofactor for macrophage-tropic HIV-1. Science (New York, N.Y.) 272, 1955-1958.

Amirache, F., Lévy, C., Costa, C., Mangeot, P.-E., Torbett, B.E., Wang, C.X., Nègre, D., Cosset, F.-L., and Verhoeyen, E. (2014). Mystery solved: VSV-G-LVs do not allow efficient gene transfer into unstimulated T cells, B cells, and HSCs because they lack the LDL receptor. Blood 123, 1422-1424.

Anliker, B., Abel, T., Kneissl, S., Hlavaty, J., Caputi, A., Brynza, J., Schneider, I.C., Münch, R.C., Petznek, H., and Kontermann, R.E., et al. (2010). Specific gene transfer to neurons, endothelial cells and hematopoietic progenitors with lentiviral vectors. Nature methods 7, 929-935.

Aoki, T., Miyauchi, K., Urano, E., Ichikawa, R., and Komano, J. (2011). Protein transduction by pseudotyped lentivirus-like nanoparticles. Gene Ther. 18, 936-941.

Bach, P., Abel, T., Hoffmann, C., Gal, Z., Braun, G., Voelker, I., Ball, C.R., Johnston, Ian C D, Lauer, U.M., and Herold-Mende, C., et al. (2013). Specific elimination of CD133+ tumor cells with targeted oncolytic measles virus. Cancer research 73, 865-874.

Bachmann, M.F., and Jennings, G.T. (2010). Vaccine delivery: a matter of size, geometry, kinetics and molecular patterns. Nature reviews. Immunology 10, 787-796.

Baldauf, H.-M., Pan, X., Erikson, E., Schmidt, S., Daddacha, W., Burggraf, M., Schenkova, K., Ambiel, I., Wabnitz, G., and Gramberg, T., et al. (2012). SAMHD1 restricts HIV-1 infection in resting CD4(+) T cells. Nat. Med. 18, 1682-1687.

Banchereau, J., Briere, F., Caux, C., Davoust, J., Lebecque, S., Liu, Y.J., Pulendran, B., and Palucka, K. (2000). Immunobiology of dendritic cells. Annual review of immunology 18, 767-811.

Banchereau, J., and Steinman, R.M. (1998). Dendritic cells and the control of immunity. Nature 392, 245-252.

Barnden, M.J., Allison, J., Heath, W.R., and Carbone, F.R. (1998). Defective TCR expression in transgenic mice constructed using cDNA-based alpha- and beta-chain genes under the control of heterologous regulatory elements. Immunol. Cell Biol. 76, 34-40.

Barry, M., and Bleackley, R.C. (2002). Cytotoxic T lymphocytes: all roads lead to death. Nature reviews. Immunology 2, 401-409.

Bennett, S.R., Carbone, F.R., Karamalis, F., Flavell, R.A., Miller, J.F., and Heath, W.R. (1998). Help for cytotoxic-T-cell responses is mediated by CD40 signalling. Nature 393, 478-480.

Berger, A., Sommer, Andreas F R, Zwarg, J., Hamdorf, M., Welzel, K., Esly, N., Panitz, S., Reuter, A., Ramos, I., and Jatiani, A., et al. (2011). SAMHD1-deficient CD14+ cells from individuals with Aicardi-Goutières syndrome are highly susceptible to HIV-1 infection. PLoS Pathog. 7, e1002425.

Bevan, M.J. (1976). Cross-priming for a secondary cytotoxic response to minor H antigens with H-2 congenic cells which do not cross-react in the cytotoxic assay. The Journal of experimental medicine 143, 1283-1288.

Beverley, P.C.L. (2002). Immunology of vaccination. British medical bulletin 62, 15-28.

Beyer, W.R., Westphal, M., Ostertag, W., and Laer, D. von (2002). Oncoretrovirus and Lentivirus Vectors Pseudotyped with Lymphocytic Choriomeningitis Virus Glycoprotein: Generation, Concentration, and Broad Host Range. Journal of Virology 76, 1488-1495.

Binz, H.K., Stumpp, M.T., Forrer, P., Amstutz, P., and Plückthun, A. (2003). Designing repeat proteins: well-expressed, soluble and stable proteins from combinatorial libraries of consensus ankyrin repeat proteins. J. Mol. Biol. 332, 489-503.

Bleharski, J.R., Niazi, K.R., Sieling, P.A., Cheng, G., and Modlin, R.L. (2001). Signaling lymphocytic activation molecule is expressed on CD40 ligand-activated dendritic cells and directly augments production of inflammatory cytokines. Journal of immunology (Baltimore, Md. : 1950) 167, 3174-3181.

Blömer, U., Naldini, L., Kafri, T., Trono, D., Verma, I.M., and Gage, F.H. (1997). Highly efficient and sustained gene transfer in adult neurons with a lentivirus vector. Journal of Virology 71, 6641-6649.

Bodmer, B.S. (2015). Vergleich stabil transgener DC-Zelllinien zur Analyse muriner T-Zell-Immunantworten.

Bolt, G., and Pedersen, I.R. (1998). The role of subtilisin-like proprotein convertases for cleavage of the measles virus fusion glycoprotein in different cell types. Virology 252, 387-398.

Boyman, O., and Sprent, J. (2012). The role of interleukin-2 during homeostasis and activation of the immune system. Nat. Rev. Immunol. 12, 180-190.

Briggs, J.A.G., Simon, M.N., Gross, I., Kräusslich, H.-G., Fuller, S.D., Vogt, V.M., and Johnson, M.C. (2004). The stoichiometry of Gag protein in HIV-1. Nat. Struct. Mol. Biol. 11, 672-675.

Broux, B., Markovic-Plese, S., Stinissen, P., and Hellings, N. (2012). Pathogenic features of CD4+CD28- T cells in immune disorders. Trends in molecular medicine 18, 446-453.

Buchholz, C.J., Koller, D., Devaux, P., Mumenthaler, C., Schneider-Schaulies, J., Braun, W., Gerlier, D., and Cattaneo, R. (1997). Mapping of the primary binding site of measles virus to its receptor CD46. J. Biol. Chem. 272, 22072-22079.

Buchholz, C.J., Schneider, U., Devaux, P., Gerlier, D., and Cattaneo, R. (1996). Cell entry by measles virus: long hybrid receptors uncouple binding from membrane fusion. Journal of Virology 70, 3716-3723.

Bukrinsky, M. (2004). A hard way to the nucleus. Molecular medicine (Cambridge, Mass.) 10, 1-5.

Burns, J.C., Friedmann, T., Driever, W., Burrascano, M., and Yee, J.K. (1993). Vesicular stomatitis virus G glycoprotein pseudotyped retroviral vectors: concentration to very high titer and efficient gene transfer into mammalian and nonmammalian cells. Proceedings of the National Academy of Sciences of the United States of America 90, 8033-8037.

Cambi, A., Beeren, I., Joosten, B., Fransen, J.A., and Figdor, C.G. (2009). The C-type lectin DC-SIGN internalizes soluble antigens and HIV-1 virions via a clathrin-dependent mechanism. European journal of immunology 39, 1923-1928.

Campadelli-Fiume, G., Cocchi, F., Menotti, L., and Lopez, M. (2000). The novel receptors that mediate the entry of herpes simplex viruses and animal alphaherpesviruses into cells. Reviews in medical virology 10, 305-319.

Cann, A.J., Stanway, G., Hughes, P.J., Minor, P.D., Evans, D.M., Schild, G.C., and Almond, J.W. (1984). Reversion to neurovirulence of the live-attenuated Sabin type 3 oral poliovirus vaccine. Nucleic Acids Res. 12, 7787-7792.

Casasnovas, J.M., Larvie, M., and Stehle, T. (1999). Crystal structure of two CD46 domains reveals an extended measles virus-binding surface. The EMBO journal 18, 2911-2922.

Cassol, E., Cassetta, L., Rizzi, C., Alfano, M., and Poli, G. (2009). M1 and M2a polarization of human monocyte-derived macrophages inhibits HIV-1 replication by distinct mechanisms. J. Immunol. 182, 6237-6246.

Cathomen, T., Buchholz, C.J., Spielhofer, P., and Cattaneo, R. (1995). Preferential initiation at the second AUG of the measles virus F mRNA: a role for the long untranslated region. Virology 214, 628-632.

Cattoglio, C., Facchini, G., Sartori, D., Antonelli, A., Miccio, A., Cassani, B., Schmidt, M., Kalle, C. von, Howe, S., and Thrasher, A.J., et al. (2007). Hot spots of retroviral integration in human CD34+ hematopoietic cells. Blood 110, 1770-1778.

Caux, C., and Dubois, B. (2001). Antigen uptake by dendritic cells. Methods in molecular medicine 64, 369-376.

Cavalieri, S., Cazzaniga, S., Geuna, M., Magnani, Z., Bordignon, C., Naldini, L., and Bonini, C. (2003). Human T lymphocytes transduced by lentiviral vectors in the absence of TCR activation maintain an intact immune competence. Blood 102, 497-505.

Centers for Disease Control and Prevention (1996). Measles pneumonitis following measles-mumps-rubella vaccination of a patient with HIV infection, 1993. MMWR. Morbidity and mortality weekly report 45, 603-606.

Ciré, S., Da Rocha, S., Yao, R., Fisson, S., Buchholz, C.J., Collins, M.K., and Galy, A. (2014). Immunization of mice with lentiviral vectors targeted to MHC class II+ cells is due to preferential transduction of dendritic cells in vivo. PloS one 9, e101644.

Clem, A.S. (2011). Fundamentals of vaccine immunology. Journal of global infectious diseases 3, 73-78.

Clever, J.L., and Parslow, T.G. (1997). Mutant human immunodeficiency virus type 1 genomes with defects in RNA dimerization or encapsidation. Journal of Virology 71, 3407-3414.

Cobos Jiménez, V., Booiman, T., de Taeye, Steven W, van Dort, Karel A, Rits, Maarten A N, Hamann, J., and Kootstra, N.A. (2012). Differential expression of HIV-1 interfering factors in monocyte-derived macrophages stimulated with polarizing cytokines or interferons. Scientific reports 2, 763.

Cocchi, F., Menotti, L., Mirandola, P., Lopez, M., and Campadelli-Fiume, G. (1998). The ectodomain of a novel member of the immunoglobulin subfamily related to the poliovirus receptor has the attributes of a bona fide receptor for herpes simplex virus types 1 and 2 in human cells. Journal of Virology 72, 9992-10002.

Cocks, B.G., Chang, C.C., Carballido, J.M., Yssel, H., de Vries, J E, and Aversa, G. (1995). A novel receptor involved in T-cell activation. Nature 376, 260-263.

Coffman, R.L., Sher, A., and Seder, R.A. (2010). Vaccine adjuvants: putting innate immunity to work. Immunity 33, 492-503.

Coico, R., and Sunshine, G. (2009). Immunology. A short course (Hoboken, N.J.: Wiley-Blackwell).

Cornetta, K., and Anderson, W.F. (1989). Protamine sulfate as an effective alternative to polybrene in retroviral-mediated gene-transfer: implications for human gene therapy. J. Virol. Methods 23, 187-194.

Cronin, J., Zhang, X.-Y., and Reiser, J. (2005). Altering the tropism of lentiviral vectors through pseudotyping. Current gene therapy 5, 387-398.

Dai, B., Yang, L., Yang, H., Hu, B., Baltimore, D., and Wang, P. (2009). HIV-1 Gag-specific immunity induced by a lentivector-based vaccine directed to dendritic cells. Proc. Natl. Acad. Sci. U.S.A. 106, 20382-20387.

Dalgleish, A.G., Beverley, P.C., Clapham, P.R., Crawford, D.H., Greaves, M.F., and Weiss, R.A. (1984). The CD4 (T4) antigen is an essential component of the receptor for the AIDS retrovirus. Nature 312, 763-767.

de Swart, Rik L, Yüksel, S., and Osterhaus, Albert D M E (2005). Relative contributions of measles virus hemagglutinin- and fusion protein-specific serum antibodies to virus neutralization. Journal of Virology 79, 11547-11551.

Dearman, R.J., Cumberbatch, M., Maxwell, G., Basketter, D.A., and Kimber, I. (2009). Toll-like receptor ligand activation of murine bone marrow-derived dendritic cells. Immunology 126, 475-484.

Demaison, C., Parsley, K., Brouns, G., Scherr, M., Battmer, K., Kinnon, C., Grez, M., and Thrasher, A.J. (2002). High-level transduction and gene expression in hematopoietic repopulating cells using a human immunodeficiency [correction of imunodeficiency] virus type 1-based lentiviral vector containing an internal spleen focus forming virus promoter. Hum. Gene Ther. 13, 803-813.

Deng, H., Liu, R., Ellmeier, W., Choe, S., Unutmaz, D., Burkhart, M., Di Marzio, P., Marmon, S., Sutton, R.E., and Hill, C.M., et al. (1996). Identification of a major co-receptor for primary isolates of HIV-1. Nature 381, 661-666.

Donnelly, M.L., Luke, G., Mehrotra, A., Li, X., Hughes, L.E., Gani, D., and Ryan, M.D. (2001). Analysis of the aphthovirus 2A/2B polyprotein 'cleavage' mechanism indicates not a proteolytic reaction, but a novel translational effect: a putative ribosomal 'skip'. The Journal of general virology 82, 1013-1025.

Dörig, R.E., Marcil, A., Chopra, A., and Richardson, C.D. (1993). The human CD46 molecule is a receptor for measles virus (Edmonston strain). Cell 75, 295-305.

Dragic, T., Litwin, V., Allaway, G.P., Martin, S.R., Huang, Y., Nagashima, K.A., Cayanan, C., Maddon, P.J., Koup, R.A., and Moore, J.P., et al. (1996). HIV-1 entry into CD4+ cells is mediated by the chemokine receptor CC-CKR-5. Nature 381, 667-673.

Dunn, T.B. (1954). Normal and pathologic anatomy of the reticular tissue in laboratory mice, with a classification and discussion of neoplasms. J. Natl. Cancer Inst. 14, 1281-1433.

Durocher, Y., Pham, P.L., St-Laurent, G., Jacob, D., Cass, B., Chahal, P., Lau, C.J., Nalbantoglu, J., and Kamen, A. (2007). Scalable serum-free production of recombinant adeno-associated virus type 2 by transfection of 293 suspension cells. Journal of virological methods 144, 32-40.

Dutton, R.W., Bradley, L.M., and Swain, S.L. (1998). T cell memory. Annual review of immunology 16, 201-223.

Enders, J.F., Katz, S.L., Milovanovic, M.V., and Holloway, A. (1960). Studies on an attenuated measles-virus vaccine. I. Development and preparations of the vaccine: technics for assay of effects of vaccination. The New England journal of medicine 263, 153-159.

Enders, J.F., and Peebles, T.C. (1954). Propagation in tissue culture of cytopathogenic agents from patients with measles. Proceedings of the Society for Experimental Biology and Medicine. Society for Experimental Biology and Medicine (New York, N.Y.) 86, 277-286.

Engering, A., Geijtenbeek, Teunis B H, van Vliet, Sandra J, Wijers, M., van Liempt, E., Demaurex, N., Lanzavecchia, A., Fransen, J., Figdor, C.G., and Piguet, V., et al. (2002). The dendritic cell-specific adhesion receptor DC-SIGN internalizes antigen for presentation to T cells. Journal of immunology (Baltimore, Md. : 1950) 168, 2118-2126.

Enkirch, T., Kneissl, S., Hoyler, B., Ungerechts, G., Stremmel, W., Buchholz, C.J., and Springfeld, C. (2013). Targeted lentiviral vectors pseudotyped with the Tupaia paramyxovirus glycoproteins. Gene therapy 20, 16-23.

Ertl, O.T., Wenz, D.C., Bouche, F.B., Berbers, G A M, and Muller, C.P. (2003). Immunodominant domains of the Measles virus hemagglutinin protein eliciting a neutralizing human B cell response. Archives of virology 148, 2195-2206.

Esslinger, C., Romero, P., and MacDonald, H.R. (2002). Efficient transduction of dendritic cells and induction of a T-cell response by third-generation lentivectors. Human gene therapy 13, 1091-1100.

Fabre, S., Reymond, N., Cocchi, F., Menotti, L., Dubreuil, P., Campadelli-Fiume, G., and Lopez, M. (2002). Prominent role of the Ig-like V domain in trans-interactions of nectins. Nectin3 and nectin 4 bind to the predicted C-C'-C''-D beta-strands of the nectin1 V domain. J. Biol. Chem. 277, 27006-27013.

Fabre-Lafay, S., Garrido-Urbani, S., Reymond, N., Gonçalves, A., Dubreuil, P., and Lopez, M. (2005). Nectin-4, a new serological breast cancer marker, is a substrate for tumor necrosis factor-alpha-converting enzyme (TACE)/ADAM-17. J. Biol. Chem. 280, 19543-19550.

Fan, Y., Sahdev, P., Ochyl, L.J., J Akerberg, J., and Moon, J.J. (2015). Cationic liposome-hyaluronic acid hybrid nanoparticles for intranasal vaccination with subunit antigens. Journal of controlled release : official journal of the Controlled Release Society.

Farina, C., Theil, D., Semlinger, B., Hohlfeld, R., and Meinl, E. (2004). Distinct responses of monocytes to Toll-like receptor ligands and inflammatory cytokines. International immunology 16, 799-809.

Feng, Y., Broder, C.C., Kennedy, P.E., and Berger, E.A. (1996). HIV-1 entry cofactor: functional cDNA cloning of a seven-transmembrane, G protein-coupled receptor. Science (New York, N.Y.) 272, 872-877.

Ferrara, J.L., Cooke, K.R., Pan, L., and Krenger, W. (1996). The immunopathophysiology of acute graft-versus-host-disease. Stem Cells 14, 473-489.

Finkelshtein, D., Werman, A., Novick, D., Barak, S., and Rubinstein, M. (2013). LDL receptor and its family members serve as the cellular receptors for vesicular stomatitis virus. Proc. Natl. Acad. Sci. U.S.A. 110, 7306-7311.

Fish, R.E. (2008). Anesthesia and analgesia in laboratory animals (Amsterdam, Boston: Elsevier/Academic Press).

Follenzi, A., Battaglia, M., Lombardo, A., Annoni, A., Roncarolo, M.G., and Naldini, L. (2004). Targeting lentiviral vector expression to hepatocytes limits transgene-specific immune response and establishes long-term expression of human antihemophilic factor IX in mice. Blood 103, 3700-3709.

Forrer, P., Stumpp, M.T., Binz, H., and Plückthun, A. (2003). A novel strategy to design binding molecules harnessing the modular nature of repeat proteins. FEBS Letters 539, 2-6.

Frecha, C., Costa, C., Lévy, C., Nègre, D., Russell, S.J., Maisner, A., Salles, G., Peng, K.-W., Cosset, F.-L., and Verhoeyen, E. (2009). Efficient and stable transduction of resting B lymphocytes and primary chronic lymphocyte leukemia cells using measles virus gp displaying lentiviral vectors. Blood 114, 3173-3180.

Frecha, C., Costa, C., Nègre, D., Gauthier, E., Russell, S.J., Cosset, F.-L., and Verhoeyen, E. (2008a). Stable transduction of quiescent T cells without induction of cycle progression by a novel lentiviral vector pseudotyped with measles virus glycoproteins. Blood 112, 4843-4852.

Frecha, C., Lévy, C., Costa, C., Nègre, D., Amirache, F., Buckland, R., Russell, S.J., Cosset, F.-L., and Verhoeyen, E. (2011). Measles virus glycoprotein-pseudotyped lentiviral vector-mediated gene transfer into quiescent lymphocytes requires binding to both SLAM and CD46 entry receptors. J. Virol. 85, 5975-5985.

Frecha, C., Szécsi, J., Cosset, F.-L., and Verhoeyen, E. (2008b). Strategies for targeting lentiviral vectors. Current gene therapy 8, 449-460.

Friedel, T., Hanisch, L.J., Muth, A., Honegger, A., Abken, H., Plückthun, A., Buchholz, C.J., and Schneider, I.C. (2015). Receptor-targeted lentiviral vectors are exceptionally sensitive toward the biophysical properties of the displayed single-chain Fv. Protein engineering, design & selection : PEDS.

Froelich, S., Tai, A., and Wang, P. (2010). Lentiviral vectors for immune cells targeting. Immunopharmacology and immunotoxicology 32, 208-218.

Funke, S., Maisner, A., Mühlebach, M.D., Koehl, U., Grez, M., Cattaneo, R., Cichutek, K., and Buchholz, C.J. (2008). Targeted cell entry of lentiviral vectors. Mol. Ther. 16, 1427-1436.

Funke, S., Schneider, I.C., Glaser, S., Mühlebach, M.D., Moritz, T., Cattaneo, R., Cichutek, K., and Buchholz, C.J. (2009). Pseudotyping lentiviral vectors with the wild-type measles virus glycoproteins improves titer and selectivity. Gene Ther. 16, 700-705.

Galla, M., Will, E., Kraunus, J., Chen, L., and Baum, C. (2004). Retroviral pseudotransduction for targeted cell manipulation. Molecular cell 16, 309-315.

Gaspari, A.A., and Tyring, S.K. (2008). Clinical and basic immunodermatology (London: Springer).

Geginat, J., Paroni, M., Facciotti, F., Gruarin, P., Kastirr, I., Caprioli, F., Pagani, M., and Abrignani, S. (2013). The CD4-centered universe of human T cell subsets. Seminars in immunology 25, 252-262.

Geng, X., Doitsh, G., Yang, Z., Galloway, N L K, and Greene, W.C. (2014). Efficient delivery of lentiviral vectors into resting human CD4 T cells. Gene Ther. 21, 444-449.

Gerlach, N., Schimmer, S., Weiss, S., Kalinke, U., and Dittmer, U. (2006). Effects of type I interferons on Friend retrovirus infection. J. Virol. 80, 3438-3444.

Ghani, K., Garnier, A., Coelho, H., Transfiguracion, J., Trudel, P., and Kamen, A. (2006). Retroviral vector production using suspension-adapted 293GPG cells in a 3L acoustic filter-based perfusion bioreactor. Biotechnology and bioengineering 95, 653-660.

Golay, J.T., Clark, E.A., and Beverley, P.C. (1985). The CD20 (Bp35) antigen is involved in activation of B cells from the G0 to the G1 phase of the cell cycle. Journal of immunology (Baltimore, Md. : 1950) 135, 3795-3801.

Goldschmidt, V., Ciuffi, A., Ortiz, M., Brawand, D., Muñoz, M., Kaessmann, H., and Telenti, A. (2008). Antiretroviral activity of ancestral TRIM5alpha. Journal of Virology 82, 2089-2096.

Grgacic, E.V.L., and Anderson, D.A. (2006). Virus-like particles: passport to immune recognition. Methods (San Diego, Calif.) 40, 60-65.

Griffin, D.E., and Oldstone, M.B.A (2008). Measles: History and Basic Biology (Berlin, London: Springer).

Haglund, K., Leiner, I., Kerksiek, K., Buonocore, L., Pamer, E., and Rose, J.K. (2002). Robust Recall and Long-Term Memory T-Cell Responses Induced by Prime-Boost Regimens with Heterologous Live Viral Vectors Expressing Human Immunodeficiency Virus Type 1 Gag and Env Proteins. Journal of Virology 76, 7506-7517.

Hamilton, D.L., and Abremski, K. (1984). Site-specific recombination by the bacteriophage P1 lox-Cre system. Cre-mediated synapsis of two lox sites. J. Mol. Biol. 178, 481-486.

Hanes, J., and Plückthun, A. (1997). In vitro selection and evolution of functional proteins by using ribosome display. Proceedings of the National Academy of Sciences of the United States of America 94, 4937-4942.

Hashiguchi, T., Maenaka, K., and Yanagi, Y. (2011a). Measles virus hemagglutinin: structural insights into cell entry and measles vaccine. Frontiers in microbiology 2, 247.

Hashiguchi, T., Ose, T., Kubota, M., Maita, N., Kamishikiryo, J., Maenaka, K., and Yanagi, Y. (2011b). Structure of the measles virus hemagglutinin bound to its cellular receptor SLAM. Nature structural & molecular biology 18, 135-141.

Hearps, A.C., and Jans, D.A. (2007). Regulating the functions of the HIV-1 matrix protein. AIDS research and human retroviruses 23, 341-346.

Hermida-Matsumoto, L., and Resh, M.D. (2000). Localization of human immunodeficiency virus type 1 Gag and Env at the plasma membrane by confocal imaging. Journal of Virology 74, 8670-8679.

Hilleman, M.R., Buynak, E.B., Weibel, R.E., Stokes, J., Whitman, J.E., and Leagus, M.B. (1968). Development and evaluation of the Moraten measles virus vaccine. JAMA 206, 587-590.

Hogquist, K.A., Jameson, S.C., Heath, W.R., Howard, J.L., Bevan, M.J., and Carbone, F.R. (1994). T cell receptor antagonist peptides induce positive selection. Cell 76, 17-27.

Hombach, A., Heuser, C., Marquardt, T., Wieczarkowiecz, A., Groneck, V., Pohl, C., and Abken, H. (2001). CD4+ T cells engrafted with a recombinant immunoreceptor efficiently lyse target cells in a MHC antigen- and Fas-independent fashion. Journal of immunology (Baltimore, Md. : 1950) 167, 1090-1096.

Hombach, A., Köhler, H., Rappl, G., and Abken, H. (2006). Human CD4+ T cells lyse target cells via granzyme/perforin upon circumvention of MHC class II restriction by an antibody-like immunoreceptor. Journal of immunology (Baltimore, Md. : 1950) 177, 5668-5675.

Horton, R.M., Hunt, H.D., Ho, S.N., Pullen, J.K., and Pease, L.R. (1989). Engineering hybrid genes without the use of restriction enzymes: gene splicing by overlap extension. Gene 77, 61-68.

Hsu, E.C., Dörig, R.E., Sarangi, F., Marcil, A., Iorio, C., and Richardson, C.D. (1997). Artificial mutations and natural variations in the CD46 molecules from human and monkey cells define regions important for measles virus binding. Journal of Virology 71, 6144-6154.

Hübner, W., Chen, P., Del Portillo, A., Liu, Y., Gordon, R.E., and Chen, B.K. (2007). Sequence of human immunodeficiency virus type 1 (HIV-1) Gag localization and oligomerization monitored with live confocal imaging of a replication-competent, fluorescently tagged HIV-1. Journal of Virology 81, 12596-12607.

Humbert, J.-M., Frecha, C., Amirache Bouafia, F., N'Guyen, T.H., Boni, S., Cosset, F.-L., Verhoeyen, E., and Halary, F. (2012). Measles virus glycoprotein-pseudotyped lentiviral vectors are highly superior to vesicular stomatitis virus G pseudotypes for genetic modification of monocyte-derived dendritic cells. Journal of Virology 86, 5192-5203.

Hunder, N.N., Wallen, H., Cao, J., Hendricks, D.W., Reilly, J.Z., Rodmyre, R., Jungbluth, A., Gnjatic, S., Thompson, J.A., and Yee, C. (2008). Treatment of metastatic melanoma with autologous CD4+ T cells against NY-ESO-1. N. Engl. J. Med. 358, 2698-2703.

Ibrahimi, A., Vande Velde, G., Reumers, V., Toelen, J., Thiry, I., Vandeputte, C., Vets, S., Deroose, C., Bormans, G., and Baekelandt, V., et al. (2009). Highly efficient multicistronic lentiviral vectors with peptide 2A sequences. Human gene therapy 20, 845-860.

Indraccolo, S., Minuzzo, S., Feroli, F., Mammano, F., Calderazzo, F., Chieco-Bianchi, L., and Amadori, A. (1998). Pseudotyping of Moloney leukemia virus-based retroviral vectors with simian immunodeficiency virus envelope leads to targeted infection of human CD4+ lymphoid cells. Gene therapy 5, 209-217.

Iorio, R.M., Melanson, V.R., and Mahon, P.J. (2009). Glycoprotein interactions in paramyxovirus fusion. Future virology 4, 335-351.

Jacks, T., Power, M.D., Masiarz, F.R., Luciw, P.A., Barr, P.J., and Varmus, H.E. (1988). Characterization of ribosomal frameshifting in HIV-1 gag-pol expression. Nature 331, 280-283.

Janeway, C.A., Murphy, K., Travers, P., and Walport, M. (2008). Janeway's immunobiology (New York, London: Garland Science Taylor and Francis Group).

Janssen, E.M., Lemmens, E.E., Wolfe, T., Christen, U., von Herrath, Matthias G, and Schoenberger, S.P. (2003). CD4+ T cells are required for secondary expansion and memory in CD8+ T lymphocytes. Nature 421, 852-856.

Jetten, N., Verbruggen, S., Gijbels, M.J., Post, M.J., De Winther, Menno P J, and Donners, Marjo M P C (2014). Anti-inflammatory M2, but not pro-inflammatory M1 macrophages promote angiogenesis in vivo. Angiogenesis 17, 109-118.

Johnson, C., Hohenboken, M., Poling, T., Jaehnig, P., and Kanesa-Thasan, N. (2014). Safety and Immunogenicity of Cell Culture-Derived A/H3N2 Variant Influenza Vaccines: A Phase I Randomized, Observer-Blind, Dose-Ranging Study. The Journal of infectious diseases.

Kaczmarczyk, S.J., Sitaraman, K., Young, H.A., Hughes, S.H., and Chatterjee, D.K. (2011). Protein delivery using engineered virus-like particles. Proceedings of the National Academy of Sciences of the United States of America 108, 16998-17003.

Kafri, T., Blömer, U., Peterson, D.A., Gage, F.H., and Verma, I.M. (1997). Sustained expression of genes delivered directly into liver and muscle by lentiviral vectors. Nature genetics 17, 314-317.

Kahl, C.A., Marsh, J., Fyffe, J., Sanders, D.A., and Cornetta, K. (2004). Human Immunodeficiency Virus Type 1-Derived Lentivirus Vectors Pseudotyped with Envelope Glycoproteins Derived from Ross River Virus and Semliki Forest Virus. Journal of Virology 78, 1421-1430.

Kamphorst, A.O., and Ahmed, R. (2013). CD4 T-cell immunotherapy for chronic viral infections and cancer. Immunotherapy 5, 975-987.

Kärber, G. (1931). Beitrag zur kollektiven Behandlung pharmakologischer Reihenversuche. Arch. Exp. Pathol. Pharmakol., 480-483.

Kastenmüller, W., Kastenmüller, K., Kurts, C., and Seder, R.A. (2014). Dendritic cell-targeted vaccines - hope or hype? Nat. Rev. Immunol. 14, 705-711.

Kim, K.S., Park, S.A., Ko, K.-N., Yi, S., and Cho, Y.J. (2014). Current status of human papillomavirus vaccines. Clinical and experimental vaccine research 3, 168-175.

Kimpel, J., Braun, S.E., Qiu, G., Wong, F.E., Conolle, M., Schmitz, J.E., Brendel, C., Humeau, L.M., Dropulic, B., and Rossi, J.J., et al. (2010). Survival of the fittest: positive selection of CD4+ T cells expressing a membrane-bound fusion inhibitor following HIV-1 infection. PLoS ONE 5, e12357.

Klatzmann, D., Champagne, E., Chamaret, S., Gruest, J., Guetard, D., Hercend, T., Gluckman, J.C., and Montagnier, L. (1984). T-lymphocyte T4 molecule behaves as the receptor for human retrovirus LAV. Nature 312, 767-768.

Kneissl, S., Abel, T., Rasbach, A., Brynza, J., Schneider-Schaulies, J., and Buchholz, C.J. (2012). Measles virus glycoprotein-based lentiviral targeting vectors that avoid neutralizing antibodies. PLoS ONE 7, e46667.

Kneissl, S., Zhou, Q., Schwenkert, M., Cosset, F.-L., Verhoeyen, E., and Buchholz, C.J. (2013). CD19 and CD20 targeted vectors induce minimal activation of resting B lymphocytes. PLoS ONE 8, e79047.

Kobinger, G.P., Weiner, D.J., Yu, Q.C., and Wilson, J.M. (2001). Filovirus-pseudotyped lentiviral vector can efficiently and stably transduce airway epithelia in vivo. Nature biotechnology 19, 225-230.

Kobune, F., Sakata, H., and Sugiura, A. (1990). Marmoset lymphoblastoid cells as a sensitive host for isolation of measles virus. J. Virol. 64, 700-705.

Korin, Y.D., and Zack, J.A. (1998). Progression to the G1b phase of the cell cycle is required for completion of human immunodeficiency virus type 1 reverse transcription in T cells. J. Virol. 72, 3161-3168.

Kornfeld, H., Cruikshank, W.W., Pyle, S.W., Berman, J.S., and Center, D.M. (1988). Lymphocyte activation by HIV-1 envelope glycoprotein. Nature 335, 445-448.

Kreutz, M., Tacken, P.J., and Figdor, C.G. (2013). Targeting dendritic cells--why bother? Blood 121, 2836-2844.

Kruse, M., Meinl, E., Henning, G., Kuhnt, C., Berchtold, S., Berger, T., Schuler, G., and Steinkasserer, A. (2001). Signaling Lymphocytic Activation Molecule Is Expressed on Mature CD83+ Dendritic Cells and Is Up-Regulated by IL-1. The Journal of Immunology 167, 1989-1995.

Kuball, J., Schmitz, F.W., Voss, R.-H., Ferreira, E.A., Engel, R., Guillaume, P., Strand, S., Romero, P., Huber, C., and Sherman, L.A., et al. (2005). Cooperation of human tumor-reactive CD4+ and CD8+ T cells after redirection of their specificity by a high-affinity p53A2.1-specific TCR. Immunity 22, 117-129.

Kugelmann, S. (2013). Nachweis von intrazytoplamatischem Proteintransfer mittels lentiviraler Vektoren. Bachelor thesis (Frankfurt am Main).

Kumar, M., Keller, B., Makalou, N., and Sutton, R.E. (2001). Systematic determination of the packaging limit of lentiviral vectors. Human gene therapy 12, 1893-1905.

Laemmli, U.K. (1970). Cleavage of structural proteins during the assembly of the head of bacteriophage T4. Nature 227, 680-685.

Laguette, N., Sobhian, B., Casartelli, N., Ringeard, M., Chable-Bessia, C., Ségéral, E., Yatim, A., Emiliani, S., Schwartz, O., and Benkirane, M. (2011). SAMHD1 is the dendritic- and myeloid-cell-specific HIV-1 restriction factor counteracted by Vpx. Nature 474, 654-657.

Lampe, M., Briggs, John A. G., Endress, T., Glass, B., Riegelsberger, S., Kräusslich, H.-G., Lamb, D.C., Bräuchle, C., and Müller, B. (2007). Double-labelled HIV-1 particles for study of virus-cell interaction. Virology 360, 92-104.

Larson, D.R., Johnson, M.C., Webb, W.W., and Vogt, V.M. (2005). Visualization of retrovirus budding with correlated light and electron microscopy. Proceedings of the National Academy of Sciences of the United States of America 102, 15453-15458.

Lee, B., Sharron, M., Montaner, L.J., Weissman, D., and Doms, R.W. (1999). Quantification of CD4, CCR5, and CXCR4 levels on lymphocyte subsets, dendritic cells, and differentially conditioned monocyte-derived macrophages. Proc. Natl. Acad. Sci. U.S.A. 96, 5215-5220.

Leonard, V.H.J., Sinn, P.L., Hodge, G., Miest, T., Devaux, P., Oezguen, N., Braun, W., McCray, P.B., McChesney, M.B., and Cattaneo, R. (2008). Measles virus blind to its epithelial cell receptor remains virulent in rhesus monkeys but cannot cross the airway epithelium and is not shed. J. Clin. Invest. 118, 2448-2458.

Lever, A., Gottlinger, H., Haseltine, W., and Sodroski, J. (1989). Identification of a sequence required for efficient packaging of human immunodeficiency virus type 1 RNA into virions. Journal of Virology 63, 4085-4087.

Levine, B.L., Humeau, L.M., Boyer, J., MacGregor, R.-R., Rebello, T., Lu, X., Binder, G.K., Slepushkin, V., Lemiale, F., and Mascola, J.R., et al. (2006). Gene transfer in humans using a conditionally replicating lentiviral vector. Proceedings of the National Academy of Sciences of the United States of America 103, 17372-17377.

Lévy, C., Amirache, F., Costa, C., Frecha, C., Muller, C.P., Kweder, H., Buckland, R., Cosset, F.-L., and Verhoeyen, E. (2012). Lentiviral vectors displaying modified measles virus gp overcome pre-existing immunity in in vivo-like transduction of human T and B cells. Mol. Ther. 20, 1699-1712.

Lewis, P., Hensel, M., and Emerman, M. (1992). Human immunodeficiency virus infection of cells arrested in the cell cycle. EMBO J. 11, 3053-3058.

Li, L., Li, H.S., Pauza, C.D., Bukrinsky, M., and Zhao, R.Y. (2005). Roles of HIV-1 auxiliary proteins in viral pathogenesis and host-pathogen interactions. Cell research 15, 923-934.

Liang, M., Morizono, K., Pariente, N., Kamata, M., Lee, B., and Chen, Irvin S Y (2009). Targeted transduction via CD4 by a lentiviral vector uses a clathrin-mediated entry pathway. J. Virol. 83, 13026-13031.

Lingappa, J.R., Reed, J.C., Tanaka, M., Chutiraka, K., and Robinson, B.A. (2014). How HIV-1 Gag assembles in cells: Putting together pieces of the puzzle. Virus research 193, 89-107.

Lopez, M., Aoubala, M., Jordier, F., Isnardon, D., Gomez, S., and Dubreuil, P. (1998). The human poliovirus receptor related 2 protein is a new hematopoietic/endothelial homophilic adhesion molecule. Blood 92, 4602-4611.

Louis, J.M., Weber, I.T., Tözsér, J., Clore, G.M., and Gronenborn, A.M. (2000). HIV-1 protease: maturation, enzyme specificity, and drug resistance. Advances in pharmacology (San Diego, Calif.) 49, 111-146.

Luckheeram, R.V., Zhou, R., Verma, A.D., and Xia, B. (2012). $CD4^+$T cells: differentiation and functions. Clinical & developmental immunology 2012, 925135.

Maetzig, T., Baum, C., and Schambach, A. (2012). Retroviral protein transfer: falling apart to make an impact. Current gene therapy 12, 389-409.

Mahnke, K., Schmitt, E., Bonifaz, L., Enk, A.H., and Jonuleit, H. (2002). Immature, but not inactive: the tolerogenic function of immature dendritic cells. Immunology and cell biology 80, 477-483.

Mak, T.W., and Saunders, M.E. (2006). The immune response. Basic and clinical principles (Amsterdam, Boston: Elsevier/Academic).

Mammano, F., Salvatori, F., Indraccolo, S., Rossi, A. de, Chieco-Bianchi, L., and Göttlinger, H.G. (1997). Truncation of the human immunodeficiency virus type 1 envelope glycoprotein allows efficient pseudotyping of Moloney murine leukemia virus particles and gene transfer into CD4+ cells. Journal of Virology 71, 3341-3345.

Marktel, S., Magnani, Z., Ciceri, F., Cazzaniga, S., Riddell, S.R., Traversari, C., Bordignon, C., and Bonini, C. (2003). Immunologic potential of donor lymphocytes expressing a suicide gene for early immune reconstitution after hematopoietic T-cell-depleted stem cell transplantation. Blood 101, 1290-1298.

Marodon, G., Mouly, E., Blair, E.J., Frisen, C., Lemoine, F.M., and Klatzmann, D. (2003). Specific transgene expression in human and mouse CD4+ cells using lentiviral vectors with regulatory sequences from the CD4 gene. Blood 101, 3416-3423.

Martin-Serrano, J., and Neil, S.J.D. (2011). Host factors involved in retroviral budding and release. Nature reviews. Microbiology 9, 519-531.

Matlin, K.S., Reggio, H., Helenius, A., and Simons, K. (1982). Pathway of vesicular stomatitis virus entry leading to infection. Journal of molecular biology 156, 609-631.

Maurice, M., Verhoeyen, E., Salmon, P., Trono, D., Russell, S.J., and Cosset, F.-L. (2002). Efficient gene transfer into human primary blood lymphocytes by surface-engineered lentiviral vectors that display a T cell-activating polypeptide. Blood 99, 2342-2350.

McBurney, S.P., Young, K.R., and Ross, T.M. (2007). Membrane embedded HIV-1 envelope on the surface of a virus-like particle elicits broader immune responses than soluble envelopes. Virology 358, 334-346.

Medzhitov, R., and Janeway, C. (2000). Innate immunity. The New England journal of medicine 343, 338-344.

Mendelsohn, C.L., Wimmer, E., and Racaniello, V.R. (1989). Cellular receptor for poliovirus: molecular cloning, nucleotide sequence, and expression of a new member of the immunoglobulin superfamily. Cell 56, 855-865.

Mitchell, R.S., Beitzel, B.F., Schroder, Astrid R W, Shinn, P., Chen, H., Berry, C.C., Ecker, J.R., and Bushman, F.D. (2004). Retroviral DNA integration: ASLV, HIV, and MLV show distinct target site preferences. PLoS biology 2, E234.

Mitta, B., Rimann, M., Ehrengruber, M.U., Ehrbar, M., Djonov, V., Kelm, J., and Fussenegger, M. (2002). Advanced modular self-inactivating lentiviral expression vectors for multigene interventions in mammalian cells and in vivo transduction. Nucleic acids research 30, e113.

Miyoshi, H., Blömer, U., Takahashi, M., Gage, F.H., and Verma, I.M. (1998). Development of a self-inactivating lentivirus vector. Journal of Virology 72, 8150-8157.

Moll, M., Klenk, H.-D., and Maisner, A. (2002). Importance of the Cytoplasmic Tails of the Measles Virus Glycoproteins for Fusogenic Activity and the Generation of Recombinant Measles Viruses. Journal of Virology 76, 7174-7186.

Montini, E., Cesana, D., Schmidt, M., Sanvito, F., Ponzoni, M., Bartholomae, C., Sergi Sergi, L., Benedicenti, F., Ambrosi, A., and Di Serio, C., et al. (2006). Hematopoietic stem cell gene transfer in a tumor-prone mouse model uncovers low genotoxicity of lentiviral vector integration. Nature biotechnology 24, 687-696.

Morizono, K., Bristol, G., Xie, Y.M., Kung, S.K., and Chen, I.S. (2001). Antibody-directed targeting of retroviral vectors via cell surface antigens. Journal of Virology 75, 8016-8020.

Mosavi, L.K., Cammett, T.J., Desrosiers, D.C., and Peng, Z.-Y. (2004). The ankyrin repeat as molecular architecture for protein recognition. Protein science : a publication of the Protein Society 13, 1435-1448.

Mosser, D.M., and Edwards, J.P. (2008). Exploring the full spectrum of macrophage activation. Nat. Rev. Immunol. 8, 958-969.

Mrkic, B., Pavlovic, J., Rülicke, T., Volpe, P., Buchholz, C.J., Hourcade, D., Atkinson, J.P., Aguzzi, A., and Cattaneo, R. (1998). Measles virus spread and pathogenesis in genetically modified mice. Journal of Virology 72, 7420-7427.

Mühlebach, M.D., Mateo, M., Sinn, P.L., Prüfer, S., Uhlig, K.M., Leonard, V.H.J., Navaratnarajah, C.K., Frenzke, M., Wong, X.X., and Sawatsky, B., et al. (2011). Adherens junction protein nectin-4 is the epithelial receptor for measles virus. Nature 480, 530-533.

Müller, B., Daecke, J., Fackler, O.T., Dittmar, M.T., Zentgraf, H., and Kräusslich, H.-G. (2004). Construction and characterization of a fluorescently labeled infectious human immunodeficiency virus type 1 derivative. Journal of Virology 78, 10803-10813.

Münch, R.C., Mühlebach, M.D., Schaser, T., Kneissl, S., Jost, C., Plückthun, A., Cichutek, K., and Buchholz, C.J. (2011). DARPins: an efficient targeting domain for lentiviral vectors. Molecular therapy : the journal of the American Society of Gene Therapy 19, 686-693.

Muranski, P., and Restifo, N.P. (2009). Adoptive immunotherapy of cancer using CD4(+) T cells. Current opinion in immunology 21, 200-208.

Murray, W.S., and Little, C.C. (1935). The Genetics of Mammary Tumor Incidence in Mice. Genetics 20, 466-496.

Myers, R.M., Greiner, S.M., Harvey, M.E., Griesmann, G., Kuffel, M.J., Buhrow, S.A., Reid, J.M., Federspiel, M., Ames, M.M., and Dingli, D., et al. (2007). Preclinical pharmacology and toxicology of intravenous MV-NIS, an oncolytic measles virus administered with or without cyclophosphamide. Clinical pharmacology and therapeutics 82, 700-710.

Nakamura, T., Peng, K.-W., Harvey, M., Greiner, S., Lorimer, Ian A J, James, C.D., and Russell, S.J. (2005). Rescue and propagation of fully retargeted oncolytic measles viruses. Nature biotechnology 23, 209-214.

Nakamura, T., Peng, K.-W., Vongpunsawad, S., Harvey, M., Mizuguchi, H., Hayakawa, T., Cattaneo, R., and Russell, S.J. (2004). Antibody-targeted cell fusion. Nature biotechnology 22, 331-336.

Naldini, L. (2011). Ex vivo gene transfer and correction for cell-based therapies. Nature reviews. Genetics 12, 301-315.

Naldini, L., Blömer, U., Gallay, P., Ory, D., Mulligan, R., Gage, F.H., Verma, I.M., and Trono, D. (1996). In vivo gene delivery and stable transduction of nondividing cells by a lentiviral vector. Science (New York, N.Y.) 272, 263-267.

Naniche, D., Varior-Krishnan, G., Cervoni, F., Wild, T.F., Rossi, B., Rabourdin-Combe, C., and Gerlier, D. (1993). Human membrane cofactor protein (CD46) acts as a cellular receptor for measles virus. J. Virol. 67, 6025-6032.

Navaratnarajah, C.K., Oezguen, N., Rupp, L., Kay, L., Leonard, V.H.J., Braun, W., and Cattaneo, R. (2011). The heads of the measles virus attachment protein move to transmit the fusion-triggering signal. Nature structural & molecular biology 18, 128-134.

Neil, S., Martin, F., Ikeda, Y., and Collins, M. (2001). Postentry restriction to human immunodeficiency virus-based vector transduction in human monocytes. Journal of Virology 75, 5448-5456.

Ngoi, S.M., Chien, A.C., and Lee, C G L (2004). Exploiting internal ribosome entry sites in gene therapy vector design. Current gene therapy 4, 15-31.

Nijkamp, F.P., and Parnham, M.J. (2011). Principles of immunopharmacology (Basel, Boston: Birkhäuser Verlag).

Noguchi, M., Yi, H., Rosenblatt, H.M., Filipovich, A.H., Adelstein, S., Modi, W.S., McBride, O.W., and Leonard, W.J. (1993). Interleukin-2 receptor gamma chain mutation results in X-linked severe combined immunodeficiency in humans. Cell 73, 147-157.

Noyce, R.S., Bondre, D.G., Ha, M.N., Lin, L.-T., Sisson, G., Tsao, M.-S., and Richardson, C.D. (2011). Tumor cell marker PVRL4 (nectin 4) is an epithelial cell receptor for measles virus. PLoS Pathog. 7, e1002240.

O'Hagan, D.T., Singh, M., Dong, C., Ugozzoli, M., Berger, K., Glazer, E., Selby, M., Wininger, M., Ng, P., and Crawford, K., et al. (2004). Cationic microparticles are a potent delivery system for a HCV DNA vaccine. Vaccine 23, 672-680.

Ohno, S., Ono, N., Seki, F., Takeda, M., Kura, S., Tsuzuki, T., and Yanagi, Y. (2007). Measles virus infection of SLAM (CD150) knockin mice reproduces tropism and immunosuppression in human infection. J. Virol. 81, 1650-1659.

Ono, N., Tatsuo, H., Hidaka, Y., Aoki, T., Minagawa, H., and Yanagi, Y. (2001a). Measles Viruses on Throat Swabs from Measles Patients Use Signaling Lymphocytic Activation Molecule (CDw150) but Not CD46 as a Cellular Receptor. Journal of Virology 75, 4399-4401.

Ono, N., Tatsuo, H., Tanaka, K., Minagawa, H., and Yanagi, Y. (2001b). V domain of human SLAM (CDw150) is essential for its function as a measles virus receptor. Journal of Virology 75, 1594-1600.

Ou, W., Marino, M.P., Suzuki, A., Joshi, B., Husain, S.R., Maisner, A., Galanis, E., Puri, R.K., and Reiser, J. (2012). Specific targeting of human interleukin (IL)-13 receptor α2-positive cells with lentiviral vectors displaying IL-13. Human gene therapy methods 23, 137-147.

Paal, T., Brindley, M.A., St Clair, C., Prussia, A., Gaus, D., Krumm, S.A., Snyder, J.P., and Plemper, R.K. (2009). Probing the spatial organization of measles virus fusion complexes. Journal of Virology 83, 10480-10493.

Page, K.A., Landau, N.R., and Littman, D.R. (1990). Construction and use of a human immunodeficiency virus vector for analysis of virus infectivity. Journal of Virology 64, 5270-5276.

Palmowski, M.J., Lopes, L., Ikeda, Y., Salio, M., Cerundolo, V., and Collins, M.K. (2004). Intravenous injection of a lentiviral vector encoding NY-ESO-1 induces an effective CTL response. J. Immunol. 172, 1582-1587.

Pariente, N., Morizono, K., Virk, M.S., Petrigliano, F.A., Reiter, R.E., Lieberman, J.R., and Chen, Irvin S Y (2007). A novel dual-targeted lentiviral vector leads to specific transduction of prostate cancer bone metastases in vivo after systemic administration. Molecular therapy : the journal of the American Society of Gene Therapy 15, 1973-1981.

Pashine, A., Valiante, N.M., and Ulmer, J.B. (2005). Targeting the innate immune response with improved vaccine adjuvants. Nature medicine 11, S63-8.

Patel, J.M., Vartabedian, V.F., Kim, M.-C., He, S., Kang, S.-M., and Selvaraj, P. (2015). Influenza virus-like particles engineered by protein transfer with tumor-associated antigens induces protective antitumor immunity. Biotechnology and bioengineering.

Pelchen-Matthews, A., Armes, J.E., and Marsh, M. (1989). Internalization and recycling of CD4 transfected into HeLa and NIH3T3 cells. The EMBO journal 8, 3641-3649.

Peng, C., Ho, B.K., Chang, T.W., and Chang, N.T. (1989). Role of human immunodeficiency virus type 1-specific protease in core protein maturation and viral infectivity. J. Virol. 63, 2550-2556.

Peng, G., Greenwell-Wild, T., Nares, S., Jin, W., Lei, K.J., Rangel, Z.G., Munson, P.J., and Wahl, S.M. (2007). Myeloid differentiation and susceptibility to HIV-1 are linked to APOBEC3 expression. Blood 110, 393-400.

Perrin-Tricaud, C., Davoust, J., and Jones, I.M. (1999). Tagging the human immunodeficiency virus gag protein with green fluorescent protein. Minimal evidence for colocalisation with actin. Virology 255, 20-25.

Petrovsky, N., and Aguilar, J.C. (2004). Vaccine adjuvants: current state and future trends. Immunology and cell biology 82, 488-496.

Pion, M., Granelli-Piperno, A., Mangeat, B., Stalder, R., Correa, R., Steinman, R.M., and Piguet, V. (2006). APOBEC3G/3F mediates intrinsic resistance of monocyte-derived dendritic cells to HIV-1 infection. The Journal of experimental medicine 203, 2887-2893.

Platt, C.D., Ma, J.K., Chalouni, C., Ebersold, M., Bou-Reslan, H., Carano, Richard A D, Mellman, I., and Delamarre, L. (2010). Mature dendritic cells use endocytic receptors to capture and present antigens. Proceedings of the National Academy of Sciences of the United States of America 107, 4287-4292.

Plemper, R.K. (2011). Cell entry of enveloped viruses. Current opinion in virology 1, 92-100.

Plemper, R.K., Brindley, M.A., and Iorio, R.M. (2011). Structural and mechanistic studies of measles virus illuminate paramyxovirus entry. PLoS pathogens 7, e1002058.

Plemper, R.K., Hammond, A.L., and Cattaneo, R. (2001). Measles virus envelope glycoproteins hetero-oligomerize in the endoplasmic reticulum. The Journal of biological chemistry 276, 44239-44246.

Plotkin, S.A., Orenstein, W.A., and Offit, P.A. (2012). Vaccines.

Plückthun, A. (2015). Designed Ankyrin Repeat Proteins (DARPins): Binding Proteins for Research, Diagnostics, and Therapy. Annual review of pharmacology and toxicology 55, 489-511.

Pornillos, O., Higginson, D.S., Stray, K.M., Fisher, R.D., Garrus, J.E., Payne, M., He, G.-P., Wang, H.E., Morham, S.G., and Sundquist, W.I. (2003). HIV Gag mimics the Tsg101-recruiting activity of the human Hrs protein. The Journal of cell biology 162, 425-434.

Poznansky, M., Lever, A., Bergeron, L., Haseltine, W., and Sodroski, J. (1991). Gene transfer into human lymphocytes by a defective human immunodeficiency virus type 1 vector. Journal of Virology 65, 532-536.

Pulendran, B., and Ahmed, R. (2011). Immunological mechanisms of vaccination. Nature immunology 12, 509-517.

Radbruch, A., Muehlinghaus, G., Luger, E.O., Inamine, A., Smith, Kenneth G C, Dörner, T., and Hiepe, F. (2006). Competence and competition: the challenge of becoming a long-lived plasma cell. Nature reviews. Immunology 6, 741-750.

Reusch, J. (2013). Erzeugung und Charakterisierung lentiviraler Vektorpartikel. Bachelor thesis (Gießen).

Reymond, N., Imbert, A.-M., Devilard, E., Fabre, S., Chabannon, C., Xerri, L., Farnarier, C., Cantoni, C., Bottino, C., and Moretta, A., et al. (2004). DNAM-1 and PVR regulate monocyte migration through endothelial junctions. The Journal of experimental medicine 199, 1331-1341.

Richardson, C.D., Scheid, A., and Choppin, P.W. (1980). Specific inhibition of paramyxovirus and myxovirus replication by oligopeptides with amino acid sequences similar to those at the N-termini of the F1 or HA2 viral polypeptides. Virology 105, 205-222.

Ridge, J.P., Di Rosa, F., and Matzinger, P. (1998). A conditioned dendritic cell can be a temporal bridge between a CD4+ T-helper and a T-killer cell. Nature 393, 474-478.

Rizzo, M.A., Springer, G.H., Granada, B., and Piston, D.W. (2004). An improved cyan fluorescent protein variant useful for FRET. Nat. Biotechnol. 22, 445-449.

Rock, K.L., York, I.A., Saric, T., and Goldberg, A.L. (2002). Protein degradation and the generation of MHC class I-presented peptides. Advances in immunology 80, 1-70.

Sakaguchi, M., Yoshikawa, Y., Yamanouchi, K., Sata, T., Nagashima, K., and Takeda, K. (1986). Growth of measles virus in epithelial and lymphoid tissues of cynomolgus monkeys. Microbiology and immunology 30, 1067-1073.

Sakuma, T., Barry, M.A., and Ikeda, Y. (2012). Lentiviral vectors: basic to translational. Biochem. J. 443, 603-618.

Sallusto, F., Lenig, D., Förster, R., Lipp, M., and Lanzavecchia, A. (1999). Two subsets of memory T lymphocytes with distinct homing potentials and effector functions. Nature 401, 708-712.

Sanber, K.S., Knight, S.B., Stephen, S.L., Bailey, R., Escors, D., Minshull, J., Santilli, G., Thrasher, A.J., Collins, M.K., and Takeuchi, Y. (2015). Construction of stable packaging cell lines for clinical lentiviral vector production. Scientific reports 5, 9021.

Sandrin, V., Russell, S.J., and Cosset, F.L. (2003). Targeting retroviral and lentiviral vectors. Current topics in microbiology and immunology 281, 137-178.

Santiago, C., Celma, M.L., Stehle, T., and Casasnovas, J.M. (2010). Structure of the measles virus hemagglutinin bound to the CD46 receptor. Nature structural & molecular biology 17, 124-129.

Sato, H., Yoneda, M., Honda, T., and Kai, C. (2012). Morbillivirus receptors and tropism: multiple pathways for infection. Front Microbiol 3, 75.

Sauce, D., Bodinier, M., Garin, M., Petracca, B., Tonnelier, N., Duperrier, A., Melo, J.V., Apperley, J.F., Ferrand, C., and Hervé, P., et al. (2002a). Retrovirus-mediated gene transfer in primary T lymphocytes impairs their anti-Epstein-Barr virus potential through both culture-dependent and selection process-dependent mechanisms. Blood 99, 1165-1173.

Sauce, D., Tonnelier, N., Duperrier, A., Petracca, B., de Carvalho Bittencourt, Marcelo, Saadi, M., Saas, P., Ferrand, C., Herve, P., and Tiberghien, P., et al. (2002b). Influence of ex vivo expansion and retrovirus-mediated gene transfer on primary T lymphocyte phenotype and functions. Journal of hematotherapy & stem cell research 11, 929-940.

Schnierle, B.S., Stitz, J., Bosch, V., Nocken, F., Merget-Millitzer, H., Engelstädter, M., Kurth, R., Groner, B., and Cichutek, K. (1997). Pseudotyping of murine leukemia virus with the envelope glycoproteins of HIV generates a retroviral vector with specificity of infection for CD4-expressing cells. Proceedings of the National Academy of Sciences of the United States of America 94, 8640-8645.

Schoenberger, S.P., Toes, R.E., van der Voort, E I, Offringa, R., and Melief, C.J. (1998). T-cell help for cytotoxic T lymphocytes is mediated by CD40-CD40L interactions. Nature 393, 480-483.

Schoenborn, J.R., and Wilson, C.B. (2007). Regulation of interferon-gamma during innate and adaptive immune responses. In (Elsevier), pp. 41–101.

Schroeder, M.A., and DiPersio, J.F. (2011). Mouse models of graft-versus-host disease: advances and limitations. Dis Model Mech 4, 318-333.

Schüle, S., Steidl, S., Panitz, S., Coulibaly, C., Kalinke, U., Cichutek, K., and Schweizer, M. (2006). Selective gene transfer to T lymphocytes using coreceptor-specific [MLV(HIV)] pseudotype vectors in a transgenic mouse model. Virology 351, 237-247.

Schülke, S., Waibler, Z., Mende, M.-S., Zoccatelli, G., Vieths, S., Toda, M., and Scheurer, S. (2010). Fusion protein of TLR5-ligand and allergen potentiates activation and IL-10 secretion in murine myeloid DC. Mol. Immunol. 48, 341-350.

Schwartz, R.H. (2003). T cell anergy. Annual review of immunology 21, 305-334.

Schweizer, A., Rusert, P., Berlinger, L., Ruprecht, C.R., Mann, A., Corthésy, S., Turville, S.G., Aravantinou, M., Fischer, M., and Robbiani, M., et al. (2008). CD4-specific designed ankyrin repeat proteins are novel potent HIV entry inhibitors with unique characteristics. PLoS Pathog. 4, e1000109.

Sedgwick, S.G., and Smerdon, S.J. (1999). The ankyrin repeat: a diversity of interactions on a common structural framework. Trends in biochemical sciences 24, 311-316.

Segura, M.M., Garnier, A., Durocher, Y., Coelho, H., and Kamen, A. (2007). Production of lentiviral vectors by large-scale transient transfection of suspension cultures and affinity chromatography purification. Biotechnology and bioengineering 98, 789-799.

Shedlock, D.J., and Shen, H. (2003). Requirement for CD4 T cell help in generating functional CD8 T cell memory. Science (New York, N.Y.) 300, 337-339.

Sherer, N.M., Lehmann, M.J., Jimenez-Soto, L.F., Ingmundson, A., Horner, S.M., Cicchetti, G., Allen, P.G., Pypaert, M., Cunningham, J.M., and Mothes, W. (2003). Visualization of retroviral replication in living cells reveals budding into multivesicular bodies. Traffic (Copenhagen, Denmark) 4, 785-801.

Shieh, J.T., Albright, A.V., Sharron, M., Gartner, S., Strizki, J., Doms, R.W., and González-Scarano, F. (1998). Chemokine receptor utilization by human immunodeficiency virus type 1 isolates that replicate in microglia. Journal of Virology 72, 4243-4249.

Shimada, T., Fujii, H., Mitsuya, H., and Nienhuis, A.W. (1991). Targeted and highly efficient gene transfer into CD4+ cells by a recombinant human immunodeficiency virus retroviral vector. The Journal of clinical investigation 88, 1043-1047.

Shultz, L.D., Brehm, M.A., Garcia-Martinez, J.V., and Greiner, D.L. (2012). Humanized mice for immune system investigation: progress, promise and challenges. Nat. Rev. Immunol. 12, 786-798.

Shultz, L.D., Lyons, B.L., Burzenski, L.M., Gott, B., Chen, X., Chaleff, S., Kotb, M., Gillies, S.D., King, M., and Mangada, J., et al. (2005). Human lymphoid and myeloid cell development in NOD/LtSz-scid IL2R gamma null mice engrafted with mobilized human hemopoietic stem cells. J. Immunol. 174, 6477-6489.

Shurin, M.R., and Salter, R.D. (2009). Dendritic cells in cancer (New York, London: Springer).

Sidorenko, S.P., and Clark, E.A. (1993). Characterization of a cell surface glycoprotein IPO-3, expressed on activated human B and T lymphocytes. Journal of immunology (Baltimore, Md. : 1950) 151, 4614-4624.

Silver, D.P., and Livingston, D.M. (2001). Self-excising retroviral vectors encoding the Cre recombinase overcome Cre-mediated cellular toxicity. Mol. Cell 8, 233-243.

Sinn, P.L., Sauter, S.L., and McCray, P.B. (2005). Gene therapy progress and prospects: development of improved lentiviral and retroviral vectors--design, biosafety, and production. Gene therapy 12, 1089-1098.

Smith, G.P., and Petrenko, V.A. (1997). Phage Display. Chemical reviews 97, 391-410.

Spearman, C. (1908). The method of 'right and wrong cases' (constant stimuli) without Gauss`s formulae. Br. J. Psychol., 227-242.

Steidl, S. (2004). Genetic engineering of onco/lentivirus hybrids results in formation of infectious but not of replication-competent viruses. Journal of General Virology 85, 665-678.

Steiner, D., Forrer, P., and Plückthun, A. (2008). Efficient selection of DARPins with sub-nanomolar affinities using SRP phage display. Journal of molecular biology 382, 1211-1227.

Steinman, R.M., and Mellman, I. (2004). Immunotherapy: bewitched, bothered, and bewildered no more. Science (New York, N.Y.) 305, 197-200.

Sternberg, N., and Hamilton, D. (1981). Bacteriophage P1 site-specific recombination. I. Recombination between loxP sites. J. Mol. Biol. 150, 467-486.

Stitz, J., Steidl, S., Merget-Millitzer, H., König, R., Müller, P., Nocken, F., Engelstädter, M., Bobkova, M., Schmitt, I., and Kurth, R., et al. (2000). MLV-derived retroviral vectors selective for CD4-expressing cells and resistant to neutralization by sera from HIV-infected patients. Virology 267, 229-236.

Stremlau, M., Perron, M., Lee, M., Li, Y., Song, B., Javanbakht, H., Diaz-Griffero, F., Anderson, D.J., Sundquist, W.I., and Sodroski, J. (2006). Specific recognition and accelerated uncoating of retroviral capsids by the TRIM5alpha restriction factor. Proceedings of the National Academy of Sciences of the United States of America 103, 5514-5519.

Stumpp, M.T., Binz, H.K., and Amstutz, P. (2008). DARPins: a new generation of protein therapeutics. Drug discovery today 13, 695-701.

Sun, J.C., and Bevan, M.J. (2003). Defective CD8 T cell memory following acute infection without CD4 T cell help. Science (New York, N.Y.) 300, 339-342.

Takaki, H., Oshiumi, H., Matsumoto, M., and Seya, T. (2014). Dendritic cell subsets involved in type I IFN induction in mouse measles virus infection models. The international journal of biochemistry & cell biology 53, 329-333.

Takeda, M., Tahara, M., Hashiguchi, T., Sato, T.A., Jinnouchi, F., Ueki, S., Ohno, S., and Yanagi, Y. (2007). A human lung carcinoma cell line supports efficient measles virus growth and syncytium formation via a SLAM- and CD46-independent mechanism. Journal of Virology 81, 12091-12096.

Takeda, M., Takeuchi, K., Miyajima, N., Kobune, F., Ami, Y., Nagata, N., Suzaki, Y., Nagai, Y., and Tashiro, M. (2000). Recovery of pathogenic measles virus from cloned cDNA. Journal of Virology 74, 6643-6647.

Takeuchi, K., Miyajima, N., Nagata, N., Takeda, M., and Tashiro, M. (2003). Wild-type measles virus induces large syncytium formation in primary human small airway epithelial cells by a SLAM(CD150)-independent mechanism. Virus Res. 94, 11-16.

Tatsuo, H., Ono, N., Tanaka, K., and Yanagi, Y. (2000). SLAM (CDw150) is a cellular receptor for measles virus. Nature 406, 893-897.

Uhlig, K.M., Schülke, S., Scheuplein, Vivian A M, Malczyk, A.H., Reusch, J., Kugelmann, S., Muth, A., Koch, V., Hutzler, S., and Bodmer, B.S., et al. (2015). Lentiviral protein transfer vectors are an efficient vaccine-platform inducing strong antigen-specific cytotoxic T cell response. Journal of Virology.

van Montfoort, N., Camps, M.G., Khan, S., Filippov, D.V., Weterings, J.J., Griffith, J.M., Geuze, H.J., van Hall, T., Verbeek, J.S., and Melief, C.J., et al. (2009). Antigen storage compartments in mature dendritic cells facilitate prolonged cytotoxic T lymphocyte cross-priming capacity. Proceedings of the National Academy of Sciences of the United States of America 106, 6730-6735.

Verhoeyen, E., and Cosset, F.-L. (2004). Surface-engineering of lentiviral vectors. The journal of gene medicine 6 Suppl 1, S83-94.

Verhoeyen, E., Costa, C., and Cosset, F.-L. (2009). Lentiviral vector gene transfer into human T cells. Methods in molecular biology (Clifton, N.J.) 506, 97-114.

Vignali, D.A.A., Collison, L.W., and Workman, C.J. (2008). How regulatory T cells work. Nature reviews. Immunology 8, 523-532.

Villadangos, J.A., and Ploegh, H.L. (2000). Proteolysis in MHC class II antigen presentation: who's in charge? Immunity 12, 233-239.

Voelkel, C., Galla, M., Dannhauser, P.N., Maetzig, T., Sodeik, B., Schambach, A., and Baum, C. (2012). Pseudotype-independent nonspecific uptake of gammaretroviral and lentiviral particles in human cells. Hum. Gene Ther. 23, 274-286.

Voelkel, C., Galla, M., Maetzig, T., Warlich, E., Kuehle, J., Zychlinski, D., Bode, J., Cantz, T., Schambach, A., and Baum, C. (2010). Protein transduction from retroviral Gag precursors. Proc. Natl. Acad. Sci. U.S.A. 107, 7805-7810.

Vongpunsawad, S., Oezgun, N., Braun, W., and Cattaneo, R. (2004). Selectively receptor-blind measles viruses: Identification of residues necessary for SLAM- or CD46-induced fusion and their localization on a new hemagglutinin structural model. Journal of Virology 78, 302-313.

Wagner, K.W., Punnoose, E.A., Januario, T., Lawrence, D.A., Pitti, R.M., Lancaster, K., Lee, D., Goetz, M. von, Yee, S.F., and Totpal, K., et al. (2007). Death-receptor O-glycosylation controls tumor-cell sensitivity to the proapoptotic ligand Apo2L/TRAIL. Nat. Med. 13, 1070-1077.

Weigand, L.U., Liang, X., Schmied, S., Mall, S., Klar, R., Stötzer, O.J., Salat, C., Götze, K., Mautner, J., and Peschel, C., et al. (2012). Isolation of human MHC class II-restricted T cell receptors from the autologous T-cell repertoire with potent anti-leukaemic reactivity. Immunology 137, 226-238.

Weinberg, J.B., Matthews, T.J., Cullen, B.R., and Malim, M.H. (1991). Productive human immunodeficiency virus type 1 (HIV-1) infection of nonproliferating human monocytes. J. Exp. Med. 174, 1477-1482.

Wetzel, S.K., Settanni, G., Kenig, M., Binz, H.K., and Plückthun, A. (2008). Folding and unfolding mechanism of highly stable full-consensus ankyrin repeat proteins. Journal of molecular biology 376, 241-257.

Witte, L. de, Abt, M., Schneider-Schaulies, S., van Kooyk, Y., and Geijtenbeek, Teunis B H (2006). Measles virus targets DC-SIGN to enhance dendritic cell infection. Journal of Virology 80, 3477-3486.

Woodland, D.L. (2004). Jump-starting the immune system: prime-boosting comes of age. Trends in immunology 25, 98-104.

Wu, D.-T., and Roth, M.J. (2014). MLV based viral-like-particles for delivery of toxic proteins and nuclear transcription factors. Biomaterials 35, 8416-8426.

Wykes, M., and MacPherson, G. (2000). Dendritic cell-B-cell interaction: dendritic cells provide B cells with CD40-independent proliferation signals and CD40-dependent survival signals. Immunology 100, 1-3.

Wykes, M., Pombo, A., Jenkins, C., and MacPherson, G.G. (1998). Dendritic cells interact directly with naive B lymphocytes to transfer antigen and initiate class switching in a primary T-dependent response. Journal of immunology (Baltimore, Md. : 1950) 161, 1313-1319.

Yang, L., Yang, H., Rideout, K., Cho, T., Joo, K.I., Ziegler, L., Elliot, A., Walls, A., Yu, D., and Baltimore, D., et al. (2008). Engineered lentivector targeting of dendritic cells for in vivo immunization. Nat. Biotechnol. 26, 326-334.

Yoder, A., Yu, D., Dong, L., Iyer, S.R., Xu, X., Kelly, J., Liu, J., Wang, W., Vorster, P.J., and Agulto, L., et al. (2008). HIV envelope-CXCR4 signaling activates cofilin to overcome cortical actin restriction in resting CD4 T cells. Cell 134, 782-792.

Yu, X., Yuan, X., Matsuda, Z., Lee, T.H., and Essex, M. (1992). The matrix protein of human immunodeficiency virus type 1 is required for incorporation of viral envelope protein into mature virions. Journal of Virology 66, 4966-4971.

Zack, J.A., Arrigo, S.J., Weitsman, S.R., Go, A.S., Haislip, A., and Chen, I.S. (1990). HIV-1 entry into quiescent primary lymphocytes: molecular analysis reveals a labile, latent viral structure. Cell 61, 213-222.

Zandberg, D.P., Rollins, S., Goloubeva, O., Morales, R.E., Tan, M., Taylor, R., Wolf, J.S., Schumaker, L.M., Cullen, K.J., and Zimrin, A., et al. (2015). A phase I dose escalation trial of MAGE-A3- and HPV16-specific peptide immunomodulatory vaccines in patients with recurrent/metastatic (RM) squamous cell carcinoma of the head and neck (SCCHN). Cancer immunology, immunotherapy : CII 64, 367-379.

Zhang, X., Lu, G., Qi, J., Li, Y., He, Y., Xu, X., Shi, J., Zhang, C.W.-H., Yan, J., and Gao, G.F. (2013). Structure of measles virus hemagglutinin bound to its epithelial receptor nectin-4. Nat. Struct. Mol. Biol. 20, 67-72.

Zhang, X.-Y., Kutner, R.H., Bialkowska, A., Marino, M.P., Klimstra, W.B., and Reiser, J. (2010). Cell-specific targeting of lentiviral vectors mediated by fusion proteins derived from Sindbis virus, vesicular stomatitis virus, or avian sarcoma/leukosis virus. Retrovirology 7, 3.

Zhou, Q., Schneider, I.C., Edes, I., Honegger, A., Bach, P., Schönfeld, K., Schambach, A., Wels, W.S., Kneissl, S., and Uckert, W., et al. (2012). T-cell receptor gene transfer exclusively to human CD8(+) cells enhances tumor cell killing. Blood 120, 4334-4342.

Zhou, Q., Schneider, I.C., Gallet, M., Kneissl, S., and Buchholz, C.J. (2011). Resting lymphocyte transduction with measles virus glycoprotein pseudotyped lentiviral vectors relies on CD46 and SLAM. Virology 413, 149-152.

Zhou, Q., Uhlig, K.M., Muth, A., Kimpel, J., Lévy, C., Münch, R.C., Seifried, J., Pfeiffer, A., Trkola, A., and Coulibaly, C., et al. (2015) Exclusive transduction of human CD4+ T cells upon systemic delivery of CD4-targeted lentiviral vectors. Journal of Immunology, accepted.

Zufferey, R., Dull, T., Mandel, R.J., Bukovsky, A., Quiroz, D., Naldini, L., and Trono, D. (1998). Self-inactivating lentivirus vector for safe and efficient in vivo gene delivery. Journal of Virology 72, 9873-9880.

Zufferey, R., Nagy, D., Mandel, R.J., Naldini, L., and Trono, D. (1997). Multiply attenuated lentiviral vector achieves efficient gene delivery in vivo. Nat. Biotechnol. 15, 871-875.

8. Abbreviations

α	Anti
A	Absorbance
AIDS	Acquired immune deficiency syndrome
Alum	Aluminium potassium sulphate
Amp	Ampicillin
APC	Antigen presenting cell or Allophycocyanin (dye)
APS	Ammonium peroxydisulfate
ATCC	American type culture collection
AR	Ankyrin repeat
BCR	B cell receptor
bp	Base pairs
BSA	Bovine serum albumin
CA	capsid protein
CAR	Chimeric antigen receptor
CD	Cluster of differentiation
CD4-LV	CD4-targeted lentiviral vector
CD8-LV	CD8-targeted lentiviral vector
cDNA	Complementary DNA
CHO	Chinese hamster ovary
CMV	Cytomegalovirus
ConA	Concanavalin A
C-terminus	Carboxy-terminus
CTL	cytotoxic T lymphocyte
d	Day
DAMP	Danger-associated molecular pattern
DARPin	Designed ankyrin repeat protein
DC	Dendritic cell
DC-SIGN	Dendritic cell-specific intercellular adhesion molecule-3-grabbing non-integrin
DMEM	Dulbecco's modified eagle medium
DMSO	Dimethyl sulfoxide
DNA	Desoxyribonucleic acid
dNTP	Deoxynucleoside triphosphate
DTT	Dithiothreitol
ECL	Enhanced chemiluminescence
E. coli	Escherichia coli
EDTA	Ethylene diamine tetraacetic acid
ELISA	Enzyme linked immunosorbent assay
ELISpot	Enzyme linked immuno spot assay
EM	Electron microscope
EMEM	Eagle's minimum essential medium
Env	Envelope glycoprotein
EpR	Epithelial cell receptor
ER	Endoplasmatic reticulum
et al.	Et alii (and others)
F	Measles virus fusion protein
FACS	Fluorescence activated cell sorting
FCS	Fetal calf serum
FDA	Food and drug administration
FIP	Fusion inhibiting peptide
FSC	Forward scatter
G	Gauge (unit for the size of the outer needle diameter)

Gag	Group-specific antigen
GFP	Green fluorescent protein
GM-CSF	Granulocyte macrophage colony-stimulating factor
GP	Glycoprotein
GvHD	Graft versus host disease
h	hour
H	Measles virus hemagglutinin protein
HEPES	4-(2-hydroxyethyl)-1-piperazineethanesulfonic acid
Her2/neu	Human epithelial growth factor receptor 2
HIV	Human immunodeficiency virus
HRP	Horseradish peroxidase
HSC	Hematopoietic stem cell
IFNAR	Interferon-α/β receptor
$IFNAR^{-/-}$	Interferon-α/β receptor knockout mouse ($IFNAR^{-/-}$ N20 C57BL/6)
IFN	Interferon
Ig	Immunoglobulin
i.h.	Intrahepatic
IL	Interleukin
IN	Integrase
INSERM	Institut nationale de la santé et de la recherche médicale
i.p.	Intraperitoneal
IRES	Internal ribosomal entry site
i.s.	Intrasplenic
IU	International unit
i.v.	Intravenous
IVC	Individually ventilated cage
Ig	Immunoglobulin
kDa	Kilodalton
LB	Lysogeny broth (medium)
LDL-R	Low-density lipoprotein receptor
LSM	Laser scanning microscope
LTR	Long terminal repeat
Luc	Luciferase
LV	Lentiviral vector
MA	Matrix protein
MACS	Magnetic cell sorting
M-CSF	Macrophage colony-stimulating factor
mDC	Myeloid dendritic cell
MFI	Mean fluorescence intensity
MHC	Major histocompatibility complex
MLV	Murine leukemia virus
MOI	Multiplicity of infection
mRNA	Messenger ribonucleic acid
MST1R	Macrophage stimulating 1 receptor
mut	Mutated
MV	Measles virus
MV_{NSe}	Measles virus strain derived from vaccine strain Edmonston B
MV_{vac}	Measles virus vaccine strain
MV_{wt}	Measles virus wild-type strain
NC	Nucleocapsid protein
NEA	Non-essential amino acids
NEB	New England Biolabs
NK cells	Natural killer cells
NSG	NOD-scid IL2Rγ-/- mice
o/n	overnight
ORF	Open reading frame

Ova	Ovalbumin
$Ova_{257-264}$	MHC I (kb)-restricted immunodominant peptide epitope of ovalbumin
$Ova_{323-339}$	Immunodominant peptide epitope of ovalbumin binding to I-A(d) MHC II
PAGE	Polyacrylamid gel electrophoresis
PAMP	Pathogen-associated molecular pattern
PBMC	Peripheral blood mononuclear cell
PBS	Phosphate buffered saline
PCR	Polymerase chain reaction
PE	Phycoerythrin
PEI	Polyethyleneimine
Pol	Polymerase
PR	Protease
PRR	Pathogen recognition receptor
Ψ	Psi - packaging signal of retroviral genomic RNA
PVR	Polio virus receptor
PTV	Protein transfer vector
PVDF	Polyvinylidene fluoride
RNA	Ribonucleic acid
rpm	Revolutions per minute
RPMI	Roswell Park Memorial Institute (Medium)
RT	Reverse transcriptase
SAMHD1	SAM domain and HD domain-containing protein 1
scFv	Single chain fragment variable (single chain antibody)
SDS	Sodium dodecyl sulfate
SFFV	Spleen focus forming virus
SIV	Simian immunodeficiency virus
SLAM	Signaling lymphocyte activation molecule
$SLAM^{ki}$	$IFNAR^{-/-}$ $SLAM^{ki}$ C57BL/6 mouse (Interferon-α/β receptor knockout, SLAM knock-in)
S.O.C	Super optimal broth with catabolite repression
SPF	Specified pathogen-free
SSC	Side scatter
TAE	Tris-acetate-EDTA buffer
$TCID_{50}$	Tissue culture infective dose 50
TCM	T cell medium
T_{CM}	central memory T cell
TCR	T cell receptor
T_{EM}	effector memory T cell
TEMED	N,N,N',N'-Tetramethylethylendiamin
Th1	T helper type 1 cell
Th2	T helper type 2 cell
Th17	T helper type 17 cell
Tm	Melting temperature
Treg	regulatory T cell
Tris	tris(hydroxymethyl)aminomethane
t.u.	Transducing unit
U	Unit
UV	Ultraviolet
VLP	Virus-like particle
Vpx	Viral protein X
VSV	Vesicular stomatitis virus
VSV-G	Glycoprotein of vesicular stomatitis virus
w/o	Without
wt	Wild-type

Terminology used for vectors:

Envelope-cargo protein-kind of vector-transgene

Examples:

$VSV\text{-}Ova\text{-}LV_{Katushka}$ = VSV-G pseudotyped lentiviral Ova protein transfer vector encoding Katushka

$CD4\text{-}LV_{Luc,GFP}$ = CD4-targeted lentiviral vector transferring *luciferase* and *gfp*

9. Curriculum Vitae

Persönliche Daten

Name	Katharina Monika Uhlig
Geburtsdatum	25.10.1986
Geburtsort	Karl-Marx-Stadt
Staatsangehörigkeit	deutsch
Familienstand	ledig

Beruflicher Werdegang

ab 06/15	Applikationsspezialistin, ALS Automated Lab Solutions GmbH, Jena

Akademische Bildung

07/15	Abgabe der Dissertation am Fachbereich Biologie, TU Darmstadt
11/14 – 05/15	Arbeitssuchend; Fertigstellung von Dissertation und Publikationen
03/11 – 11/14	Doktorandin am Paul-Ehrlich-Institut, Langen • Anfertigung der Doktorarbeit in AG Prof. Dr. Buchholz und AG Dr. Mühlebach • Thema: Entry targeted lentiviral vectors for the specific modification of distinct subsets of immune cells
10/05 – 12/10	Biologiestudium an der Friedrich-Schiller-Universität Jena • Vertiefung Genetik (Hauptfach), Biochemie und Immun- und Infektionsbiologie (Nebenfächer) • Diplomarbeit am Zentrum für Molekulare Biomedizin der Friedrich-Schiller-Universität Jena, AG Prof. Dr. Heinzel, Thema: Charakterisierung der SUMO-Modifikation der murinen Histondeacetylase 2 • Abschluss: Diplom-Biologin (Note 1,0)

Schulausbildung

09/97 – 07/05	Gymnasium Burgstädt, Abschluss Abitur (Note 1,4)
09/93 – 08/97	Grundschule Köthensdorf

Auszeichnungen & Stipendien

03/14	Best Poster Prize beim 20. Jahrestreffen der Deutschen Gesellschaft für Gentherapie (DG-GT)
10/13	Travel Award der Europäischen Gesellschaft für Gen- und Zelltherapie (ESGCT)

03/13	Travel Award der Deutschen Gesellschaft für Gentherapie (DG-GT)
04/09 – 07/09	Stipendiatin des Leonardo Da Vinci Programms für einen Forschungsaufenthalt am Imperial College London
06/05	Auszeichnung für außergewöhnliche Leistungen im Abitur 2005 (überreicht durch den Förderverein des Gymnasiums Burgstädt)

10. Publications

Parts of this thesis have been published

Uhlig KM, Schülke S, Scheuplein VAM, Malczyk AH, Reusch J, Kugelmann S, Muth A, Koch V, Hutzler S, Bodmer BS, Schambach A, Buchholz CJ, Waibler Z, Scheurer S, Mühlebach MD. Lentiviral protein transfer vectors are an efficient vaccine-platform inducing strong antigen-specific cytotoxic T cell response (2015). Journal of Virology, accepted.

Zhou Q*, **Uhlig KM***, Muth A, Kimpel J, Lévy C, Münch RC, Seifried J, Pfeiffer A, Trkola A, Coulibaly C, von Laer D, Wels WS, Hartwig UF, Verhoeyen E, Buchholz CJ. Exclusive transduction of human $CD4^+$ T cells upon systemic delivery of CD4-targeted lentiviral vectors (2015). Journal of Immunology, accepted.

Mühlebach MD, Mateo M, Sinn PL, Prüfer S, **Uhlig KM**, Leonard VH, Navaratnarajah CK, Frenzke M, Wong XX, Sawatsky B, Ramachandran S, McCray PB Jr, Cichutek K, von Messling V, Lopez M, Cattaneo R (2011). Adherens junction protein nectin-4 is the epithelial receptor for measles virus. *Nature*. 480(7378):530-3

Further publications, not included in this thesis

Seifried J*, Patasic L*, Tondera C, Schmitz H, Prüfer S, Koch V, **Uhlig KM**, Cichutek K, Mühlebach MD. Characterizing viral factors counteracting resistance to measles virus infection. Manuscript in preparation.

Oral presentations at scientific meetings

Uhlig KM, Zhou Q, Trinschek B, Abel T, Münch RC, Rasbach A, Trkola A, Jonuleit H, Buchholz CJ. Entry targeted gene transfer into functional subpopulations of human T cells. European Society of Gene and Cell Therapy Meeting 2013, Madrid, Spain, 10/25/2013 – 10/28/2013

Uhlig KM, Zhou Q, Trinschek B, Abel T, Münch RC, Rasbach A, Trkola A, Jonuleit H, Buchholz CJ. Selective gene transfer into functional subpopulations of human T cells. Cancer Immunotherapy Meeting 2013, Mainz, Germany, 05/14/2013 – 05/16/2013

* shared first authors

Uhlig KM, Zhou Q, Abel T, Münch RC, Rasbach A, Trkola A, Buchholz CJ. Selective gene transfer into functional subpopulations of human T cells. German Society of Gene Therapy Meeting 2013, Hamburg, Germany, 02/28/2013 – 03/02/2013

Poster presentations at scientific meetings

Uhlig KM, Schülke S, Scheuplein VAM, Rasbach A, Koch V, Schambach A, Cichutek K, Buchholz CJ, Waibler Z, Scheurer S, Mühlebach MD. Protein transfer vectors: an efficient tool to induce antigen-specific cytotoxic T cell responses. Cancer Immunotherapy Meeting 2014, Mainz, Germany, 05/06/2014 – 05/08/2014

Uhlig KM, Schülke S, Scheuplein V, Rasbach A, Koch V, Schambach A, Cichutek K, Buchholz CJ, Waibler Z, Scheurer S, Mühlebach MD. Protein transfer vectors: an efficient tool to induce antigen-specific immune responses. German Society of Gene Therapy Meeting 2014, Ulm, Germany, 03/20/2014 – 03/22/2014

Uhlig KM, Schülke S, Schambach A, Cichutek K, Buchholz CJ, Scheurer S, Waibler Z, Mühlebach MD. Protein transfer vectors as targeted and safe antigen carriers. European Society of Gene and Cell Therapy Meeting 2013, Madrid, Spain, 10/25/2013 – 10/28/2013

Uhlig KM, Zhou Q, Trinschek B, Abel T, Münch RC, Rasbach A, Trkola A, Jonuleit H, Buchholz CJ. Selective gene transfer into functional subpopulations of human T cells. Cancer Immunotherapy Meeting 2013, Mainz, Germany, 05/14/2013 – 05/16/2013

Mühlebach M, **Uhlig K**, Schülke S, Scheuplein V, Schambach A, Cichutek K, Buchholz C, Scheurer S, Waibler Z. Protein transfer vectors as targeted, safe, and effective vaccines. German Society of Gene Therapy Meeting 2013, Hamburg, Germany, 02/28/2013 – 03/02/2013

11. Danksagung

Mein herzlicher Dank gilt Prof. Dr. Christian Buchholz und Dr. Michael Mühlebach für die Vergabe der interessanten und anspruchsvollen Themen, ihre stete Bereitschaft zu konstruktiven, fachlichen Diskussionen, die hervorragende wissenschaftliche Betreuung und nicht zuletzt die angenehme und freundliche Arbeitsatmosphäre.

Des Weiteren danke ich Prof. Dr. Beatrix Süß für die freundliche und unkomplizierte Betreuung seitens der TU Darmstadt und auch Prof. Dr. Bodo Laube möchte ich für seine Einwilligung, als Zweitgutachter zu fungieren, danken.

Allen meinen Kollegen aus den Arbeitsgruppen „Molekulare Biotechnologie und Gentherapie“ und „Onkolytische Masernviren und Impfvektoren“ möchte ich für das angenehme Arbeitsklima, eure Hilfsbereitschaft und die fachlichen Diskussionen danken. Es hat Spaß gemacht, mit euch zusammenzuarbeiten und auch außerhalb des Labors Zeit mit euch zu verbringen, wie beispielsweise dienstags im Langener Kino mit „einem Film vor dem Bundesstart in Ton und Farbe“.

Besonders herzlich möchte ich mich dabei bei Dr. Katrin Friedrich und Jan Hanauer bedanken – ihr wart beide in den kleinen und großen Dingen immer für mich da und seid von Kollegen zu Freunden geworden, die ich nicht mehr missen möchte. Ich habe die gemeinsame Zeit mit euch sehr genossen!

Sven Flindt, Dr. Verena Schummer und Dr. Kendra Schafti danke ich für viele schöne Mittwoch-Mittagspausen, seelisch-moralische Unterstützung und unkonventionelle Unterhaltungen.

Ferner möchte ich mich bei all den Menschen bedanken, die auf die eine oder andere Weise zum Gelingen meiner Doktorarbeit beigetragen haben und ohne die diese Arbeit so nicht möglich gewesen wäre - angefangen bei Frau Varga, der guten Seele des Labors, über das Tierstallteam, bis hin zu internen und externen Kooperationspartnern.

Auch meinen Freunden danke ich herzlich für die schönen gemeinsamen Momente fernab der Wissenschaft und vor allem ihr Verständnis dafür, dass wir für wichtige Experimente manches Treffen verschieben mussten.

Mein besonderer Dank aber gilt meiner wundervollen Familie und meinem wunderbaren Freund Gregor, auf deren vorbehaltslose Unterstützung und Liebe ich immer zählen konnte. Danke, dass ihr mir in den Jahren meiner Doktorarbeit - wie auch in sonst allen Lebenslagen - immer treu zur Seite gestanden habt und für mich da wart! Gregor, danke für geschätzte 40.000 km Jena - Langen.

12. Ehrenwörtliche Erklärung

Ich erkläre hiermit ehrenwörtlich, dass ich die vorliegende Arbeit entsprechend den Regeln guter wissenschaftlicher Praxis selbstständig und ohne unzulässige Hilfe Dritter angefertigt habe.

Sämtliche aus fremden Quellen direkt oder indirekt übernommenen Gedanken sowie sämtliche von Anderen direkt oder indirekt übernommenen Daten, Techniken und Materialien sind als solche kenntlich gemacht. Die Arbeit wurde bisher bei keiner anderen Hochschule zu Prüfungszwecken eingereicht.

Darmstadt, den 14.07.2015

_____

Katharina Uhlig